Naval Surface Warfare Center
Carderock Division
West Bethesda, MD 20817-5700

NSWCCD-50-TR–2008/070 September 2008
Hydromechanics Department Report

Evaluation of Multi-Vessel Ship Motion Prediction Codes

by
A.L. Silver
M.J. Hughes
R.E. Conrad
S.S. Lee
J.T. Klamo
J.T. Park

REPORT DOCUMENTATION PAGE

Form Approved
OMB No. 0704-0188

1. REPORT DATE *(DD-MM-YYYY)*	2. REPORT TYPE	3. DATES COVERED *(From - To)*
20-Sep-2008	Final	10/2005 - 9/2008

4. TITLE AND SUBTITLE
Evaluation of Multi-vessel Ship Motion Prediction Codes

5a. CONTRACT NUMBER

5b. GRANT NUMBER

5c. PROGRAM ELEMENT NUMBER

6. AUTHOR(S)
A.L. Silver, M.J. Hughes, R.E. Conrad, S.S. Lee, J.T. Klamo, and J.T. Park

5d. PROJECT NUMBER

5e. TASK NUMBER

5f. WORK UNIT NUMBER
05-1-5500-719, 06-1-5500-734

7. PERFORMING ORGANIZATION NAME(S) AND ADDRESS(ES) AND ADDRESS(ES)

Naval Surface Warfare Center
Carderock Division
9500 Macarthur Boulevard
West Bethesda, MD 20817-5700

8. PERFORMING ORGANIZATION REPORT NUMBER

NSWCCD-50-TR-2008/070

9. SPONSORING / MONITORING AGENCY NAME(S) AND ADDRESS(ES)
Attn: Paul Hess ONR 331
Chief of Naval Research
875 North Randolph Street
Arlington, VA 22217-5660

10. SPONSOR/MONITOR'S ACRONYM(S)

11. SPONSOR/MONITOR'S REPORT NUMBER(S)

12. DISTRIBUTION / AVAILABILITY STATEMENT
Approved for Public Release, Distribution Unlimited

13. SUPPLEMENTARY NOTES

14. ABSTRACT

An evaluation of six different multiple body ship motion prediction codes, MVS-CSC, MVTDS, AQWA, ShipMo3D, AEGIR, and LAMP-MULTI, was performed by the Naval Surface Warfare Center, Carderock Division (NSWCCD). Each of the codes in this evaluation was chosen based on its accessibility to the Navy or its use by US regulatory agencies. The evaluation was performed in two parts. The first part compared the capabilities of each code against a matrix of capabilities that were important for predicting the usefulness of a base at sea to transfer military equipment and personnel from a larger to smaller vessel. Results of this evaluation show that all the codes have the same capabilities for estimating the environment, calculating the motions of the ships in any configuration with respect to each other, and accounting for the hydrodynamic effects between the hulls. The major differences in the capabilities of the codes were in the non-hydrodynamic factors and in the degree of complexity used to model the hydrodynamic factors. AEGIR, LAMP-MULTI, and AQWA allow for user supplied force routines in the time domain and AQWA, LAMP-MULTI and MVS include some built-in models for mooring lines and fenders. Also, the autopilot feature for multiple ships was available only in the MVS and LAMP-MULTI codes.

(The abstract is continued on the following page)

15. SUBJECT TERMS

16. SECURITY CLASSIFICATION OF:			17. LIMITATION OF ABSTRACT	18. NUMBER OF PAGES	19a. NAME OF RESPONSIBLE PERSON
a. REPORT	b. ABSTRACT	c. THIS PAGE			Andrew Silver
UNCLASSIFIED	UNCLASSIFIED	UNCLASSIFIED	SAR	190	19b. TELEPHONE NUMBER *(include area code)* 301-227-5119

Block 14. ABSTRACT (Continued)

The second part of the evaluation correlated two-ship model data from a test performed at the Maritime Research Institute Netherlands (MARIN) with the output from each of the codes. This correlation of the codes yielded differing results. Overall all codes predicted heave and pitch motions within 10% of the model test results except for the CSC MultiVessel Simulator (MVS) and the D&P MultiVessel Time Domain Simulator (MVTDS) which was 30% off of the model tests. For surge and sway forces and roll and yaw moments LAMP-MULTI and AEGIR were 20% different from the model test, AQWA was 35%, the MVS code from CSC and the MVTDS from D&P were 60 to75 percent different, and the ShipMo3D was 160% different. The phase correlation yielded similar results for pitch and heave, but was more uniform for the forces and moments, resulting in 20 to 25 percent difference.

CONTENTS

CONTENTS (continued)

FIGURES

FIGURES (continued)

TABLES

TABLES (continued)

ABSTRACT

An evaluation of six different multiple body ship motion prediction codes, MVS-CSC, MVTDS, AQWA, ShipMo3D, AEGIR, and LAMP-MULTI, was performed by the Naval Surface Warfare Center, Carderock Division (NSWCCD). Each of the codes in this evaluation was chosen based on its accessibility to the Navy or its use by US regulatory agencies. The evaluation was performed in two parts. The first part compared the capabilities of each code against a matrix of capabilities that were important for predicting the usefulness of a base at sea to transfer military equipment and personnel from a larger to smaller vessel. Results of this evaluation show that all the codes have the same capabilities for estimating the environment, calculating the motions of the ships in any configuration with respect to each other, and accounting for the hydrodynamic effects between the hulls. The major differences in the capabilities of the codes were in the non-hydrodynamic factors and in the degree of complexity used to model the hydrodynamic factors. AEGIR, LAMP-MULTI, and AQWA allow for user supplied force routines in the time domain and AQWA, LAMP-MULTI and MVS include some built-in models for mooring lines and fenders. Also, the autopilot feature for multiple ships was available only in the MVS and LAMP-MULTI codes.

The second part of the evaluation correlated two-ship model data from a test performed at the Maritime Research Institute Netherlands (MARIN) with the output from each of the codes. This correlation of the codes yielded differing results. Overall all codes predicted heave and pitch motions within 10% of the model test results except for the CSC MultiVessel Simulator (MVS) and the D&P MultiVessel Time Domain Simulator (MVTDS) which was 30% off of the model tests. For surge and sway forces and roll and yaw moments LAMP-MULTI and AEGIR were 20% different from the model test, AQWA was 35%, the MVS code from CSC and the MVTDS from D&P were 60 to 75 percent different, and the ShipMo3D was 160% different. The phase correlation yielded similar results for pitch and heave, but was more uniform for the forces and moments, resulting in 20 to 25 percent difference.

ADMINISTRATIVE INFORMATION

This work was performed by the Seakeeping Division (Code 5500) of the Hydromechanics Department at the Naval Surface Warfare Center, Carderock Division (NSWCCD). Funding for this study was provided through Work Request Numbers N0001405WX20968, N0001406WX21051, N0001407WX20703, N0001407WX20704, 1445, and N0001408WX21041 by the Office of Naval Research Code 331. The work was performed under NSWCCD Work Unit Numbers 05-1-5500-719, 06-1-5500-734, 07-1-5500-760, 07-1-5500-761, and 08-1-5500-779.

INTRODUCTION

The US Navy is preparing for a scenario in which a conflict area is not near a full service port for the logistic delivery of military equipment and personnel. The port that may be available near the conflict, could be one that is classified as 'austere' as it would allow only smaller vessels and have few aids to navigation. Military cargo is generally transported by Large Medium Speed Roll-on Roll-off (LMSR) ships. Establishing an offshore seabase with multiple ships in close proximity would allow the transfer of military equipment and personnel from the LMSR to a smaller one. This smaller ship could then navigate the austere port and thus mitigate this logistics problem. It is planned that this seabase could be formed as far as 100 nautical miles from the shore. At this distance, the seabase could encounter a wide variety of seaways. It is anticipated that the seabase would only be set up and operational if the sea conditions were at or lower than Sea State 4.

When two ships are in close proximity in a seaway, as in an operational seabase configuration, complex hydrodynamic interactions take place. Large wave induced motions of each of the ships could diminish its functionality. The motions of a wide variety of ships in close proximity can be predicted using multiple-ship motion simulation codes. There are many multiple-ship motion prediction codes available to use. The Office of Naval Research (ONR) sponsored an investigation by NSWCCD to evaluate the capabilities of the various codes and the accuracy of their motions predictions.

Each of the computer simulation codes that were included in this evaluation were chosen based on either their availability to be used by NSWCCD, or if the code is being used by a regulating agency such as the American Bureau of Shipping (ABS). The final set of six codes included the MultiVessel Simulator (MVS) written by Computer Sciences Corporation (CSC)[1*], the Multiple Vessel Time Domain Simulator (MVTDS) written by British Maritime Technology Designers and Planners (BMT D&P)[2], Large Amplitude Motion Program (LAMP) for multiple ships or LAMP-MULTI by Science Applications International Corporation (SAIC)[3], AEGIR developed initially at the Massachusetts Institute of Technology (MIT) and now supported by Flight Safety Technologies[4], AQWA developed by ANSYS Inc.[5], and ShipMo3D developed by Defence Research and Development Canada (DRDC) Atlantic[†]. Two additional codes, WAMIT[6] developed at MIT and marketed by WAMIT Inc., and FD-Waveload from MARTEC Ltd[7] were also examined but not formally included in the evaluation.

The evaluation of these codes was performed in two parts. First, a matrix of capabilities was established that represented the required functions that any simulation code should have for evaluating the motions of the ships composing a seabase. The documentation for each of the codes was then reviewed to determine if the capabilities listed in the matrix were addressed. The second part of the evaluation determined the veracity of the predicted motions of each code. This was conducted by running each code for eight conditions that were part of an overall model test matrix of two ships in close proximity. The results of the predictions of the codes were then compared to the

---

[*] References are located on page 189.

[†] McTaggart, K., "ShipMo3D Version 1.0 User Manual for Frequency Domain Seakeeping Predictions for Two Ships in a Seaway," unpublished manuscript Defence R&D Canada, Atlantic.

model test results. This report documents the procedure of the evaluation and provides the results. As is the case with many computational tools, the codes evaluated in this effort are constantly being revised and improved by their developers. This evaluation, therefore, only includes the versions of each of these codes as they were on 1 January 2008.

MATRIX OF CODE CAPABILITIES

The task of evaluating each of the multiple ship motion prediction codes to assess their respective capabilities was twofold. First, a matrix of core required capabilities for determining the functionality of the seabase in a prevailing seaway had to be established, then, second, determine if each of the codes addressed those capabilities. The capabilities were broken down into four major categories; environment, seabase configuration, hydrodynamic factors and non-hydrodynamic factors.

The first major category of capabilities was the representation of the environment, specifically waves, wind, current and water depth, and how it was modeled in each of the codes. The waves should be represented in both irregular spectral format and regular sinusoidal form. These two environmental factors, regular and irregular representations of the seaway, are the most important factors the codes should be able to accommodate. The irregular waves should be able to be represented as Bretschneider, JONSWAP and Ochi-Hubble bimodal spectra. The ability to model the forces from wind and current, accounting for both their speed and direction, is also desirable, but it is of secondary importance. Finally, since the seabase could be located closer than 100 nautical miles to shore, the computational model ship motion calculations should be able to handle cases in finite depth water. This capability, too, is of secondary importance.

The next major category was the configuration of the seabase of which there were four elements considered. First, each code should be able to predict the motions of at least two ships, and possibly more, in close proximity. Second, the motion prediction code should be able to accommodate a variety of ships of different hull geometries including multi-hulled vessels, Surface Effect Ships (SES), and Air Cushion Vehicles (ACV). Third, the codes should model motion control systems such as active fins and rudder roll stabilization. Finally, the codes should be able to model the motions of the ships of the seabase when they are in any arbitrary alignment. This would include close-in or far-apart, amidships-to-amidships, Med-moor, and bow-to-stern among others. Of these factors, the number of vessels composing the seabase, and the arrangement of the seabase are the two primary capabilities the codes should have. The capability to include different hull geometries is also important (for the seabase may need to accommodate the Joint High Speed Vessel (JHSV), a possible catamaran vessel and the SES T-Craft) but not as important as the other two factors.

The hydrodynamic factors category includes a number of different elements. First, the programs should account for forward speed. Although the speeds of the ships while in a seabase formation are generally slow, much less than a Froude Number of 0.4, it is still important to make sure that the programs can account for forward speed. The second hydrodynamic factor is whether the program runs in the frequency or time domain. Frequency domain calculations are generally quicker and the response amplitude operator (RAO) spectrum can be easily determined. However, the non-linear aspects of the motions and mooring configurations cannot be discerned. Time domain

calculations can include the non-linear hydrostatic and Froude-Krylov forces and some other important hydrodynamic forces, such as viscous roll damping, as well as outside forces, such as those from mooring lines and fenders. Third, because in many cases during the formation of the seabase one ship will be in the lee of the other, the program should include wave shadowing effects on the motions. Next the codes should account for the different types of hydrodynamic forces acting on the ships. These forces include the propulsors/thruster forces, the appendage forces including rudders, bilge keels, skegs and fins, and any second order drift forces. Finally, the code documentation was reviewed to determine if non-linear effects of the free surface, hydrostatics, and dynamic motions were accounted for in the programs. These capabilities are less important as they account for small and second order effects.

The final capability category includes the non-hydrodynamic factors that could be present in a two ship scenario and whether the codes account for those forces and attributes. The forces include the mooring and fender systems that may be deployed for a skin-to-skin operation, and ramp forces that would be applied if a ramp were used for cargo transfer. Other non-hydrodynamic factors in the code capability matrix include autopilot, ship overtaking scenarios, and whether the codes are able to fix some of the motion calculations to yield only forces and moments. Again, the non-hydrodynamic capabilities that show the utility of the seabase would be in the mooring, ramp, and fender systems so these capabilities would be the most important.

This capability matrix is shown in Tables 1 through 4. Once the matrix was established, the capabilities of each of the codes in this evaluation were compared against it. These capabilities were determined primarily from the documentation that came with each code. Additionally, no documentation or code updates were accepted after January 1, 2008. Several codes allow the user to create his own subroutine to be either compiled with the code or linked through a DLL. This utility can be used to include a non-hydrodynamic force or other capability that is not inherent in the code itself. Instances in which the capability was not currently present in the code but could be added by a user-supplied program are noted in Tables 1 through 4.

A review of the documentation of the six codes was then conducted to determine how well each code fulfills the capabilities in the matrix. As shown in Table 1, all codes can model the seaway by regular waves and all except ShipMo3D can model irregular waves according to the user documentation that was in hand as of 1 January 2008. The developer of ShipMo3D[‡] has stated that the capability to model irregular seaways has been coded into the multiple vessel ShipMo3D model, but the documentation as of the freeze date does not reflect that. The irregular wave environment can be modeled by each of the other codes by using one of the following spectra: Bretschneider, JONSWAP, and Ochi-Hubble. Most simulations, except ShipMo3D, can include routines to model the effect of wind and current speed and direction. Finite water depth effects can be accounted for in LAMP-MULTI, AEGIR, and AQWA. For the MVS and MVTDS codes, the finite depth effects are only included in the resulting predicted motions if the programs, such as FD-Waveload[7], that were used to calculate the added mass, damping and other hydrodynamic parameters for the formulation of the impulse response function include finite depth effects.

[‡] McTaggart, K., ibid

The next major category was the configurations of ship geometries and the seabase, as shown in Table 2. All of the codes can predict the motions with two or more vessels and they can all accommodate multi-hull vessels and arbitrary but steady body-to-body alignment. None of the codes can predict the motions of surface effect ships (SESs) or fully skirted air cushion vehicles (ACVs) in the presence of other ships. Simulation of motion control systems on ships in the multi-vessel environment can only be addressed by LAMP-MULTI and ShipMo3D. LAMP-MULTI can add passive anti-roll tanks, a moving mass system for ride control, force-specified anti-rolling fins, rudder roll stabilizer and a general foil controller. ShipMo3D can model passive motion control such as bilge keels, skegs, and fins, and active motion control of rudder roll stabilization. AQWA and AEGIR can accept an external program with motion control algorithms.

Hydrodynamic capabilities of each of the codes are not as straightforward. Although all of the codes in this evaluation can account for the hydrodynamic effects on the ship motions of forward speed and wave shadowing, each of the codes has varying capabilities in accounting for the other hydrodynamics. LAMP-MULTI, AQWA, and ShipMo3D include routines integrated in their code to include the propulsor and thruster forces. AEGIR can account for these forces if the user adds an external routine, and the MVS code handles these forces in AgileShip which is then fed into MVS. It is not evident from the documentation of the version supplied to NSWCCD how MVTDS includes the propulsor and thruster forces. The types of hydrodynamic calculations also differ with each of the codes. LAMP-MULTI, AEGIR, and AQWA run time domain calculations, though AQWA also has a frequency domain module that can be exercised. ShipMo3D currently calculates the multi-ship motions only in the frequency domain, and MVS and MVTDS codes are time domain tools, although the initial program that calculates the added mass and damping coefficients, FD-Waveload[7], is a frequency domain program. Appendage forces are also handled differently between each of the codes. For the MVS, MVTDS, AQWA, and ShipMo3D, the lift force from the rudders and viscous roll damping from the bilge keels are accounted for within the programs. Within LAMP-MULTI, the forces from wing-like and plate-like appendages are computed from empirical formulae to account for rudder and bilge keel forces. AEGIR can model fins and rudders directly as part of the hydrodynamic boundary value solution or include the forces on these appendages using empirical lift and drag coefficients, while bilge keel forces are included through a simple linear model that calculates viscous damping. The final hydrodynamic factors that are included in the code capabilities include the non-linear effects of the free surface, non-linear hydrostatics and Froude-Krylov forces, and the second order drift forces. Modeling the free surface is linear in all but AEGIR where the user has the option of selecting non-linear wave radiation and diffraction. Accounting for the non-linear hydrostatic and Froude Krylov forces is only performed in LAMP-MULTI, AEGIR, and AQWA. MVS, MVTDS and ShipMo3D provide only linear results. None of the codes, except AQWA, provide calculations to determine the second order drift forces.

Table 1. Matrix of Code Capabilities - Environment

Environment	MVS	MVTDS	LAMP-MULTI	AEGIR	AQWA	ShipMo3D
Irregular Waves	**Yes** - available irregular spectrum types are not specifically reported in MVS documentation	**Yes** - Bretschneider, Ochi Hubble, and JONSWAP; all longcrested (modification necessary for short crested)	**Yes** - Pierson-Moskowitz, Bretschneider, Ochi Hubble, JONSWAP; both short and long crested seas	**Yes** - represented as a superposition of many regular waves	**Yes** - Pierson-Moskowitz and JONSWAP longcrested only; user defined spectrum can also be used	**Yes** - Bretschneider, Ochi-Hubble, JONSWAP, 10 parameter wave spectrum; both longcrested and shortcrested but not in current documentation.
Regular Waves	**Yes**	**Yes**	**Yes**	**Yes**	**Yes**	**Yes**
Wind	**Yes**	**Yes** - but in full version only	**Yes** - through external force in autopilot file	**No** - but possible for user to add as external force	**Yes** - using a force coefficient	**No** - not evident from documentation
Current	**Yes**	**Yes** - but in full version only	**Yes**	**No** - not evident from the documentation	**Yes** - using a force coefficient	**No** - not evident from the documentation
Finite water depth	Depends on tool used to generate impulse repsonse functions	Depends on tool used to generate impulse repsonse functions	**Yes**	**Yes**	**Yes**	**No** - not evident from the documentation

Configurations	MVS	MVTDS	LAMP-MULTI	AEGIR	AQWA	ShipMo3D
Number of Bodies	Two	Two or more	Currently restricted to three.	Two or more	up to ten bodies	Two
Multihull Vessels	**Yes** - but handled in FD-Waveload	**Yes** - but handled in FD-Waveload	**Yes** - but total closed wetted surfaces limited to three unless using a user-specified free surface	**Yes**	**Yes** - can handle up to fifty structures	**Yes**
Arbitrary Body-to-Body Alignment	**Yes**	**Yes**	**Yes**	**Yes**	**Yes** - determined by the input structure locations	**Yes**
Surface Effect Ships	**No**	**No**	Single ship version only	Single ship version only	**No** - However, Alion has a DLL	**No**
ACV's (fully skirted)	**No**	**No**	**No**	Single ship version only	**No**	**No**
Motion Control Systems	No active appendages except rudders	Not evident from documentation	Passive anti-roll tanks, moving mass system for roll control, force-specified anti-rolling fins, rudder roll stabilization, and a general foil controller	Not evident from documentation, future addition as an external module	Models rudder lift and bilge keel forces. External forces can be added through a user-supplied program.	Passive motion control such as bilge keels, skegs, and fins can be modelled. The only active appendage to mitigate roll motion is the rudder. There is no mention of trim tabs or other active fins in the documentation.

Table 2. Matrix of Code Capabilities - Configurations

Table 3. Matrix of Code Capabilities – Hydrodynamics

Hydrodynamics	MVS	MVTDS	LAMP-MULTI	AEGIR	AQWA	ShipMo3D
Forward Speed; up to Fn=0.4	**Yes**	**Yes**	**Yes**	**Yes**	**Yes**	**Yes**
Propulsor/thruster forces	**Yes** - propeller forces can be handled in AgileShip but not thruster forces.	Not evident from documentation	**Yes** - models propeller propulsors but not waterjet or thrusters, unless an external force code is written	Possible for user to add as external force	Up to ten thruster forces may be applied to each body	**Yes**
Time domain/frequency domain	MVS is a time domain code, FD-Waveload is a frequency domain code	MVS is a time domain code, FD-Waveload is a frequency domain code	Time domain	Time domain only	AQWA-LINE is frequency domain; AQWA-NAUT is time domain; AQWA-FER is frequency domain.	Frequency domain only for multi-ship calculations
Wave shadowing effects on motions	**Yes**	**Yes**	**Yes**	**Yes**	**Yes**	**Yes**
Appendage Forces	Rudders and nonlinear viscous roll damping from bilge keels	Rudders and nonlinear viscous roll damping from bilge keels	Can specify wing-like and plate-like appendages	Simple linear model for viscous damping	Rudder lift and bilge keels modeled	Bilge keels, skegs, fins, and rudders modeled
Free surface non-linearity	Free-surface is linearized about calm water; hull boundary is lineanzed about mean position	Free-surface is linearized about calm water; hull boundary is linearized about mean position	Linear free surface condition, with option of where to apply the condition	Option of linear or nonlinear wave radiation and diffraction	Linear	Linear
Body non-linearity	Linear	Linear	Nonlinear hydrostatics and Froude-Krylov wave forces	Linear added mass, damping and diffraction; nonlinear hydrostatics and Froude-Krylov forces	Linear added mass, damping and diffraction; nonlinear hydrostatics and Froude-Krylov forces	Linear added-mass, damping and diffraction
Drift forces	Not evident from the documenation	Not evident from the documenation	Not evident from the documenation	Not evident from the documenation	Second order mean wave drift forces calculated in AQWA-LINE; slowly varying drift forces calculated in AQWA-DRIFT	Not evident from the documenation

Table 4. Matrix of Code Capabilities – Non-Hydrodynamic Factors

Non-Hydrodynamic Factors	MVS	MVTDS	LAMP-MULTI	AEGIR	AQWA	ShipMo3D
Mooring System Forces on Bodies	**Yes**	**Yes** - but not in the version that was evaluated for this study	**Yes** - using the CABLE input module	**Yes** - as an external model	**Yes** - using both linear and non-linear models	Not evident from the documenation
Fender Forces and Dynamics on Bodies	**Yes**	**Yes** - but not in the version that was evaluated for this study	**Yes** - Using the FENDER input module	**Yes** - as an external model	**Yes** - as a nonlinear cable force	Not evident from the documenation
Ramp Forces and Structural Dynamics on Bodies	Modifications to code required to add ramp forces	Modifications to code required to add ramp forces	Modifications to code required to add ramp forces	Modifications to code required to add ramp forces	Modifications to code required to add ramp forces	Modifications to code required to add ramp forces
Autopilot	**Yes**	Not evident from the documenation	**Yes** - numerous options including maintain speed, maintain heading, and rudder commands	Not evident from the documenation	Not evident from the documenation	**Yes** - but only utilized in the single ship time domain version which was not evaluated
Ship Degrees of Freedom	Six when in free running mode or two (pitch and heave) in captive mode	In version used in this study only two DOF. Understand program can calculate 6 DOF.	6 DOF in free running mode or user specified in captive mode	Can specify free and forced modes	Can specify any degree of freedom, but only 0 or 6 DOF for AQWA-LINE	6 DOF in free running mode or user specified in captive mode
Simulate overtaking scenarios	Can simulate the overtaking scenarios using different initial speeds for each ship	Not implemented in version used for this evaluation	Can simulate the overtaking scenarios using different initial speeds for each ship	Only one ship speed can be input	**No**	**No**

MODEL TEST

The second part of the evaluation process was to correlate the output from each of these codes with two-ship model tests that were performed at MARIN[8, 9, 10]. The ships that were tested were 45th scale models of the T-AKR 300 class (BOB HOPE) and the T-AK 3008 (BOBO). The setup of the test required a new sub-carriage to be built on to the existing carriage in the Seakeeping basin at MARIN. The BOB HOPE was attached to the main carriage, and the BOBO was attached to the new sub-carriage as shown in Figure 1. Both models were free to pitch and heave and constrained in all other modes. During the test, the heave and pitch motions, surge and sway forces and roll and yaw moments were measured. The waves for this set of tests were regular with a nominal height of 0.75 meters full-scale and frequencies at 0.4, 0.5, 0.6, 0.7, 0.8, and 0.95 radians per second. The ship-to-wave heading conditions included head to following waves with the BOB HOPE on the weather side of the carriage at the following headings: 180°, 150°, 135°, 120°, 90°, 30°, and 0° (where 180 ° is head and 0 ° is following). There were also a few runs made with the BOBO on the weather side at headings of 330°, 270°, and 225°. The tests were also run for three full-scale separations: 3 meters, 16.5 meters and 33 meters when the models were amidships-to-amidships, and at speeds of 0, 5 and 16 knots. Other conditions tested included the BOBO both abaft and ahead of the BOB HOPE and the BOBO passing the BOB HOPE.

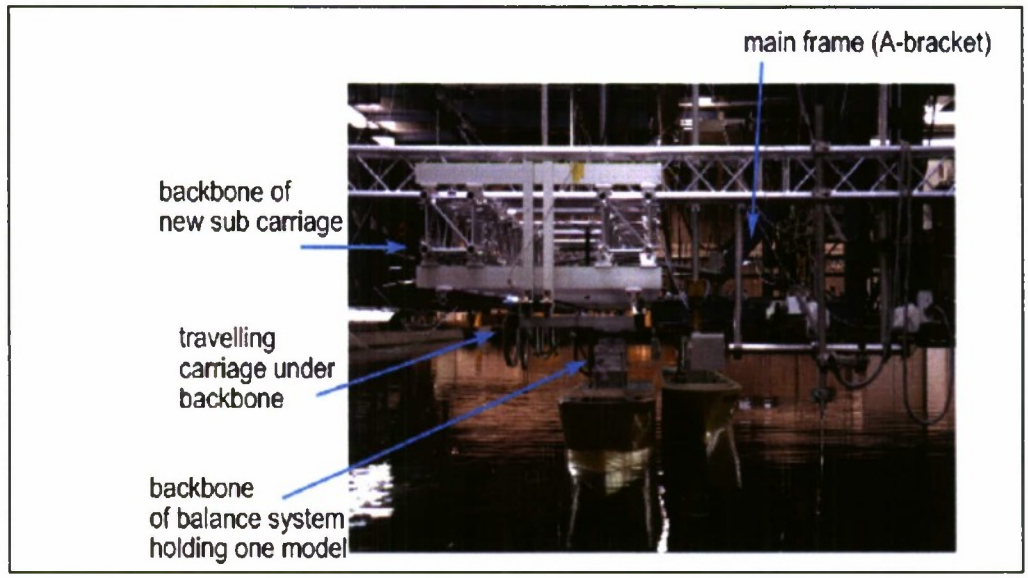

Figure 1. Carriage setup for the MARIN two ship test

Of the complete data set, eight cases were chosen to compare with the output from the six simulation codes included in our evaluation, as shown in Table 5. Each of the eight conditions had the BOBO and the BOB HOPE amidships-to-amidships in steady state mode. The chosen conditions included a case with a slow speed and close separation, a case at the highest speed and medium distance separation, and another case at the highest speed with the largest separation distance. The basis for the selection of the eight conditions was to include a wide range of conditions in the amidships-to-amidships configuration. It was thought that for this initial investigation of multi-ship seakeeping

eodes, it would be best to evaluate them in the eondition that the seabase was most likely to be eonfigured. One example correlation case was diseussed in the body of this report and the other seven are provided in the appendiees of this report. The case shown in the body of the report is the eondition that represents a 3 meter separation, 135° heading, and 5 knot ship speed.

Table 5. Model Test Conditions used in the Multi Body Simulation Code Evaluation

	3 meter separation	16.5 meter separation	33 meter separation
Speed	5 knots	16 knots	16 knots
Heading	180°,135°	180°, 150°, 120°	180°, 150°, 120°

UNCERTAINTY ESTIMATES OF MARIN MODEL TESTS

Beeause the model test data are to be used to eorrelate the motion predietions of eaeh of the six simulation eodes, it is important to determine the uneertainty of these model tests. First, the aeeuraey of the instrumentation was investigated. Seeond, an uneertainty analysis of the piteh and heave response amplitude operator (RAO) motions was eondueted and finally the variability of the data eolleetion was determined from 10 repeat test runs for the exaet same eonditions. The result of this uneertainty analysis provided a measure of the error band of the model test data.

Instrument Accuracy

For proper eomparison to theory, uneertainty estimates have been formulated for the MARIN multi-vessel tests. The information on uneertainty of these tests provided in the MARIN reports, referenees 8 through 10, was inadequate for the eomputation of uneertainty estimates. Uneertainty estimates were provided for the heave and piteh measurements [8], but these estimates were based upon manufaeturer's speeifieations and not on any ealibration. Piteh angle was eheeked at an angle of 0.50° with an error of 0.01° deg with an inelinometer [8] for the BOB HOPE, but the uneertainty in the inelinometer was not provided. For the foree measurements, the aeeuracy was elaimed as ±2 %[8], but no evidence was provided to support this elaim other than experienee. Typieally for sueh a measurement, the uneertainty in load is fixed in physieal units. A pereent in uneertainty is normally refereneed to full-seale, and the full-seale loads were not provided.

The only useable information provided for uncertainty estimates was the performanee of the wave-maker. The wave frequeney was reported as within ±2.5 % for a wave frequeney range of $0.3 < \omega < 0.95$ rad/s and the wave amplitude within ±5 % at a nominal wave amplitude of $A = 0.75$ m for no model in the basin[8].

As a eomparison, uneertainty estimates were performed for heave and piteh. Suffieient information was not available from the MARIN reports for the forees and moments. The deviees for the heave and piteh measurements were a pair of Fiama PF700 potentiometers. The aeeuraeies of these deviees were elaimed to be ±0.0045 m in heave and ±0.17° in piteh at full-seale[8]. Careful review of these deviees from manufaeturer's speeifieations indieates that these values are ineorreet. These deviees were not ealibrated, but piteh was eheeked with an error of 0.01° deg at 0.50° for the Bob Hope model as stated previously[8]. None of the measurements as reported by MARIN are traeeable to their national metrology laboratory, Nederlands Meetinstituut (NMi).

The actual specification for the Fiama PF700 is a resolution of 0.1 mm and linearity of ±0.25 %. These values are not the same as uncertainty or accuracy of the measurement. Since the scale factor is $\lambda = 45$, then the resolution is 0.0045 m, which is the apparent claim for accuracy. For a 700 mm measurement device at 0.25 % linearity, the uncertainty without calibration may be as high as 1.75 mm or 0.079 m full-scale (17.5 times the stated value). Furthermore, the MARIN reports do not report any details on the use of the 2 potentiometers. For estimation purposes, heave will be assumed to be the average of the 2 potentiometers. Full-scale heave is then

$$H = \lambda(y_1 + y_2)/2 \tag{1}$$

where λ is the scale factor and y_1 and y_2 are the 2 laboratory scale heave measurements. From the law of propagation of uncertainty from the ISO Uncertainty Guide[11], the uncertainty in the full-scale heave measurement is then

$$U_H = \lambda U_y/\sqrt{2} \tag{2}$$

where the uncertainty in y_1 and y_2 are assumed to be the same and uncorrelated and the uncertainty in scale factor is zero. If the two transducers were calibrated against the same reference standard, then the uncertainties would be correlated, and a different result would occur. For the purpose of this analysis, the uncertainty in the potentiometer at the 95 % confidence level is assumed to be the resolution. The uncertainty in heave is then 0.0032 m. The non-dimensional heave or Response Amplitude Operator (RAO) is defined as

$$RAO_H = H/A \tag{3}$$

The non-dimensional relative uncertainty in heave is then

$$U_{RAO}/RAO_H = \sqrt{(U_H/H)^2 + (U_A/A)^2} \tag{4}$$

where the relative uncertainty in amplitude is assumed to be ±5 % at the 95 % confidence level.

The pitch angle as measured by the two potentiometers is given by

$$\sin\alpha = (y_1 - y_2)/x \tag{5}$$

or for small pitch angles

$$\alpha = (y_1 - y_2)/x \tag{6}$$

The uncertainty in pitch angle is then

$$U_\alpha = \sqrt{2(U_y/x)^2 + (\alpha U_x/x)^2} \tag{7}$$

With the assumption that the second term will be small, this equation reduces to

$$U_\alpha = \sqrt{2}(U_y/x) \tag{8}$$

From the MARIN report, the distance, x, between the two potentiometers is 3 meters. The uncertainty in angle is then ±0.0027° and not ±0.17° claimed in the report. As a practical matter, a good laboratory inclinometer will have an uncertainty between 0.1° and 0.01°. For the purpose of these estimates, a value of ±0.01° at the 95 % confidence will be assumed. This value is also consistent with the error reported by a comparison with an inclinometer.

The non-dimensional pitch angle is defined by

$$RAO_\alpha = \alpha L/A \tag{9}$$

The relative uncertainty in the RAO is then

$$U_{RAO} / RAO_{\alpha} = \sqrt{(U_{\alpha} / \alpha)^2 + (U_L / L)^2 + (U_A / A)^2} \quad (10)$$

The referenee length for sealing was the full-seale length of the BOB HOPE of 269.45 m from Table 1 of Appendix A of referenee 8. The reported toleranee was 5 mm on length per Seetion 1, p. 5 in referenee 10. With a seale faetor of 45, the full-seale uneertainty was assumed to be 0.225 m. The estimated uncertainties of the individual measurements for heave and piteh are summarized in Table 6.

Table 6. Uneertainty of Measurement Quantities for Heave and Piteh

Quantity	Symbol	U_{95}	Units
Amplitude	A	5.0	%
Frequency	ω	2.5	%
Heave	H	0.0032	m
Length	L	0.225	m
Pitch	α	0.01	deg

The results for propagation of the uneertainties are presented in Figure and 3, for non-dimensional heave and piteh, respeetively. In both eases, the uneertainties are dominated by primarily the uneertainty in wave amplitude. However, the uneertainty in the heave and pitch measurements eould easily be underestimated by a faetor of 10. In whieh ease, those terms would be dominant. The effeet of uneertainty in length on piteh is essentially nil.

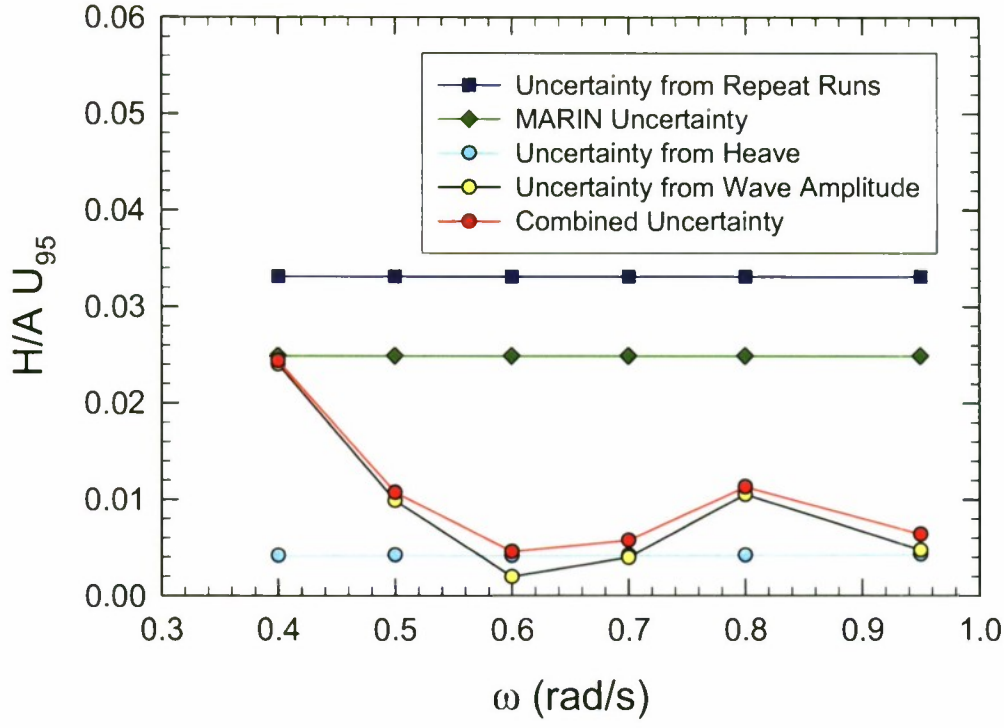

a) HOPE

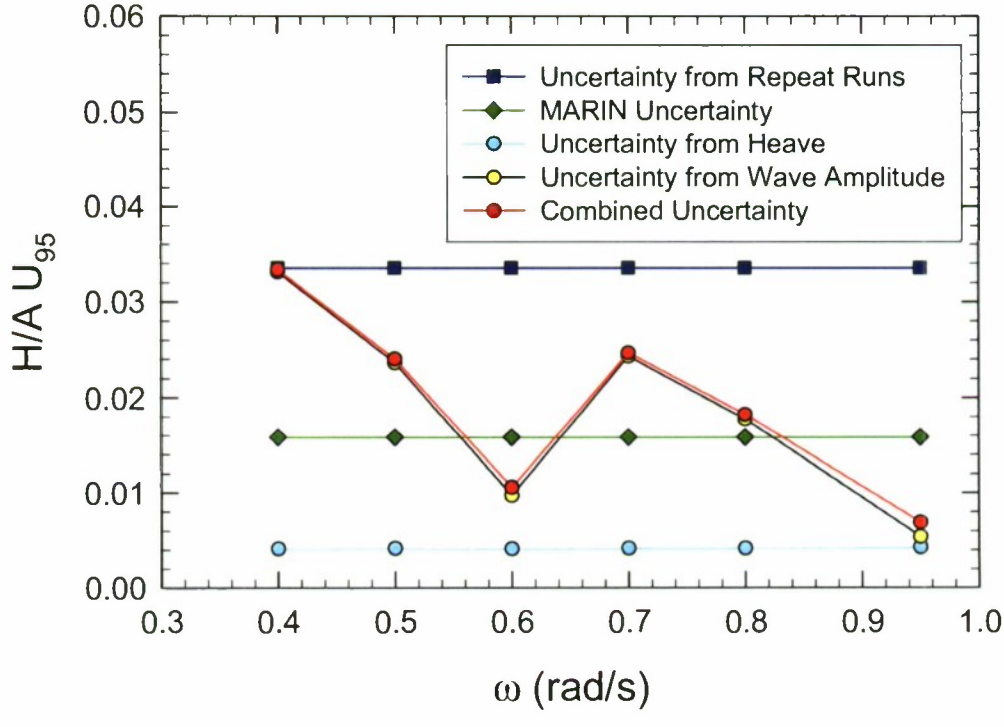

b) BOBO

Figure 2. Uncertainty Estimates in Heave for Zero Speed and 0° Heading

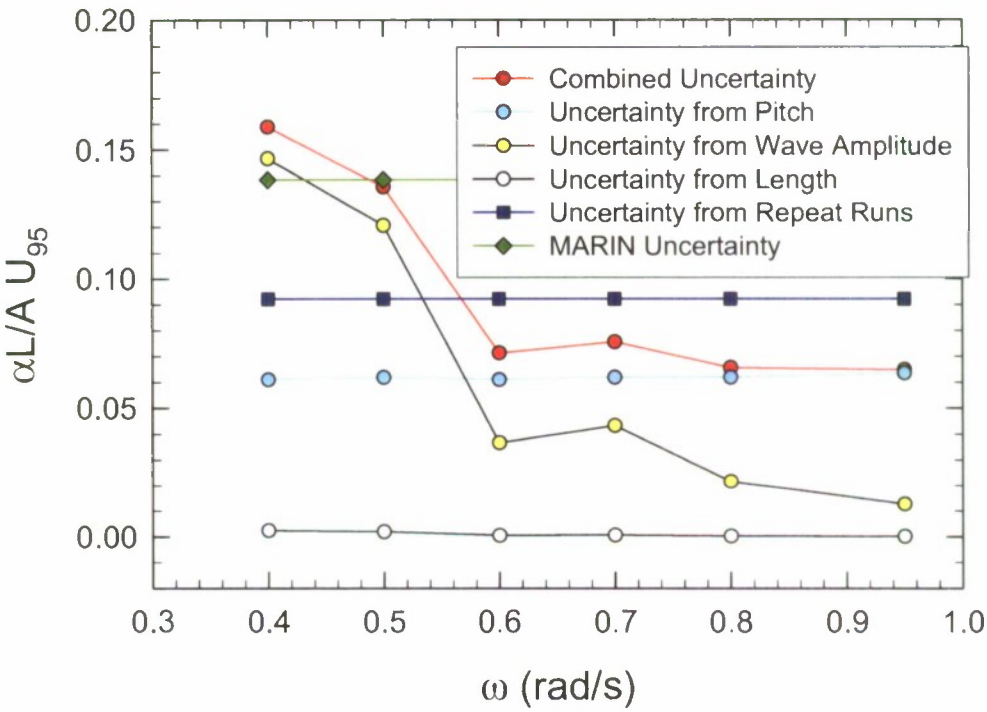

a) HOPE

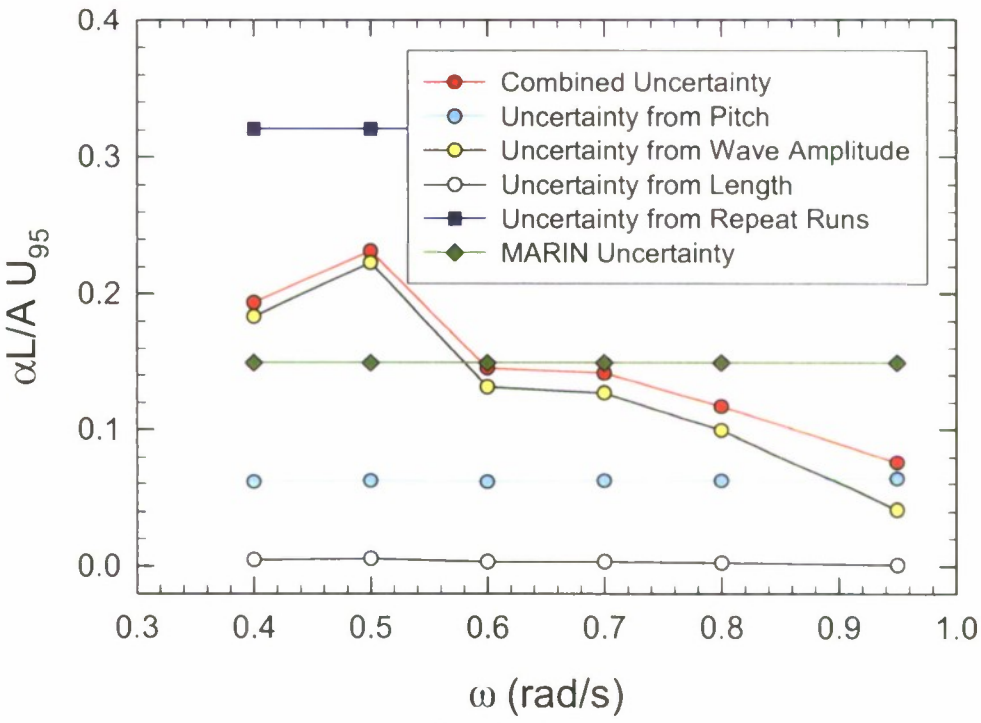

b) BOBO

Figure 3. Uncertainty Estimates in Pitch for Zero Speed and 0° Heading

Repeat Tests

MARIN performed a series of 10 repeat tests for a heading of 135° and speed of 5 knots. The wave amplitude was an average of 0.728 m and frequency of 0.60 radians per second. The wave amplitude of 0.75 m in the table was the nominal test value. The actual measured values are located in the *.LOG files for each run.

As a practical matter, the variability in the repeat tests is probably larger than uncertainty estimates from the instrument calibrations. Also, since inadequate information was available for computation of the uncertainties by the methods of the previous section, uncertainty estimates were computed from the standard deviation in the mean values for the 10 repeat runs.

Data for the MARIN tests were computed from a harmonic analysis. A more appropriate calculation appears to be one from standard statistics. The results were presented as a Response Amplitude Operator (RAO). A ratio was taken of the measured quantity of motion and the wave amplitude. From a statistical point of view, the ratio is computed as a ratio of the standard deviations. For a pure sine wave, the resulting ratio is the same. For a sine wave, the standard deviation and amplitude are related by the following:

$$A = \sqrt{2}\sigma \tag{11}$$

where σ is the standard deviation. The statistics were recomputed from the original time series in the MARIN data files. The results are summarized in Table 7a at the 95 % confidence limit. In most cases, the resulting uncertainty is higher than reported in reference 8. These values in non-dimensional physical units are applied as the vertical error bars in subsequent plots with the uncertainty in frequency as ±2.5 %. The uncertainty estimates for the different methods are compared in Figures 4 and 5 for heave and pitch, respectively. For comparison with the percent difference tables computed for each computational tool, the uncertainty values from the repeat runs were recomputed using the same normalization that was used to compute the percent difference values quantifying the difference between the numerical predictions and the model test data. These values are listed in Table 7b. The standard deviations used in Table 7b represent the standard deviation of the magnitude of the first harmonic from the repeat runs computed from harmonic analysis, and are slightly different than the values computed from standard statistics used in Table 7a. The harmonic values were used here to be consistent with the percent difference calculations, which were computed from the RAOs computed for the MARIN tests from harmonic analysis. The percentage values in Table 7b for the 95% confidence limit are normalized with respect to the maximum value of the quantity over all six frequencies that were tested. This was done to match the normalization used in the percent difference calculations.

Two examples of the time series for the test results at zero speed, zero heading (following seas), and a wave frequency of 0.4 rad/s are shown in Figure 6. In this case, the heave response, Figure 6a, is quite sinusoidal; however, the roll response, Figure 6b, is relatively random. Consequently, a harmonic analysis will provide results that are essentially the same in heave in comparison to a statistical analysis, but the results will be quite different for the roll moment due to the randomness of the data.

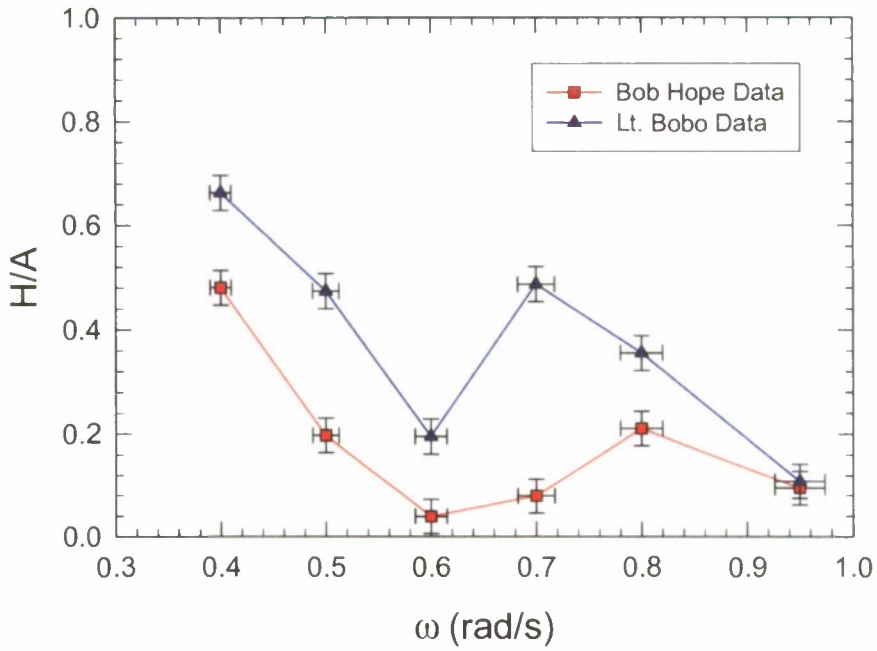

Figure 4. Heave at Zero Speed and 0° Heading

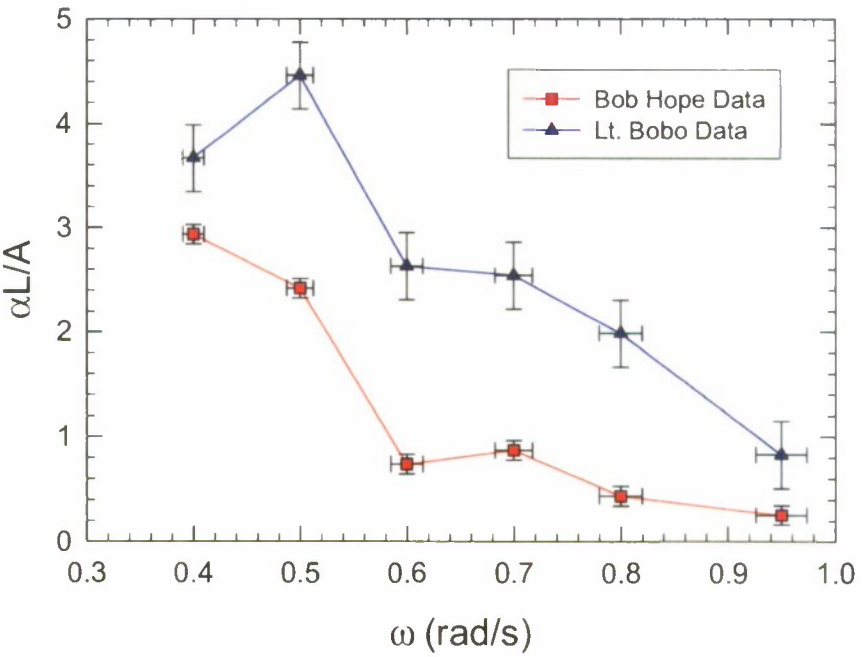

Figure 5. Pitch at Zero Speed and 0° Heading

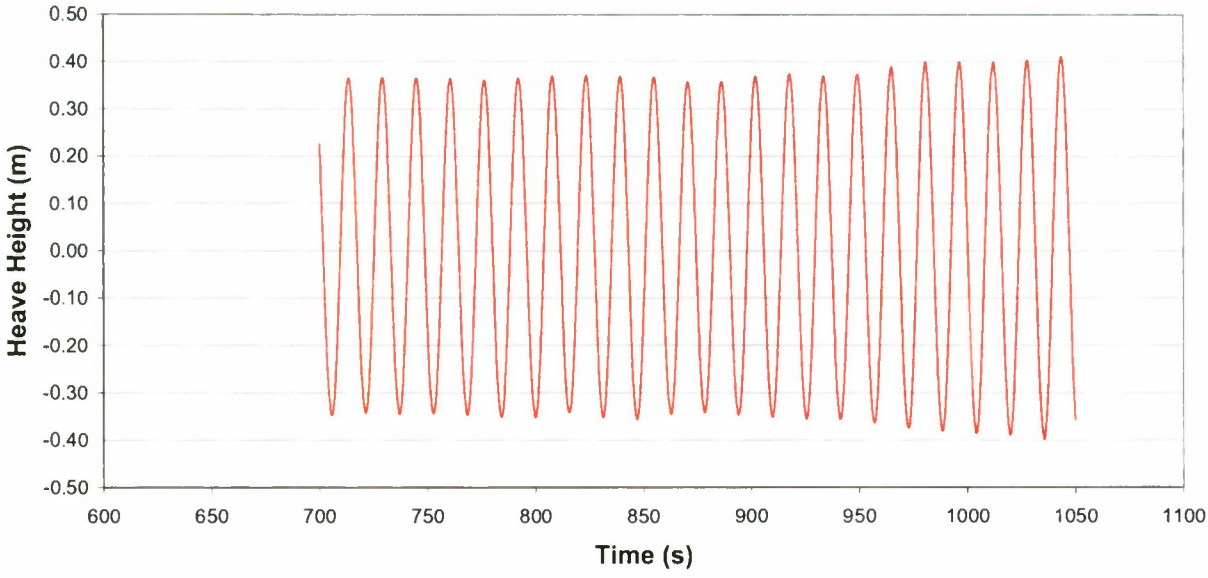

a. Heave

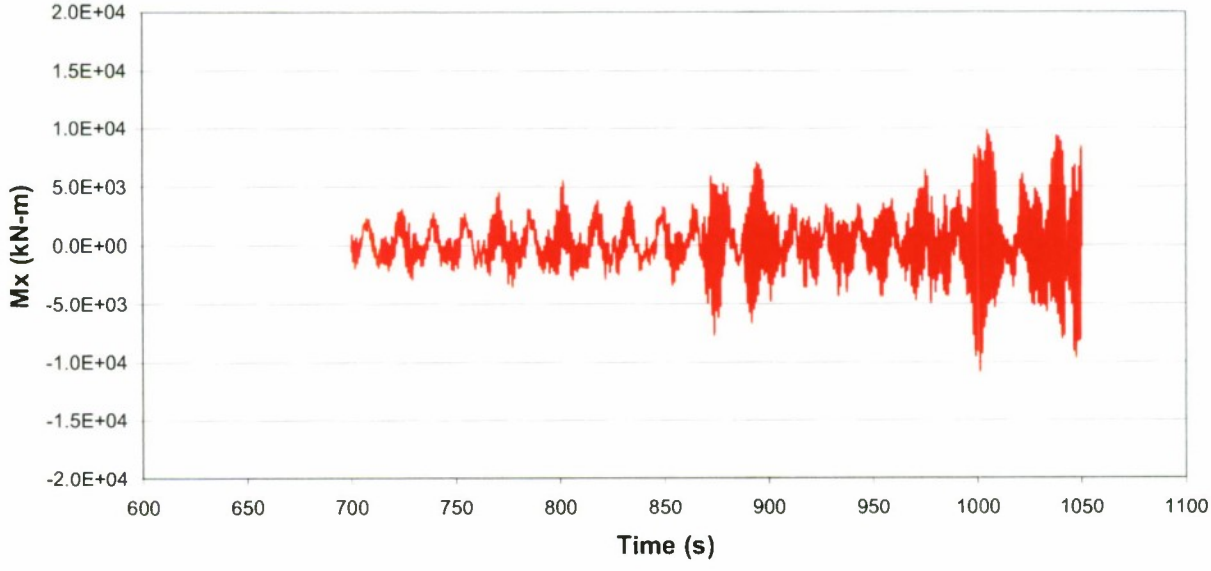

b. Roll Moment

Figure 6. Time Series for BOB HOPE at Zero Speed, 0° Heading, and 0.4 rad/s Wave Frequency

Table 7a. Uncertainty Estimates from Repeat Tests at 95 % Confidence Limit

		BOB HOPE				BOBO			
Quantity	Formula	Average	Std Dev	U95	U95 (%)	Average	Std Dev	U95	U95 (%)
Heave	H/σ	0.1224	0.0146	0.0331	27.1	0.3509	0.0148	0.0336	9.6
Pitch	α^*L/σ	2.6191	0.0407	0.0922	3.5	3.57	0.142	0.321	9.0
Surge	$Fx/\rho gL^2\sigma$	0.013111	0.000951	0.00215	16.4	0.006745	0.000329	0.000745	11.0
Sway	$Fy/\rho gL^2\sigma$	0.008061	0.000475	0.00107	13.3	0.00715	0.000360	0.000815	11.4
Roll	$Mx/\rho gL^3\sigma$	0.000267	1.96E-05	4.43E-05	16.6	0.000242	4.61E-05	0.000104	43.1
Yaw	$Mz/\rho gL^3\sigma$	0.003382	9.81E-05	0.000222	6.6	0.001129	2.73E-05	6.19E-05	5.5

Table 7b. Uncertainty Estimates from Repeat Tests at 95 % Confidence Limit, normalized in same manner as Percent Difference values for computational methods

		HOPE				BOBO			
Quantity	Units	Max	Std. Dev.	U95	U95%	Max	Std. Dev.	U95	U95%
Heave	m/m	0.820	0.01136	0.02568	3.13	0.990	0.00688	0.01554	1.57
Pitch	deg/m	0.660	0.01251	0.02826	4.28	0.790	0.01369	0.03093	3.91
Surge	kN/m	3907.62	84.50	190.97	4.89	3006.72	58.10	131.32	4.37
Sway	kN/m	7365.06	146.80	331.76	4.50	7067.98	100.18	226.41	3.20
Roll	(kNm)/m	37564.81	186.85	422.28	1.12	22498.54	302.13	682.81	3.03
Yaw	(kNm)/m	641320.5	15217.2	34390.9	5.36	330438.6	7535.16	17029.5	5.15

DESCRIPTION OF COMPUTATIONAL TOOLS

This section provides a general discussion of the computational methods used by the prediction codes in this study. All of the numerical methods employed by the computational hydrodynamic tools were based on potential flow theory and were either panel methods or used coefficients obtained from panel methods. Panel methods are the most practical tools currently available for predicting the motions of multiple ships in moderate seas. The methods differed in the type of singularity distributed on the panels and whether the panel methods solved the problem in the time domain or frequency domain. The types of methods used by the tools in this study to predict the response of two or more ships operating in a seaway can be grouped into the following categories:

1. Time domain tools based on externally computed impulse response functions
2. Time domain / frequency domain tools that are based on the zero-speed free surface Green's Function
3. Time domain Rankine panel methods
4. Frequency domain tools that are based on the zero speed free surface Green's function.

There are other types of computational methods that could be used to predict the motion of two or more ships in a seaway. Strip theory methods that are traditionally used

for single ship seakeeping predictions could also be applied for multiple ships, but it is very difficult for strip theory to capture the interactions between the two ships, and these methods would probably not be adequate for predicting the "wave shadowing" effect of one ship operating in the lee of another ship. Unsteady Reynolds Averaged Navier-Stokes (URANS) tools can be used for this problem as well. URANS codes are computationally intensive, and no URANS tools were examined as part of the current study. A URANS solution would require a computer with about twenty processors on the order of one week to complete a single two ship simulation. The University of Iowa has used their CFD-Ship URANS code to compute a limited subset of two ship model test cases examined in this study, and they have shown good correlation with MARIN model tests data for those runs[12].

Time domain tools based on externally computed impulse response functions

The first category of tools employ methods that perform a time domain simulation of the motions of two ships using force coefficients supplied as input to the program. The tools in this study that fall into this category are the CSC Multi-Vessel Simulator (MVS) and the BMT D&P Multiple Vessel Time Domain Simulator (MVTDS). These tools do not directly compute the hydrodynamic forces based on the geometry and relative position of the ships. The forces are obtained at each time step during the simulation from tables of coefficients and impulse response functions computed by other programs at a series of speeds and headings. To generate the tables of force coefficients, a few other programs are run prior to running the time domain simulation tool, and the output from these other programs is used to build the input files for the simulation tool. The total force on each ship at each time step is broken down into several component forces. These force components are:

- The steady interaction force. This is the force present on the two ships traveling at constant speed in calm water. It includes the "suction" force from the accelerated flow between the two ship hulls as well as forces which would change the draft and trim of the ship at constant forward speed. Either a steady flow panel method or Reynolds Averaged Navier-Stokes (RANS) method would be suitable for computing the steady flow interaction forces. For very low speeds (FN<0.1) even a method that treats the water surface as a flat rigid wall would provide a sufficiently accurate approximation for the suction force between the two ships. For running the MVS tool, CSC used the ShipFlow code marketed by Flowtech AB of Sweden for these calculations while NSWCCD used AEGIR.
- The wave induced forces. These include the wave exciting forces (composed of incident wave and diffraction components) and the radiation forces. They represent the largest unsteady force component for the simulations run to correlate with the model test data. The wave induced forces are computed by using a set of frequency domain added mass, damping and wave exciting force coefficients generated by a commercially available code such as WAMIT or FD-Waveload. These frequency domain coefficients are then transformed into tables of impulse response functions, which are interpolated and evaluated at each time step during the time domain simulation. It would also be possible to use a time domain panel method to compute the impulse response functions directly, but none of the codes used this approach.

- The maneuvering forces. These forces include the rudder and control surface forces as well as the steady and very low frequency hull motion forces. The maneuvering forces are difficult to predict directly from a numerical simulation so empirical methods are generally used. They are computed individually for each ship, so it is assumed in these methods that the presence of the other ship does not influence the maneuvering forces.

The user may choose which programs to use to compute the impulse response functions, maneuvering force coefficients and steady hull interaction forces. The MVS tool includes an intermediate processor program which can create input files for the MVS from the output files of programs used to compute the force coefficients. This intermediate processor was the only option available for building input for the MVS tool at the time of this study, however, and it required the use of FD-Waveload for the frequency domain seakeeping coefficients and AgileShip for the maneuvering forces.

As mentioned previously, the results of model tests were used for correlation in this study. During these tests, the two ship models were traveling at a constant speed with a fixed separation distance between them. For the simulations run to correlate with these model tests, the maneuvering force and steady interaction force will only change the mean force on each vessel, not the amplitude of the unsteady force. The correlation performed in this study compared the response amplitude operators obtained from the model test data with the values obtained from the simulations. Therefore, for the comparisons with the model test predictions shown in this report, the tools in this first category can do no better than the frequency domain tool used to generate the added mass, damping and wave exciting force coefficients.

Time domain / Frequency domain tools based on zero-speed free surface Green's Functions

The second category of tools are methods capable of predicting both the time domain and frequency domain response of one or more ships using a panel method based on the zero-speed Green's function. The tools in this category are actually very similar to those in the first category, except that the method for computing frequency domain seakeeping coefficients, the method for transforming the frequency domain coefficients into impulse response functions and the actual time domain simulation tool are all combined into a single software package. Note that the frequency domain tools used to generate the input files for codes that fall in the first category are also based on the zero-speed free surface Green's function. These are boundary element methods that are commonly referred to as "panel methods" since they represent the hulls with quadrilateral surface elements or "panels." A source distribution is placed on each panel, and the strengths of the sources are computed to satisfy the hull boundary condition. The term "zero-speed free surface Green's function" refers to the mathematical form of the source distribution on the panels, which for these methods automatically satisfies a linearized boundary condition on the water surface. As the name implies, the function assumes that the ships have zero forward speed. The effect of the steady forward speed of the ships is included through corrections to the zero-speed solution, which are typically referred to as "*m-terms*" (see Ogilvie 1969[13]). This approach gives acceptable results for forward speeds up to a Froude Number of about 0.4. Transient Green's functions exist that do not

assume zero-speed; however, these functions are more complicated than the zero-speed functions and require significantly more computational effort to evaluate. Only a few tools (TiMIT and Martec's TD-Waveload are examples) have been developed utilizing the transient Green's function, and none of the methods examined in the current study used the transient Green's function.

The tools in this category require the user to create a panel mesh to represent the ship hull geometry up to the static waterline. The geometry of the hull above the static waterline is ignored during the frequency domain calculations, and no panels are placed on the calm water surface. It is possible to partially account for the geometry above the static waterline in the time domain solution, by including the incident wave and hydrostatic pressure forces up to the incident wave surface at each time step. The tools in the current study that fall into this category are AQWA and ShipMo3D. These tools contain a separate program or module for computing the frequency domain coefficients and another program or module for computing the time domain simulation. At the time the tool evaluation was performed, the two ship version of ShipMo3D was only capable of performing frequency domain calculations, and time domain calculations could only be performed for a single ship in ShipMo3D. While time domain modules of AQWA are functional for two ships, only the frequency domain module was exercised for the present correlation study.

Time domain Rankine panel methods

The third category of tools is time domain Rankine panel methods. These are boundary element methods, similar to tools in the previous category, except these tools use simple source and/or dipole distributions on each panel that are called Rankine singularities. Rankine singularities do not automatically satisfy any boundary condition on the free surface. The singularities themselves are easier and faster to evaluate compared with free surface Green's functions, but the methods based on Rankine singularities require that panels be placed on the water surface in addition to the hull surface so that the boundary condition can be applied directly on the free surface. In contrast to the methods in the previous categories, these methods obtain a potential flow solution directly in the time domain, without first computing a set of frequency domain solutions over a range of frequencies. There are also no assumptions made by these methods concerning forward speed, so they are not limited to Froude Numbers below 0.4.

Generally these tools required more computational effort than the tools in the first two categories to complete the simulations required for the correlation study. More user expertise is required as well, because panel meshes must be generated on both the free surface as well as on the ship hulls. As these tools do not rely on the form of the singularity distribution to satisfy the free surface condition, different forms of the linearized free surface boundary condition (i.e. linearization about double body flow instead of free stream flow) or even non-linear boundary conditions can be applied. Incorporating modifications to the free surface boundary condition, as would be required to model a surface effect ship or air cushion vehicle, is also more straightforward in a Rankine panel method. The tools examined as part of the current study that are Rankine panel methods include LAMP-MULTI and AEGIR. Both of these tools include three options for specifying "body non-linearity", where increasing the level of non-linearity increases the computational effort. The option used most often with these tools is to compute "body-linear" (modeling the hull geometry only up to the static waterline) wave

radiation and damping forces and "body-nonlinear" (modeling the hull geometry up to the incident wave surface) incident wave and hydrostatic pressure forces. The main difference between LAMP-MULTI and AEGIR is that LAMP-MULTI uses flat quadrilateral panels with constant strength source distributions, whereas AEGIR does not use traditional "panels" but instead defines both the hull and free surface geometry and the singularity distribution with NURBS (Non-Uniform Rational B-Spline) surfaces.

Frequency domain tools based on the zero-speed free surface Green's function

In addition to the six tools described above, two purely frequency domain tools were also used during this study. They were used to generate input for the computational tools in the first category. These tools can be useful by themselves for predicting the statistics for the relative motions between two ships; however, they are limited to purely linear calculations. For multiple ship simulations any forces from mooring lines, fenders or thrusters used for dynamic positioning could only be included as equivalent linearized terms. Although the behavior of the hydrodynamic forces acting on two ships in a sea base are primarily linear, other external forces such as those from mooring lines and fenders or from dynamic positioning thrusters are quite non-linear. The two frequency domain tools used in this study were WAMIT and FD-Waveload. They are both based on the zero-speed free surface Green's function and are similar to the tools in the second category, except they do not include modules for computing a time domain solution. The WAMIT package includes a program for computing impulse response functions from the frequency domain coefficients but no module for computing the time domain response. WAMIT includes the option of using either traditional quadrilateral panels with a uniform source distribution on each panel, or using NURBS surfaces to describe both the geometry and singularity distribution in the same manner as AEGIR. WAMIT, however, is limited to zero-speed. FD-Waveload includes forward speed correction terms through the use of m-terms (see Ogilvie 1969[13]). Neither WAMIT nor FD-Waveload was officially included in the evaluation of tools for this report. However, WAMIT was run for several wave headings for the HOPE and BOBO with a 3m separation distance and zero forward speed and showed good correlation with the MARIN model test data for these conditions. FD-Waveload was run for all the correlation cases as this code was used to generate the input for the MVS and MVTDS simulation tools, and direct comparison of the FD-Waveload predictions with the model test results is included later in this report.

Overall Model Complexity, Computational Issues and Efficiency

Certain computation issues are common to all of the methods evaluated in this report. For example, all of the time domain methods require that a time step size be specified that is small enough such that a converged solution is obtained but not so small that the computational time required becomes burdensome. For the regular wave correlation studies in this report, care was also be taken to ensure the total time simulated was sufficiently long to perform the harmonic analysis and that the transient startup portion of the simulation was removed so that only the steady state response was analyzed. For simulations in irregular waves, even longer simulation times would be required to obtain meaningful statistics. All the methods require that the geometry of the ship hulls be defined with either a mesh of quadrilateral or triangular panels or using a NURBS surface. For the traditional panel methods, the sensitivity to the panel size must be examined to ensure a converged solution. The panel size and time step size required

are dependent on the geometry, speed, and sea spectrum. For instance, higher incident wave frequencies result in shorter wavelengths and wave periods, which in turn require a smaller panel size and time step size to resolve. For resolving the response accurately at high frequencies, the methods using NURBS surfaces for the geometry and singularity distribution have an advantage. However, in practice these methods have some issues as well, in that the surfaces taken from IGES files produced by CAD software typically need to be faired to remove some of the irregularities typical of NURBS surfaces produced by CAD software. Although the methods that use NURBS surfaces do not have a "panel size" in the traditional sense, the issue of choosing a converged spatial discretization still exists, as the user must specify the order of the B-Splines and the number of "knot intervals" in each direction along the NURBS surface.

Another complication that arises when examining multiple ships is the existence of resonant waves in the gap between the ships (see Newman 2004[14]). When the distance separating the ships is a multiple of half the wavelength of one of the wave components, (i.e. separation distances of ½λ, λ, 1½λ, 2λ,...) standing transverse waves can become "trapped" between the two ships. These waves and the forces associated with them can become unrealistically large in a potential flow prediction, and some artificial damping must be included to account for the viscous damping not included directly in the potential flow simulations. In the model tests used for the correlation in this report, the separation gap sizes examined were such that this resonant wave effect would only occur at wave frequencies greater than 1.0 radian/sec, and all the model tests were performed at wave frequencies lower than that. Although this effect did not directly influence the correlation study, care must be taken to account for viscous damping when analyzing the response of two ships in an irregular sea if the spectrum has significant energy at wave frequencies that would result in resonant waves in the gap.

The computational methods that rely on the zero-speed Greens' function require the user to take care to remove irregular frequency effects. These panel methods obtain a solution for the potential both external to the ship hulls and internal to the ship hulls. Although only the external potential is of interest, numerical solutions will be erroneous near the Dirichlet Eigen-frequencies of the interior domain bounded by the inner surface of the hull and the calm water plane inside the hull. This can lead to erroneous spikes in the predicted added mass and damping coefficients near these frequencies. Although these spikes are typically observed only at higher frequencies, their existence can still corrupt the computation of impulse response functions if they are not removed. The effects of irregular frequencies can be suppressed by placing a "lid" of panels on the calm water plane inside the hull and applying a special boundary condition there (see Lee et. al. 1996[15]), or by simply plotting the added mass and damping coefficients as a function of wave frequency and throwing out the solutions at the higher frequencies where spikes are observed. When computing impulse response functions from the frequency domain coefficients, an integral must be evaluated with the integration limits from zero to infinite frequency. Care must be taken such that a sufficient number of frequencies are computed to accurately evaluate this integral and that a sufficiently large frequency is used for the highest frequency where the numerical integration is truncated.

The Rankine panel methods require that the user create a separate panel mesh covering a portion of the water surface. The extent of the free water surface modeled, the length of the "numerical beach" required for damping out waves at the boundaries of the

domain, and the panel size used for the free surface mesh are all things that must be considered. The Rankine panel methods are very sensitive to the free surface paneling around blunt sterns such as that of the BOBO and to the "squeezed" mesh in the gap between the hulls. This sensitivity was noticed in both LAMP and AEGIR. When running a Rankine panel method, the user must visually observe the pressure distributions on the hull and the wave patterns on the free surface, to ensure that there are no pressure spikes on the hull or wave spikes on the free surface resulting from the panel mesh. These can occur when the aspect ratio of the free surface panels are too large, when some of the free panels become skewed as they bend to conform to the hull waterline, or when a free surface panel clips one of the hull panels. Unlike the hull mesh, reducing the panel size on the free surface is not always the solution. For codes such as LAMP-MULTI a pure convergence test cannot be performed to determine the free surface panel size, as reducing the size of the free surface panels beyond a certain point can lead to numerical instabilities. The automatic free surface generation features available in both LAMP-MULTI and AEGIR are satisfactory for many but not all cases, and a certain amount of user experience is required to determine when and how to modify the free surface mesh to obtain reliable solutions.

All the tools require the user to have some experience running hydrodynamics programs to obtain a reliable solution. None of the tools are at a stage where a user can simply set up the input and obtain time domain solutions for various conditions without first performing a convergence study and examining the output from the intermediate steps, such as examining the added mass and damping coefficients as a function of wave frequency for Green's function based methods or examining pressure distributions on the hull and wave elevations on the free surface for Rankine panel methods. For a new user to "come up to speed" running a code, the programs using the free surface Green's function may have a small edge in ease of use and required computational effort. These tools, which fall under categories 1 and 2, require the user to run a large number of frequency domain runs to build a database of coefficients, but after those coefficients are computed the time domain solution can be obtained very quickly. There are options available for improving the computational efficiency of the Rankine panel methods which bring them closer to the efficiency of the Green's function approach, such as using more efficient matrix solvers and using the Rankine panel methods to compute and store impulse response functions and then evaluating these functions during the time domain simulation.

For the evaluation of each code in this report, an attempt was made to create a set of common panel meshes for each ship, so that each tool would use the same panel mesh. This was intended to create a level playing field for all the tools, by removing the influence of panel mesh quality. To examine the influence of panel size, three different panel meshes were created for the BOBO and two different panel meshes were created for the HOPE. The three panel meshes for the BOBO used 482, 954 and 1538 panels on half of the hull and are shown in Figures 7, 8 and 9 respectively. The two meshes for the HOPE used 708 and 1461 panels on half of the hull and are shown in Figures 10 and 11 respectively. The HOPE model included a large skeg (see inset in Figure 10), which was included as part of the panel model, as it was felt the skeg would influence the sway forces and yaw and roll moments. The skeg was not included in the panel models developed at CSC for their MVS simulations or in the panel models created at SAIC for

their LAMP-MULTI simulations. WAMIT was used to examine the sensitivity of the solution to panel size for each ship run by itself at zero speed and at a wave heading of 135°. It was observed that even the coarsest grid produced a converged solution for the single ship cases in WAMIT. Figure 12 shows the convergence of the Heave RAO for the BOBO for the three meshes.

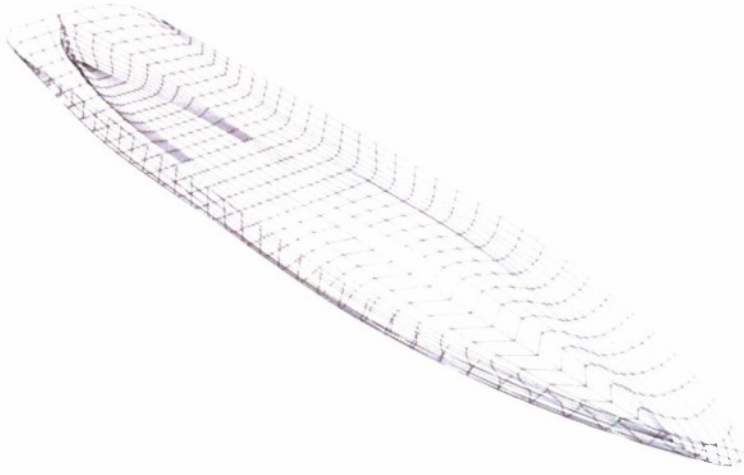

Figure 7. BOBO panel mesh with 482 panels on half of the hull

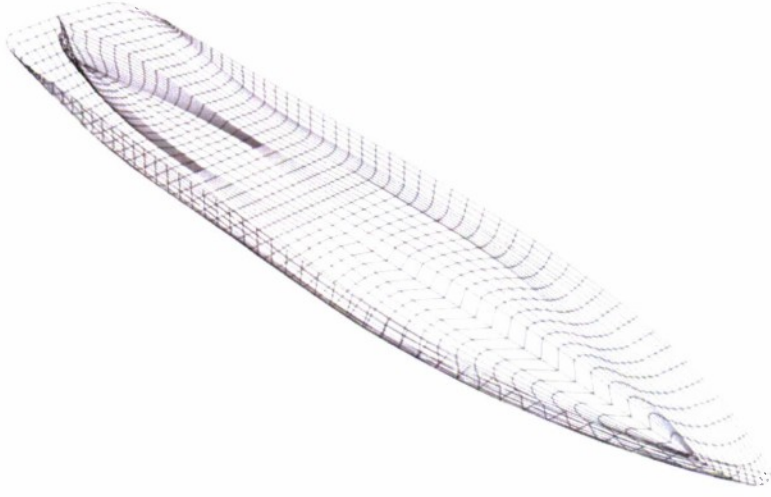

Figure 8. BOBO panel mesh with 954 panels on half of the hull

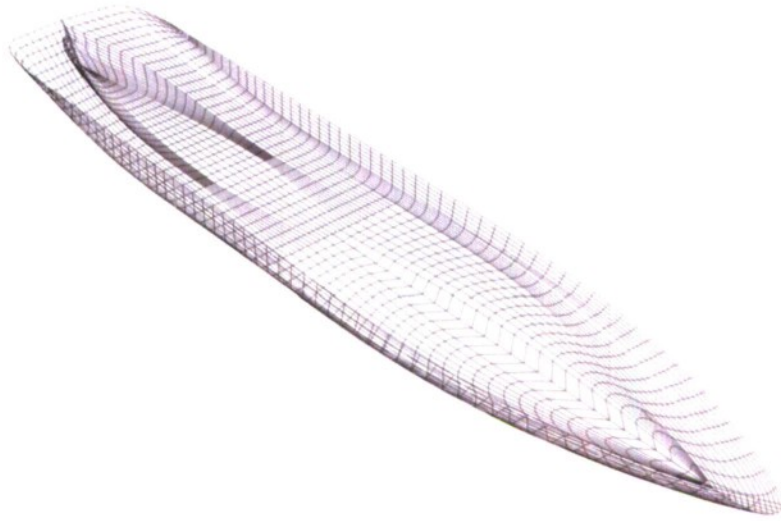

Figure 9. BOBO panel mesh with 1538 panels on half of the hull

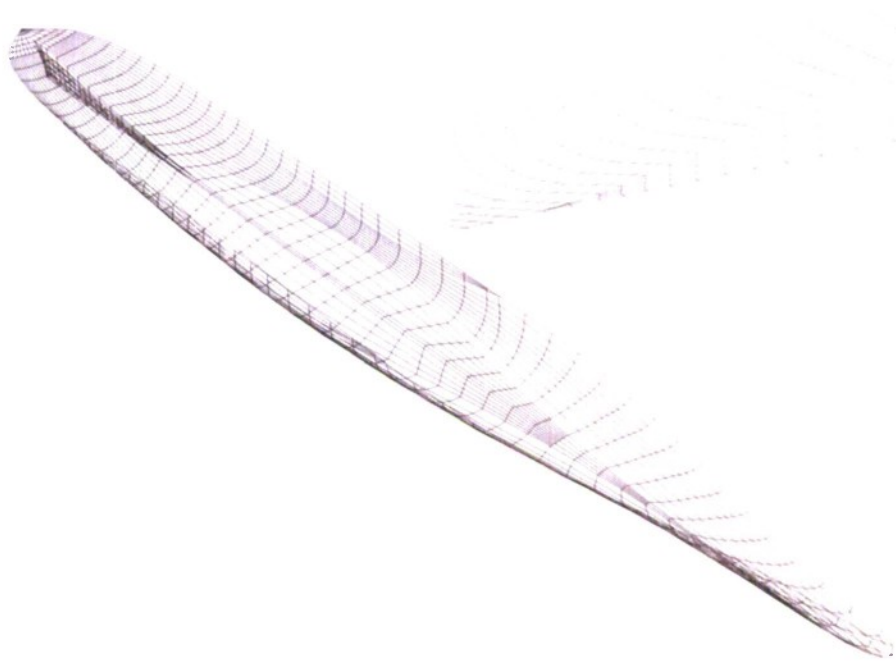

Figure 10. HOPE panel mesh with 708 panels on half of the hull

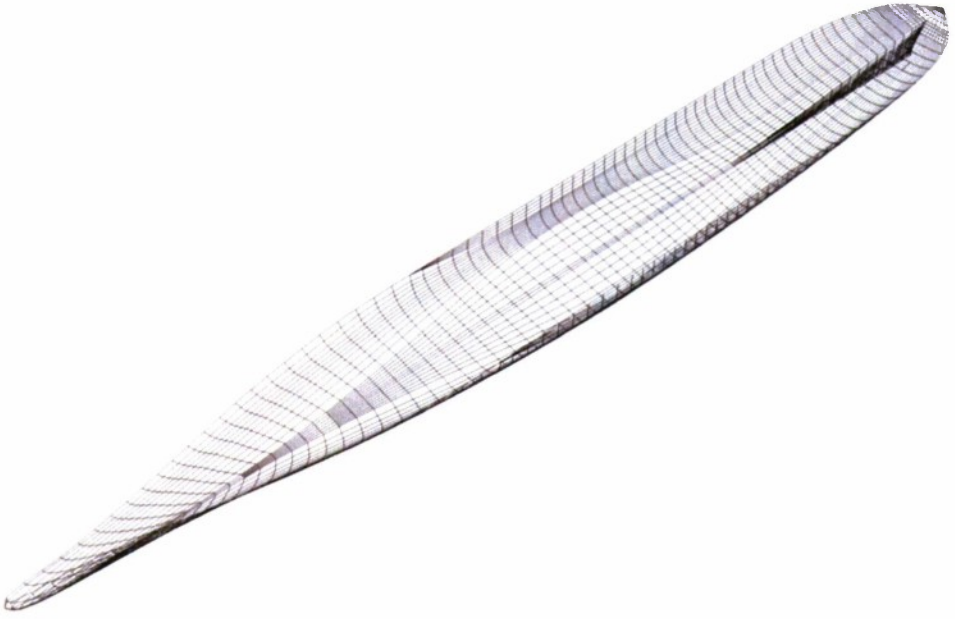

Figure 11. HOPE panel mesh with 1461 panels on half of the hull

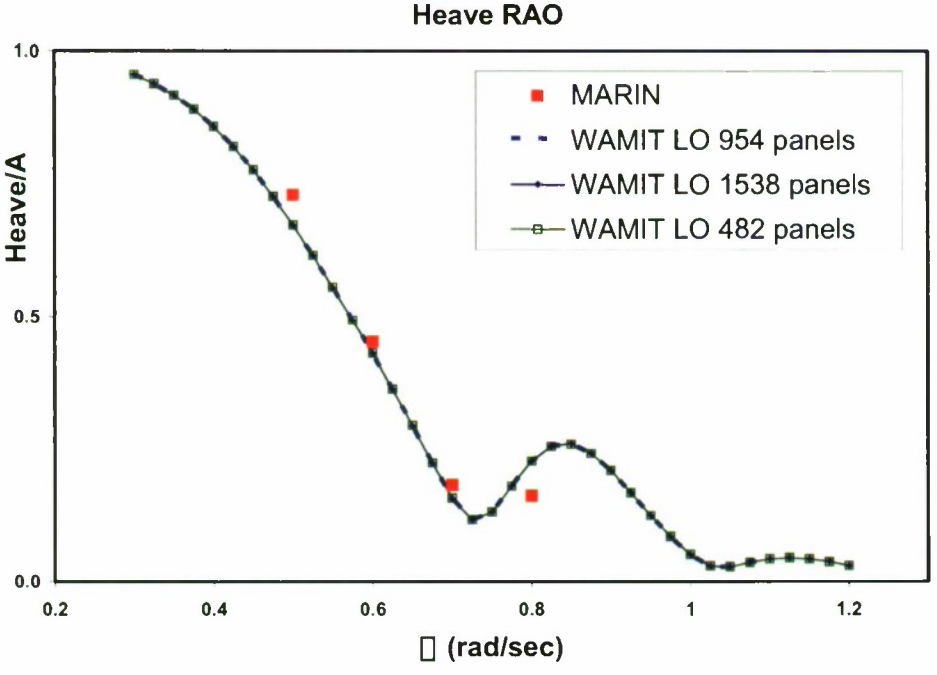

Figure 12. WAMIT convergence study for panel size on BOBO meshes

MULTI-VESSEL CODE CORRELATION WITH MODEL TEST

In the following sections each code being evaluated is briefly described, the input hull geometry is explained, and sample comparison plots of the output from each code with one model test condition are displayed. Each section concludes with a short qualitative comparison of the code output with the model test results. For this comparison, the range of the phase plots was extended beyond the conventional 360 degrees in order to make the plots continuous. With this type of display, it is easier to identify the trends of correlation of the phase relations.

CSC MULTI VESSEL SIMULATOR

The CSC MultiVessel Simulator (MVS) program was originally developed by Computer Sciences Corp Advanced Marine Center to support evaluation of the ONR High Capacity Along Side Sea Base Sustainment (HiCASS), now Large Vessel Interface Lift On Lift Off (LVI-LoLo) motion-compensated crane development program. It is now being used to support seabasing scenarios for the Maritime Pre-positioning Force (Future) (MPF(F)) office of NAVSEA. The MVS program combines calm water maneuvering forces, calm water ship interaction forces, and wave-induced motions of the two ships, which are obtained from frequency domain motions that are converted to Impulse Response Functions (IRF). The output of the program consists of time domain ship motions and forces and moments of the two ships.

Response Amplitude Operator Calculation

The MVS program combines the output from several computer programs to calculate the ship motions, forces and moments of the two ships as indicated in Figure 13. The calm water maneuvering forces and moments were calculated using the CSC AgileShip program, which uses empirical maneuvering force and moment coefficients. The calm water ship interaction forces were calculated using the AEGIR program, which determines the pressure field forces between the ships. In their running of the MVS program, CSC used a different program, ShipFlow, to calculate the calm water interaction forces between the ships. The wave-induced forces were calculated with the Martec FD-WaveLoad program. FD-WaveLoad is a linear frequency domain potential flow three dimensional panel code that is based on the zero-speed Green's function for multiple interacting ships and has a correction term to account for forward speed effects.

Initially, CSC used an undocumented complex method for generating input files for MVS using the output from the FD-WaveLoad and AgileShip programs. To improve the methodology of generating the input files, so that organizations outside of CSC could run MVS independently, CSC developed an input Intermediate Processor. This Intermediate Processor calculates the IRF for time domain ship motions from the FD-WaveLoad added mass and damping and wave excitation results. It also modifies the maneuvering forces and moments from the AgileShip results and calculates the wind forces and moments and roll damping moment coefficients.

The MultiVessel Simulator uses the Intermediate Processor and the ship interaction force results to calculate the time domain motions, forces and moments of both ships. Optionally mooring lines and fenders forces can be included in the calculation.

A Fourier analysis was then used to calculate the Response Amplitude Operator (RAO) amplitudes and phase angles from the ship motion time histories. It considered only the encounter frequency term for the steady regular waves.

Input Description

The AgileShip program version 5 requires the hull form, appendage and propeller descriptions, as well as the displacement and center of buoyancy.

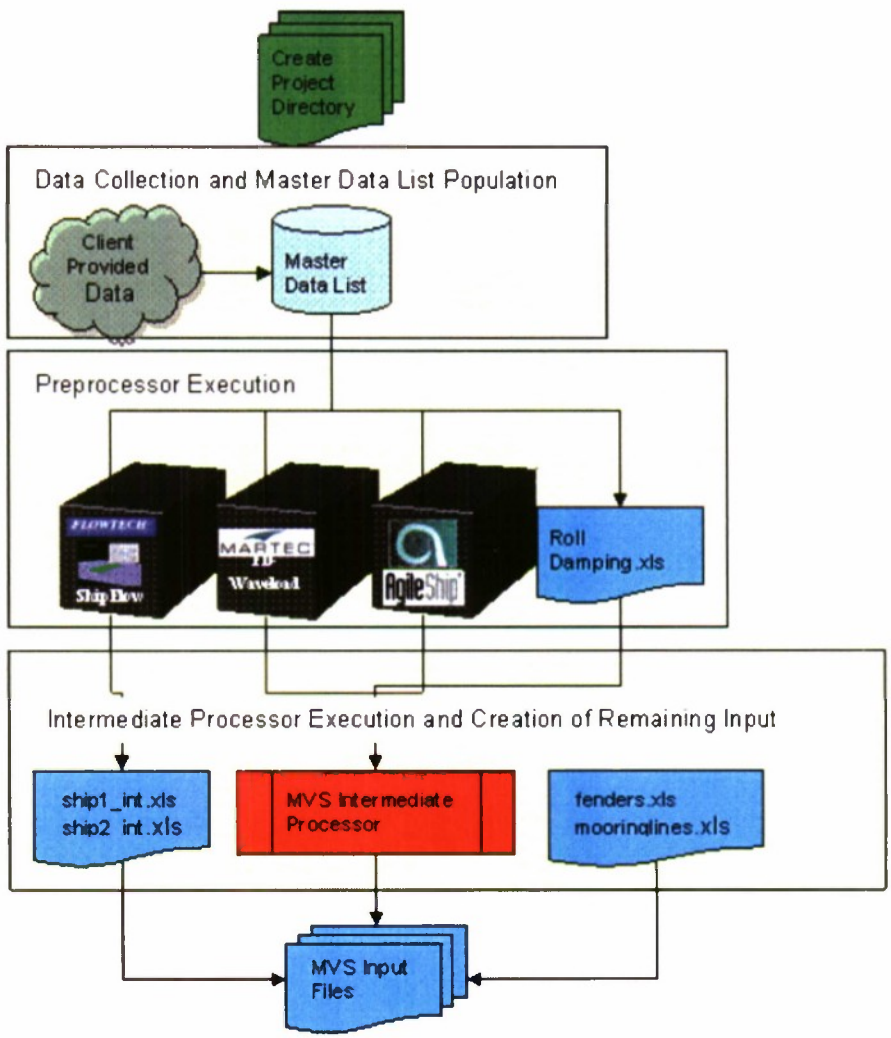

Figure 13. MultiVessel Simulator Input Process

The AEGIR program requires the hull form defined as NURBS surfaces, as well as the displacement and center of gravity. The resulting ship interaction forces and moments were required to be in a particular format for MVS.

The FD-WaveLoad program requires the hull form defined as a grid of panels, as well as the displacement, center of gravity, and gyradii. A specific set of ship speeds, headings and wave frequencies are required by the Intermediate Processor. The

Intermediate Processor version that was available for use requires that FD-WaveLoad version 2006A3 be used. The Heave and Pitch RAOs were found to be essentially the same for three hull panel densities for the BOBO hull form. The coarsest panel density for each hull was used for the final calculations as shown in Figure 14 below.

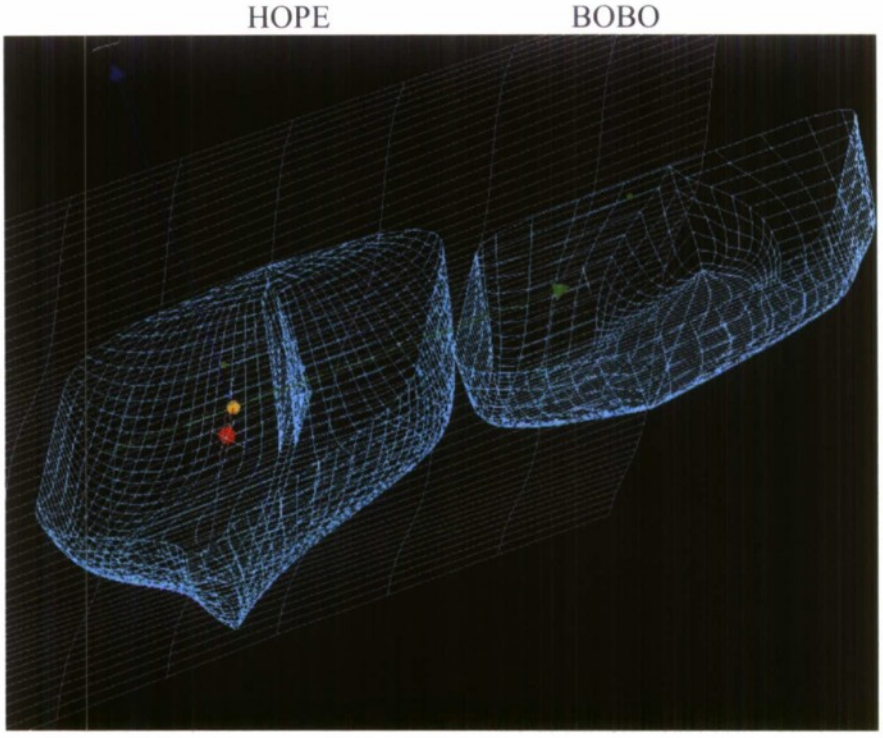

Figure 14. FD-WaveLoad Hull Panel Grids for HOPE and BOBO

The MVS Intermediate Proeessor uses the frequeney domain added mass, damping and wave exeiting results from FD-WaveLoad to ealeulate the impulse response funetions. Some ship geometry and load eondition parameters are used with the maneuvering eoeffieients from AgileShip to define the maneuvering forees. The ship's above water areas and the eenter of gravity are used to ealeulate the wind forees. The roll damping information is added to the ship motions data.

The MultiVessel Simulator requires the relative eenter of gravity position, ship speeds, sea conditions, current definitions, and simulation run preferences. Optionally data for defining the mooring lines and fenders forees can be ineluded in the ealeulations. The Fourier analysis uses the MVS ship motion time histories to ealeulate thc RAO amplitudes and phase angles.

RAO Amplitude and Phase Results and Observations

Plots of MVS predieted amplitude and phase of heave and piteh motion, surge and sway foree and yaw and roll moment RAOs for the 3-meter separation, 5 knots, 135-degree wave heading (bow seas) eondition are presented in Figures 15 through 18 along with the results of the MARIN tests. The plots for the remaining seven test eonditions are shown in Appendix A. Qualitatively eomparing the MVS RAO amplitude predietions versus the model tests, some trends are found. In general, the heave, piteh motions and

surge and sway force RAO amplitudes for the HOPE agree reasonably well with model test data, while the phases show larger scatter. The roll and yaw moment amplitudes for the HOPE have more scatter. The same is true for the BOBO, but the amplitudes, in general, do not follow the model test data as well as the HOPE. The RAO amplitudes are generally predicted more accurately than the phase angles. The phases for the BOBO results also show more scatter than those from the HOPE. The FD-WaveLoad heave and pitch results tend to be closer to the model data than the MVS results that are based on them.

CSC, independently, ran the same condition through MVS for their validation and verification (V&V) effort. The amplitudes of all the RAOs from the CSC V&V are also plotted in Figures 15 through 18 but the phases were not reported in this V&V effort so they could not be shown. The CSC V&V effort ran MVS without the use of the intermediate processor. The differences between these two results are noticeable but not substantial and generally bound the model test RAOs.

Additionally, the heave and pitch predictions from FD-WaveLoad are presented in Figure 15 for the HOPE and Figure 17 for the BOBO. The MVS Intermediate Processor requires the 2006 version of FD-WaveLoad, which does not calculate RAO values for forces or moments, That predicts the heave and pitch motion RAO values assuming the vessel is free to move in all six degrees of freedom. Therefore, only pitch and heave motions are displayed from FD-Waveload. The fact that the FD-Waveload predicted RAOs do not account for restricted degrees of freedom does not affect the IRF computed in the Intermediate Processor, as these are computed from the added mass, damping and wave exciting force coefficients. The MVS takes into account which degrees of freedom are free and fixed when evaluating the impulse response functions. The fact that the MARIN models were fixed in the modes other than heave and pitch should not have a large effect on the heave and pitch RAO values, since the vertical and lateral plane motions are not strongly coupled. It would be expected that the amplitude and phase of the pitch and heave motion predicted by the MVS would agree fairly closely with the FD-Waveload heave and pitch RAO predictions, as this is simply a matter of taking a frequency domain solution, computing IRF to compute a time domain solution, and then using harmonic analysis to recover the frequency domain values. However, this was not the case with the version of the MVS code that was evaluated for this study. CSC has identified this as a problem with MVS and has shown progress on correcting it since the completion of the current study. Both the MVS and the MVTDS code developed by D&P used IRF generated from FD-Waveload frequency domain coefficients, and both of those tools showed large discrepancies with RAO values obtained by FD-Waveload. Therefore this issue is discussed for both of these codes together at the end of the MVTDS section.

The results that are presented in Appendix A show trends that are similar to those noted above for this condition. It should be noted, however, that there are larger differences between the MVS results and the FD-Waveload results in comparison with the model test data for the 16.5 meter separation, particularly at the 180 degree heading.

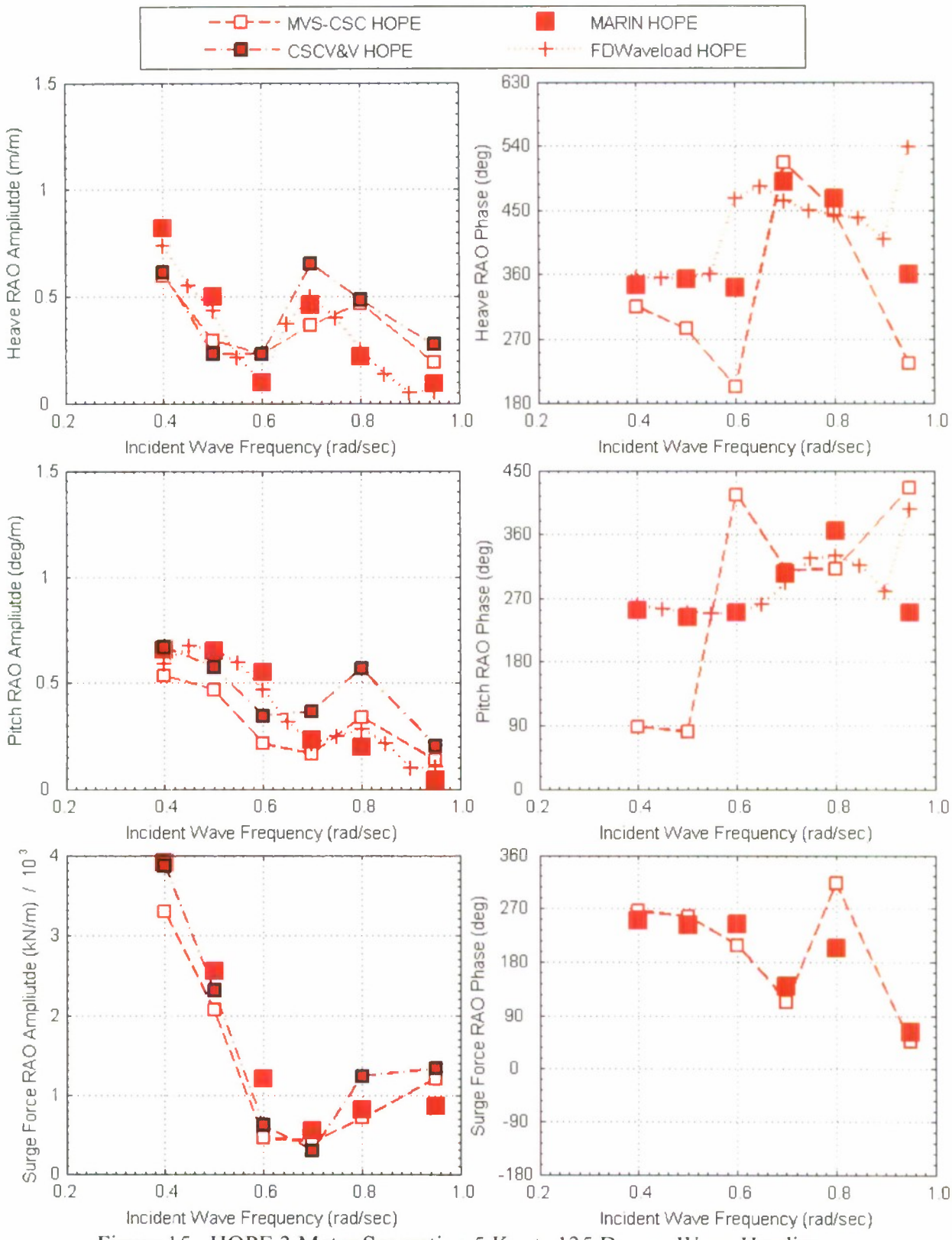

Figure 15. HOPE 3 Meter Separation 5 Knots 135 Degree Wave Heading

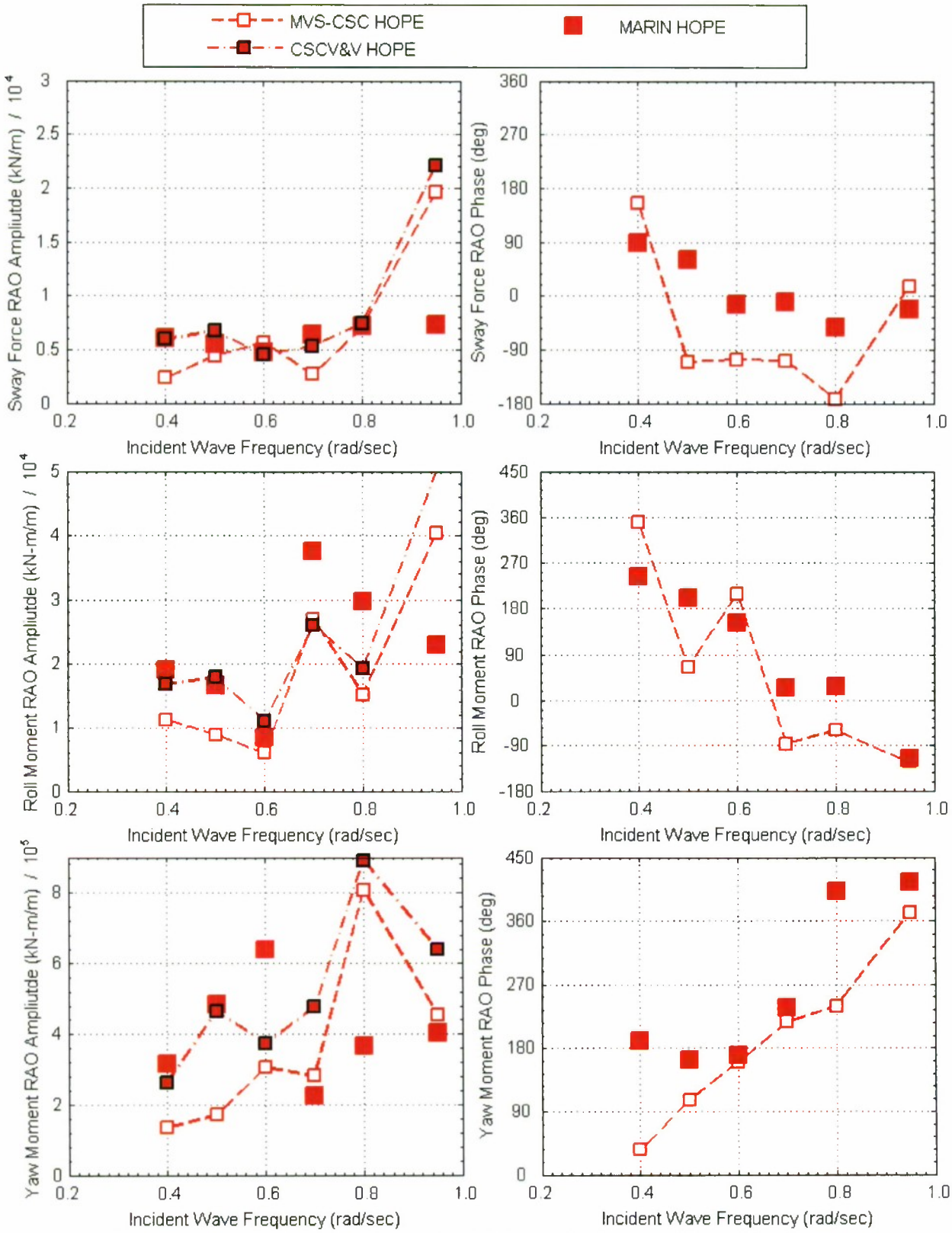

Figure 16. HOPE 3 Meter Separation 5 Knots 135 Degree Wave Heading

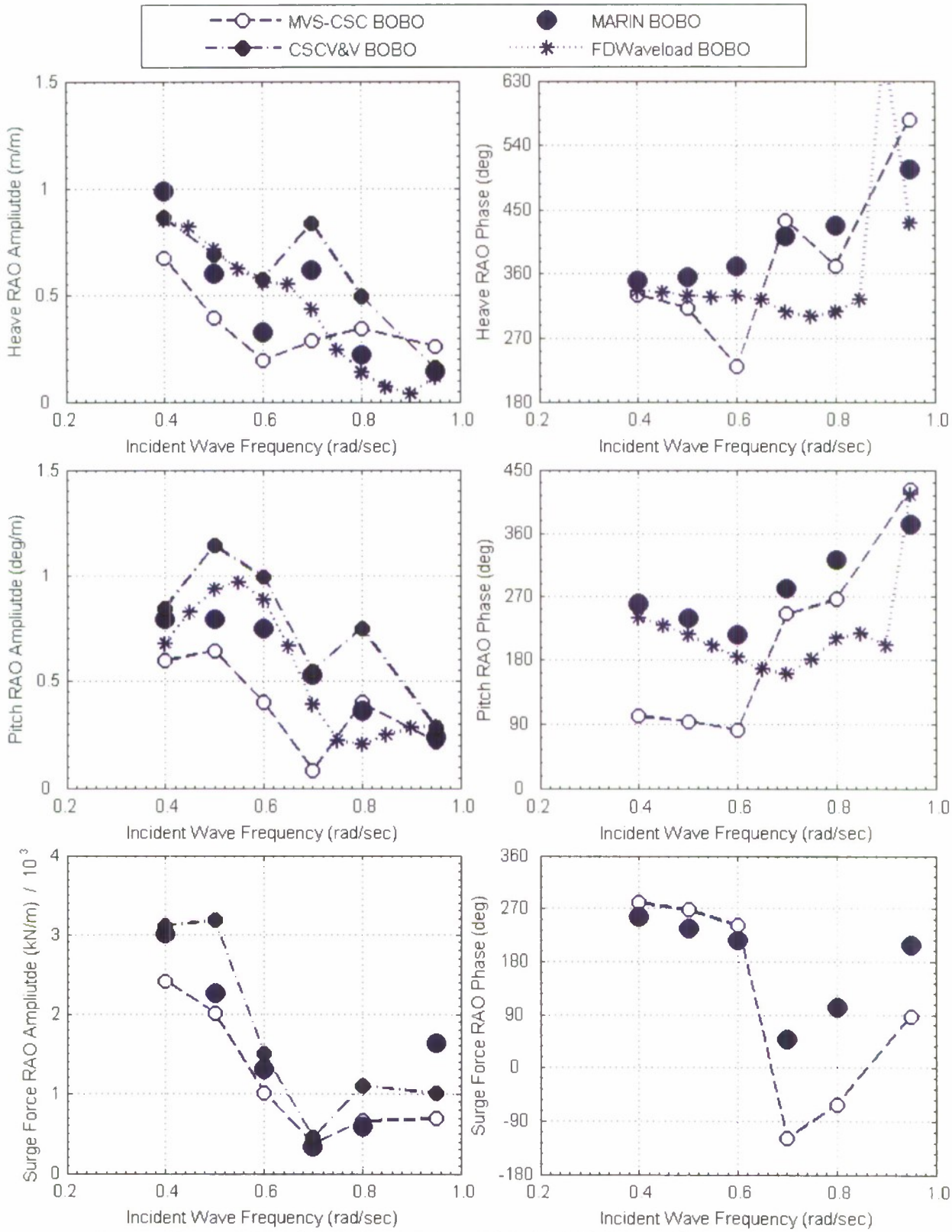

Figure 17. BOBO 3 Meter Separation 5 Knots 135 Degree Wave Heading

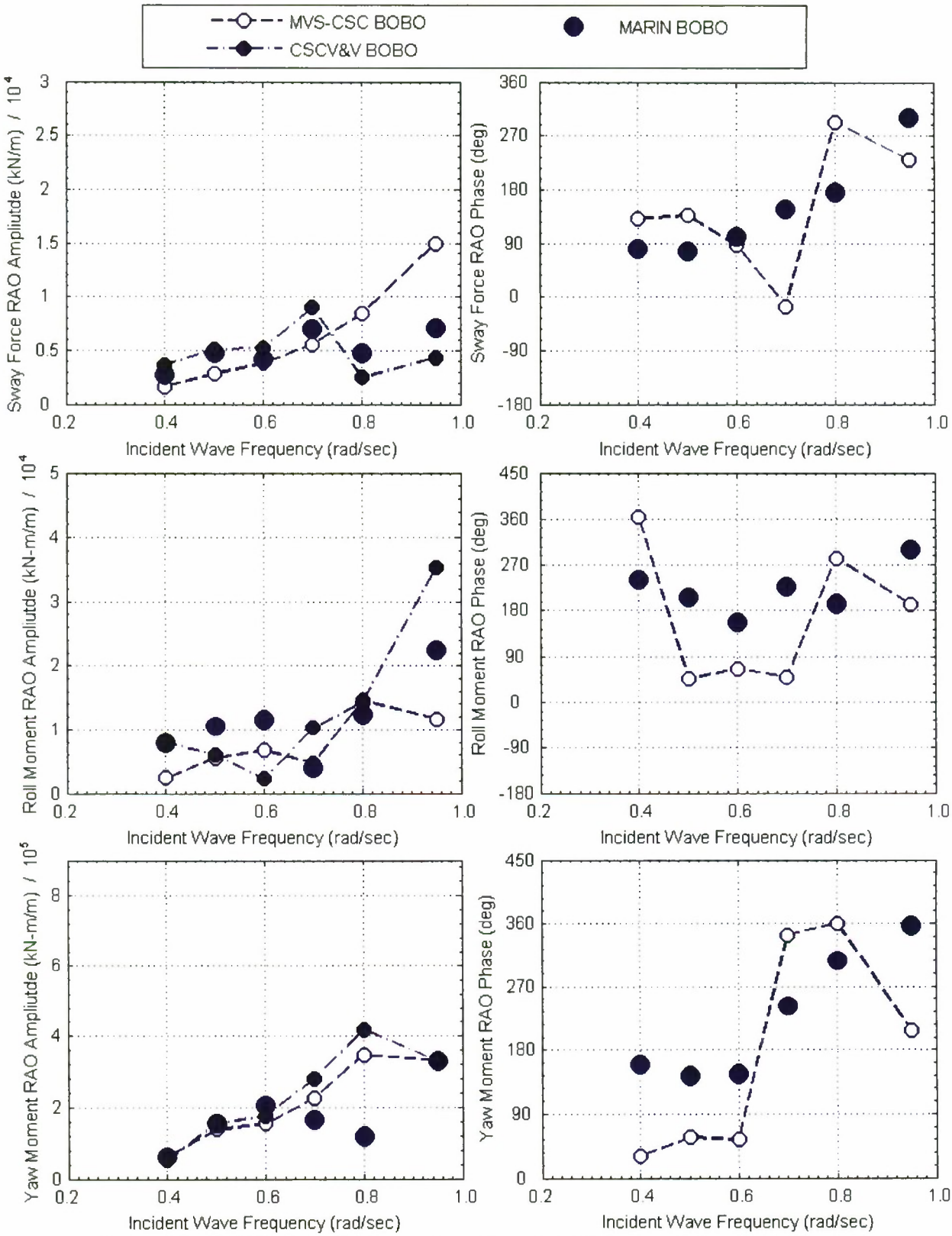

Figure 18. BOBO 3 Meter Separation 5 Knots 135 Degree Wave Heading

DESIGNERS AND PLANNERS MULTIPLE VESSEL TIME DOMAIN SIMULATOR

The Multiple Vessel Time Domain Simulator (MVTDS) was developed at Designers and Planners to support ONR projects requiring multiple vessel seakeeping predictions such as the Interface Ramp Technology (IRT) project. The MVTDS is a time domain simulation tool that obtains the forces on each ship at each time step from coefficients supplied as input to the program. The total force on each ship is computed as the sum of component forces such as the wave exciting, radiation and damping forces, the steady interactions forces, maneuvering forces, and any non-hydrodynamic forces such as those from mooring lines and fenders. The coefficients used to compute the component forces are obtained by running other available tools that are appropriate for each force component. The method allows for some flexibility in terms of which force components are included and which commercial tools are used to compute the coefficients required for input. The D&P MVTDS approach is very similar to the approach used by the MVS code developed at CSC. The main difference between the MVTDS and MVS codes is that MVTDS uses a built in maneuvering model based on the work of Kijima (2003)[16], whereas the MVS uses the CSC AgileShip program to compute maneuvering forces. Other differences are that MVTDS is written in C and includes the capability to simulate more than two vessels. The version of MVTDS that was delivered to NSWCCD was a custom version of the code that was hardwired to simulate the MARIN model tests with two vessels fixed in all modes except heave and pitch. The maneuvering forces and ability to include forces from mooring lines and fenders are not included in this custom version of the code. The delivered code contained only the parts needed to simulate the MARIN model tests so that the code could be correlated with the model test data.

Input Description and Response Amplitude Operator Calculation

The input for MVTDS consists of a series of ASCII text files containing the coefficients required to obtain the component forces on each ship at each time step along with an overall control input file to specify the relative position and velocity of the ships. Separate input files are used for the tables of coefficients for each force component. For the custom version of MVTDS delivered to NSWCCD for correlation with the MARIN model tests, input files were required containing impulse response functions (IRF) for the wave exciting forces and radiation forces along with files containing tables of the infinite frequency added masses, the restoring force coefficients and the steady interaction forces. The format of the input files for the MVTDS is nearly identical to that for the MVS code developed at CSC. For both of these tools, the tables of IRF and steady interaction forces are provided for a matrix of ship speeds and relative positions, and the values are interpolated based on the input speed and relative positions of the two vessels. D&P does not have an intermediate processor to generate the input files containing the impulse response functions directly from the FD-Waveload output files. Internally D&P used a combination of MatLab programs and Excel spreadsheets to generate the input for the simulations they performed using the MVTDS. This procedure was not documented and could not be transferred for use by NSWCCD. While, it would have been possible to create a program at NSWCCD to compute IRF from the FD-Waveload coefficients and build input files in the proper format for the MVTDS, doing so would have required a level of effort that was beyond the scope of the code evaluation effort. Guidance from

D&P suggested using the input files produced by the CSC Intermediate Processor. Therefore, the input files for the MVTDS containing the IRF tables and added mass and restoring force coefficients were generated by taking the MVS input files produced by the CSC Intermediate Processor, and making some minor modifications to these files so that they were formatted correctly for MVTDS. The input files containing the steady interaction forces were generated manually based on a series of steady flow AEGIR simulations of the two ships traveling next to each other in calm water.

One of the difficulties in verifying the correctness of the input files for the MVTDS concerns inconsistencies in the coordinates systems used by the MVTDS and the separate programs used to generate the input coefficients. For instance FD-Waveload uses a coordinate system with the z-axis positive upwards, while in MVTDS the z-axis points downwards. For the wave-exciting force IRF this transformation is done within the MVTDS, so the input file with the wave exciting force impulse response functions must be generated assuming z is positive upwards. However, this is not the case with the radiation force IRF, and the input file with the radiation force impulse response functions must be generated assuming z is positive downwards. It was believed that this is consistent with the coordinate system definitions output from CSC Intermediate Processor; however, this could not be definitively verified as the coordinate systems were not clearly defined in the program documentation for the CSC Intermediate Processor.

The MVTDS was used to perform a series of regular wave simulations corresponding to the regular wave model tests performed at MARIN. The outputs from the MVTDS consists of two text files containing the time histories of the heave and pitch motions of each ship and the force and moment histories of each ship for the surge, sway, roll and yaw modes. The RAOs were computed from the time histories using MatLab.

MVTDS RAO Amplitude and Phase Results and Observations

Plots showing the MVTDS predictions for the RAO amplitude and phase are shown in Figures 19 and 20 for the case of the HOPE and BOBO separated by 3 meters, traveling at 5 knots with a wave heading of 135° (bow quartering seas). The MVTDS predictions are compared with both the MARIN test results and the FD-Waveload predictions. Figure 19 shows the correlation for the heave and pitch motions and the surge force. Figure 20 shows the correlation for the sway force and yaw and roll moments. The correlation for the other speeds, headings, and separation distances are shown in Appendix B. The plots in Appendix B also include the comparison with the FD-Waveload predictions. The 2007A1 version of FD-Waveload was used to compute the RAO values shown in Figures 19 and 20 and in Appendix B, while the 2006A3 version was used to compute the added mass, damping and wave exciting force coefficients used to compute the IRF for the input files. The added mass, damping and wave exciting forces predicted by the 2006 and 2007 versions of FD-Waveload are nearly identical, but the 2007 version is needed to compute the RAO values with the ships free to heave and pitch but fixed in all other modes.

MVTDS obtains a time domain solution using impulse response functions computed from the added mass, damping and wave exciting force coefficients, which are computed by FD-Waveload. Other forces can also be added to the wave induced forces at each time step, but the only additional force included in NSWCCD's custom version MVTDS is the steady interaction force, which will only influence the mean value of the

total force and will have no effect on the amplitude of the unsteady forces or motions. The RAO amplitude and phase values are obtained from the MVTDS time domain solution. Within FD-Waveload, the added mass, damping and wave exciting forces are used to solve the frequency domain equations of motion to compute the RAO amplitude and phase values. In theory, the values obtained from both approaches should be very close as they are based on the same force coefficients. Therefore, a direct comparison between the MVTDS values and the FD-Waveload values is shown to verify whether the input for MVTDS was generated correctly and whether the MVTDS is computing the time domain response correctly.

As mentioned above, the CSC Intermediate Processor was used to compute the impulse response function tables used for both the D&P MVTDS and the CSC MVS codes. As both tools use a very similar approach to evaluate the IRF to obtain forces at each time step and produce a time domain response, one would expect that the RAO values predicted by these two tools would agree with each other fairly closely. Even if the IRF were computed incorrectly by the CSC Intermediate Processor, it would be expected that the two codes would produce the same incorrect time response. Figure 21 shows comparisons of the heave amplitude RAO values predicted by MVTDS, MVS and FD-Waveload for the 5 knot, 3m separation, 135° heading case. It can be seen that for this case there are significant differences between the MVTDS and MVS solutions and neither code agrees with the FD-Waveload solution. The FD-Waveload values correlate very well for the HOPE and reasonably well for the BOBO. Overall the correlation between FD-Waveload and the MARIN model test data is reasonable and similar to that seen for AQWA and ShipMo3D. This raises two questions which will be addressed in the remainder of this section: (1) Why are there large discrepancies between the time domain solutions from MVS and MVTDS, when both tools use the same impulse response function tables? and (2) What is the cause of the differences between the FD-Waveload predicted RAO values and the values computed from the MVTDS and MVS time domain solutions?

Examining first the discrepancies between the MVS and MVTDS solutions, the most likely cause is inconsistencies in the coordinate systems used when defining the impulse response functions (IRF). As mentioned above, the MVTDS input files require the radiation force IRF to be specified assuming z positive upwards, while the wave exciting force IRF must be specified assuming that z is positive downwards. Plots were generated of the IRF produced by the CSC Intermediate Processor to verify that the column order and direction were specified correctly. Determination of the compatibility of the column order and coordinate system could be discerned from some plots of the IRF, but not definitively for all of the IRF tables. An incorrect coordinate system in just one of the IRF tables could lead to large errors in the predicted time domain response. Other possible causes for the discrepancy include errors in the interpolation or evaluation of the IRF in one of the two codes.

There are several possible explanations for the discrepancies between the RAO values computed directly in the frequency domain in FD-Waveload and the RAO values obtained from the time domain analysis. These are discussed below.

Interpolation of Impulse Response Functions

One source of error could be the interpolation of the IRF with respect to speed and heading. For the cases examined in Figures 19 and 20, the matrix of FD-Waveload simulations performed to generate the input for the CSC Intermediate Processor included speeds of 0, 3 and 6 knots and wave headings spaced every 30° (runs were performed at wave headings of 180°, 150°, 120°, etc). The IRF input tables were then produced at those speeds and headings. The speeds and headings at which the IRF are computed are hard wired in the CSC Intermediate Processor. To obtain the wave exciting force impulse response functions for a wave heading of 135° at 5 knots the MVTDS or MVS must interpolate for both the speed and wave heading (essentially averaging the IRF computed at 120° and 150°). The radiation force IRF are independent of wave heading, so the interpolation must only be performed for speed. The interpolation based on speed is not likely to have a significant effect at the lower speeds, as the dependence of the coefficients on speed is small, and in fact there is little difference between the RAO values computed at 0 and 5 knots. The dependence of the wave exciting force on wave heading may result in a more noticeable error and perhaps a 15° heading spacing would be an improvement, but this error is likely small compared with the total difference between the solutions and can not fully explain the discrepancy. A large discrepancy is present even in cases where the time domain solution is obtained at one of the headings at which the IRF are specified (see for instance figures B1 and B2 in Appendix B, which show the 3m separation, 5 knot case at a wave heading of 180°).

Accuracy of Impulse Response Function Calculations

This section discusses the factors that influence the accuracy of the calculation of IRF from frequency domain coefficients and the accuracy of the time domain forces calculated by evaluating IRF . The discussion applies not only to the MVS and MVTDS codes, but is also relevant to codes such as AQWA-NAUT, which obtains a time domain solution in AQWA based on AQWA-LINE frequency domain coefficients, and to future versions of ShipMo3D which will use a similar approach.

The calculation of the IRF from the frequency domain coefficients involves evaluating an integral involving the added mass, damping or wave exciting force coefficients over a range of frequencies extending to infinite frequency. For example the formula for the radiation force impulse response function can be expressed in terms of either the frequency-dependent added mass or damping coefficients:

$$K_{ij}(t) = \frac{2}{\pi}\int_0^\infty \left[B_{ij}(\omega) - B_{ij}(\infty)\right]\cos(\omega t)d\omega = \frac{2\omega}{\pi}\int_0^\infty \left[A_{ij}(\omega) - A_{ij}(\infty)\right]\sin(\omega t)d\omega \quad (12)$$

where K_{ij} is the radiation force impulse response function, B_{ij} is the frequency-dependent damping coefficient and A_{ij} is the frequency dependent added mass coefficient. Then during the time domain solution the radiation force is evaluated as:

$$F_i(t) = \sum_{j=1}^{6}\left[-A_{ij\infty}\ddot{x}_j - B_{ij\infty}\dot{x}_j - \int_{-\infty}^{t} K_{ij}(t-\tau)\dot{x}_j(\tau)d\tau\right] \quad (13)$$

The formulae for the wave exciting force IRF are similar, but are also dependent on wave heading and use the wave exciting force frequency domain coefficients instead of added mass and damping coefficients. Numerically it is not possible to carry the integration

out to infinity so the integral must bc truncated at some finite frequeney. Also the frequency domain coefficients are computed at a discrete number of frequcncies and the number and spacing of the frequencies at which thesc coefficients are computed can influence thc accuracy of the IRF calculations.

In order to bettcr understand the process of obtaining a time domain solution from frequency domain eoefficients, Professor J. Nieholas Newman was asked to provide a tutorial on the process for NSWCCD. The tutorial was based on the WAMIT code and a module included with WAMIT called F2T, whieh computes impulse response functions. The case studied with WAMIT looked at both the HOPE and BOBO and two half ellipsoids with the length, beam and draft equal to that of the HOPE and BOBO. For the tutorial, a separation distance of 32 meters between the vessels was used and the speed was zero knots, as WAMIT does not include forward speed. For the ease of the two half ellipsoids, heave and pitch RAO values were computed from the time domain and then compare with those RAO values that were computed in the frequency domain. The two RAO values agreed to within about 1% of the each other. In the study, the influence of frequency spacing, removal of irregular frequeneies, and truneation frequency were examined. To study the influence of truneation frequency, the IRF were computed twice using a truneation frequency of 2.0 rad/sec and 4.0 rad/sec. No significant differences were found between the IRF so it was determined that a truncation frequency of 2.0 rad/sec is adequatc. The influence of removing irregular frequencies using a "lid" of panels in the panel method calculations was also examined by computing the IRF both with and without the removal of irregular frequeneies. No notieeable differenees in the IRF were observed, which indicated that irregular frequency effects are not significant for this particular problem in WAMIT. To examine the influenee of frequeney spaeing the IRF were eomputed using a frequency spacing of 0.01 rad/sec and 0.005 rad/sec and the IRF computed with both frequency spacings were eompared. It was determined that the 0.01 rad/sec spacing was adequate for surge, heave, pitch, and yaw, but that the smallcr frequency spaeing of 0.005 was important for the sway and roll.

The frequencies used to eompute the IRF using the CSC Intermediate Processor were hardwired and could not bc adjusted by the user. A frequency spacing of 0.15 rad/sec was required starting with an initial frequency of 0.1 rad/sec up to a truneation frequency of 2.95 rad/sec. Thc study using WAMIT indicates that the truneation frequency of 2.95 rad/sec should be adequate, but the frequency spacing is very eoarse compared with what was used in the tutorial. The coarse frequency spaeing used by the CSC Intermediate Processor is probably not adequate to obtain an accurate answer over the range of frequeneies examincd. However, even with this eoarse frequency spacing, thc time domain solution based on the IRF should match the frequency domain solution at the 0.4 and 0.7 wave frequeneies, since FD-Waveload ealeulations were performed to gencrate the input at these frequencies. Therefore, while the coarse frequency spacing may contribute to the discrepancies between the time domain and frequency domain RAO values seen in the correlation, it does not fully explain the discrepancy, as there are large differences between the FD-Waveload RAO values and those computed from MVS and MVTDS even at the wave frequencies specifically used to compute the IRF.

In the process of revamping the MVS code to inelude dynamie positioning forces, CSC ereated a new version of the MVS and Intermediate Processor that has addressed these issues, and they have demonstrated with some of their own ealeulations that they

now reproduce the RAO values computed by FD-Waveload fairly well. However, the new code was developed after the completion of the NSWCCD correlation study. Designers and Planners have also provided NSWCCD with calculation results from MVTDS for the HOPE and Mighty Servant 3, which demonstrate that using their internal method for building the input IRF tables, they are able to achieve a reasonable agreement between the RAO values obtained from the predicted time domain response and the FD-Waveload frequency domain values. For simulation tools that rely on impulse response functions computed from frequency domain coefficients obtained by other tools, the pre-processor program that computes the impulse response function is an important part of the calculation. This preprocessor influences the correlation of the tool at least as much if not more than the time domain simulation code itself. Therefore it is felt that a preprocessor tool to compute IRF must be included as part of the software package for this type of tool if a worthwhile correlation of the tool is to be performed.

It does not make sense to discuss in detail the quality of the correlation between the MVTDS predictions and the MARIN model test results, since it is not clear whether the impulse response function tables used as input were set up correctly and no tool was provided to generate IRF tables specifically for the MVTDS. The FD-Waveload comparison provides an indication of the best possible correlation that the MVS and MVTDS codes could achieve using the FD-Waveload solution as input. For both tools there will be some additional errors from the interpolation of component force coefficients with respect to heading, speed and relative position of the two vessels as well as from the computation and evaluation of the IRF. With care these sources of error can be minimized and a level of accuracy close to that from the direct FD-Waveload solution should be achievable. For this reason a direct correlation of FD-Waveload with the MARIN model test data is also included in this report. The time domain simulation tools can then allow nonlinear forces from mooring lines, fenders, dynamic positioning systems, etc. to be included so that many practical real world problems can be examined.

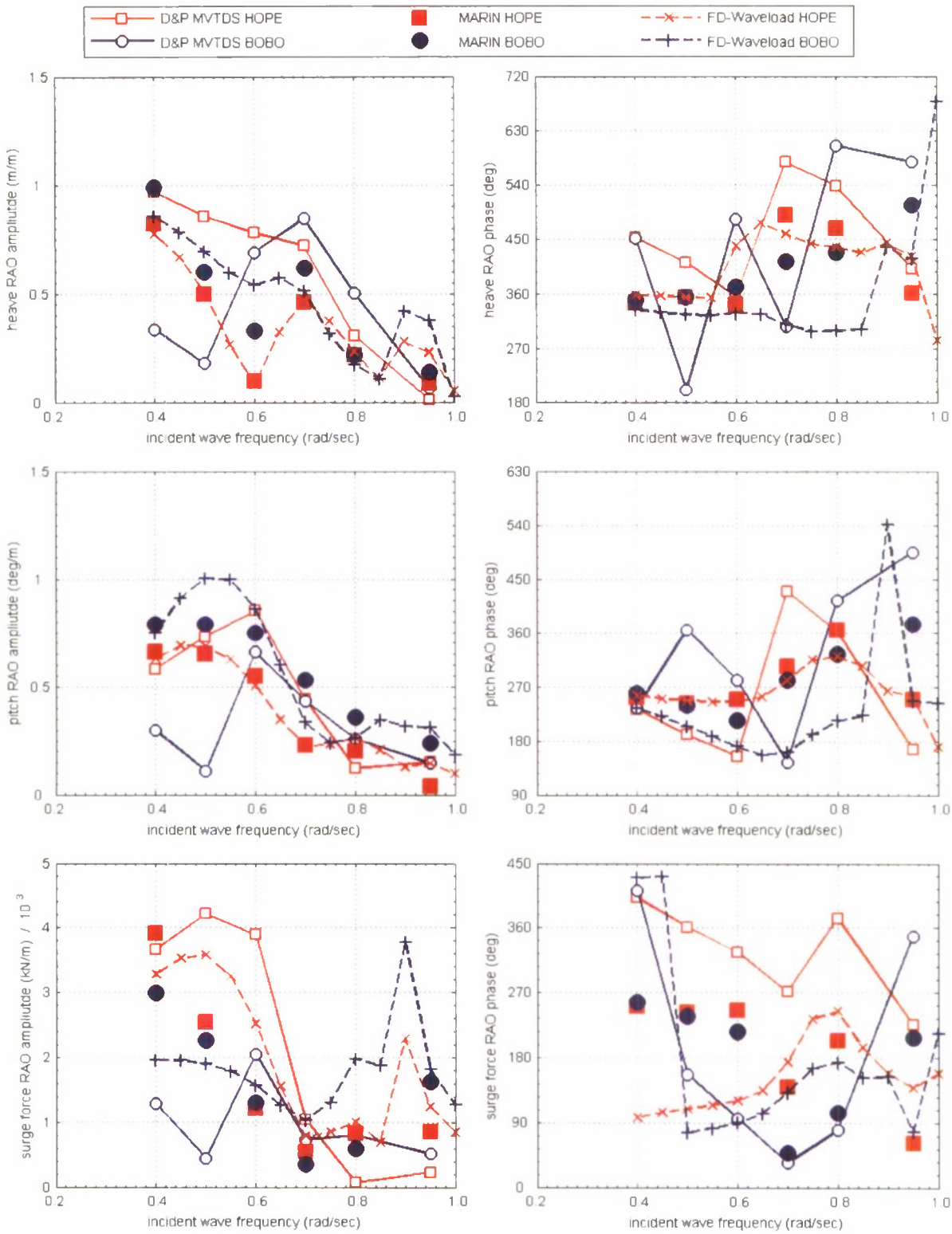

Figure 19. Heave, piteh and surge force RAOs for 3 meter separation, 135 degree wave heading, and 5 knots ship speed.

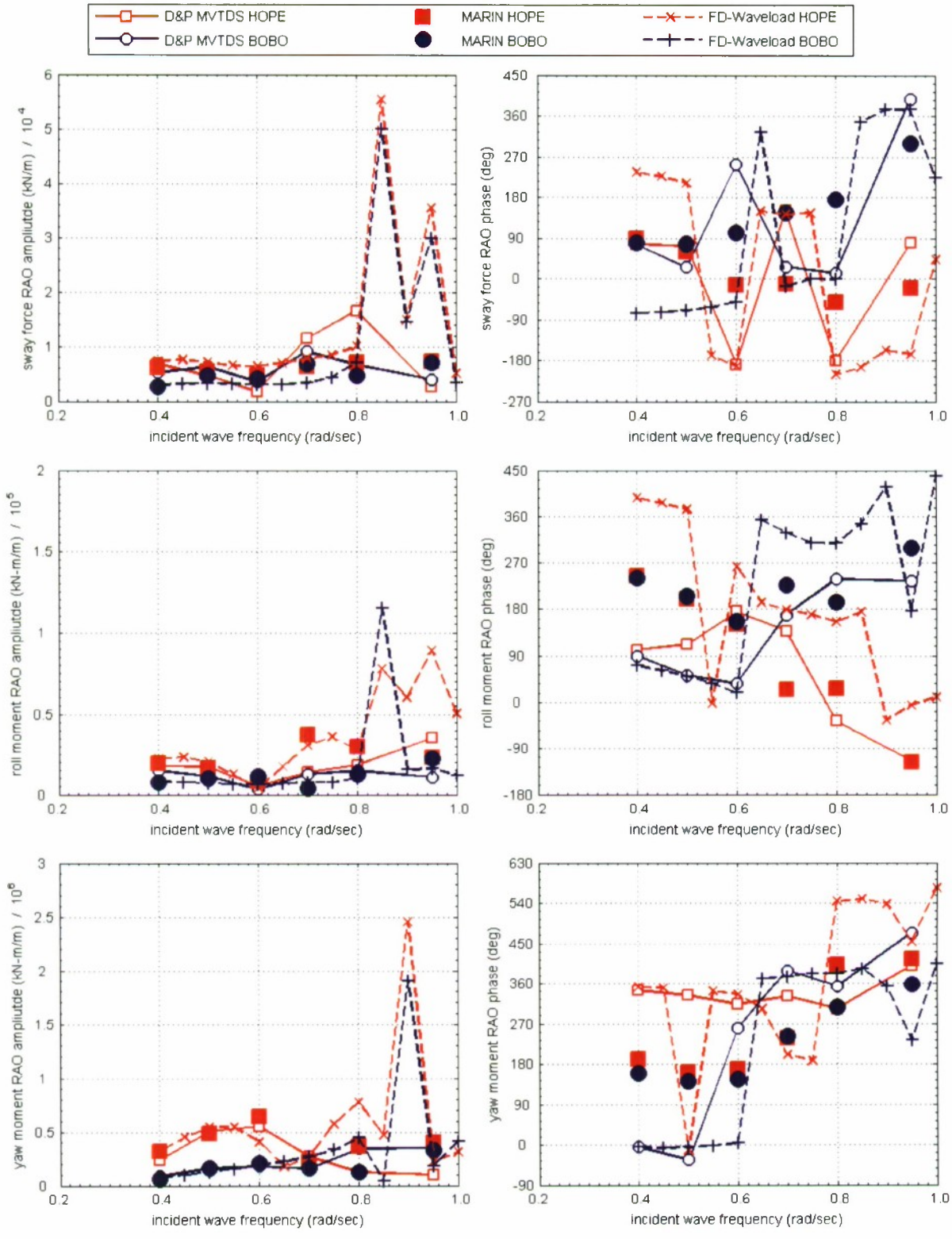

Figure 20. Sway force, roll and yaw moment RAOs for 3 meter separation, 135° wave heading, and 5 knots ship speed.

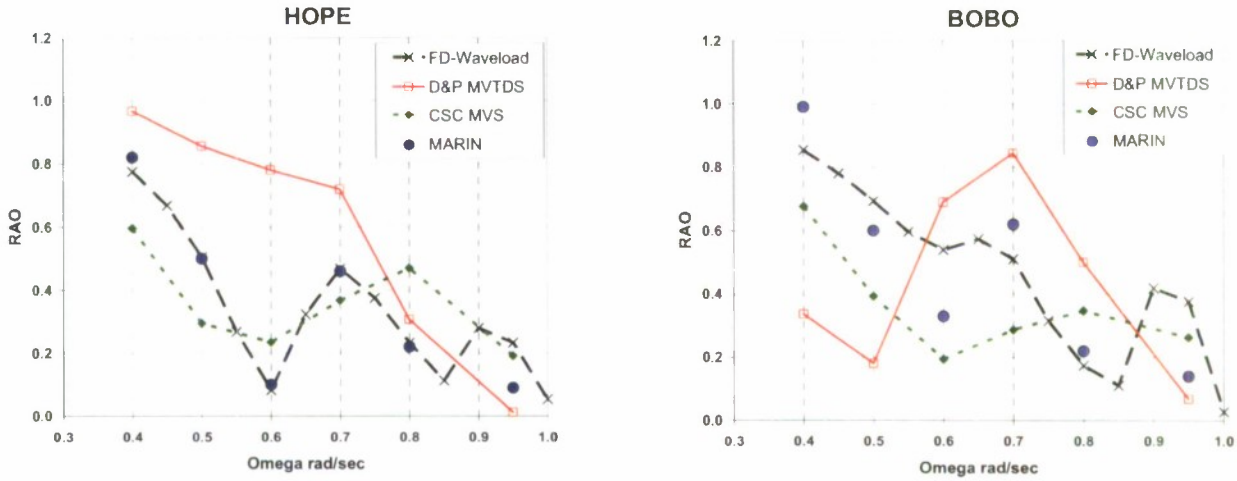

Figure 21. Comparison of D&P MVTDS with CSC MVS and FD-Waveload for the Heave RAO for the HOPE and BOBO at 5 knots, 3m separation, 135° heading.

AQWA

AQWA, developed by Century Dynamics and marketed by ANSYS, is a suite of integrated modules which predicts the hydrodynamic properties of offshore and marine structures. Each of these modules, AQWA-LINE, AQWA-FER, AQWA-NAUT, and AQWA-DRIFT, provides predictions of the hydrostatics and hydrodynamic motions of up to ten bodies in close proximity. AQWA-LINE calculates the wave loading and body response in regular waves. It also computes the linear wave forces and the second order mean wave drift forces. AQWA-FER analyzes the responses of the floating bodies in irregular seas. Both AQWA-LINE and AQWA-FER are performed in frequency domain. The time domain responses can be obtained by using AQWA-NAUT or AQWA-DRIFT.

AQWA Response Amplitude Operator Calculation

As mentioned in the description of the codes section of this report, AQWA calculates motions using linear velocity potential theory and solving the potentials with the zero speed Green's function. AQWA also uses a forward speed correction, similar to that of strip theory, to calculate the motions with forward speed. This approximation is valid for low to medium ship speeds, or Froude Numbers less than 0.3. The AQWA-LINE module is used for this evaluation to calculate the linear response of floating bodies in regular waves. For the two body case, AQWA-LINE uses three-dimensional radiation/diffraction potential theory. The amplitude of the incident wave is assumed to be small compared to the ship length. The motion is also assumed to be harmonic and the solution is obtained in the frequency domain.

AQWA Input Description

AQWA-LINE performs the ship motion calculations by representing the geometry of each of the ships as panels. Figure 22 shows the panels used for the AQWA calculations. The ship geometry was modeled by 708 panels for HOPE and 482 panels for BOBO. The panels represent the ship geometry below the still water line. AQWA-LINE uses both triangular and quadrilateral elements (panels). In an AQWA-LINE data file, the elements which are below the still water line must be denoted as diffracting elements. Although AQWA-LINE can handle mixed models of both diffracting and non-diffracting elements, the top row of diffracting elements must have their top edges aligned with the still water line.

AQWA RAO Amplitude and Phase Results and Observations

An initial investigation of the behavior of the RAOs for the example condition of 3-meter separation, 135-degree wave heading, and 5-knot ship speed was performed to determine if the amplitudes and phases were well behaved. For this investigation, AQWA-LINE was run with 105 frequencies with a variable frequency interval ranging from 0.2 radians per second to 0.001 radians per second. The smaller frequency intervals were used so that the discontinuity or spikes would be evident. Figures 23 and 24 show these RAOs computed by AQWA-LINE. Both amplitudes and phases of the RAOs of heave and pitch motions, surge and sway forces, and roll and yaw moments are compared with MARIN model test data. The AQWA values shown for the forces and moments are the wave exciting forces only, which represent the forces that would be measured on the

two ships if they were both fixed in all degrees of freedom. The radiation forces are not included in the surge and sway force or the roll and yaw moments. As the MARIN models were restricted in all modes except for pitch and heave, this means the AQWA predictions for the forces and moments in the fixed modes do not include the forces resulting from the heave and pitch motion of the two vessels. The effect of this may be small, as the vertical plane motions probably have only a small influence on the lateral plane forces. For instance it is unlikely that the heave and pitch motion of a vessel will produce a large roll or yaw moment. However, in the case of two vessels side by side, the heave motion of one vessel will generate radiated waves that may result in lateral plane forces on the other vessel which are not included in the AQWA-LINE wave exciting forces.

The heave and pitch motion RAO's are computed as if both ships were free to move in all six degrees of freedom, not just free to pitch and heave. The current version of AQWA-LINE did not allow for only some degrees of freedom to be restricted, so each ship could be modeled as either free in all six modes or fixed in all six modes. For the heave and pitch motion, the values shown in Figures 23 and 24 and in Appendix C are computed as if the vessels were free to move in all six degrees of freedom, and the values for the surge and sway forces and yaw and roll moments are computed as if the two vessels were fixed in all six degrees of freedom. If a time domain analysis were performed in AQUA-NAUT, the vessels could be restricted in all degrees of freedom except pitch and heave by including the towing carriage as a fixed moving non-hydrodynamic body and then modeling the mechanical linkages between the models and the carriage. However, the scope of the current correlation study only included the AQWA-LINE frequency domain analysis.

FD-Waveload is a frequency domain code based on a similar theory to that used in AQWA-LINE. The 2007a version of FD-Waveload has the capability to compute motion and force RAOs with the ships free to move in some degrees of freedom and fixed in others. FD-Waveload was run with the degrees of freedom set up as in the MARIN model test and also run with the degrees of freedom set up the in the same manner as was done in AQWA-LINE. The comparison of the two FD-Waveload simulations showed that neglecting the restricted degrees of freedom typically causes a difference of a few percent in the heave and pitch amplitude and differences on the order of 5 to 10% in the force and moment amplitudes.

Qualitatively, for the one condition of 3-meter separation, 135 degree wave heading, and 5 knot ship speed, the AQWA-LINE results have good agreement with the MARIN test data with the exception of the surge force. Also, in general, the predictions for the HOPE tend to be closer to the model test results than those of the BOBO. As expected, irregular spikes are evident in the heave and pitch RAOs (both amplitudes and phases) from AQWA-LINE at frequencies about 0.45 rad/sec and 0.95 rad/sec. The corresponding wavelengths are 304 meters and 68 meters, respectively. It is unusual to see the irregular behavior at the lower frequency of 0.45 rad/sec. There are also very large irregular spikes in the surge and sway forces and roll and yaw moments in the high frequency range of 0.8 to 1.0 rad/sec. This irregular behavior has been observed from free surface Green's function based simulation codes, and could be a function of the potential flow calculations which ignore the damping due to viscous effects.

The remaining seven conditions are shown in Figures C1 through C14 in Appendix C. The RAOs for these conditions were calculated by AQWA-LINE only at the frequencies of the model test. Therefore, any spikes or discontinuities in the behavior of the RAOs are essentially ignored. Straight lines are plotted between each of the RAO amplitude and phase at the specific frequencies. The conditions include separation of the two models of 3, 16.5, and 33 meters, ship speeds of 5 and 16 knots, and headings of head and bow seas. The model test results are plotted on each of these figures so as to discern the extent of the correlation between the predicted motions, forces, and moments with the model tests. In general, there is no clear pattern between the predicted results from AQWA-LINE and the model test. One observed deviation, however, is pointed out. For the 16.5-meter separation cases, the predicted pitch motion at the 0.6 rad/sec frequency and sway force at the 0.5 rad/sec frequency, the RAO amplitudes are significantly over predicted. Then, for the 33- meter spacing of the vessels, the pitch motion, surge force, and yaw moment are over predicted at the 0.8 rad/sec at 120 degree heading and 0.7 rad/sec at the 150 degree heading. Again, the rest of the predictions at the other frequencies and conditions correlated reasonably well.

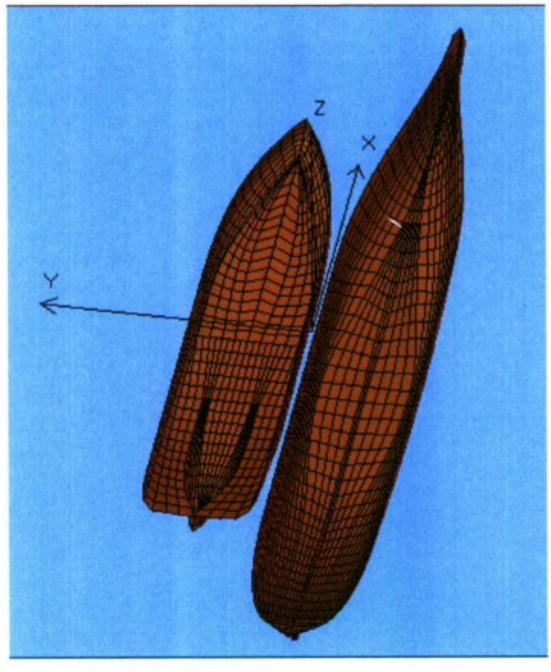

Figure 22. Panels used for AQWA-LINE simulations (Hope: 708 wet panels, Bobo:482 wet panels).

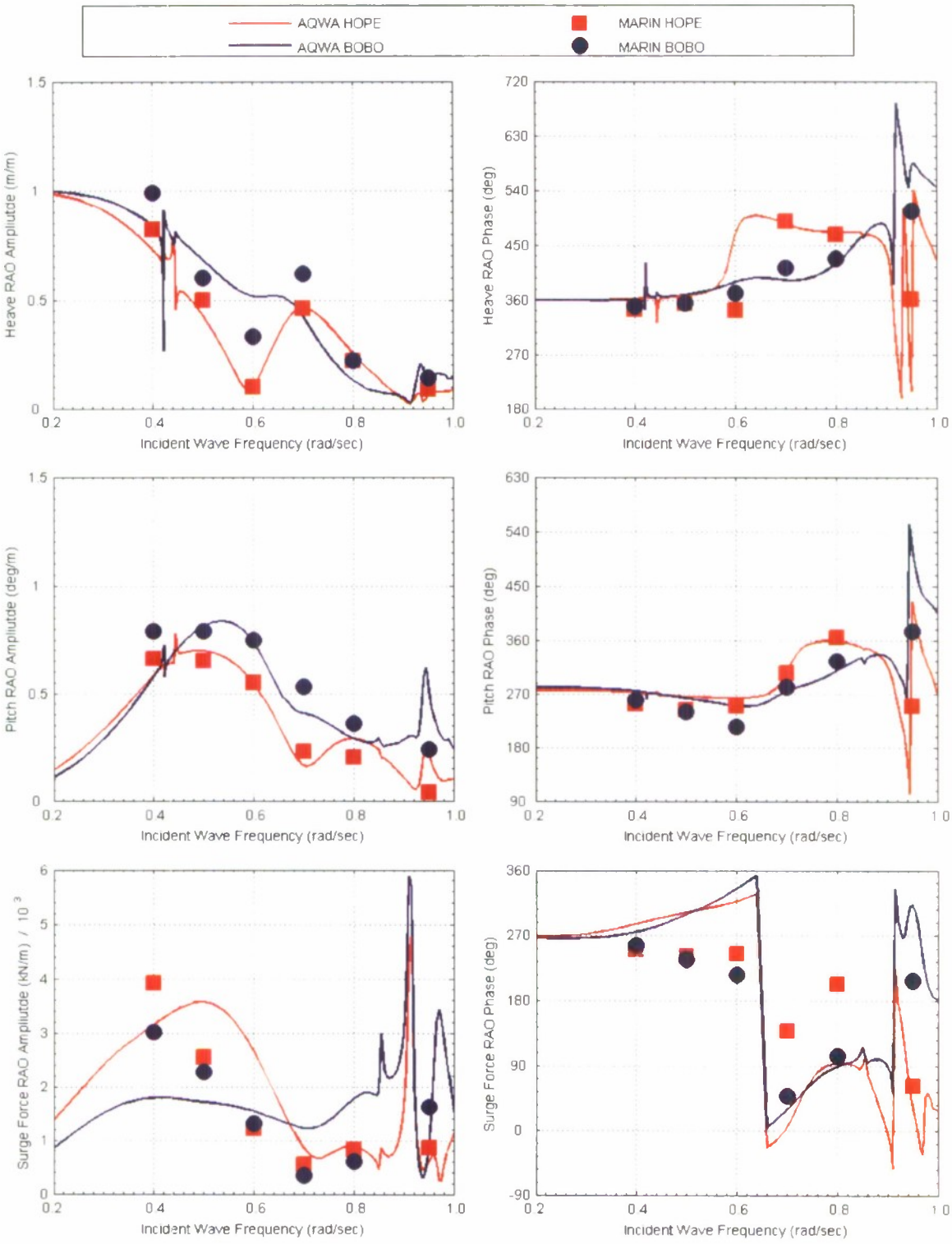

Figure 23. Heave, pitch and surge force RAOs for 3 meter separation, 135 degree wave heading, and 5 knot ship speed.

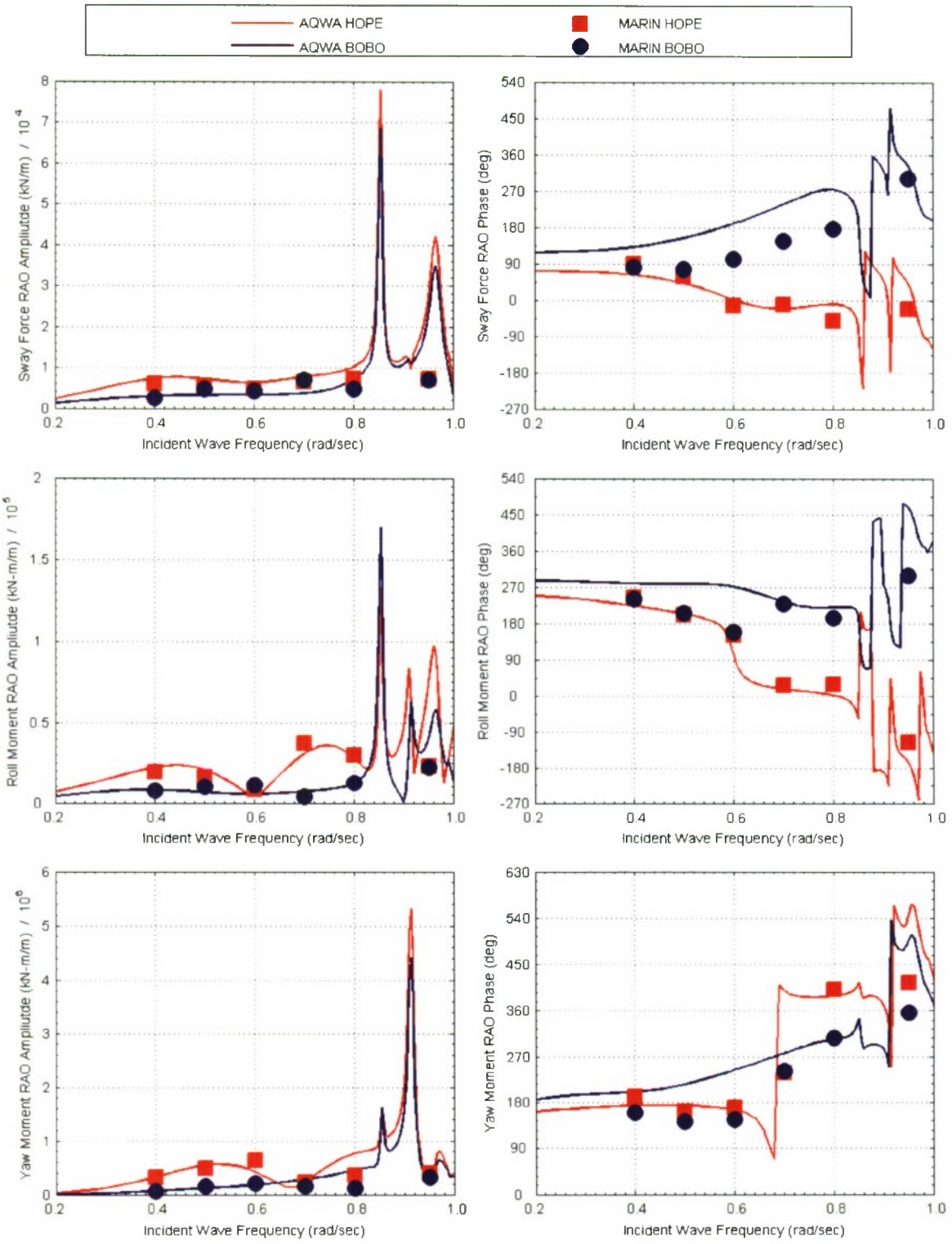

Figure 24. Sway force, roll and yaw moment RAOs for 3 meter separation, 135 degree wave heading, and 5 knot ship speed.

SHIPMO3D

The multi-vessel version of ShipMo3D belongs to the elass of purely linear frequency domain codes where the hydrodynamic coefficients are determined using a Green's function formulation. It has been developed by Kevin McTaggart of Defence R & D Canada – Atlantic and is constructed as an object-oriented library with associated user applications written in the Python programming language. Since the multi-vessel version of ShipMo3D is still in the early stages of development, many features that are currently supported in the single ship version have not yet been incorporated. As of January 1, 2008, the multi-vessel capabilities allowed for the determination of the forces on, and motions of, each vessel in the frequency domain moving at the same forward speed in regular waves. The capabilities available for a single ship simulation in ShipMo3D that are being added to the multi-vessel version involve both frequency and time domain simulations as well as both regular and irregular waves. In time domain simulations there is the option to compute nonlinear Froude-Krylov and hydrostatic forces on the instantaneous wetted hull. Other various force models that are available include hull eddy-making damping, hull cross-flow drag, input for hull maneuvering coefficients, and bilge keel viscous roll damping.

Input Description and RAO Calculation

Since ShipMo3D is an assortment of user applications, a set of stand-alone programs must be run in sequential order. As input, all of these programs require a user generated ASCII format input file, and in many cases, the python output file from previously run programs in the sequence. Many of the programs output an ASCII format file as well as graphical output. The first step is to create the vessel geometries in a python file format. This can be done by either using the program SM3DPanelHull, which reads in hull lines defined by point offsets and then generates panel corner points through interpolation, or SM3DReadPanelHull, which reads in the corner points of an already paneled hull directly. Regardless of which program is used, it must be run for each ship individually. The next step is to run SM3DRadDif; also for each ship individually. This program calculates the hydrodynamic forces due to added mass, wave radiation damping, and wave excitation in the frequency domain. The final program that is run on each ship is SM3DBuildShip. This program creates a database of all the relevant ship properties and characteristics such as the radius of gyration values, viscous force parameters, definitions of any appendages that are modeled, autopilot and rudder control parameters, and propeller characteristies. Next, the two ships are brought together in the program SM3DRadDifPair and the hydrodynamic forces due to added mass, wave radiation damping, and wave excitation for a pair of neighboring ships is computed. The ship separation is defined in this program and therefore it must be run for each separation distance between the ships of interest. Finally, SM3DSeaKeepRegularPair is run to compute the forces and motions for a pair of neighboring ships in regular waves.

Sensitivity study

A small sensitivity study was undertaken to determine the effect that the panel size (directly related to the number of panels) had on the resultant predicted transfer functions. In order to eliminate the effects that multiple ship interactions could potentially have, only a single ship, in this case the BOBO hull, was examined. In order

to generate the different panel sizes in ShipMo3D, the program SM3DPanelHull was used and the parameters controlling the interpolation were varied to systematically half the number of panels for each different case. The baseline hull geometry used throughout this total investigation had approximately 482 panels. For this study, a slightly denser paneling of 518 panels was looked at, as well as coarser geometries of 234, 111, and 53 panels respectively. Figure 25 shows the coarsest paneling used in the sensitivity study along with the bascline paneling that was used throughout this study of 482 panels.

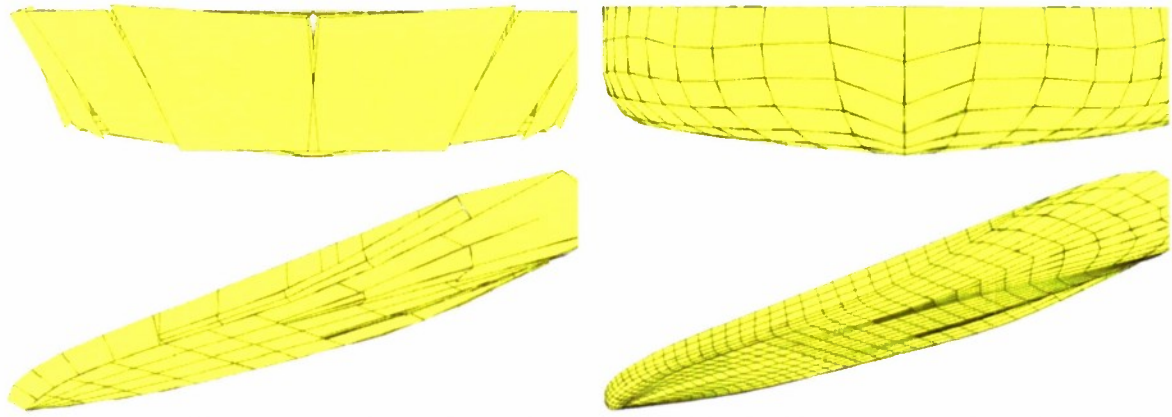

(a) coarse hull geometry using 53 panels (b) baseline hull geometry using 482 panels

Figure 25. Comparison of the extreme paneling differences in the BOBO hull geometries used in the scnsitivity study.

A frequency domain simulation was run of the BOBO in order to generate the predicted transfer functions of motion. The ShipMo3D results were also compared to data from a single ship experiment. The single ship experiment condition was conducted at MARIN with a ship speed of five knots, wave heading of 135 degrees, and a regular wave height of 0.75 meters full-scale at frequencies ranging from 0.5 to 0.8 radians per second. The heave and pitch amplitude transfer function results for the five different paneled hulls along with the experimental results are shown in Figure 26.

Both the heave and pitch transfer functions show that there is almost no differencc in the results between all of the various paneling densities if one excludes the most coarse panel geometry (53 panels). But even this extrcmely coarse panel geometry only begins to noticeably diverge from the other results at higher frequencies; frequencies above 0.60 rad/s for heave and above 0.80 rad/s for pitch. Furthermore, all the results, including thc coarsest panel geometry, agree very well with the experimental results from MARIN. Therefore, it appears that our baseline 428 panel hull geometry is more than sufficient to give accurate results.

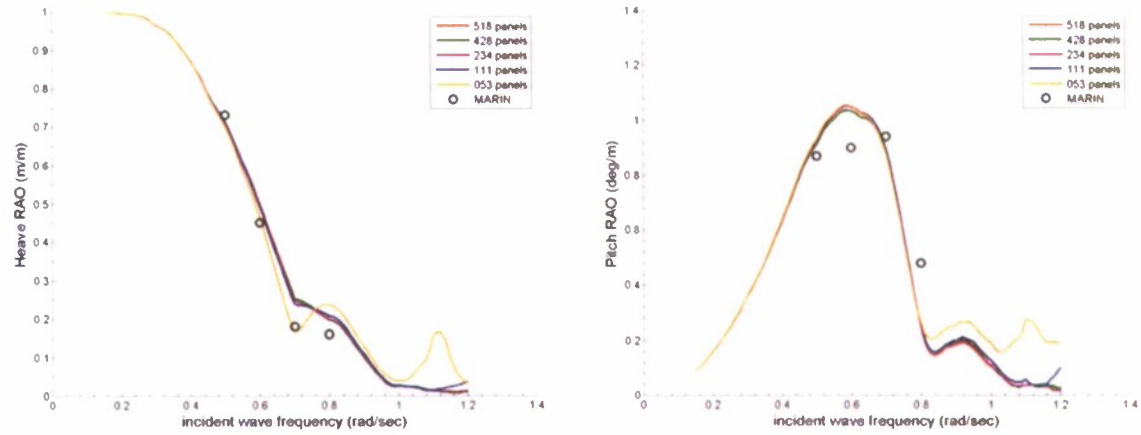

(a) heave amplitude (b) pitch amplitude

Figure 26. Hull panel sensitivity study transfer function results using the BOBO hull for condition of five knots ship speed, 135 degrees wave heading, and 0.75 meters full-scale wave height.

Irregular frequencies

Many panel-method codes, such as ShipMo3D, can be influenced by irregular frequencies. According to McTaggart[§], at these irregular frequencies, the computed hull source strengths and associated velocity potentials give unreliable results. This occurs because the source strengths on the hull become very sensitive to the influence matrix or the matrix of normal velocities from the source strengths and this causes small errors to be magnified. In order to minimize these effects, ShipMo3D allows the user to specify various frequencies that should be ignored when calculating the hydrodynamic coefficients. The program then interpolates across the excluded frequency gaps to fill in the coefficient values.

When simulating a single ship, irregular frequencies are fairly straightforward to identify. Large sudden changes, or spikes, in the added mass or damping coefficient over consecutive encounter frequencies usually signal an irregular frequency. However, when multiple ships in close proximity are involved in the simulation, it is not a simple task to determine irregular frequencies. This is because spikes in the hydrodynamic coefficients could now also be due to unexpected coupling between the motions of the ships. Unfortunately, in many cases of multiple ship simulations, the naturally weak interactions between the nearby ships are artificially magnified by the numerical solution of the problem. Therefore, leaving the coefficients unchanged or completely removing the spike at the problematic frequency are both undesired actions.

The possibility of eliminating irregular spikes that could be the result of irregular frequencies within ShipMo3D was explored. This meant skipping the hydrodynamic coefficient at a certain frequency and then later calculating its value by interpolating between neighboring points. Figure 27 shows an example using no irregular frequency

[§] McTaggart, K. ibid

control versus ignoring a frequency that produces a spike for the HOPE hull at three meter separation, 135-degree wave heading, and five knots ship speed using the sway added mass (black line) and damping (red line) hydrodynamic coefficients.

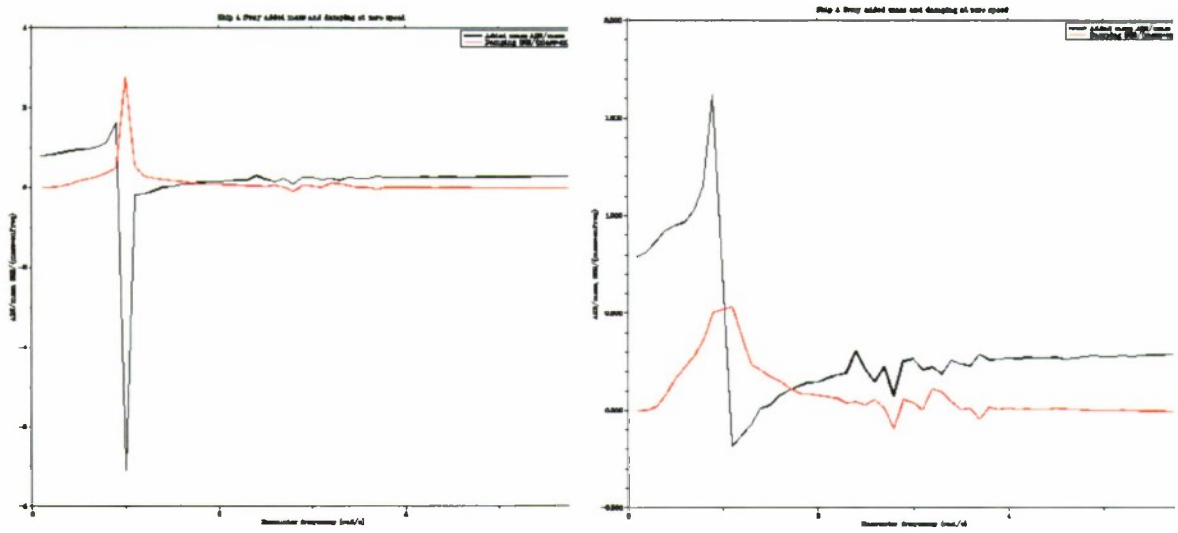

(a) without any irregular frequency control (b) with irregular frequency control

Figure 27. Sway added mass and damping coefficients computed for the HOPE hull with a three meter separation with and without irregular frequency considerations.

Without any irregular frequency considerations, the added mass sway coefficient for the HOPE hull showed a very prominent downward spike with resultant negative values around an encounter frequency of one radian per second as shown in Figure 27(a). For a single ship this would obviously be an irregular frequency since negative coefficients cannot exist. However, for multiple ships in close proximity, negative values are indeed possible. If the user chooses to suppress this spike because it is believed to be erroneous, then the ShipMo3D user has the option of ignoring that particular encounter frequency. The result is shown in Figure 27(b), where the large sway added mass, over -6.0 A22/mass, downward spike is gone, highlight the effects this change would produce.

The choice to suppress an irregular spike that could be an irregular frequency can have a large impact on the resulting transfer functions. This is shown by the results in Figure 28 where the pitch transfer functions of both ships in a multi-ship simulation are shown. In one case there were no irregular frequency considerations (the solid lines), while for the other case we removed the potential irregular frequencies (dashed lines). For the most part, the pitch responses in both cases are nearly identical. However, near the potentially irregular encounter frequency of one radian per second (0.857 radians per second incident wave frequency) the pitch responses of each vessel show large difference. The experimental results were also plotted to serve as a means to help assess the correctness of each approach. The results for the HOPE seem to suggest that it is justifiable to suppress the irregular frequencies since the result with the removed spike passes right through the experimental result at 0.95 radians per second. However, the results for the BOBO are not so clear. The experimental result at that incident wave frequency lies between the predicted RAOs with and without the irregular frequency;

perhaps suggesting the difficult situation where ship coupling does exist but is artificially magnified. Ultimately however, no definite statement can be made due to the discrete nature of the experimental results and the narrow width of the spike in question. It is possible that the observed spike predicted by ShipMo3D could exist in the experimental data if more points between 0.80 and 0.95 radians per second had been investigated. The correct handling of irregular spikes is usually even more complicated than this since, in most cases, experimental results are not available to be used as a guide. As demonstrated, even if they do exist, the proper handling of irregular spikes in the coefficient results requires much thought.

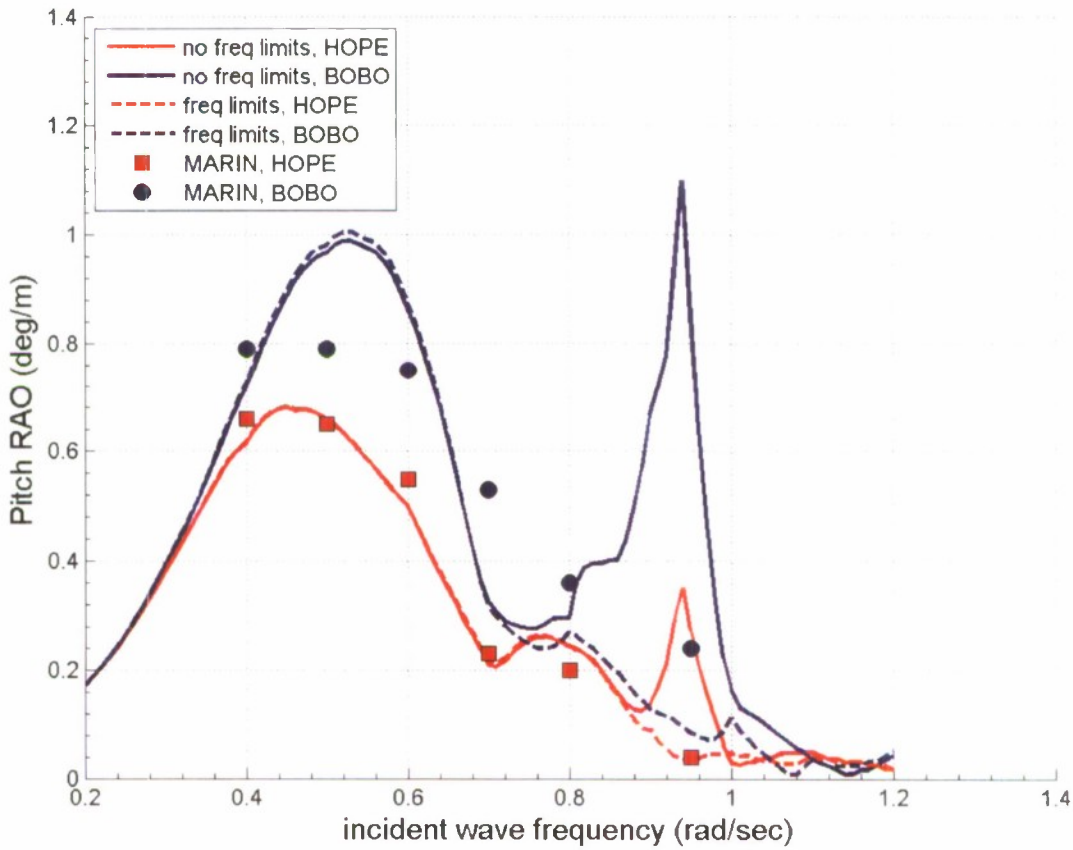

Figure 28. Effects of irregular frequency smoothing has on the resultant pitch transfer function for three meter separation, 135 degree heading, and five knots ship speed.

In order to be consistent in the evaluation of the other codes, no irregular frequency considerations were used to calculate the results in the following section. The rationale behind this was that irregular frequency handling involved the application of more advanced hydrodynamic knowledge than the average user may have at their disposal.

ShipMo3D RAO Amplitude and Phase Results and Observations

The predicted RAO amplitudes and phases using ShipMo3D for each of the two vessels, along with the experimental results from the multiple-ship tests performed at MARIN, can be seen in Figures 29 and 30 below. The results shown below are of the 135° ship heading to the waves and 5 knot ship speed and 3 meter separation between the two ships. Plots showing the remainder of the conditions studied can be found in Appendix D.

Overall, ShipMo3D does a very good job predicting the ship motion transfer functions of heave and pitch, both amplitude and phase. The amplitudes of the two motions show slightly better agreement to the experimental data for the larger ship, HOPE, than the smaller ship, BOBO. The phases of the two motions for both ships also have similar agreement to the experimental results. ShipMo3D is able to predict the surge and sway force amplitudes reasonably well. In a similar manner to the motions, it appears to do a slightly better job predicting these forces for the HOPE than the BOBO. The phases of the force predictions correlate well for the low incident wave frequency region for the surge force but deviate from the experimentally measured phases for the higher frequency region and for the sway force entirely. Finally, ShipMo3D struggles with predicting the roll and yaw moment transfer functions. The biggest problem is that the possible irregular frequencies around an encounter frequency of one radian per second appear to be extremely magnified in the moment transfer functions. There is a small, relative to the rest of the results, spike in the heave and pitch motion and surge force amplitudes results around this encounter frequency. There is a similar spike, although much larger, more than an order of magnitude, in the sway force and roll and yaw moment amplitudes. Because of the large vertical scale, the results at lower frequencies have less resolution along the abscissa. In order to resolve this scaling issue, the ShipMo3D roll moment amplitude results are cut off at 0.78 radians per second and shown in Figure 31. This figure now has a more appropriate scale and the predicted ShipMo3D results can be compared to the experimental results more easily. It is apparent, however, that the predicted results still do not capture the moment amplitudes correctly. It appears that for low frequencies, less than 0.70 radians per second, ShipMo3D over predicts the moment amplitudes by about three times. For higher frequencies, one near the possible irregular frequency as was shown in the previous figure, ShipMo3D predicts moments that are orders of magnitude too large.

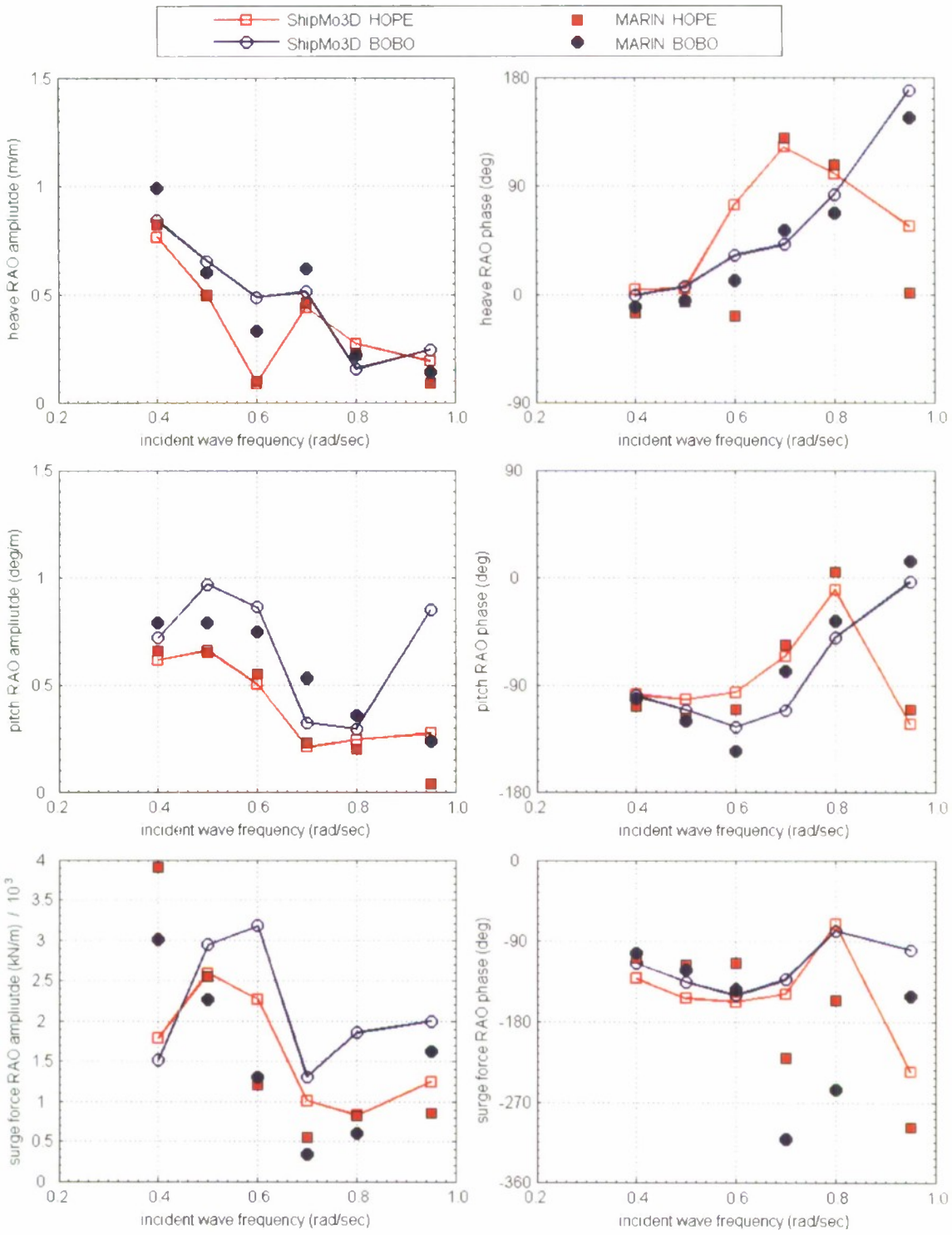

Figure 29. Heave and Pitch Motion and Surge Force RAO amplitudes and phases for three meter separation, 135 degree wave heading, and five knots ship speed.

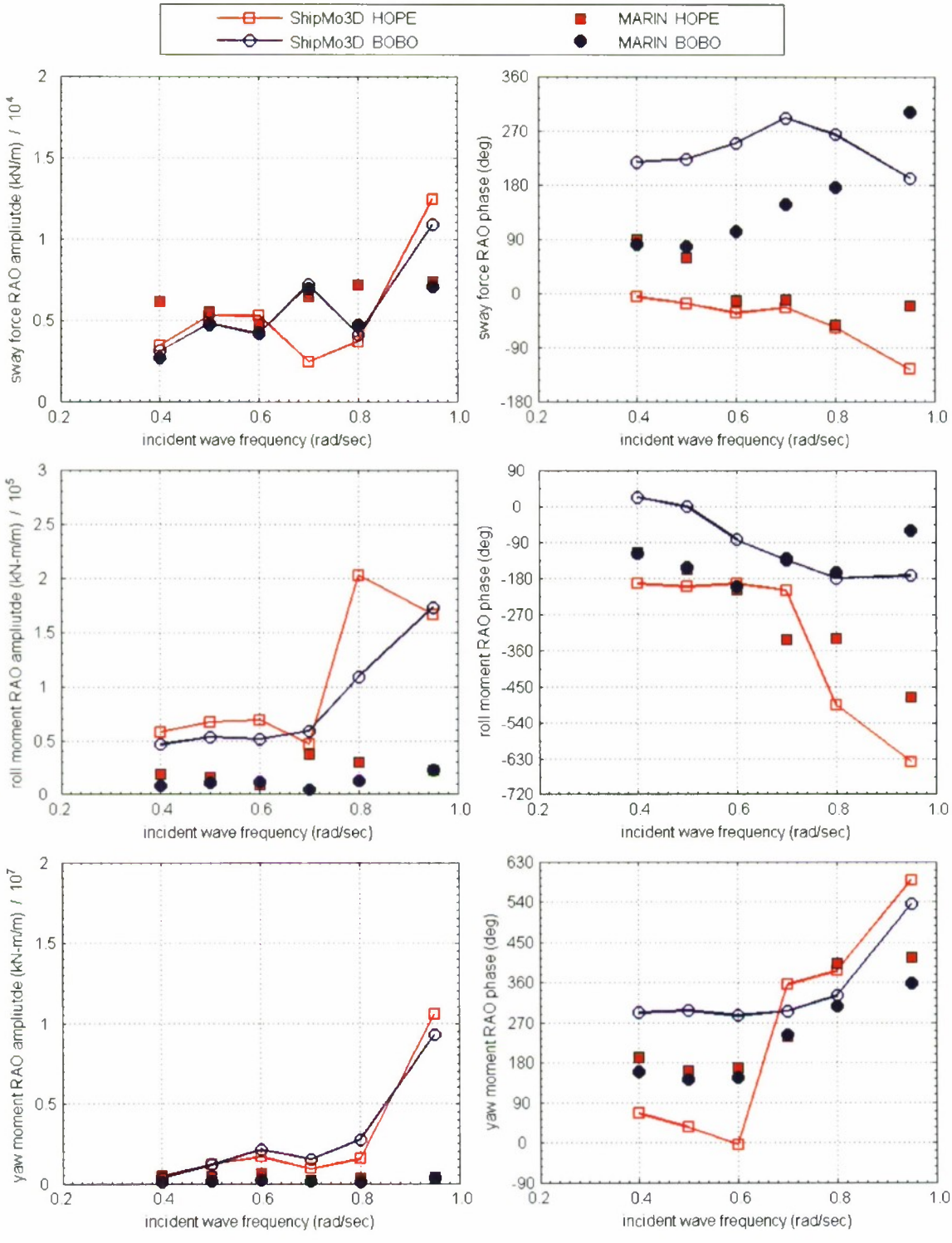

Figure 30.Sway Force and Roll and Yaw Moment RAO amplitudes and phases for three meter separation, 135 degree wave heading, and five knots ship speed.

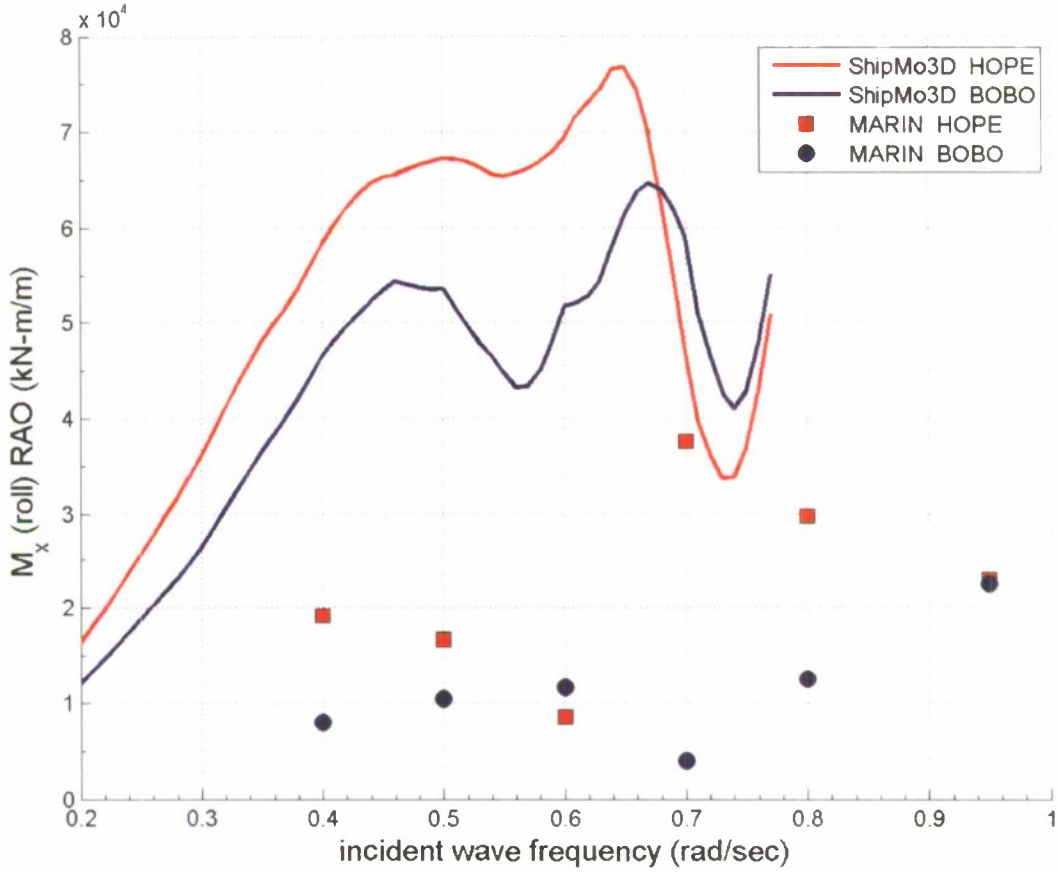

Figure 31. Partial resultant roll moment amplitude transfer function for three meter separation, 135 degree heading, and five knots ship speed.

LARGE AMPLITUDE MOTIONS PROGRAM (LAMP)

The Large Amplitude Motions Program (LAMP) was developed by Science Applications International Corporation (SAIC) to provide both linear and nonlinear ship motion predictions in the time domain. Most of the development of LAMP was performed under ONR sponsorship. The basis of LAMP is a time domain Rankine panel method. LAMP includes several options for obtaining the time domain solution on the ship hull surfaces and the free surface, with different levels of complexity and computational effort required. Using an approach referred to as LAMP 1, both the hydrostatics and hydrodynamics can be computed in a body linear manner, taking into account the hull geometry only up to the static waterline. A hybrid approach can also be used that combines body-nonlinear hydrostatic and Froude-Krylov forces with linear hydrodynamic forces. This approach is used in options referred to as LAMP 2 and LAMP 3. The difference between LAMP 2 and 3 is that LAMP 3 includes methods for predicting the maneuvering forces associated with large lateral motions, where the forces contributed by rudders, other appendages and the propeller are included using empirical formulas. The most complex and computationally intensive approach is LAMP 4, which uses a body-nonlinear method for the hydrodynamic problem as well as to compute the hydrostatic and Froude-Krylov forces. For predicting the motions of multiple ships in close proximity, SAIC produced an offshoot of the LAMP suite they called LAMP-MULTI. The LAMP-MULTI version of the program used for this seabasing evaluation was based on LAMP 2. The LAMP-MULTI program calculated the calm water maneuvering forces, calm water ship interaction forces, and time domain ship wave-induced motions, forces and moments for the two ships studied for this evaluation.

Response Amplitude Operator Calculation

The LAMP-MULTI program used the following numerical methods to calculate the essential maneuvering, ship interaction forces, and wave-induced forces. The calm water ship interaction forces are calculated by the potential flow panel method. The wave-induced forces are calculated using a three-dimensional body-linear Rankine potential flow panel hydrodynamics with body-nonlinear hydrostatic and Froude-Krylov wave forces. The hull lift forces are approximated using low aspect ratio airfoil theory. The program then combines the results of the maneuvering and ship interaction force calculations with the wave-induced forces to determine the time domain ship motions, forces and moments of both ships. Optional calculations for forces from mooring lines and fenders can be included.

A Fourier analysis was used to calculate the Response Amplitude Operator (RAO) amplitudes and phase angles from the ship motion, force and moment time histories. It considered only the encounter frequency term for the steady regular waves.

Input Description

The input to the program included the hull form panels, the appendage descriptions and dimensions, the center of gravity, roll damping, and wave conditions. The free surface geometry was defined by a set of quadrilateral panels that was generated by the LAMP automatic free surface grid generation pre-processor code. The panel density that was used for the final calculations is shown in Figure 32.

Results from LAMP numerical calculations can vary depending upon how the hull geometry and free surface are represented in the input. A sensitivity study was conducted to better understand the influence of these input variables on the LAMP output. In this study, the number of panels that were needed to represent the hull geometries of the two ships and the extent that these panels represented the free surface were varied. Variation in the time step size was also evaluated for the 16.5 meter separation 16 knots 120 degree heading condition. There was noticeable differences in the LAMP-MULTI output due to free surface panel extent and hull resolution. In general, the aim is to use as small a free surface panel extent and as large a panel size panel to represent the hull and free surface as possible without sacrificing accuracy. Figures 33 and 34 depict the influence of varying the free surface extent on the predicted motions, forces and moments. As shown, the heave and pitch motions were relatively constant with changes in panel extent, while the forces and particularly the moments varied considerably with panel extent. From this study, the free surface panel extent of 800 meters was chosen to be used for the final runs for frequencies of 0.4 and 0.8 radians per second. This extent was chosen because the variations in the output became more constant than those of smaller free surface extents. The MARIN model test data was included in the figures for reference. As shown in Figures 35 and 36, the heave and pitch motions were relatively constant with changes in panel resolution or size, while the forces and particularly the moments varied considerably with panel size. At the panel size of 16 meters that was used for the final runs, the variations were generally smaller than those of larger sizes. The smaller of the two panel sizes near 16 meters was selected to show the difference between having four panels between the hulls instead of two with mixed results. The final 3 meter and 16.5 meter separation runs were made with two panels between the hulls while the 33 meter separation runs were made with four panels. The RAO amplitudes were generally predicted more accurately than the phase angles.

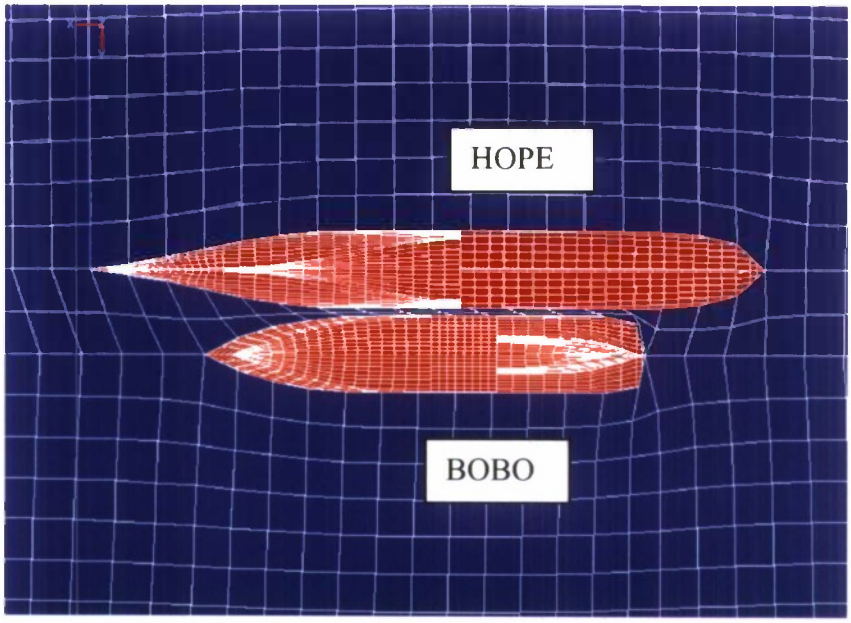

Figure 32. LAMP LAMP-MULTI Hull Panel Grids for HOPE and BOBO

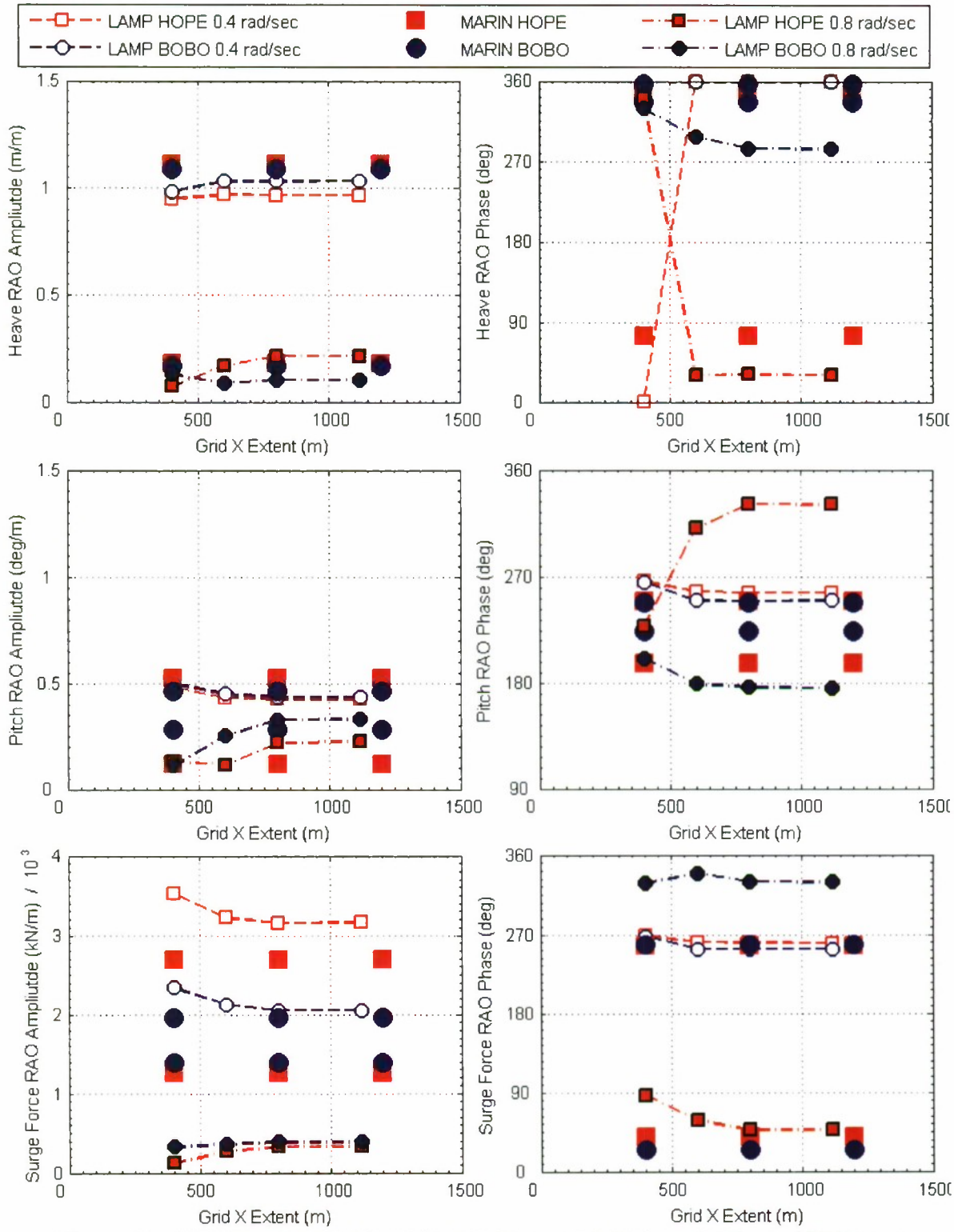

Figure 33. HOPE and BOBO LAMP Grid Extent 16.5 Meter 16 Knots 120 Degree Heading

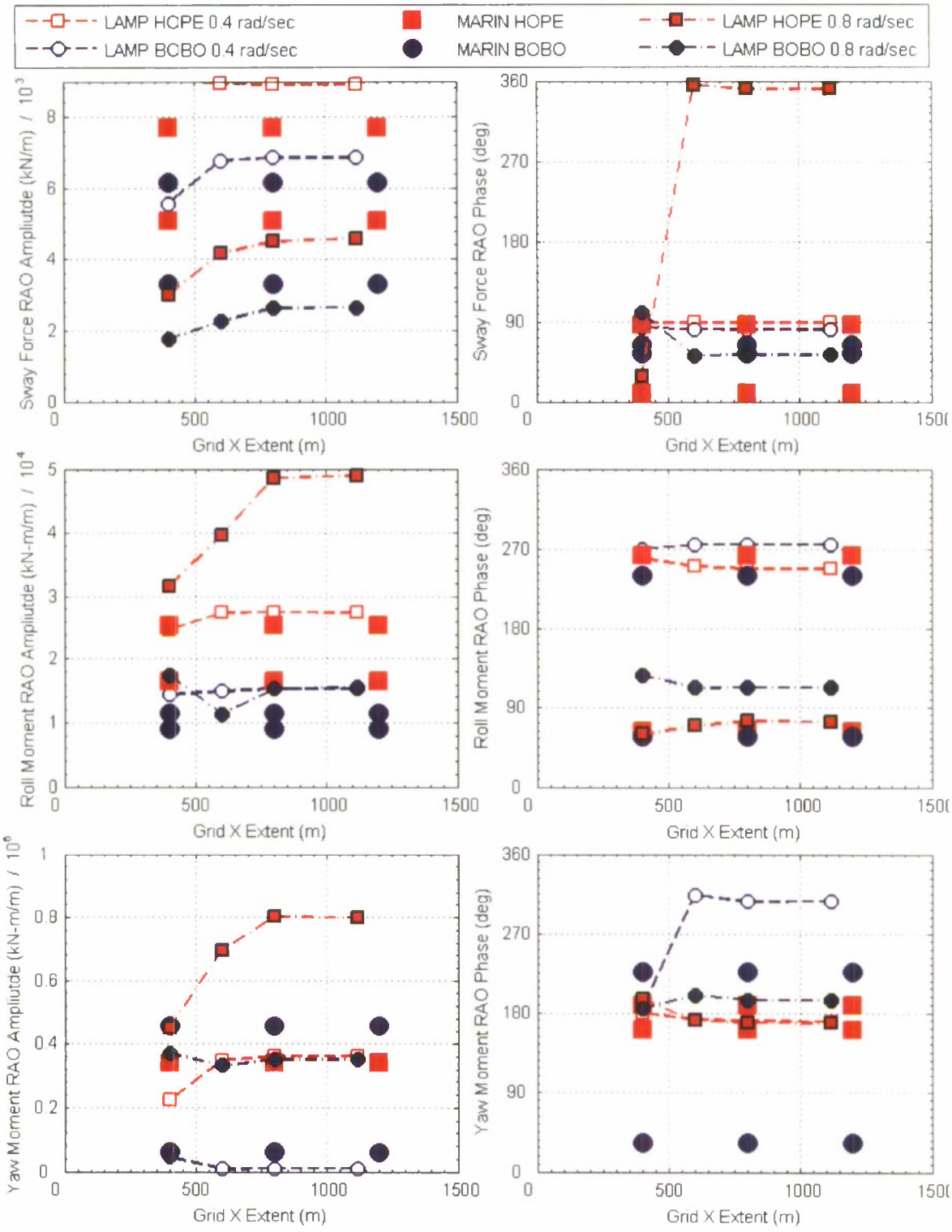

Figure 34. HOPE and BOBO LAMP Grid Extent 16.5 Meter 16 Knots 120 Degree Heading

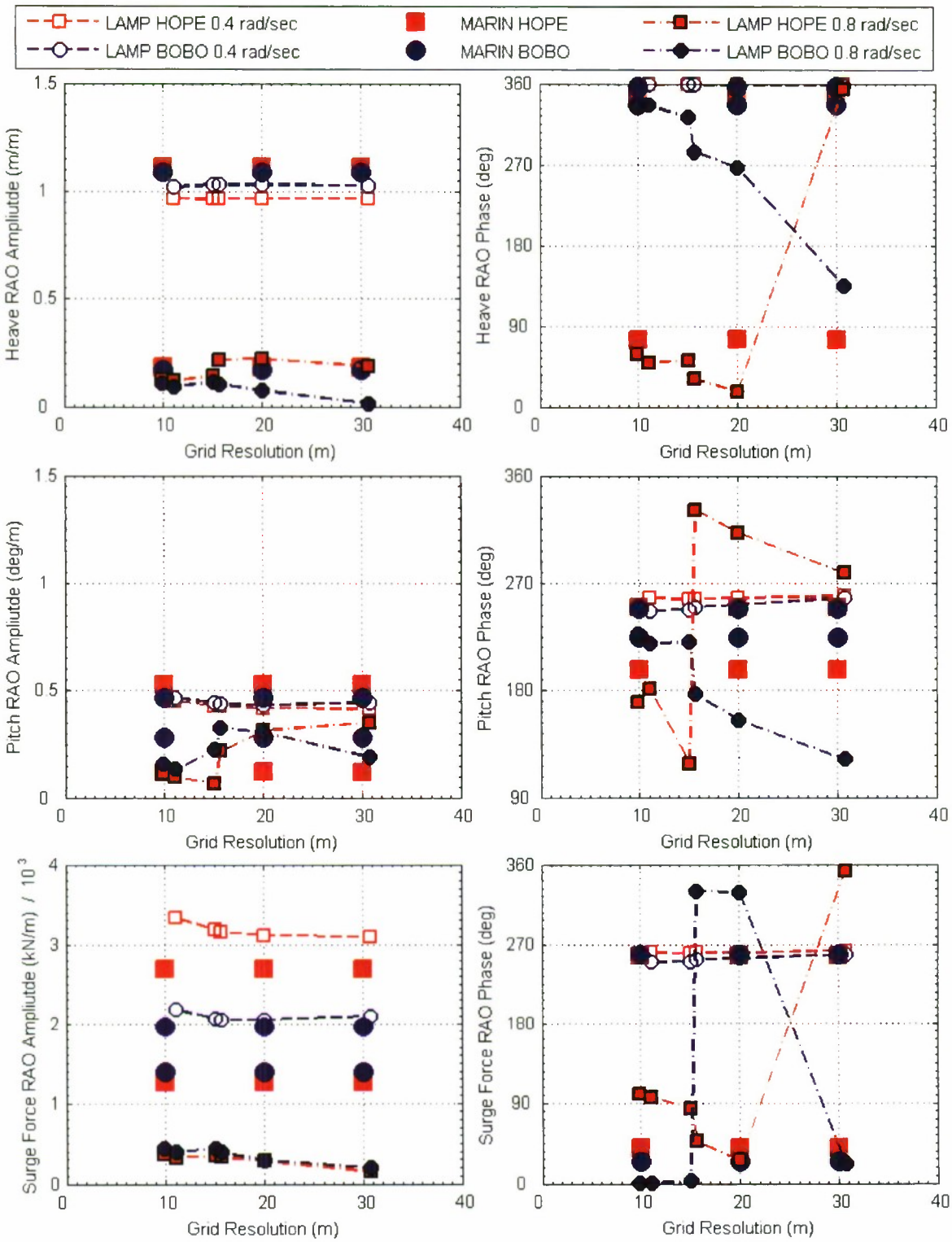

Figure 35. HOPE and BOBO LAMP Grid Resolution 16.5 Meter 16 Knots 120 Deg Heading

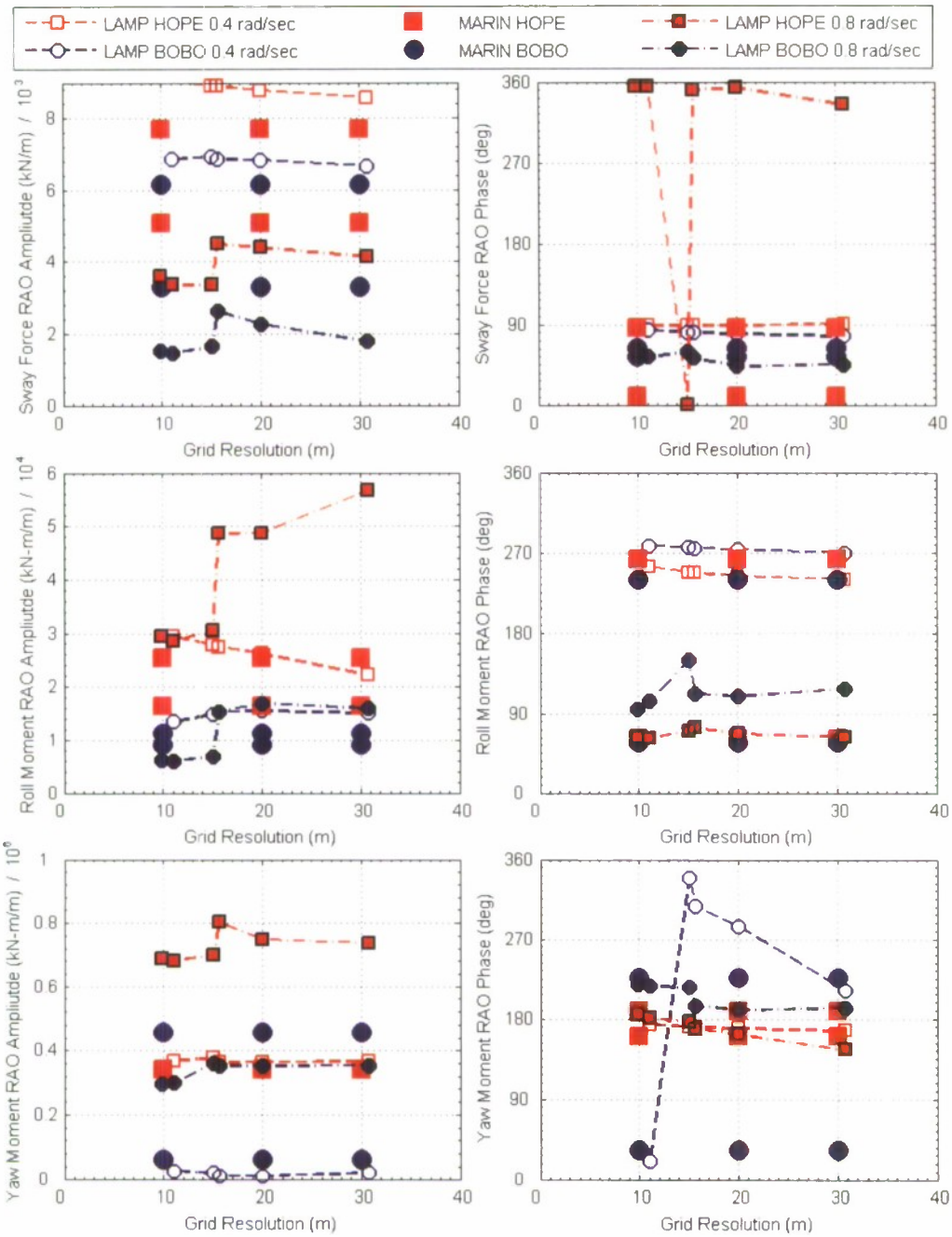

Figure 36. HOPE and BOBO LAMP Grid Resolution 16.5 Meter 16 Knots 120 Deg Heading

RAO Amplitude and Phase Results and Observations

RAO amplitude and phase of heave and pitch motion, surge and sway force and roll and yaw moment for the 3 meter separation, 5 knots, and 135° wave heading condition are shown in Figures 37 and 38. The range of the phase plots has been extended to make the plots continuous, instead of wrapping at 0° and 360°. Also plotted on Figures 37 and 38 are the RAO amplitude calculations that were developed by SAIC for the same condition. Correlation plots for the remaining seven test conditions are shown in Appendix E.

The qualitative assessment of the LAMP-MULTI results for all eight conditions shows some general trends. First, the RAO amplitudes agree quite well for all motions and slightly less well for the moments and not well for the two forces. This is especially true for the 33 and 16.5 meter separation, with a ship speed of 16 knots and 120° to 150° heading. For both separation distances at head seas, 180° heading, only the heave and pitch motions correlated well. However, the 3-meter separation with a ship speed of 5 knots, the 180° heading showed excellent correlation for all six RAO amplitudes, and for the bow sea case, 135° heading, the heave and pitch motions and sway force correlated well, and the surge force and roll and yaw moments not so well. Second, the phase results show slightly more scatter though the trends follow the model test results in a similar way to the RAO amplitudes.

In addition to the effort described above, SAIC was given two conditions from the MARIN model test and ran LAMP-MULTI for those conditions in a separate investigation. The conditions that SAIC was given were 33-meter separation, 150° heading at a ship speed of 16 knots and 3-meter separation, 135° heading and a ship speed of 5 knots. Because the output from LAMP is dependent upon the grid generation, it is interesting to note any differences in the output from LAMP-MULTI between the two organizations. The SAIC results are plotted in Figures 37 and 38 and Figures E3 and E4 in Appendix E. SAIC presented the amplitudes of each of the motions, forces and moments and the phases of the motion only. In general, the amplitudes of both results were extremely close with just a few minor deviations. There were a few cases at some frequencies where the results from the two calculations deviated from each other. In those instances, it appeared that the results from one or the other calculations aligned with the model test results. There was, however, no consistent pattern.

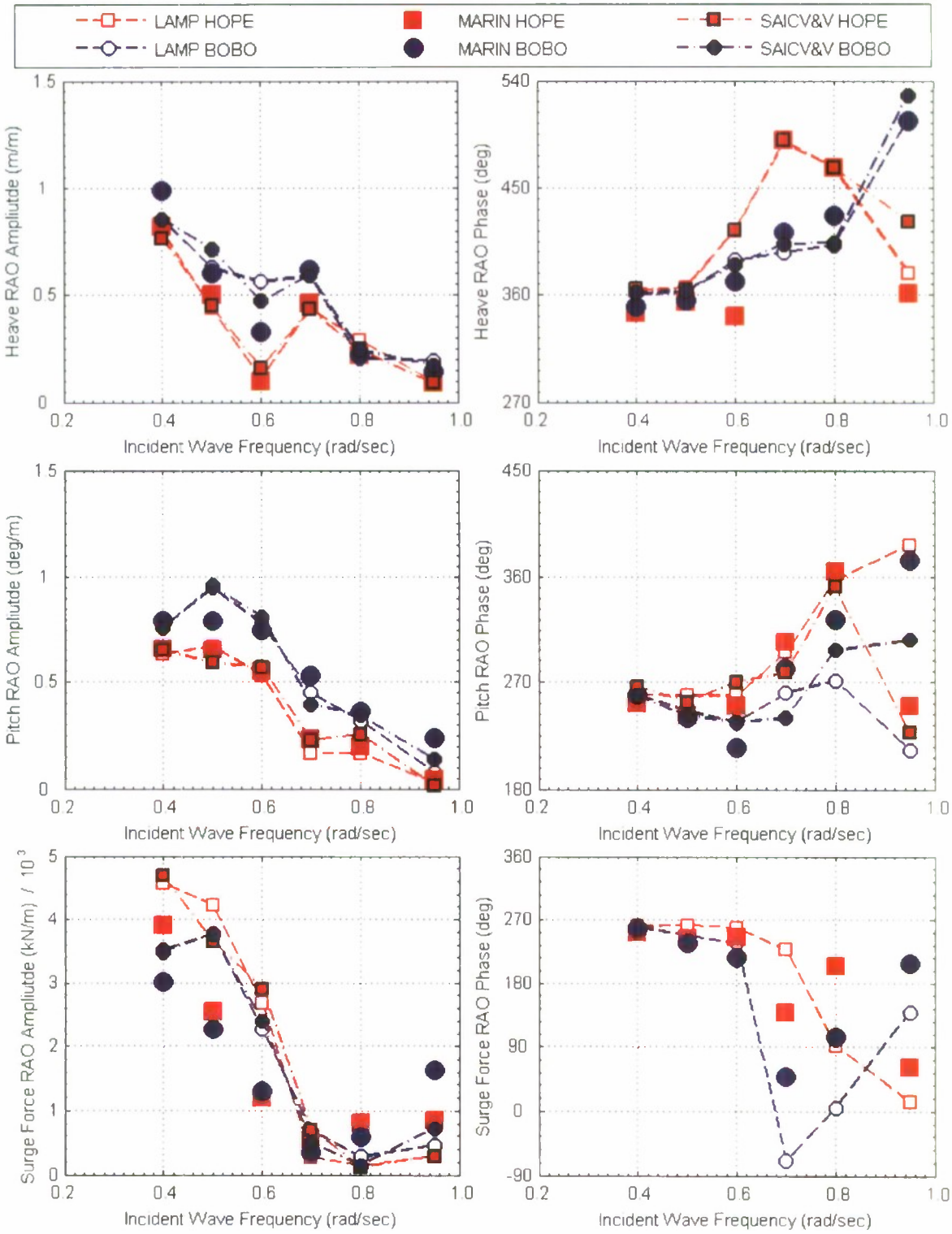

Figure 37. HOPE and BOBO 3 Meter Separation 5 Knots 135 Degree Wave Heading

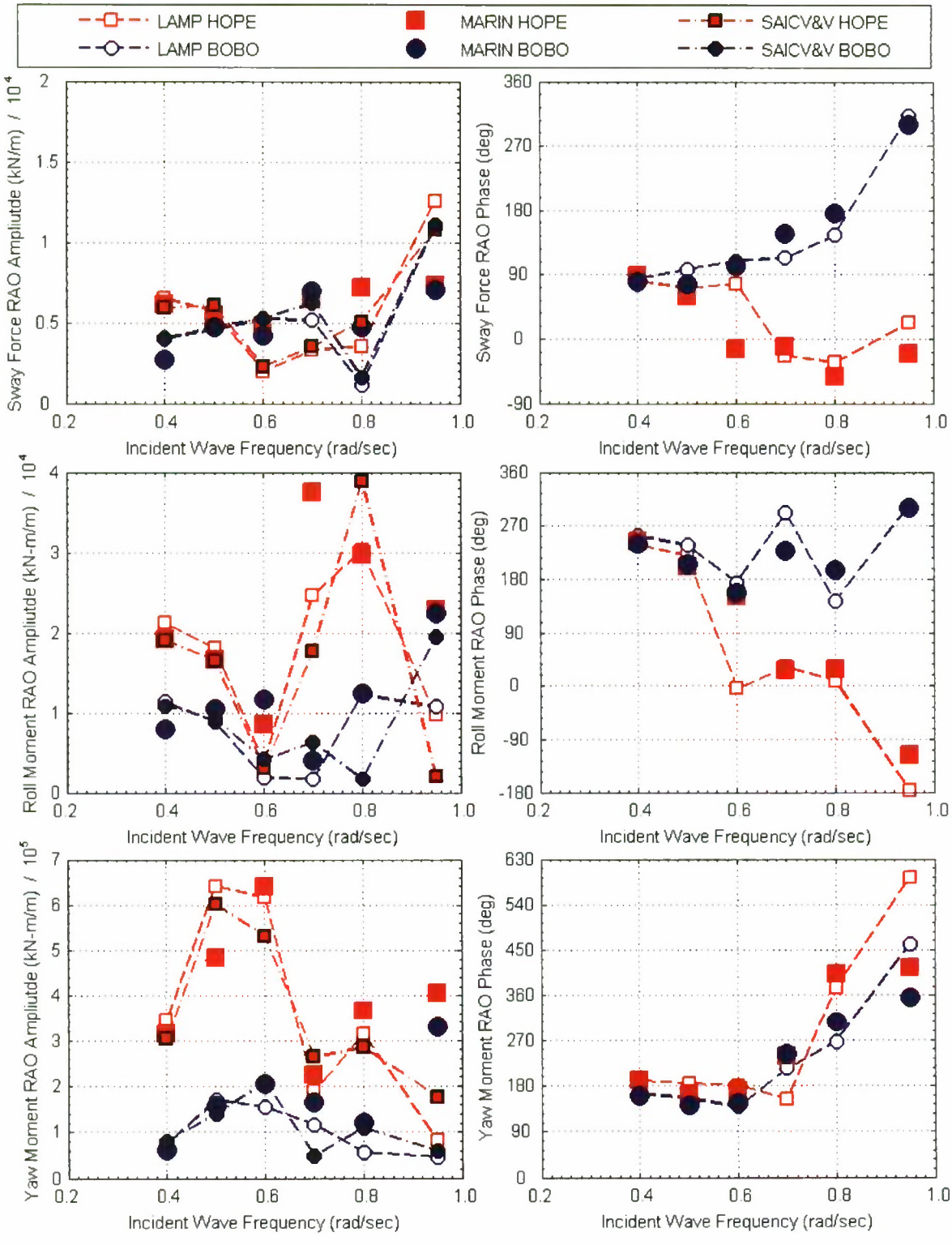

Figure 38. HOPE and BOBO 3 Meter Separation 5 Knots 135 Degree Wave Heading

AEGIR

AEGIR is currently being developed jointly at Flight Safety Technologies and Applied Physical Sciences Corp. AEGIR is a time domain three-dimensional B-spline based Rankine boundary element method that predicts the potential flow around ships on or near the water surface. It can be used both to predict the wave resistance and steady interaction forces for one or more ships in calm water or the unsteady motions and forces for one or more ships in waves. It was developed initially for a single ship and was extended to model multiple ships as part of the ONR-sponsored HSSL project. AEGIR is based on the higher-order panel formulation used in WAMIT incorporated with the time domain and Rankine singularity formulation used in SWAN-2. The initial development of AEGIR began at MIT and continued after the developers of AEGIR left MIT to work in industry. AEGIR differs from traditional panel methods in that it does not use flat quadrilateral or triangular "panels" to define the hull and water surface geometry with a constant strength singularity distribution on each panel to define the solution. Instead AEGIR uses Non-Uniform Rational B-Spline (NURBS) surfaces to describe the hull and water surface geometry as well as the shape of the singularity distributions on those surfaces. AEGIR is based on simple Rankine singularities and has no inherent limitations on the forward speed of the ships. Options are available for obtaining a purely linear solution, or a solution that combines linear hydrodynamic forces with body nonlinear incident wave and hydrostatic forces. The AEGIR formulation also allows for the modeling of lifting surfaces such as foils and rudders directly in the boundary element model, as opposed to including these as external forces. Viscous forces and non-hydrodynamic forces such as forces from fenders or mooring lines can be included as external forces in the time domain solution, but require the user to supply a routine to describe the forces.

Input description and Response Amplitude Operator Calculation

The input for AEGIR differs from the other tools evaluated for this study in that the ship hull geometry needs to be defined as a set of NURBS surfaces as opposed to a set of panel corner points. AEGIR requires that the hull geometry be defined as surfaces using the file format of the Rhinoceros™ surface modeling package, which is commonly referred to as Rhino. The NURBS surfaces can be imported into Rhino from an IGES file or the NURBS surfaces can be created within Rhino from a set of offsets or section curves. For the HOPE and BOBO hull forms, the geometry was obtained from IGES files produced at MARIN for the model construction. In principal AEGIR should have the advantage of being able to go directly from the CAD description of the hulls used to build the models to the input geometry description for the flow solver. In practice the NURBS surfaces produced for model creation or concept description are not always acceptable, and some manipulation of the surfaces in Rhino is often required. For instance the tip of the bulbous skeg on the BOBO protruded just slightly above the calm water surface which created some issues for the automatic intersection routines in AEGIR, so that the tip had to be pulled down slightly below the calm water surface. Also a few surfaces had to be regenerated by cutting section curves through the original surface and then lofting those curves to create NURBS surfaces with a more regular distribution of parametric curves. While some user expertise had to be acquired to

prepare the geometric surfaces for the hulls, the input preparation was still faster than would usually be required for building a good traditional panel model, and the fineness of the discretization could be refined by simply changing a few numbers in one of the ASCII input files.

A portion of the water surface surrounding the ships is also modeled in AEGIR. The code includes some automated free surface generation options for standard single ship configurations, but for the HOPE and BOBO configuration, a set of surfaces covering the calm water surface had to be created manually in Rhino. As the BOBO had a wide blunt stern, it was found that a separate surface patch was required behind the stern of the BOBO to obtain a good solution. The surfaces used for the 16.5-meter separation cases are shown in Figure 39 and for the 3m separation cases in Figure 40. The mesh shown on each surface does not represent a set of panel corner points, but rather indicates the knot density along the B-Splines used to define the surfaces.

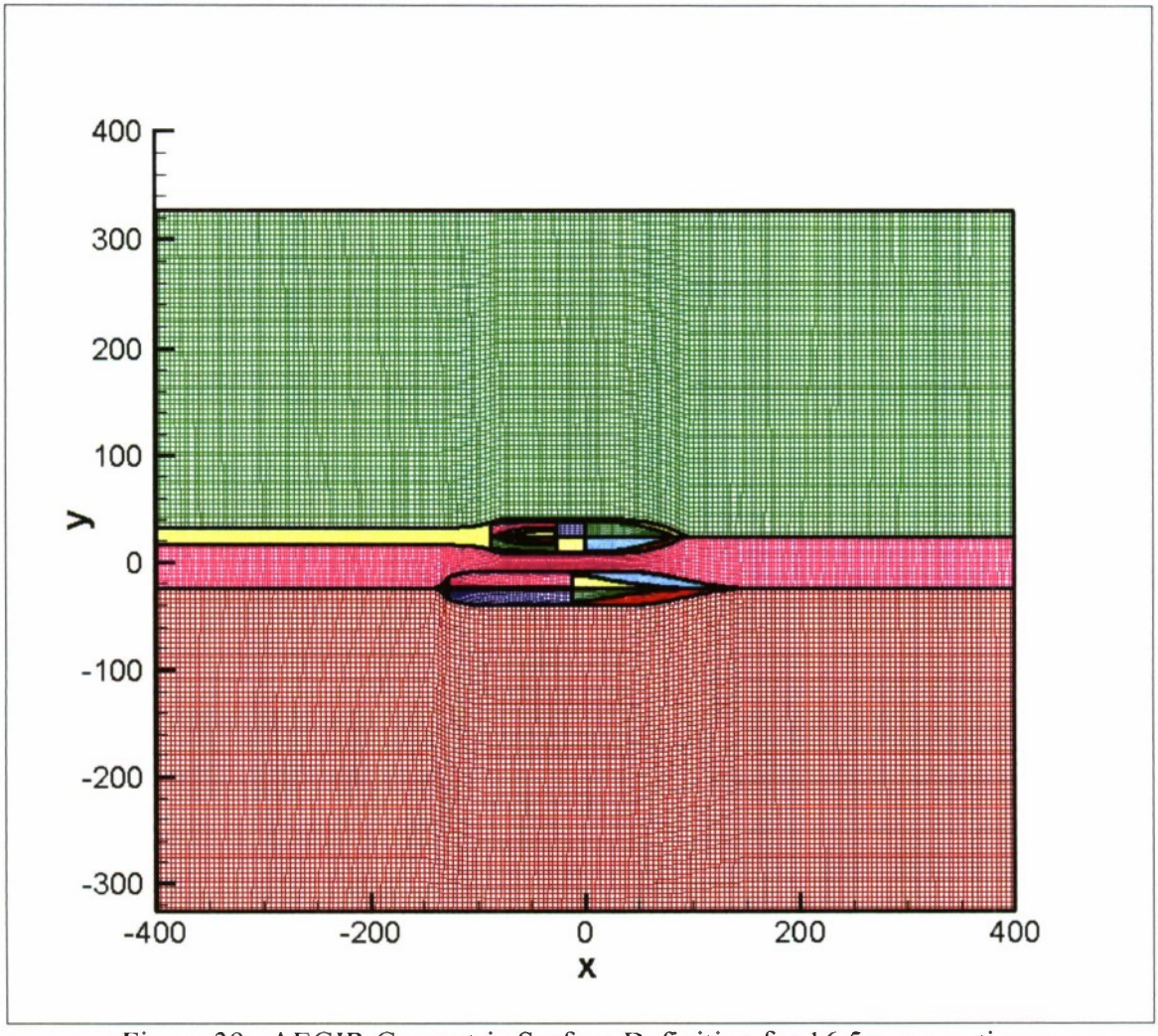

Figure 39. AEGIR Geometric Surface Definition for 16.5m separation case

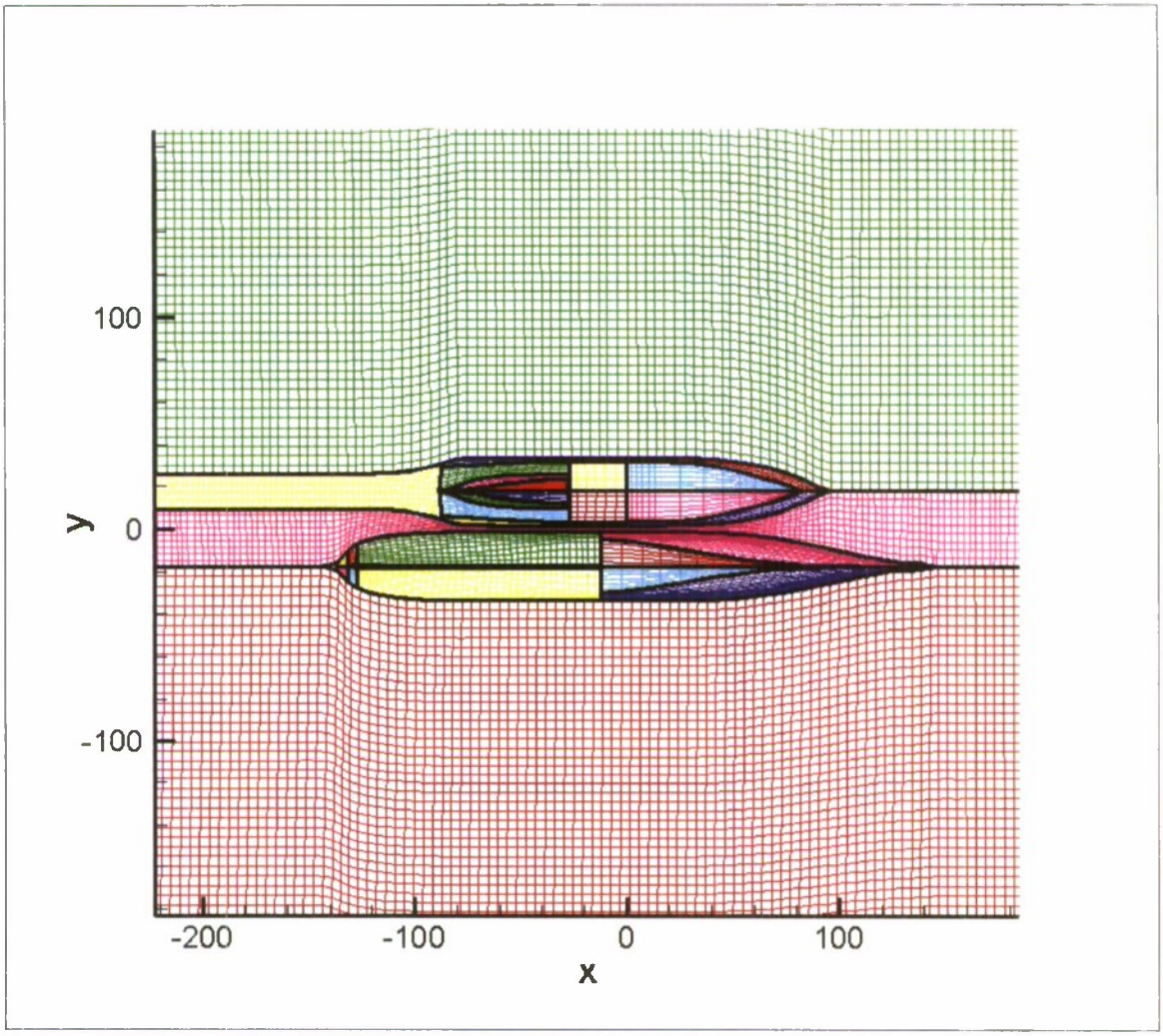

Figure 40. AEGIR Geometric Surface Definition for 3m separation case

In addition to the Rhino files containing the geometry, several ASCII files are also required to provide the values for each vessel such as speed, displacement, center of gravity, initial position, gyradii, constraints on degrees of freedom, etc. During the course of performing the AEGIR simulations, a few bugs were discovered which were fixed by the code developers. AEGIR is less mature than most of the other codes in the study, so this was not too unexpected when using the code for new applications such as multiple ships. In this study, the option to include non-linear Froude-Krylov and hydrostatic forces was not used, so a purely linear response was computed. For the 3m separation, 135° heading case, two different linearization schemes were used: the first was linearization about the undisturbed free stream flow (Neumann-Kelvin linearization), and the second was linearization about the "double body" flow, which is the flow that would result past the ships at constant speed if the water surface was replaced with a wall. For output, AEGIR produces a set of ASCII files in the TeePlot format, which provide the time histories of the motions and forces on each body. Harmonic analysis of

the time histories was performed using MatLab to compute the amplitude and phase of the transfer functions.

AEGIR RAO Amplitude and Phase Results and Observations

The correlation between the AEGIR simulations and the MARIN model test results are shown in Figures 41 and 42 for the case were the ships are traveling at five knots, separated by 3 meters at a wave heading of 135°, bow quartering seas with the BOBO on the leeward side. Plots showing the correlation for other combinations of forward speed, separation distance, and wave heading are shown in Appendix F. For the case shown in Figures 41 and 42, results from AEGIR are shown based both on the simpler Neumann-Kelvin linearization and the double body flow linearization, referred to as "AEGIR NK" and "AEGIR DB" respectively in the plot legend. The double body linearization should in theory capture more of the three dimensional flow effects. Comparing the results from the two forms of linearization indicated that this had negligible influence on the transfer function amplitude and phase predictions for this case.

In general AEGIR showed very good correlation with the MARIN data. Both the amplitude and phases were predicted reasonably well for the heave and pitch motion of both the HOPE and BOBO. As was the case for the other codes in the study, the correlation of AEGIR with the MARIN data was better for the pitch and heave motion transfer functions than it was for the force and moment transfer functions. However, the force and moment transfer functions also correlated reasonably well with the MARIN data for both amplitude and phase. The predictions for the HOPE correlated slightly better than for the BOBO across the board, but only by a couple percent. One would expect the interaction effects to be larger for the BOBO, which was on the leeward side and the smaller of the two vessels. The correlation for surge force amplitude was worse than for the other forces and moments, while the correlation for the yaw moment amplitude was the best. Overall the correlation for the moment amplitudes was better than for the force amplitudes. The correlation for phase is generally pretty good for both forces and moments with no bias seen in terms of which ship or force component is examined. On the average, phases were predicted within 40 degrees.

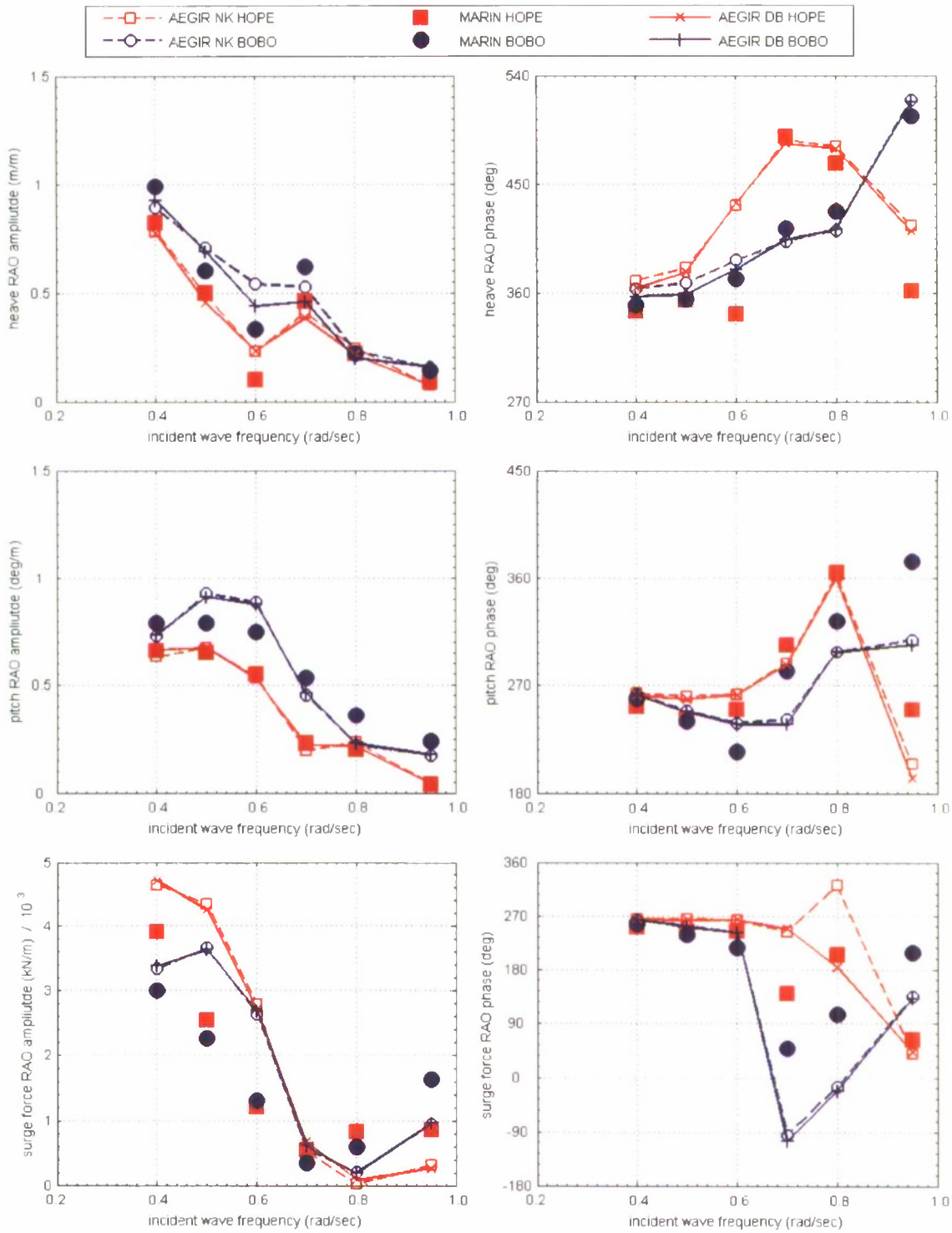

Figure 41. Heave, pitch and surge force RAOs for 3m separation, 135° heading, 5 knot ship speed. AEGIR results shown using Neumann-Kelvin linearization (AEGIR NK) and double body flow linearization (AEGIR DB).

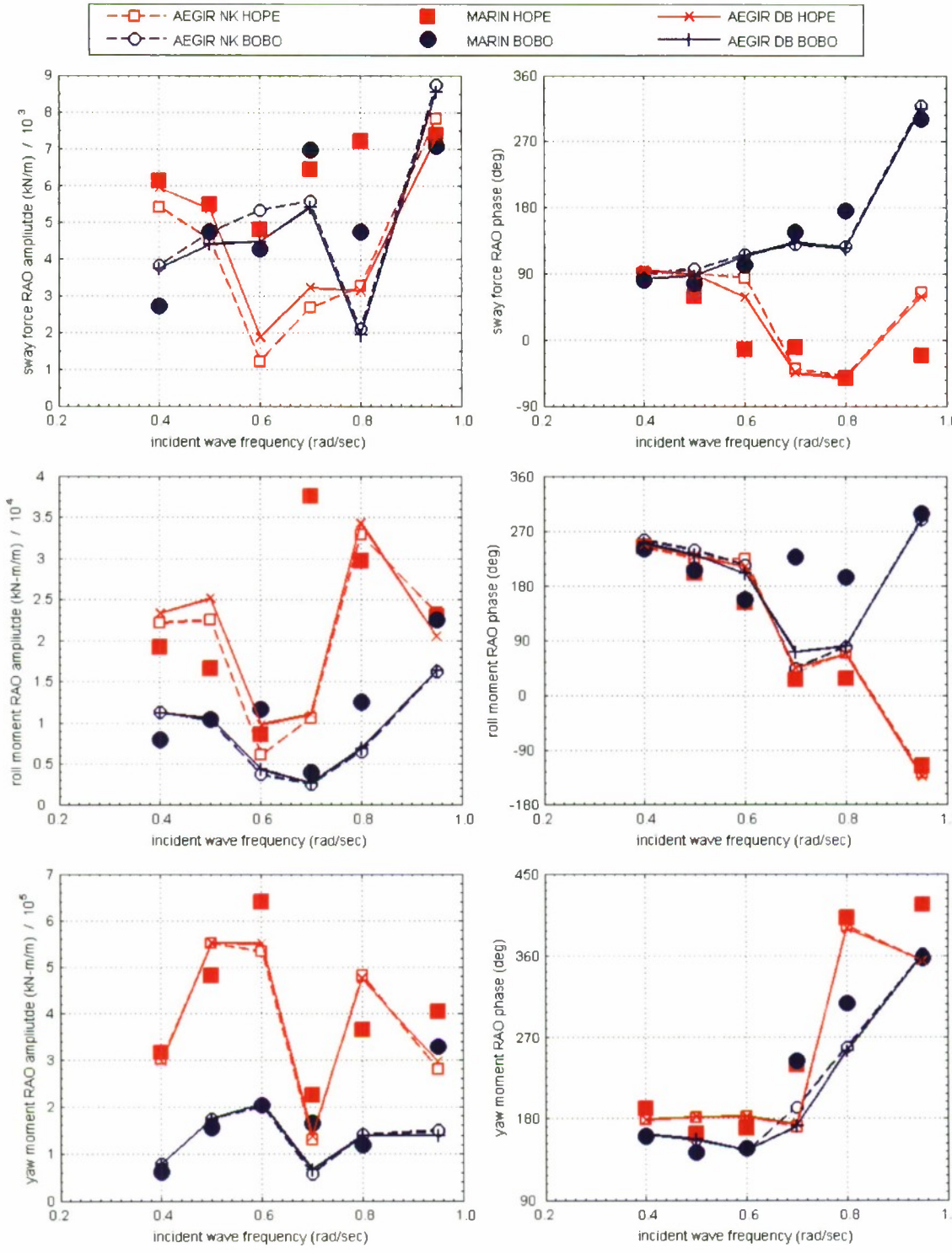

Figure 42. Sway force, yaw and roll moment RAOs for 3m separation, 135° heading, 5 knot ship speed. AEGIR results shown using both Neumann-Kelvin linearization (AEGIR NK) and double body flow linearization (AEGIR DB).

QUANTITATIVE CORRELATION – PERCENT DIFFERENCES

In order to quantitatively ascertain the degree of correlation of the predictions from each of the six programs to the model test results, percent difference tables were generated. The percent difference between the model test results and FD-Waveload predictions were also computed and are included in the tables. Although FD-Waveload was not one of the six codes selected for the correlation study, it was used to generate the input for the MVS and MVTDS tools, and represents the best correlation achievable by codes based on coefficients computed by FD-Waveload. The percent difference is calculated by first taking the difference between the predicted motion/force/moment RAO amplitude and phase at each frequency and the model test results. The resulting value for the amplitudes are then normalized by dividing the resulting difference by the largest value of amplitude over all headings and frequencies from the model test for the same separation distance and ship speed, referred to here as the baseline (see equation 14). The phase difference was normalized by dividing the result by 360 (see equation 15). The final results are then multiplied by 100 to yield the percent difference.

$$PD_{RAOAmplitude} = 100\frac{\Psi_{sim} - \Psi_{MARIN}}{\Psi_{baseline}} \tag{14}$$

$$PD_{RAOPhase} = 100\frac{\Psi_{sim} - \Psi_{MARIN}}{360} \tag{15}$$

For each of the six simulations used in this code evaluation, the percent differences were first calculated for each of the six model test frequencies of the RAO amplitude and phase of the motions, forces and moments for each of the eight model test conditions. They were calculated separately for each model, HOPE and BOBO. The signs for the percent difference were kept at this point to show if the motion, force, or moment was over or under predicted by the codes in comparison to the model test results. An example of the results of these percent difference calculations for the HOPE heave and pitch motion are shown in Tables 8 through 11. Tables 8 and 9 show heave motion RAO amplitude and phase respectively for the HOPE, and Tables 10 and 11 show the pitch motion RAO amplitude and phase respectively for the HOPE. Also in each of these tables is an average of the absolute values of the percent differences across the frequencies. This can help identify the simulation code that obtains the best overall correlation with the model test results for the particular ship and condition. A complete set of tables for both ships for each degree of freedom for all eight combinations of speed, heading and separation distance has been compiled and is available electronically in Excel format upon request from the authors. The complete list of tables was too large to include in the report. As can be seen, from just these two motions and one condition shown in Tables 8 through 11, the MVS-CSC and MVTDS correlate less well with the model test data than the other simulation codes, while FD-Waveload, which was used to generate the input force coefficients for both of those tools, correlates fairly well.

Table 8. Percent Difference of RAO Amplitudes for Heave Motion of HOPE
Test condition: 3 meter separation, 5 knots and 135 degree heading

HOPE - Heave Amplitude							
Freq (rad/s)	MVS	MVTDS	FD-Waveload	AQWA	ShipMo3D	LAMP	AEGIR
0.40	-27.48	17.88	-5.56	-11.35	-6.95	-2.72	-4.80
0.50	-25.08	43.41	0.53	-9.23	-0.73	-7.50	-1.47
0.60	16.37	82.82	-2.18	-0.34	-1.59	0.83	15.61
0.70	-11.40	31.52	0.98	0.29	-2.56	-3.01	-6.46
0.80	30.40	10.67	1.60	4.04	6.34	8.53	2.96
0.95	12.30	-9.45	17.45	-2.77	12.32	0.95	-1.72
Average	20.50	32.63	4.72	4.67	5.08	3.92	5.50

Table 9. Percent Difference of RAO Phase for Heave Motion of HOPE
Test condition: 3 meter separation, 5 knots and 135 degree heading

HOPE - Heave Phase							
Freq (rad/s)	MVS	MVTDS	FD-Waveload	AQWA	ShipMo3D	LAMP	AEGIR
0.40	-8.07	29.79	3.46	4.56	5.28	5.09	6.87
0.50	-19.36	15.77	-0.11	3.51	3.06	3.41	7.30
0.60	-38.90	3.65	26.61	34.72	25.56	19.97	24.95
0.70	7.57	24.08	-8.85	-1.46	-2.22	-0.64	-1.02
0.80	-4.93	19.74	-8.57	1.25	-1.94	0.03	4.06
0.95	-34.53	11.29	16.87	-42.14	15.28	4.93	15.22
Average	18.89	17.39	10.75	14.61	8.89	5.68	9.90

Table 10. Percent Difference of RAO Amplitude for Pitch Motion of HOPE
Test condition: 3 meter separation, 5 knots and 135 degree heading

HOPE - Pitch Amplitude							
Freq (rad/s)	MVS	MVTDS	FD-Waveload	AQWA	ShipMo3D	LAMP	AEGIR
0.40	-15.04	-9.42	-3.52	-9.31	-5.41	-3.39	-3.65
0.50	-21.81	9.58	4.12	5.87	1.06	2.12	2.87
0.60	-40.38	36.44	-5.53	-1.17	-5.95	-2.42	-2.14
0.70	-7.49	25.40	-1.05	-8.14	-2.53	-7.48	-4.17
0.80	16.76	-9.43	7.71	11.00	5.19	-3.90	4.07
0.95	11.63	13.56	12.52	21.72	28.22	-1.74	0.98
Average	18.85	17.31	5.74	9.54	8.06	3.51	2.98

Table 11. Percent Difference of RAO Phase for Pitch Motion of HOPE
Test condition: 3 meter separation, 5 knots and 135 degree heading

HOPE - Pitch Phase							
Freq (rad/s)	MVS	MVTDS	FD-Waveload	AQWA	ShipMo3D	LAMP	AEGIR
0.40	-45.49	-5.23	0.96	5.46	2.78	2.01	2.97
0.50	-44.71	-14.29	1.37	6.36	4.44	4.68	5.19
0.60	46.07	-26.44	-1.29	3.56	3.89	2.42	3.44
0.70	1.83	34.87	-6.67	0.17	-2.78	-2.52	-4.53
0.80	-14.88	-0.92	-12.67	-2.02	-4.17	-2.06	-0.77
0.95	48.67	-23.35	1.24	48.38	-3.61	38.09	-12.67
Average	33.61	17.52	4.03	10.99	3.61	8.63	4.93

To examine the quality of the correlation of the predicted output from the codes with the model test data and relative to each other for all six degrees of freedom for the 3-meter separation, 5 knot 135 degree heading case, the results for each degree of freedom were averaged over all the frequencies. This comparison is shown in Tables 12 through 15. Note that the absolute values of the percent differences are averaged over all frequencies, so any indication as to whether the codes over or underpredict the model test values is lost. Each row in Tables 12 through 15 is equivalent to the last "Average" row of a table in the format of Tables 8 though 11. For instance, the first row in Table 12 showing the average heave amplitude is the same as the last row in Table 8. It can be observed that the correlation for heave and pitch motions is better than for the forces and moments for both ships at this condition for every code included in the study. Also, by comparing Tables 11 and 12, it can be seen that all the codes with the exception of MVS and MVTDS predict the heave and pitch motions for the HOPE noticeably better than for the BOBO for this case. The BOBO was the smaller of the two ship and was on the leeward side, so it would be expected that the ship interaction effects would be have a greater influence on the BOBO. These trends were also observed for the other seven conditions that were examined. Tables showing the percent differences averaged over the frequency range for each ship and degree of freedom for the other seven conditions are included in Appendix G.

One measure of the quality of the correlation is to relate the percent differences listed in Tables 12 and 13 to the model test 95% confidence limits listed in Table 7b, which are normalized in the same manner as the percent difference values. The model test U95% values ranged from 1 to 5 percent. By this measure the heave and pitch predictions for HOPE can be judged as good for all the codes other than MVS and MVTDS as their the percent difference values fall within or are close to the 95% confidence limits of the experimental uncertainty. The percent difference values for the heave and pitch amplitude predictions for BOBO are about twice the U95% values. The percent difference values for the predictions of the surge, sway, roll and yaw amplitudes are all much larger than the U95% values listed in Table 7b. There is also uncertainty in the computational values. This was touched upon briefly in the discussion of the LAMP code, by examining the influence of gridding and comparing independent LAMP calculations for the same cases performed at SAIC and NSWCCD. However, no quantitative analysis of the computational uncertainty was performed during the current study.

Table 12. Percent Difference for motion, force and moment amplitudes for HOPE, test condition: 3 meter separation, 5 knots and 135 degree heading.

Amplitude Percent Differences for HOPE							
	MVS	MVTDS	FD-Waveload	AQWA	ShipMo3D	LAMP	AEGIR
Heave	20.50	32.63	4.72	4.67	5.08	3.92	5.50
Pitch	18.85	17.31	5.74	9.54	8.06	3.51	2.98
Surge	9.41	24.80	14.49	14.75	15.71	20.40	20.98
Sway	28.61	31.31	48.49	37.30	20.95	20.09	17.62
Roll	26.81	23.50	38.32	32.13	211.04	15.63	18.57
Yaw	35.75	20.40	24.43	23.45	363.46	16.31	13.71

Table 13. Percent Difference for motion, force and moment amplitudes for BOBO, test condition: 3 meter separation, 5 knots and 135 degree heading.

Amplitude Percent Differences for BOBO							
	MVS	MVTDS	FD-Waveload	AQWA	ShipMo3D	LAMP	AEGIR
Heave	20.89	33.81	13.96	12.78	10.76	8.43	9.00
Pitch	20.26	26.25	12.30	12.18	20.88	8.34	10.33
Surge	10.31	28.49	18.73	22.97	31.53	22.87	20.72
Sway	38.54	28.46	74.90	55.87	12.38	27.69	18.62
Roll	20.39	27.77	14.87	22.27	298.71	20.46	17.81
Yaw	18.25	15.40	31.93	30.78	818.29	23.84	17.57

Table 14. Percent Difference for motion, force and moment phases for HOPE, test condition: 3 meter separation, 5 knots and 135 degree heading.

Phase Percent Differences for HOPE							
	MVS	MVTDS	FD-Waveload	AQWA	ShipMo3D	LAMP	AEGIR
Heave	18.89	17.39	10.75	14.61	8.89	5.68	9.90
Pitch	33.61	17.52	4.03	10.99	3.61	8.63	4.93
Surge	9.92	37.70	26.08	20.43	14.86	13.52	13.58
Sway	27.12	27.40	43.24	8.16	14.63	8.58	11.56
Roll	23.39	20.09	38.50	7.41	27.08	12.30	7.45
Yaw	20.73	31.15	33.25	15.67	33.98	14.85	8.38

Table 15. Percent Difference for motion, force and moment phases for BOBO, test condition: 3 meter separation, 5 knots and 135 degree heading.

Phase Percent Differences for BOBO							
	MVS	MVTDS	FD-Waveload	AQWA	ShipMo3D	LAMP	AEGIR
Heave	16.27	33.39	19.01	6.66	4.21	3.67	3.77
Pitch	26.85	25.97	21.47	10.83	4.40	12.12	7.72
Surge	24.67	24.80	34.50	15.55	20.32	14.83	17.77
Sway	22.05	27.21	40.21	20.14	35.79	4.90	5.83
Roll	34.65	27.44	37.06	19.62	25.23	8.25	18.80
Yaw	28.31	35.50	36.57	17.98	31.48	9.25	5.69

Overall Average Percent Difference

To obtain a measure of how well the simulations correlate with the model test results over the eight conditions, the percent differences were averaged over the motions (heave and pitch), forces (surge and sway) and moments (roll and yaw) that were measured. The results of this averaging for amplitudes are shown in Table 16 and for phase in Table 17. While it is impossible to condense the entire correlation study down to a single numerical value for each code, Tables 16 and 17 give a concise overall indication of how well each tool correlated with the model test data. These tables show the MVS-CSC and MVTDS amplitudes correlate the least well with the model test data except for ShipMo3D which correlates the least well of any of the simulation predictions for the roll and yaw moment amplitudes. The methods based on Rankine panel methods, LAMP and AEGIR, show the best overall correlation for motion, force and moment amplitudes. The phase correlation is quite different in that, over all the simulation codes, the correlation was rather uniform, about 15 to 25 percent difference.

Table 16. Percent Difference of RAO Amplitudes Averaged Over All Eight Model Test Conditions for Both the HOPE and BOBO

Motion Amplitudes for Heave and Pitch							
	MVS	MVTDS	FD-Waveload	AQWA	ShipMo3D	LAMP	AEGIR
HOPE	27.83	39.90	11.48	8.56	7.20	5.90	6.02
BOBO	30.91	43.86	20.93	12.91	12.49	7.99	8.16
Both Ships	29.37	41.88	16.20	10.73	9.84	6.94	7.09
Force Amplitudes for Surge and Sway							
	MVS	MVTDS	FD-Waveload	AQWA	ShipMo3D	LAMP	AEGIR
HOPE	57.87	78.90	28.18	35.56	35.99	27.82	27.01
BOBO	77.52	91.16	32.64	41.01	38.31	29.57	31.97
Both Ships	67.70	85.03	30.41	38.28	37.15	28.70	29.49
Moment Amplitudes for Roll and Yaw							
	MVS	MVTDS	FD-Waveload	AQWA	ShipMo3D	LAMP	AEGIR
HOPE	58.23	72.22	24.04	28.32	161.32	14.18	14.36
BOBO	50.79	58.95	33.23	42.50	288.19	18.42	18.08
Both Ships	54.51	65.59	28.64	35.41	224.76	16.30	16.22
Average Percent Difference for All Amplitudes							
	MVS	MVTDS	FD-Waveload	AQWA	ShipMo3D	LAMP	AEGIR
HOPE	47.97	63.67	21.23	24.14	68.17	15.97	15.79
BOBO	53.07	64.66	28.93	32.14	113.00	18.66	19.40
Both Ships	50.52	64.16	25.08	28.14	90.58	17.31	17.60

Table 17. Percent Difference of RAO Phase Angles Averaged Over All Eight Model Test Conditions for Both the HOPE and BOBO

Phase of Heave and Pitch Motion							
	MVS	MVTDS	FD-Waveload	AQWA	ShipMo3D	LAMP	AEGIR
HOPE	23.53	26.42	13.17	9.95	10.20	9.50	8.57
BOBO	25.35	22.86	18.41	10.20	11.54	9.09	11.47
Both Ships	24.44	24.64	15.79	10.07	10.87	9.30	10.02
Phase of Surge and Sway Force							
	MVS	MVTDS	FD-Waveload	AQWA	ShipMo3D	LAMP	AEGIR
HOPE	24.54	23.77	19.45	18.78	23.36	16.37	18.78
BOBO	26.04	24.99	19.84	16.98	27.35	17.20	18.68
Both Ships	25.29	24.38	19.64	17.88	25.36	16.78	18.73
Phase of Yaw and Roll Moments							
	MVS	MVTDS	FD-Waveload	AQWA	ShipMo3D	LAMP	AEGIR
HOPE	24.39	25.75	17.60	17.75	25.60	18.43	19.18
BOBO	27.27	26.70	24.45	20.97	24.40	19.82	21.96
Both Ships	25.83	26.22	21.02	19.36	25.00	19.13	20.57
Average Percent Difference for All Phases							
	MVS	MVTDS	FD-Waveload	AQWA	ShipMo3D	LAMP	AEGIR
HOPE	24.15	25.31	16.74	15.49	19.72	14.77	15.51
BOBO	26.22	24.85	20.90	16.05	21.10	15.37	17.37
Both Ships	25.19	25.08	18.82	15.77	20.41	15.07	16.44

SUMMARY

Six multi-vessel motion prediction codes were evaluated to determine their utility in predicting the motions of ships in close proximity in a seaway. First the features of each code were compared against a matrix of required capabilities. The result of this evaluation showed the following. First, all codes can model the important environmental factors that influence ship motions in the seabase. Second, all codes can accommodate two or more vessels in close proximity with the geometry of these hulls vessels either monohull or multi-hull forms and configured in any arbitrary steady state arrangement. Modifications to all the codes are required to model SES, ACV, and forces from ramps and cranes. Third, LAMP-MULTI and AEGIR are capable of modeling the non-linear free surface boundary condition, whereas all the other codes use the free stream linearized free surface condition. Additionally, AQWA, ShipMo3D, LAMP-MULTI, and AEGIR are capable of including body nonlinear hydrostatic and Froude-Krylov wave forces. Finally, to account for the non-hydrodynamic forces and controls, LAMP-MULTI, AEGIR and AQWA allow for user supplied force routines in the time domain. Only AQWA, LAMP-MULTI, MVS and MVTDS include some built-in models for mooring lines and fenders. The autopilot feature for multiple ships and the ability to simulate overtaking scenarios can only be exercised in the MVS and MVTDS codes.

The output from each of the six codes was also correlated with specific conditions from a model test. The result of this correlation showed the following trends. First, for pitch and heave RAO amplitude correlation, LAMP-MULTI, AEGIR, AQWA, and ShipMo3D resulted in only 10% difference from the model tests whereas the MVS and MVTDS were on the order of 30% variability. The surge and sway force and roll and yaw moment amplitude correlation resulted in LAMP-MULTI and AEGIR predictions being roughly 20% different from the model test, with AQWA being 35% different, the MVS and MVTDS codes 60 and 75 percent off, and finally ShipMo3D is 130% off from the model test results. For phase correlation, pitch and heave were uniformly 10% off for all the codes except the two MVS codes which were roughly 25% off. The force and moment phases were uniformly 20 to 25 % off of the model test results with LAMP-MULTI being the best at 17%.

The final findings of this evaluation showed that the codes with more sophisticated methodology in predicting the motions yielded better prediction results by a small margin. Some of the more sophisticated codes are still in the developmental stages and therefore do not have all the functions of more mature codes. Additionally, MVS and MVTDS were developed to predict the motions for the unsteady case which this evaluation did not cover. Finally, between January 1, 2008 and the date of this report, the CSC MVS code was substantially reworked and that could potentially improve its results.

ACKNOWLEDGEMENTS

The authors would like to thank Dr. Paul Hess of ONR for his support and guidance through this study. He also suggested which multiple vessel motion codes to include in the study and suggested the concept of a capability matrix. The authors also acknowledge Dr. Geoff Main, Ms. Kelly Cooper and Ms. Katherine Mangum for their support of the study. Finally Dr. John O'Dea and Professor J. Nicholas Newman are acknowledged for their technical guidance to the authors with Dr. O'Dea's initial work

with WAMIT and Professor Newman's explanation of trapped waves between the vessels and the concept of applying the lid to account for viscous damping not present in the potential flow codes that were investigated.

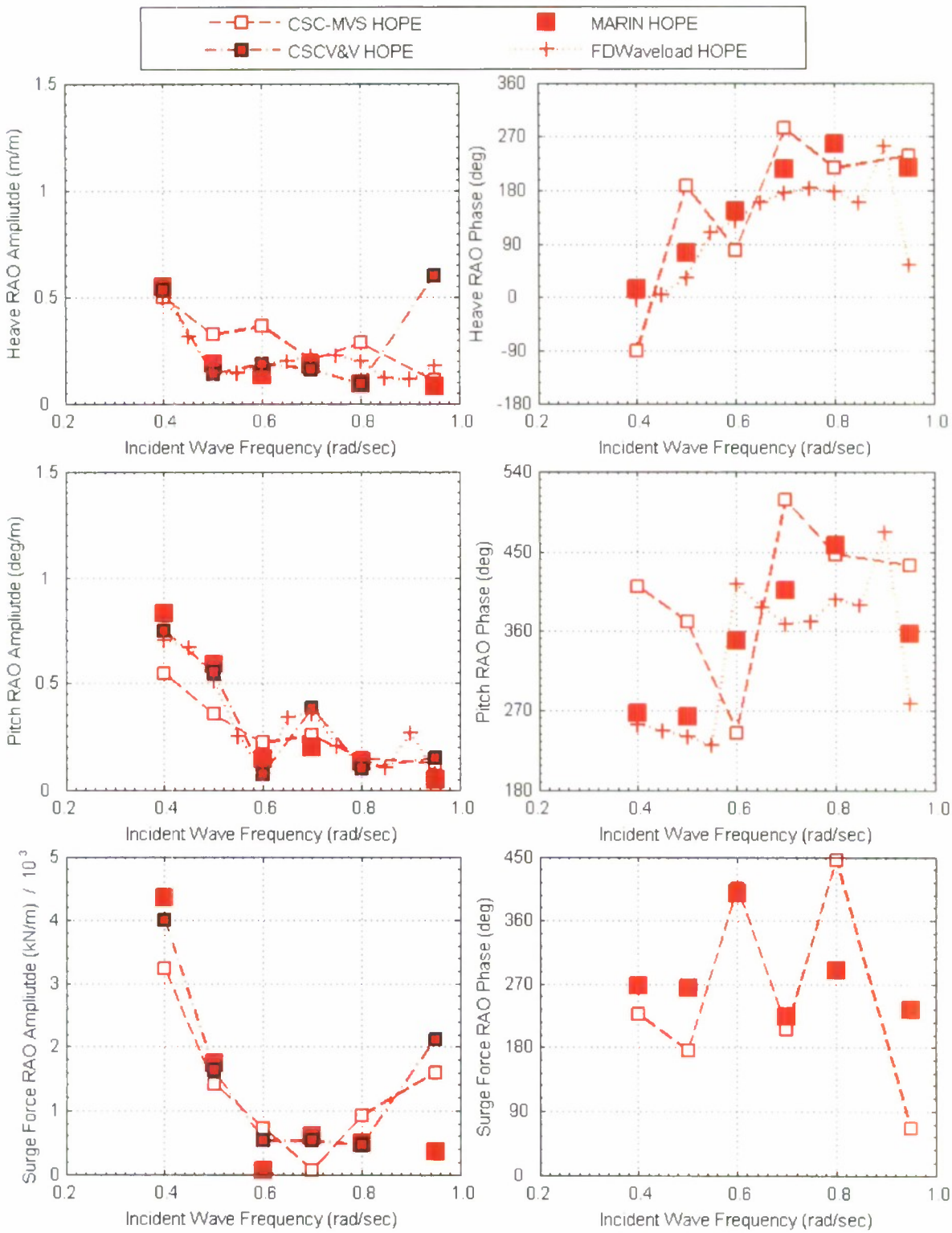

Figure A1. HOPE Heave and Pitch Motion and Surge Force RAO Amplitude and Phase for 3 meter separation, 180 degree wave heading, and 5 knots ship speed.

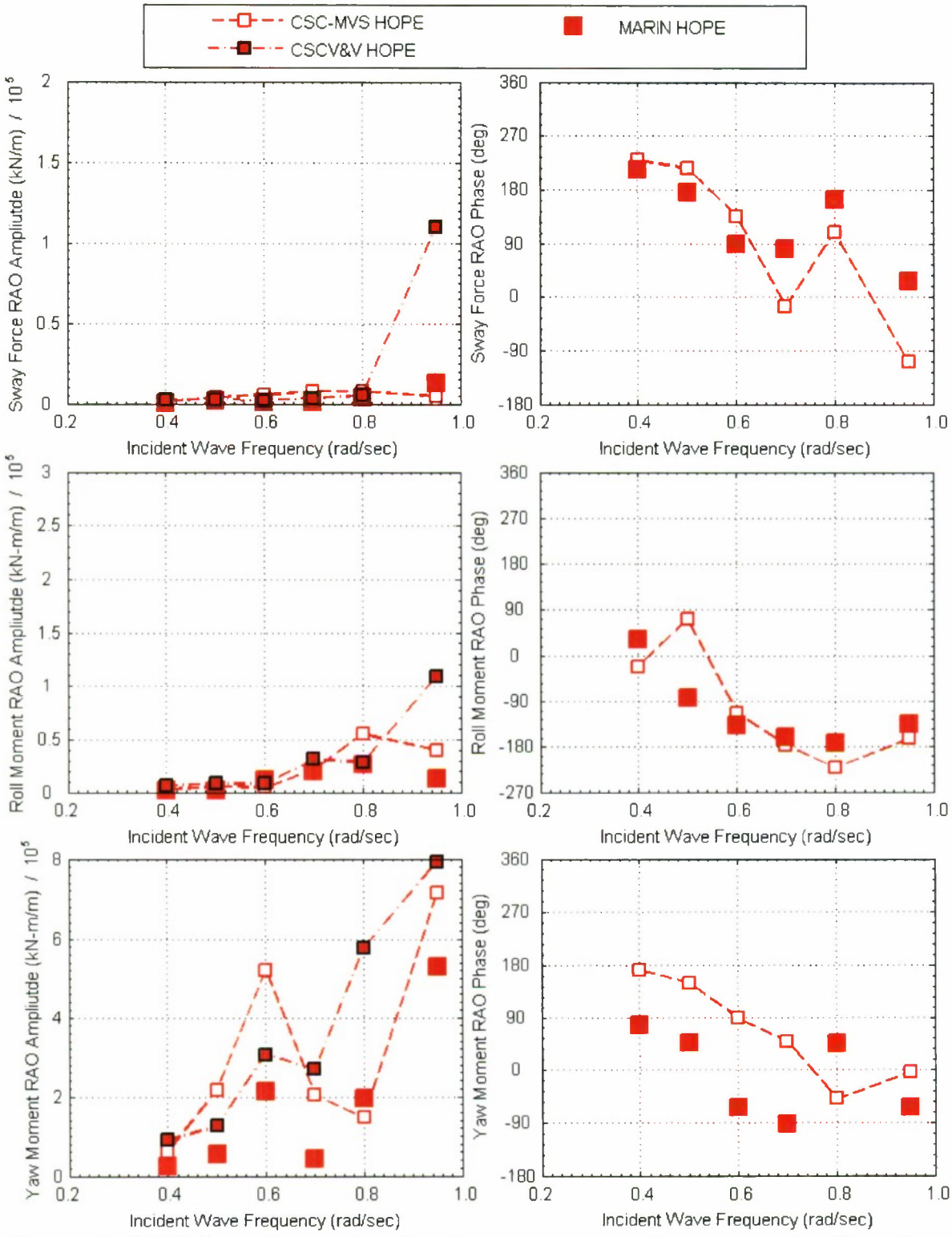

Figure A2. HOPE Sway Force and Roll and Yaw Moment RAO Amplitude and Phase for 3 meter separation, 180 degree wave heading, and 5 knots ship speed.

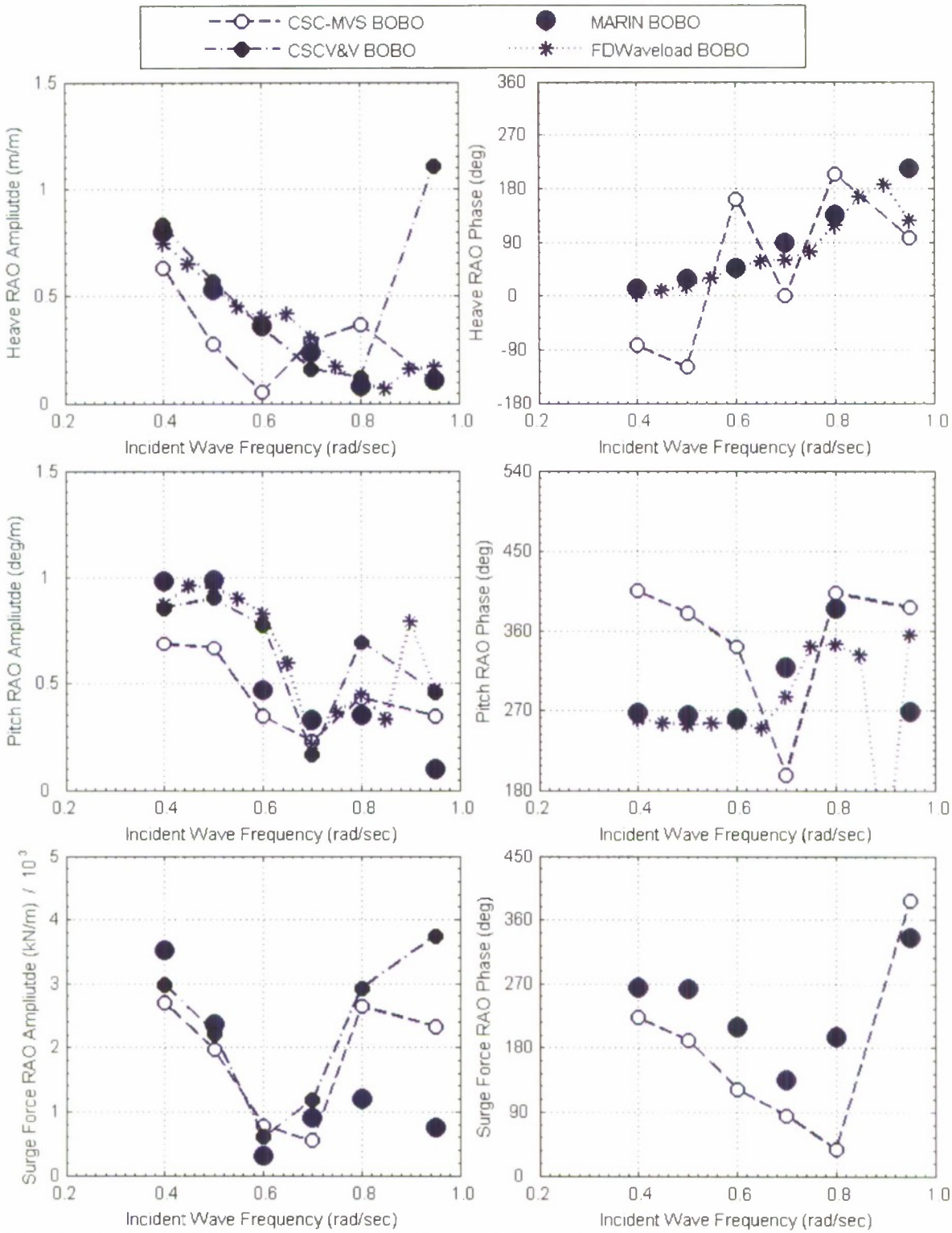

Figure A3. BOBO Heave and Pitch Motion and Surge Force RAO Amplitude and Phase for 3 meter separation, 180 degree wave heading, and 5 knots ship speed.

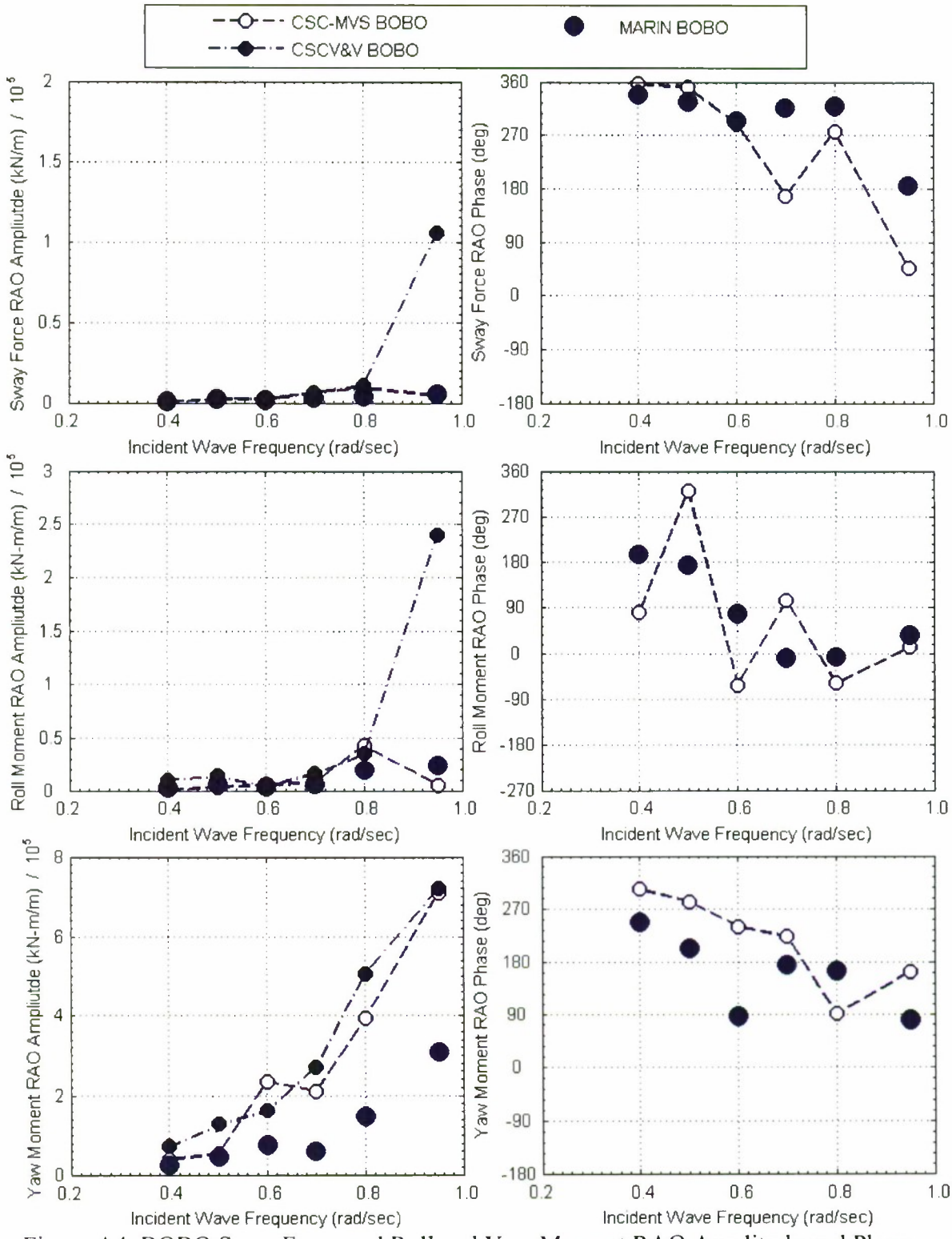

Figure A4. BOBO Sway Force and Roll and Yaw Moment RAO Amplitude and Phase for 3 meter separation, 180 degree wave heading, and 5 knots ship speed.

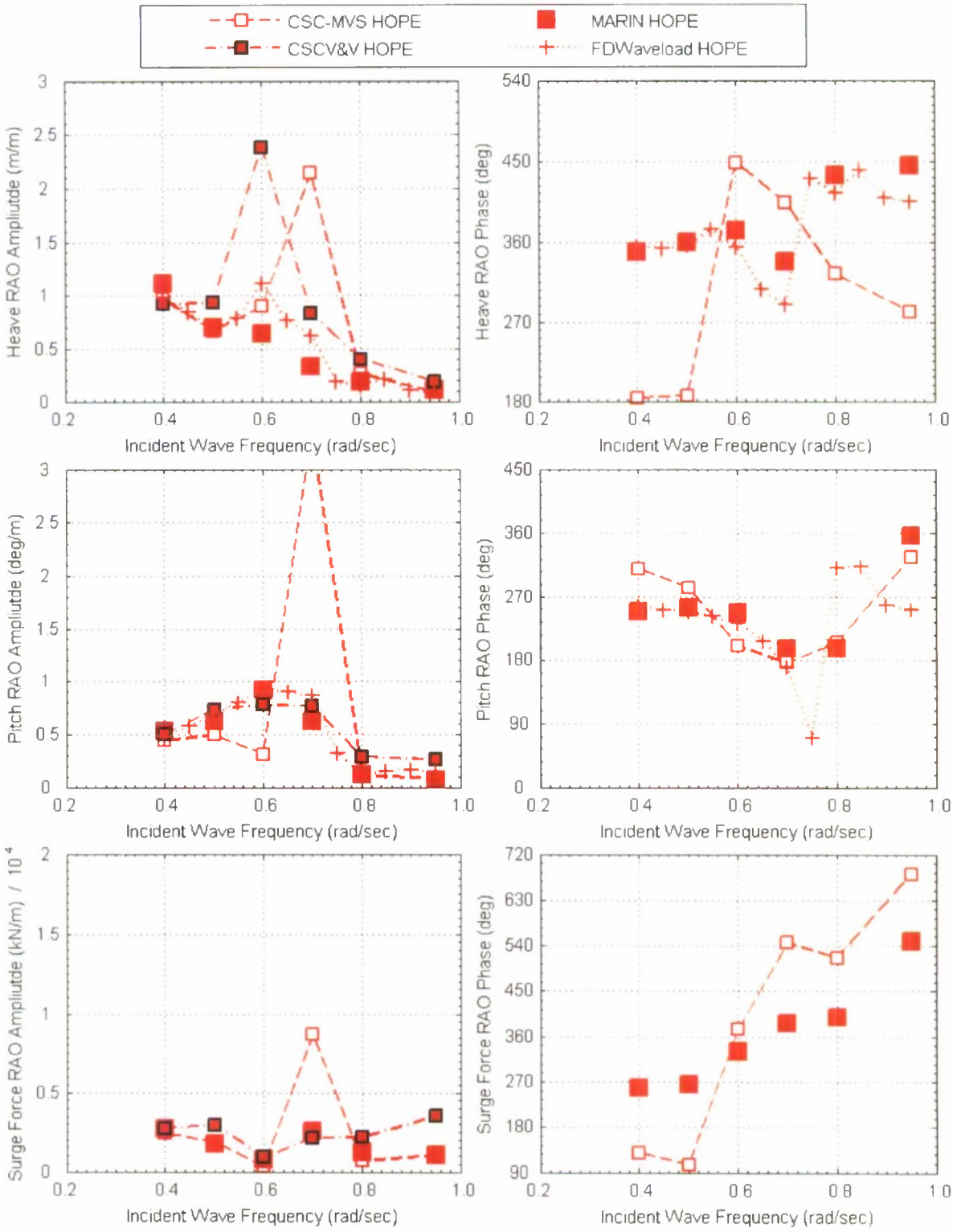

Figure A5. HOPE Heave and Pitch Motion and Surge Force RAO Amplitude and Phase for 16.5 meter separation, 120 degree wave heading, and 16 knots ship speed.

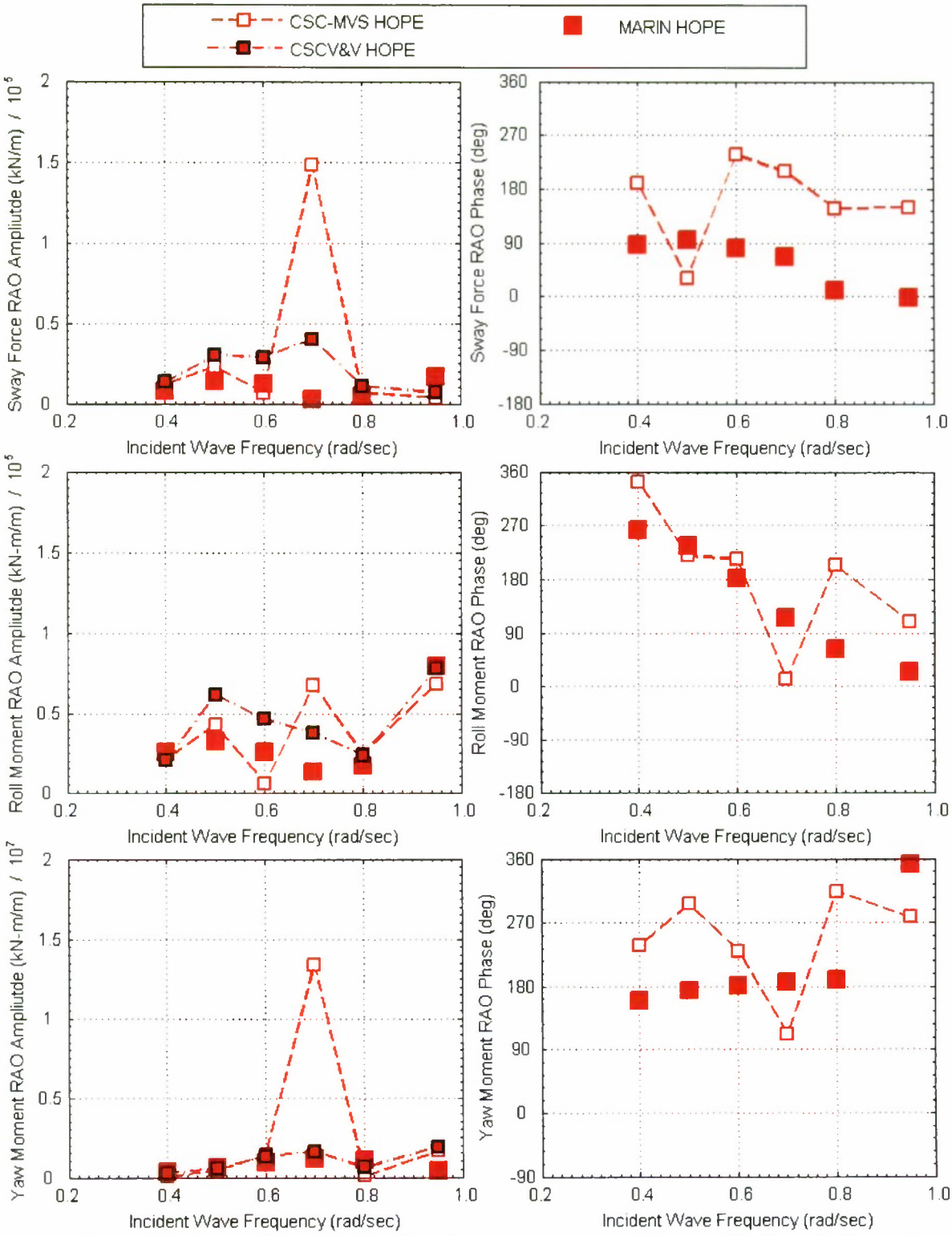

Figure A6. HOPE Sway Force and Roll and Yaw Moment RAO Amplitude and Phase for 16.5 meter separation, 120 degree wave heading, and 16 knots ship speed.

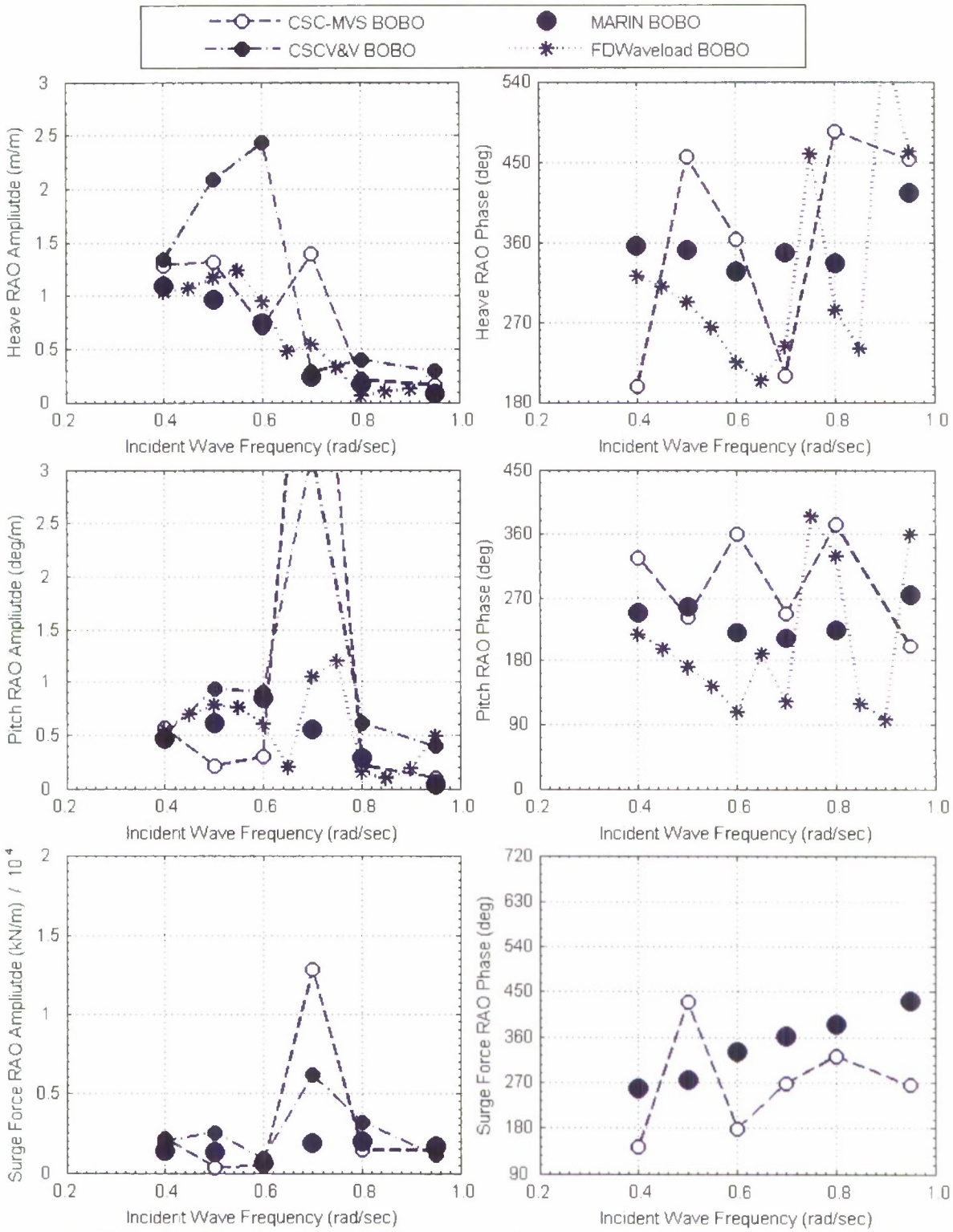

Figure A7. BOBO Heave and Pitch Motion and Surge Force RAO Amplitude and Phase for 16.5 meter separation, 120 degree wave heading, and 16 knots ship speed.

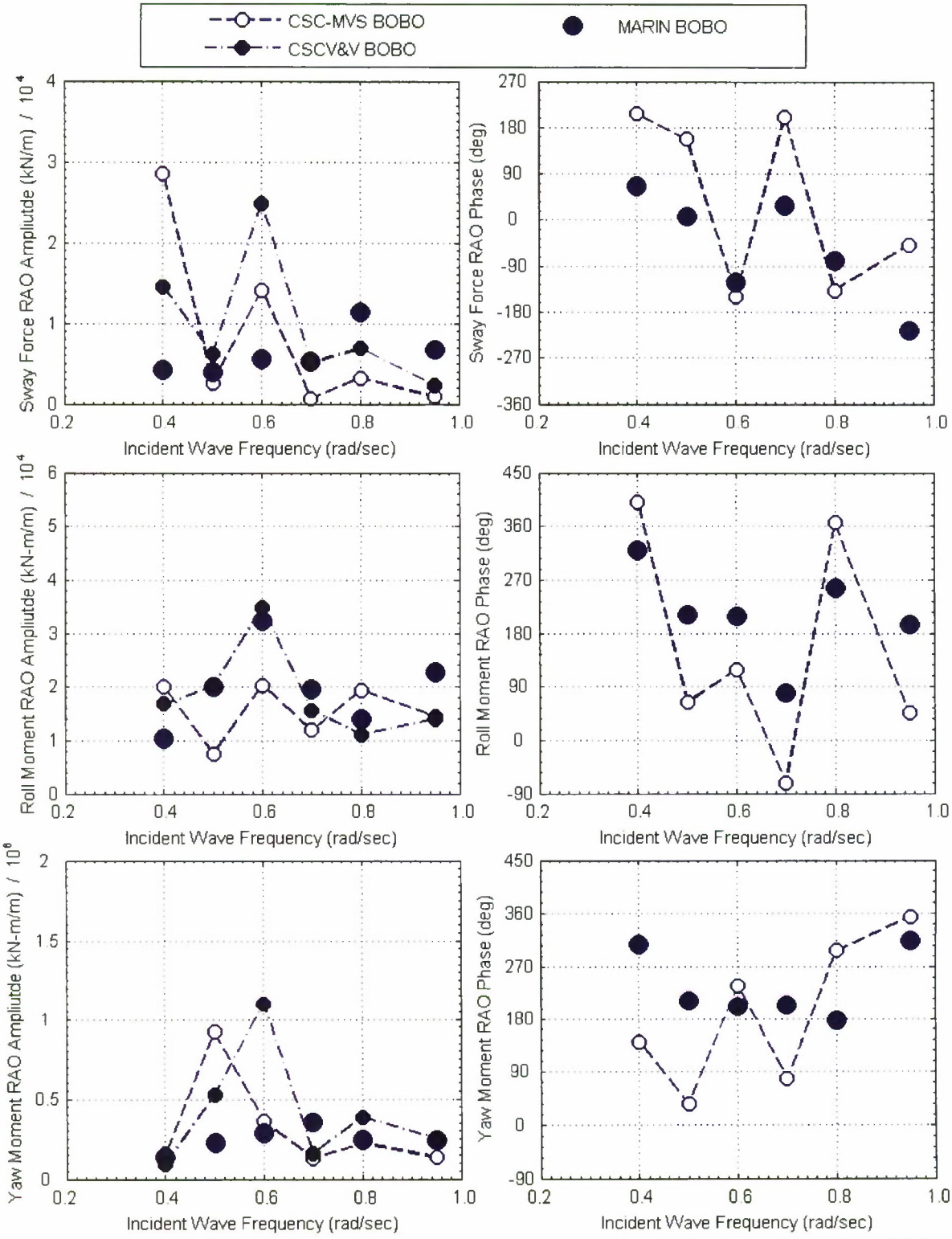

Figure A8. BOBO Sway Force and Roll and Yaw Moment for 16.5 meter separation, 120 degree wave heading, and 16 knots ship speed.

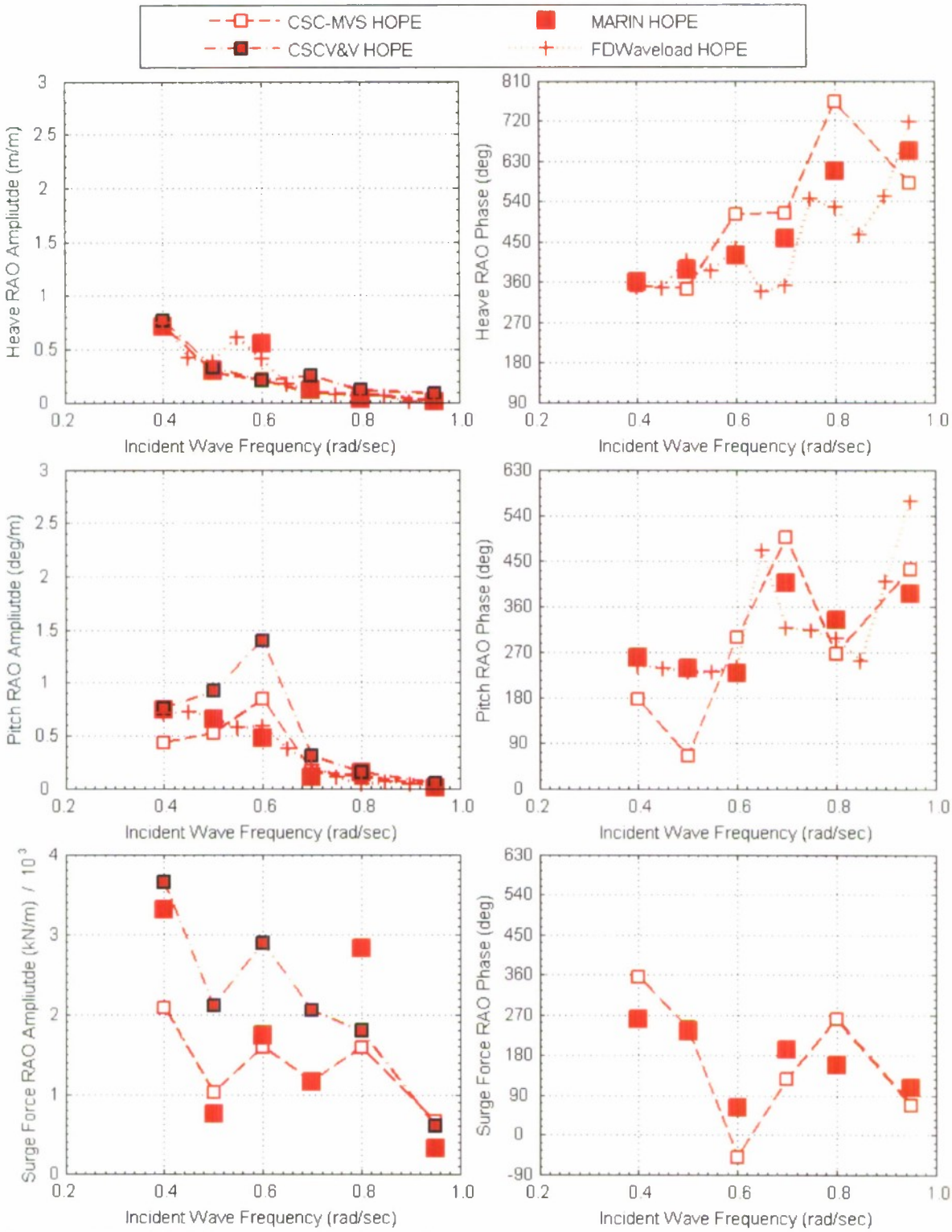

Figure A9. HOPE Heave and Pitch Motion and Surge Force RAO Amplitude and Phase for 16.5 meter separation, 150 degree wave heading, and 16 knots ship speed.

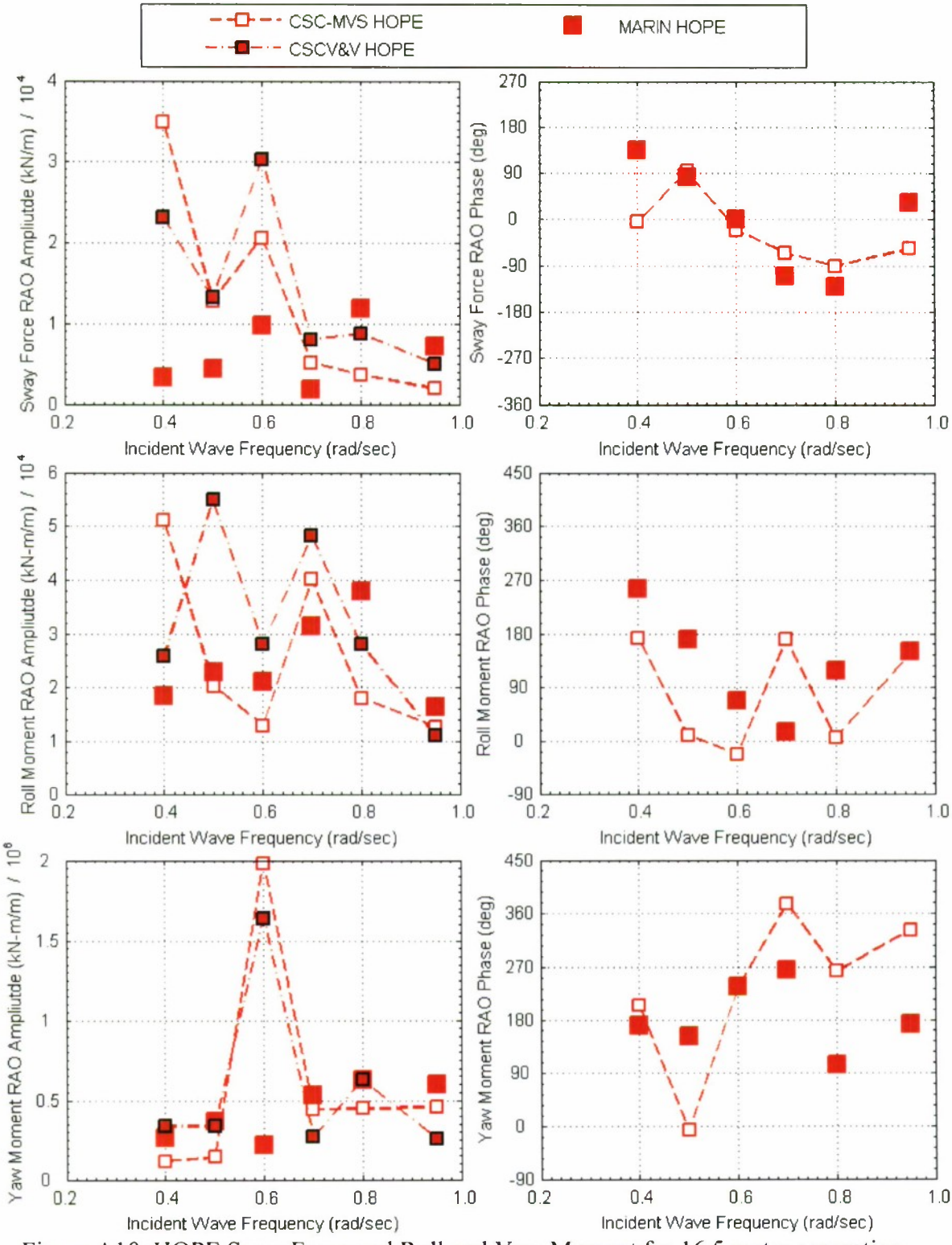

Figure A10. HOPE Sway Force and Roll and Yaw Moment for 16.5 meter separation, 150 degree wave heading, and 16 knots ship speed.

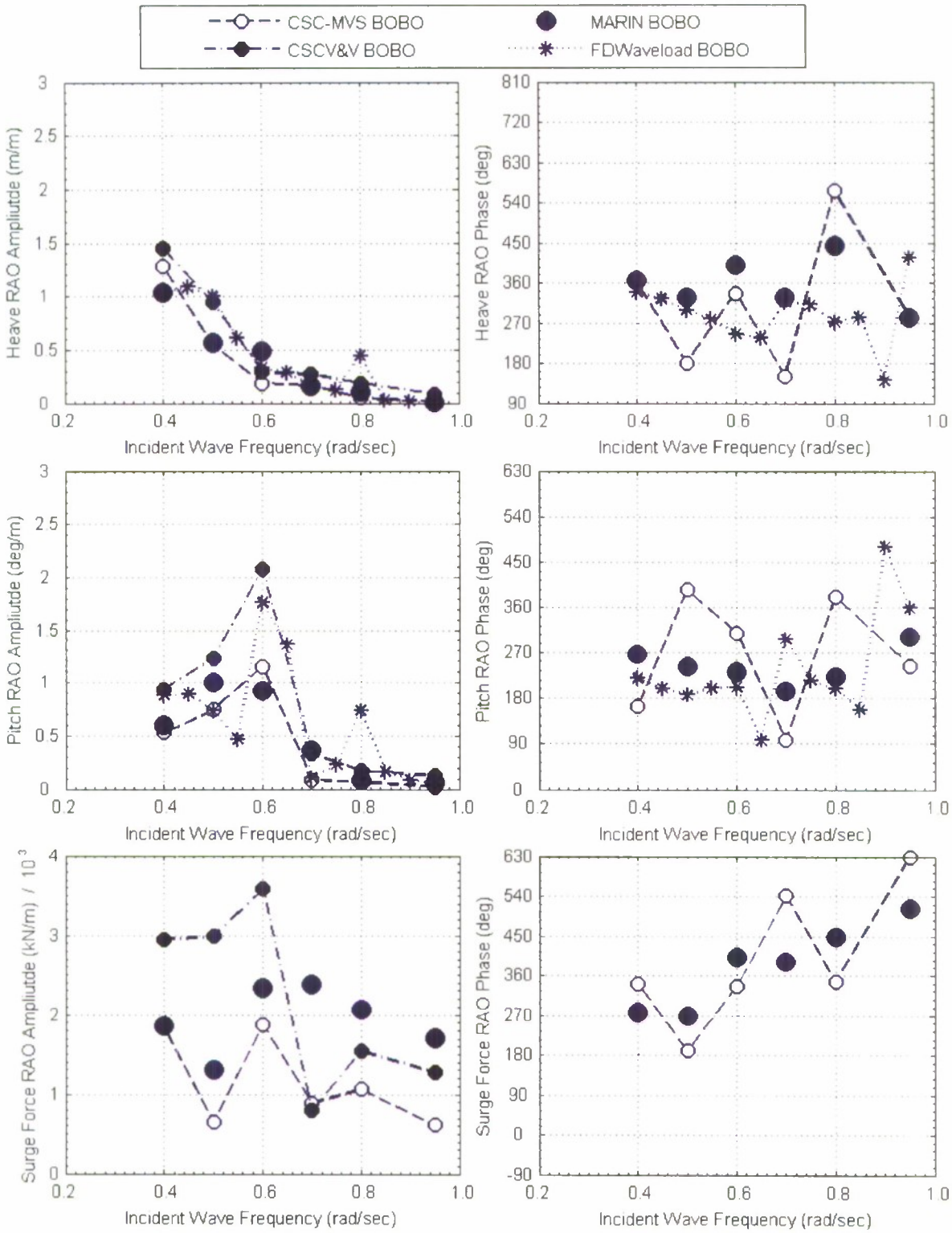

Figure A11. BOBO Heave and Pitch Motion and Surge Force RAO Amplitude and Phase for 16.5 meter separation, 150 degree wave heading, and 16 knots ship speed.

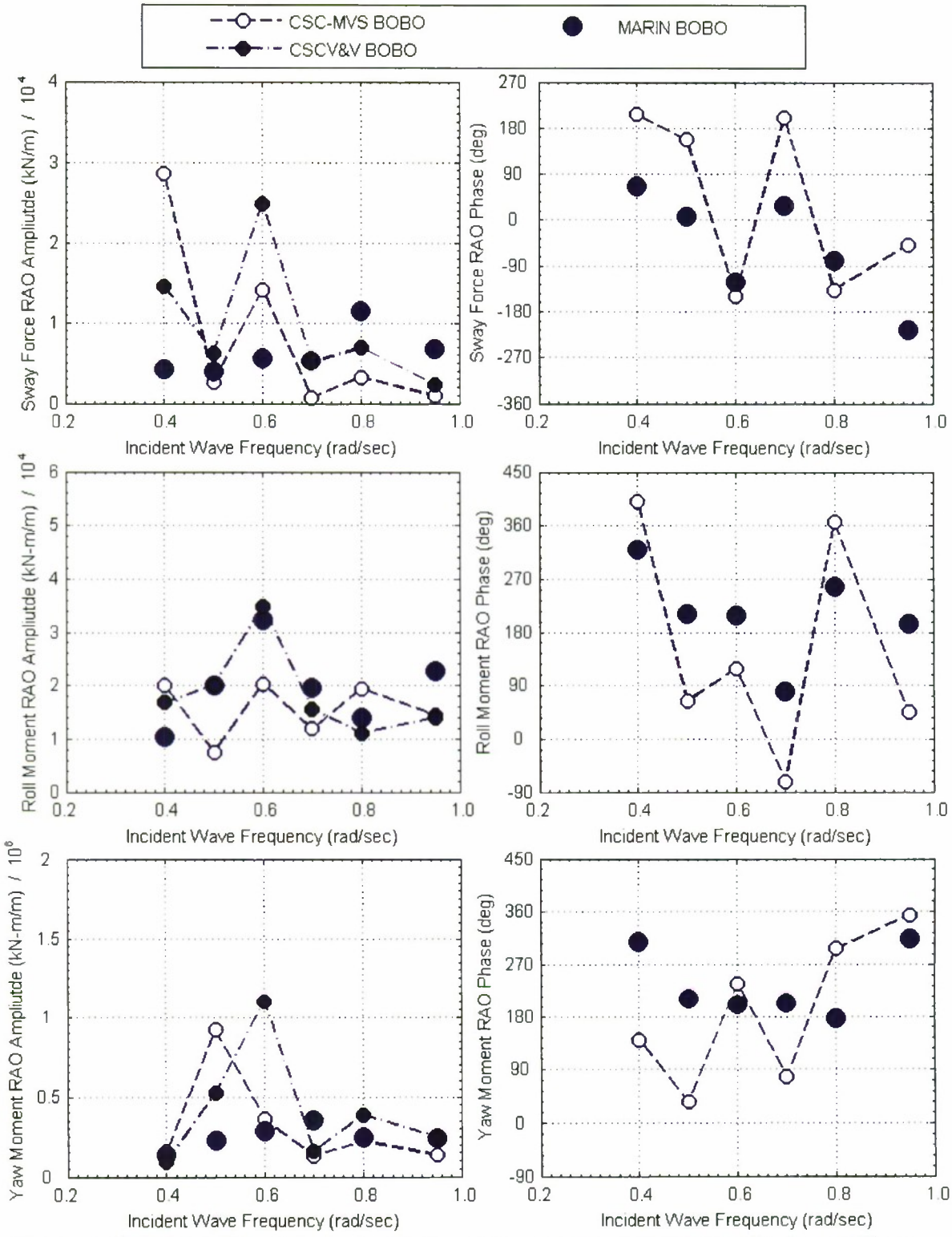

Figure A12. BOBO Sway Force and Roll and Yaw Moment RAO Amplitude and Phase for 16.5 meter separation, 150 degree wave heading, and 16 knots ship speed.

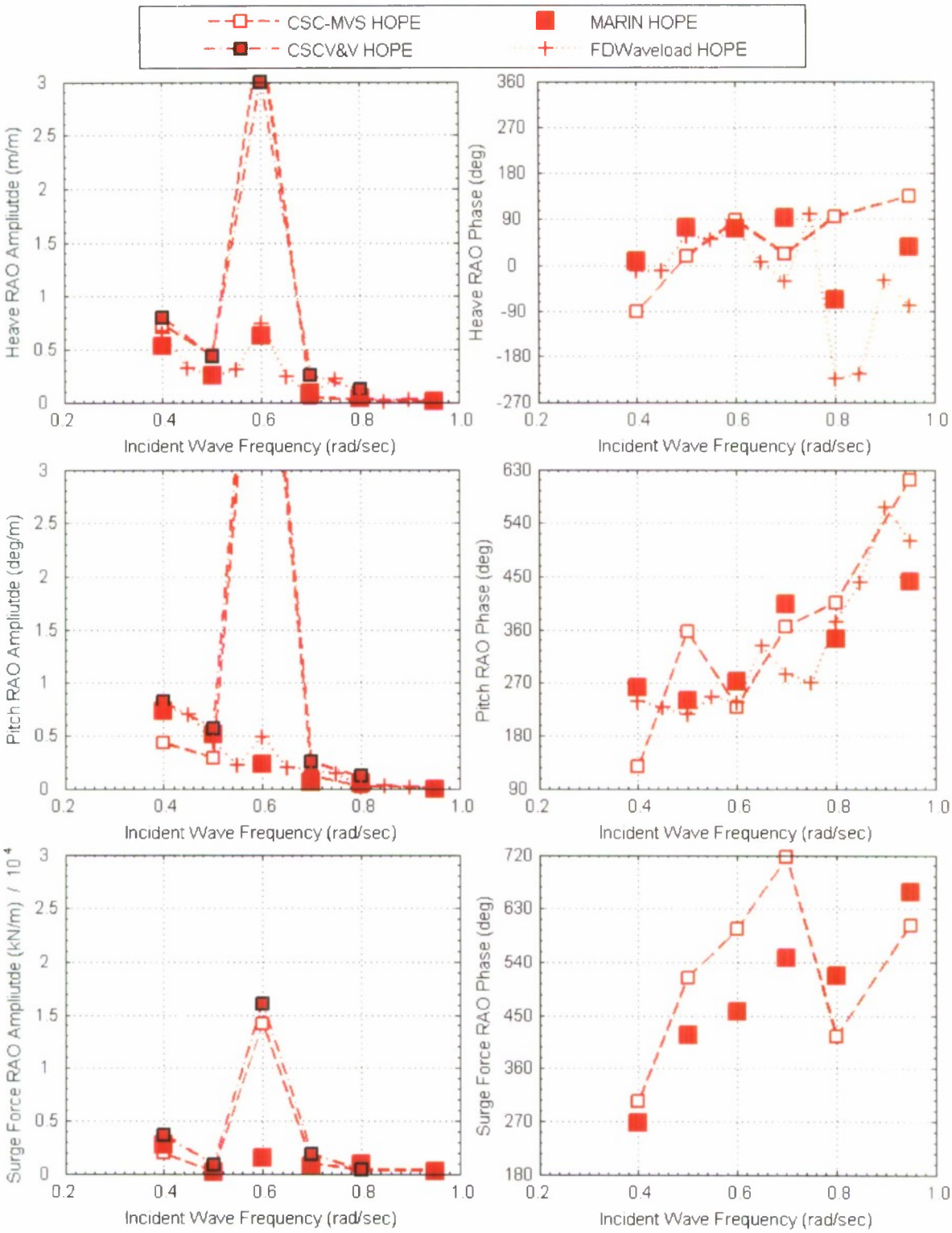

Figure A13. HOPE Heave and Pitch Motion and Surge Force RAO Amplitude and Phase for 16.5 meter separation, 180 degree wave heading, and 16 knots ship speed.

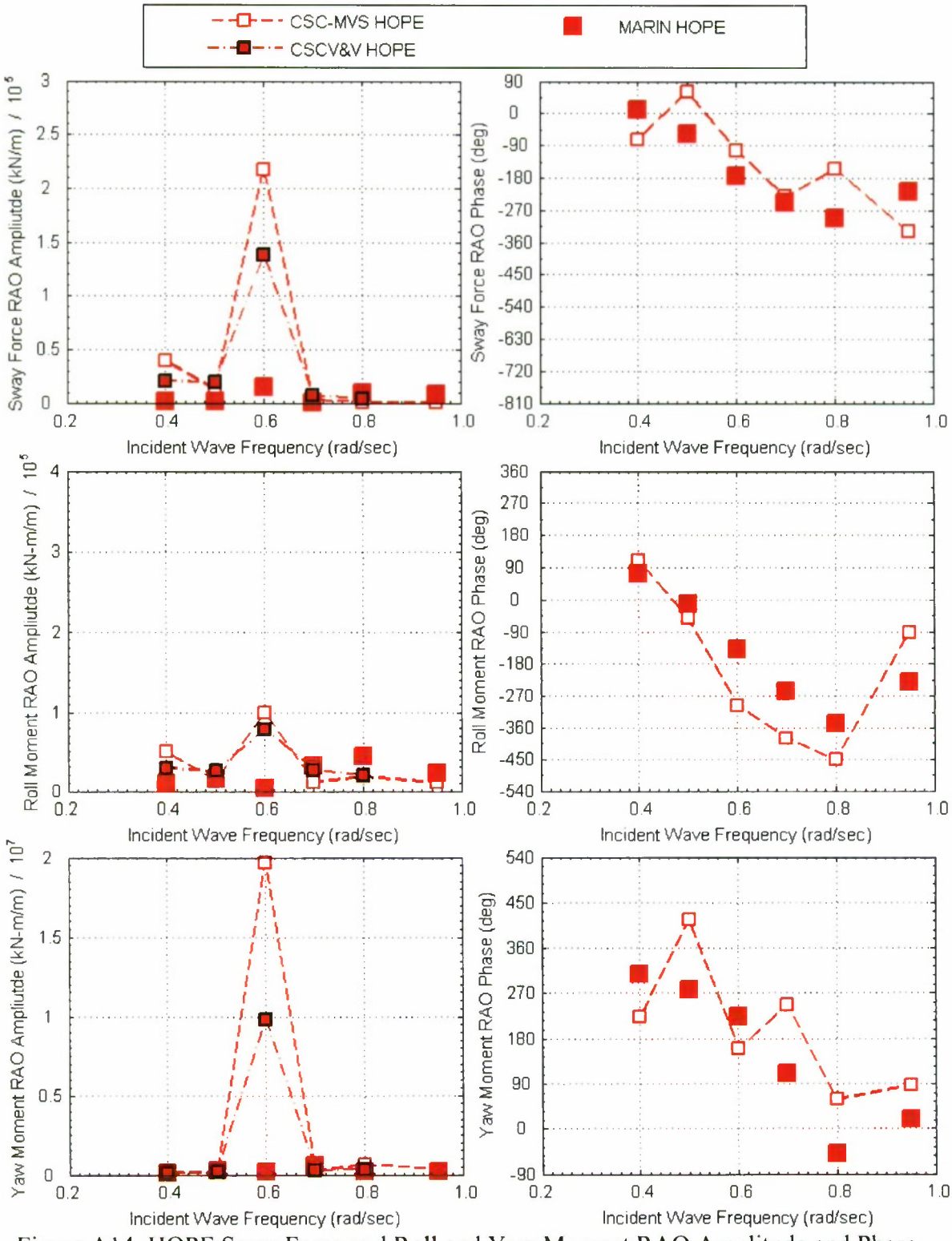

Figure A14. HOPE Sway Force and Roll and Yaw Moment RAO Amplitude and Phase for 16.5 meter separation, 180 degree wave heading, and 16 knots ship speed.

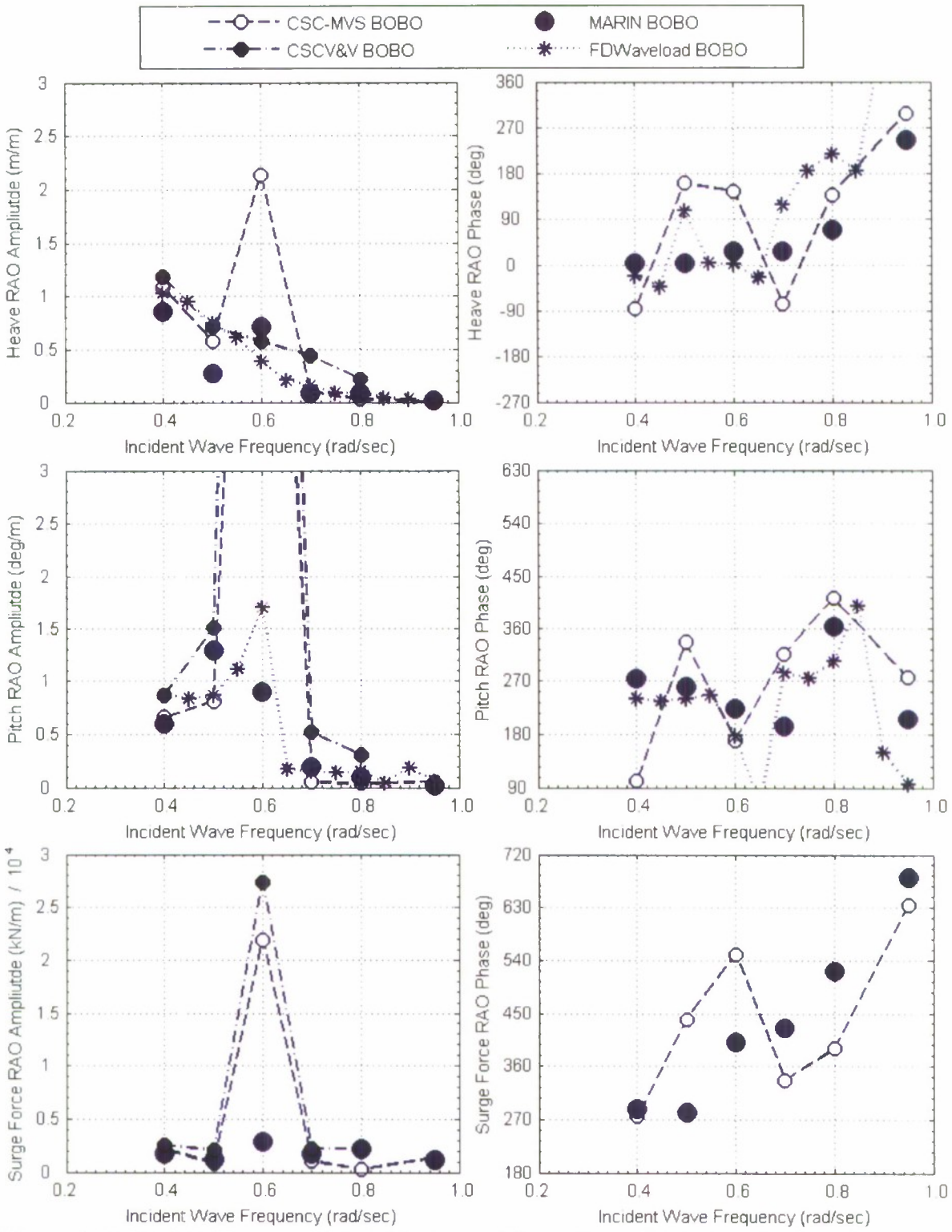

Figure A15. BOBO Heave and Piteh Motion and Surge Force RAO Amplitude and Phase for 16.5 meter separation, 180 degree wave heading, and 16 knots ship speed.

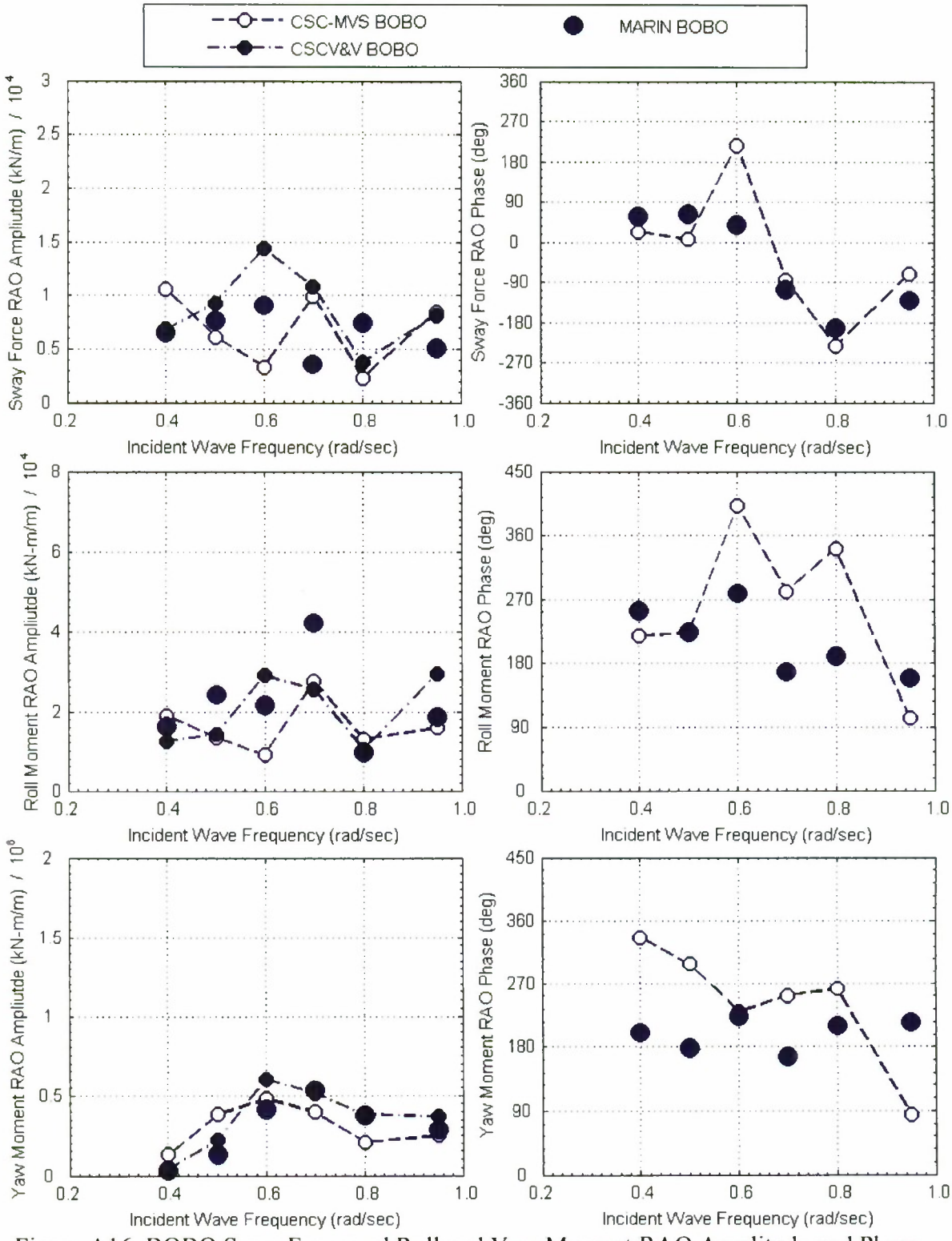

Figure A16. BOBO Sway Force and Roll and Yaw Moment RAO Amplitude and Phase for 16.5 meter separation, 180 degree wave heading, and 16 knots ship speed.

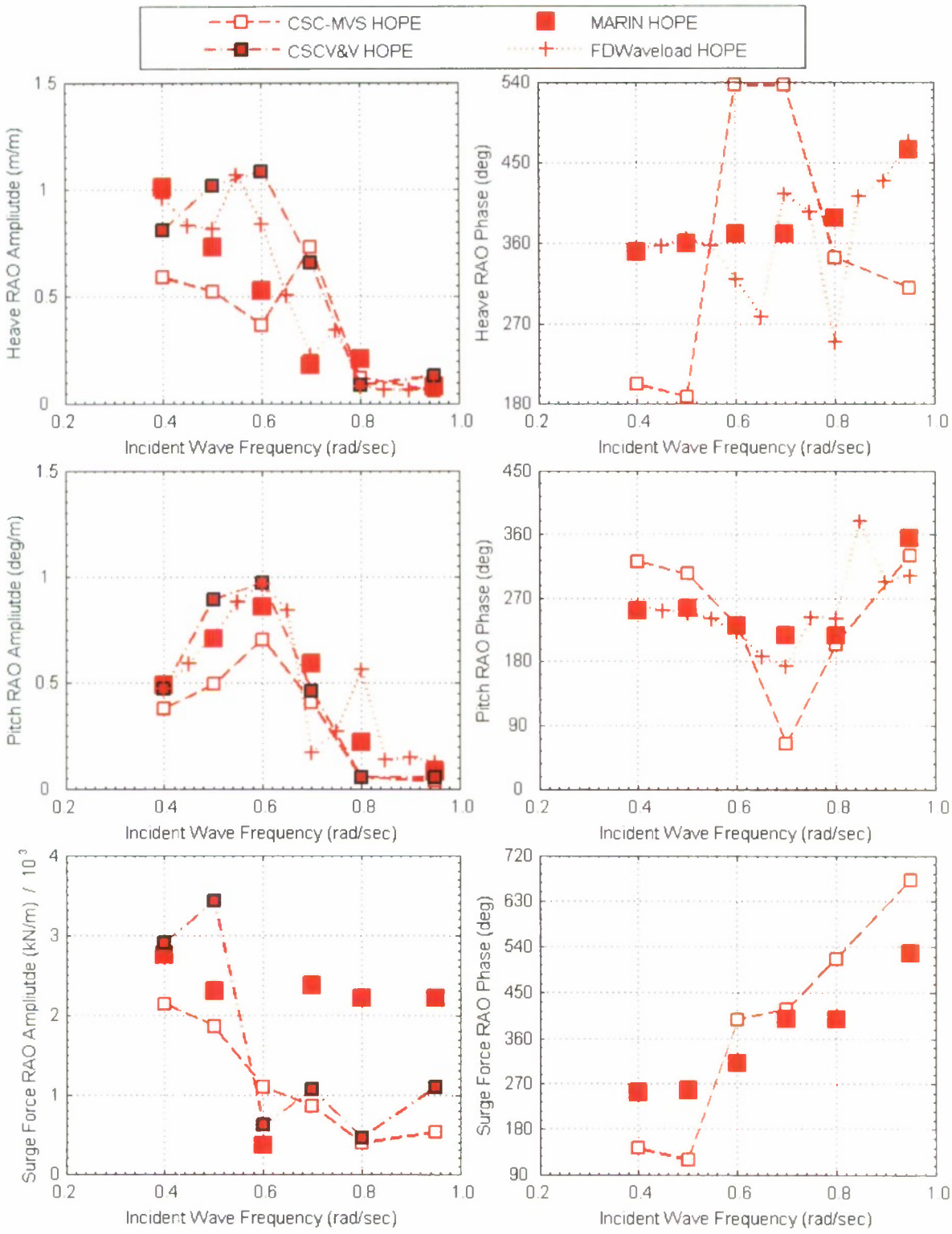

Figure A17. HOPE Heave and Pitch Motion and Surge Force RAO Amplitude and Phase for 33 meter separation, 120 degree wave heading, and 16 knots ship speed.

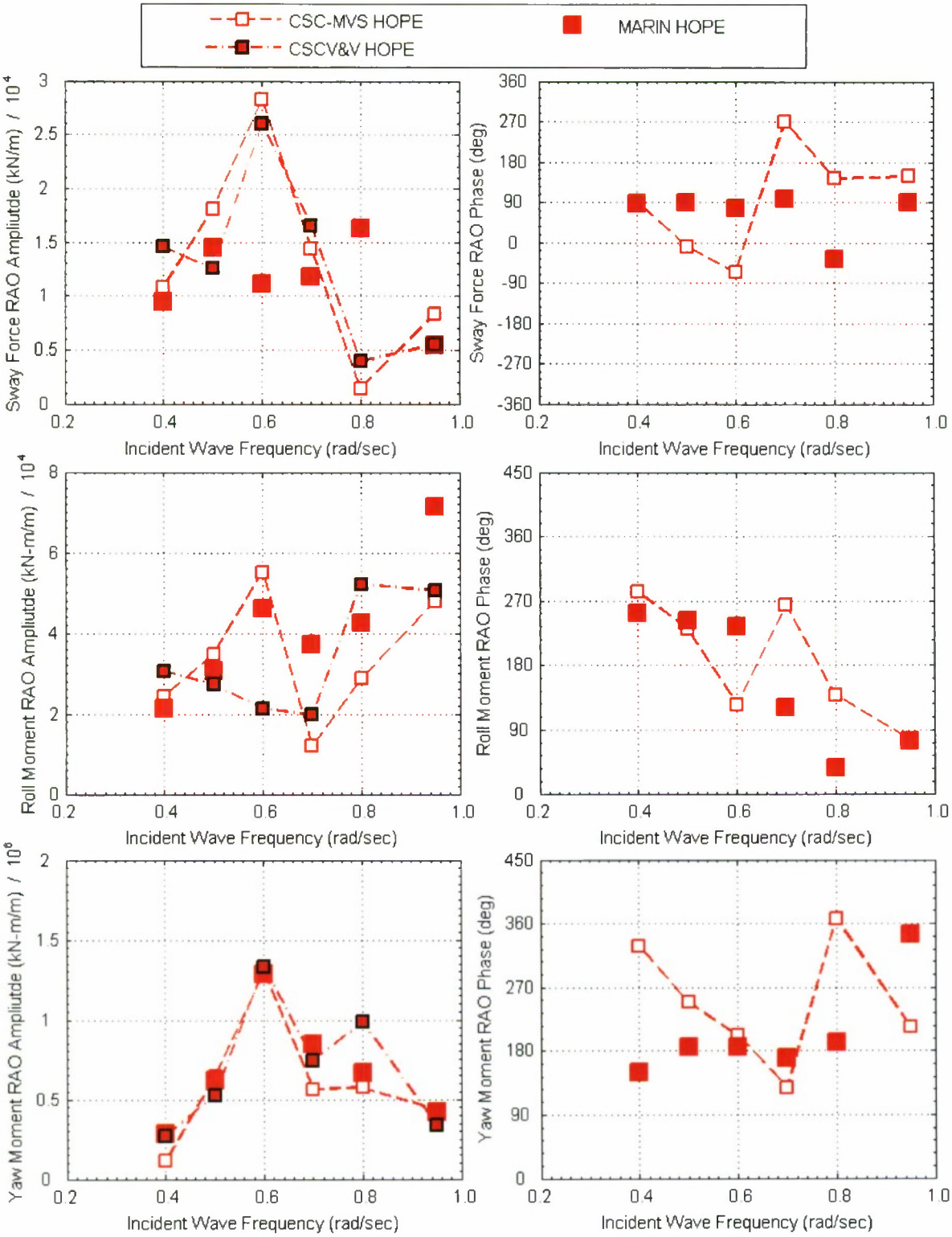

Figure A18. HOPE Sway Force and Roll and Yaw Moment RAO Amplitude and Phase for 33 meter separation, 120 degree wave heading, and 16 knots ship speed.

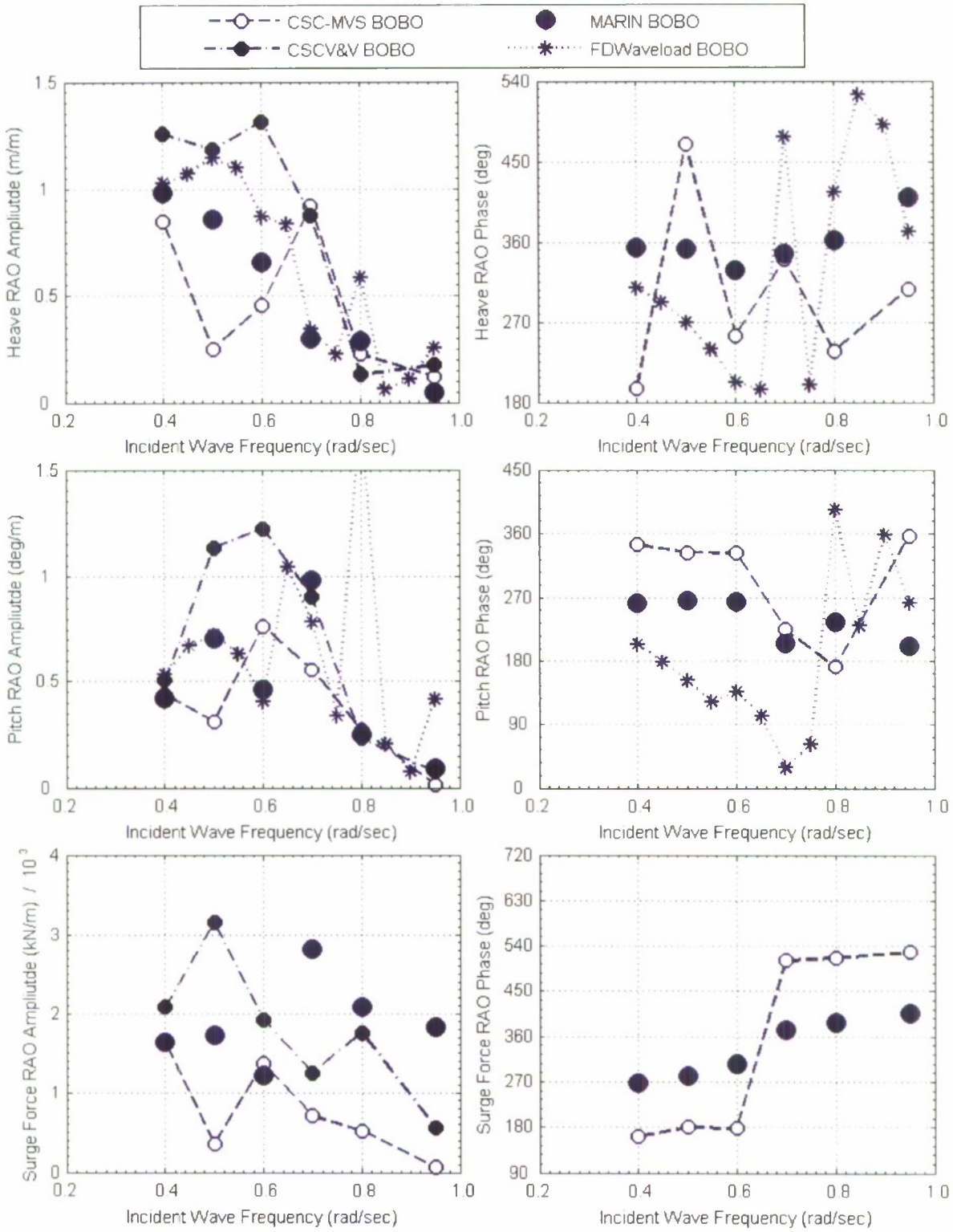

Figure A19. BOBO Heave and Pitch Motion and Surge Force RAO Amplitude and Phase for 33 meter separation, 120 degree wave heading, and 16 knots ship speed.

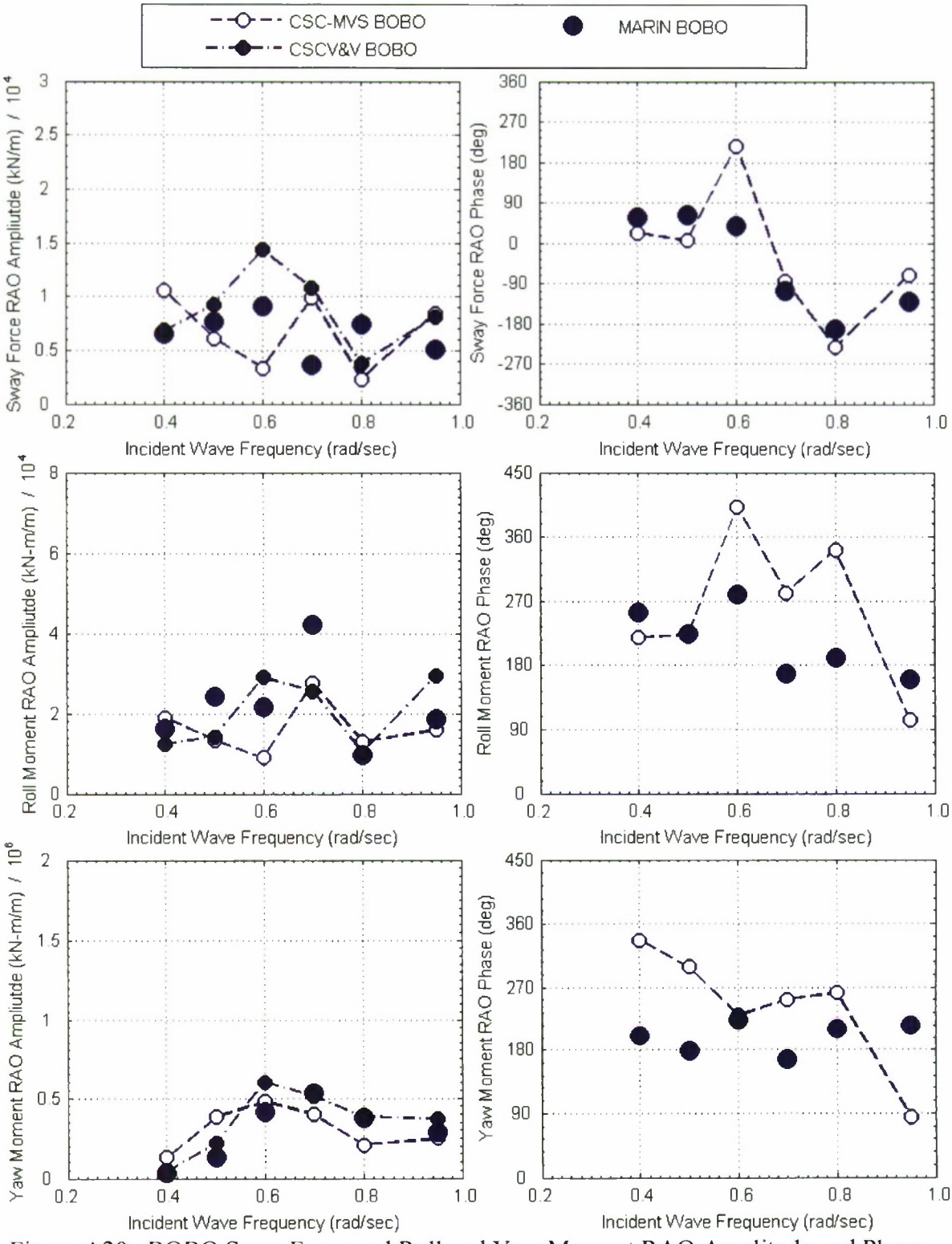

Figure A20. BOBO Sway Force and Roll and Yaw Moment RAO Amplitude and Phase for 33 meter separation, 120 degree wave heading, and 16 knots ship speed.

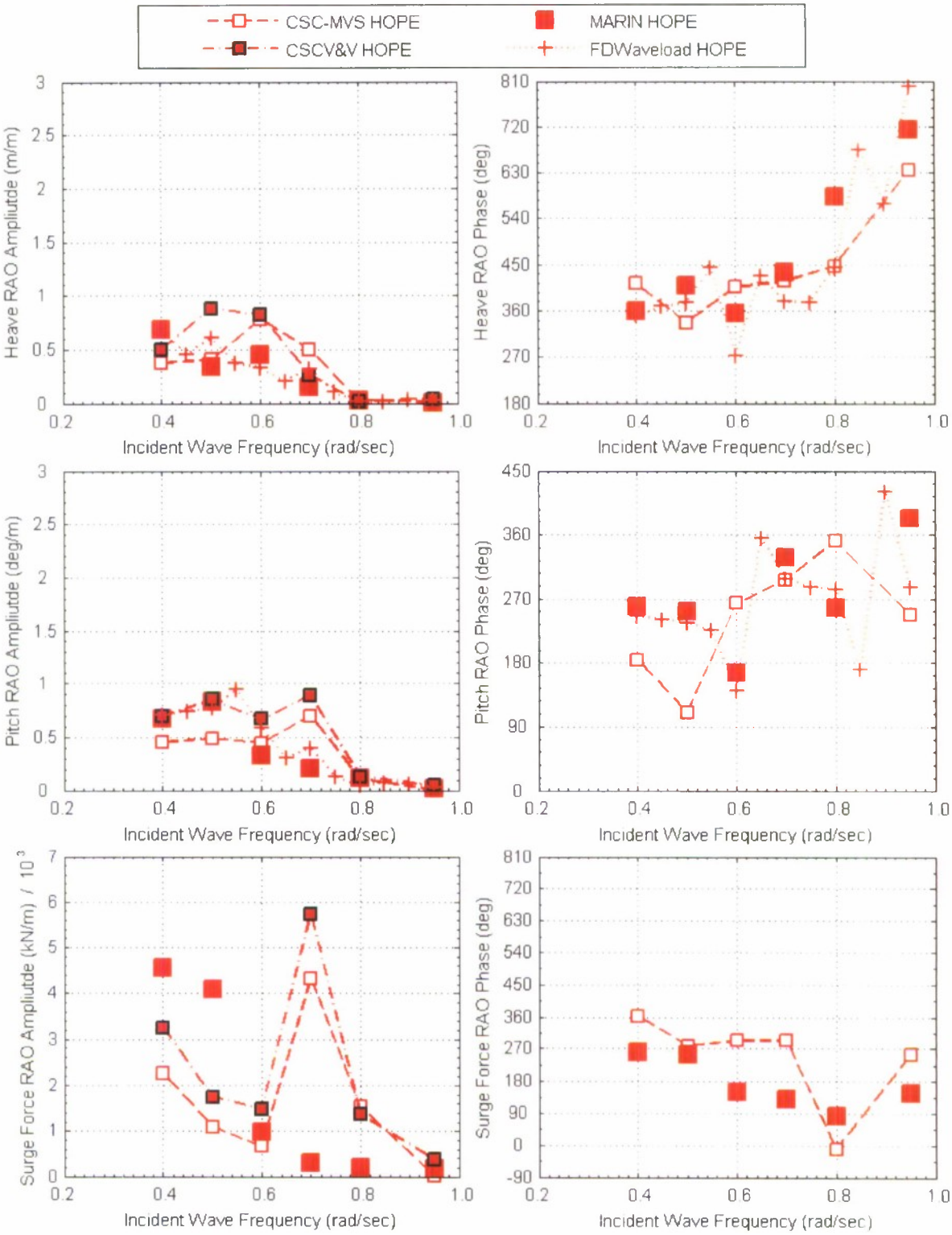

Figure A21. HOPE Heave and Pitch Motion and Surge Force RAO Amplitude and Phase for 33 meter separation, 150 degree wave heading, and 16 knots ship speed.

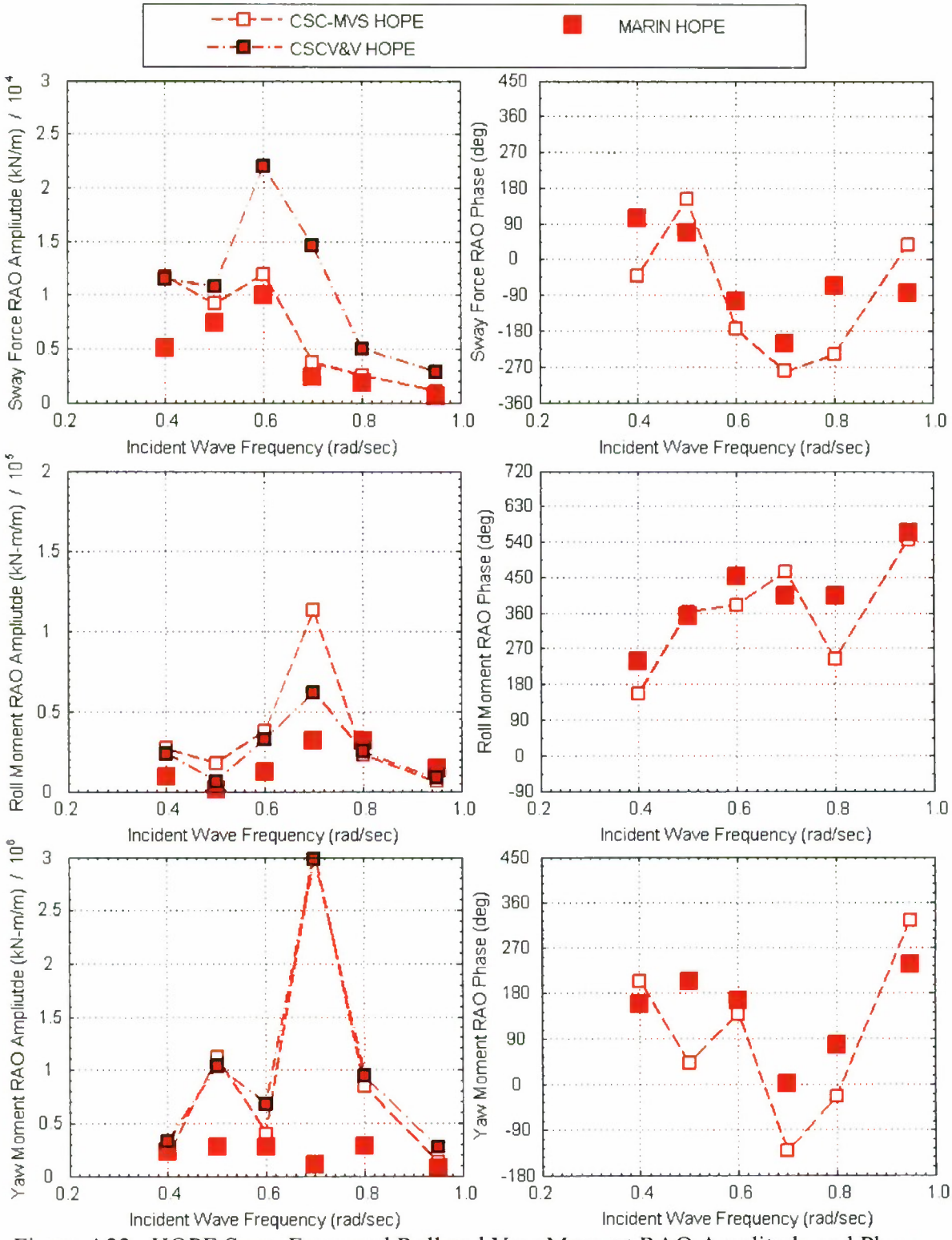

Figure A22. HOPE Sway Force and Roll and Yaw Moment RAO Amplitude and Phase for 33 meter separation, 150 degree wave heading, and 16 knots ship speed.

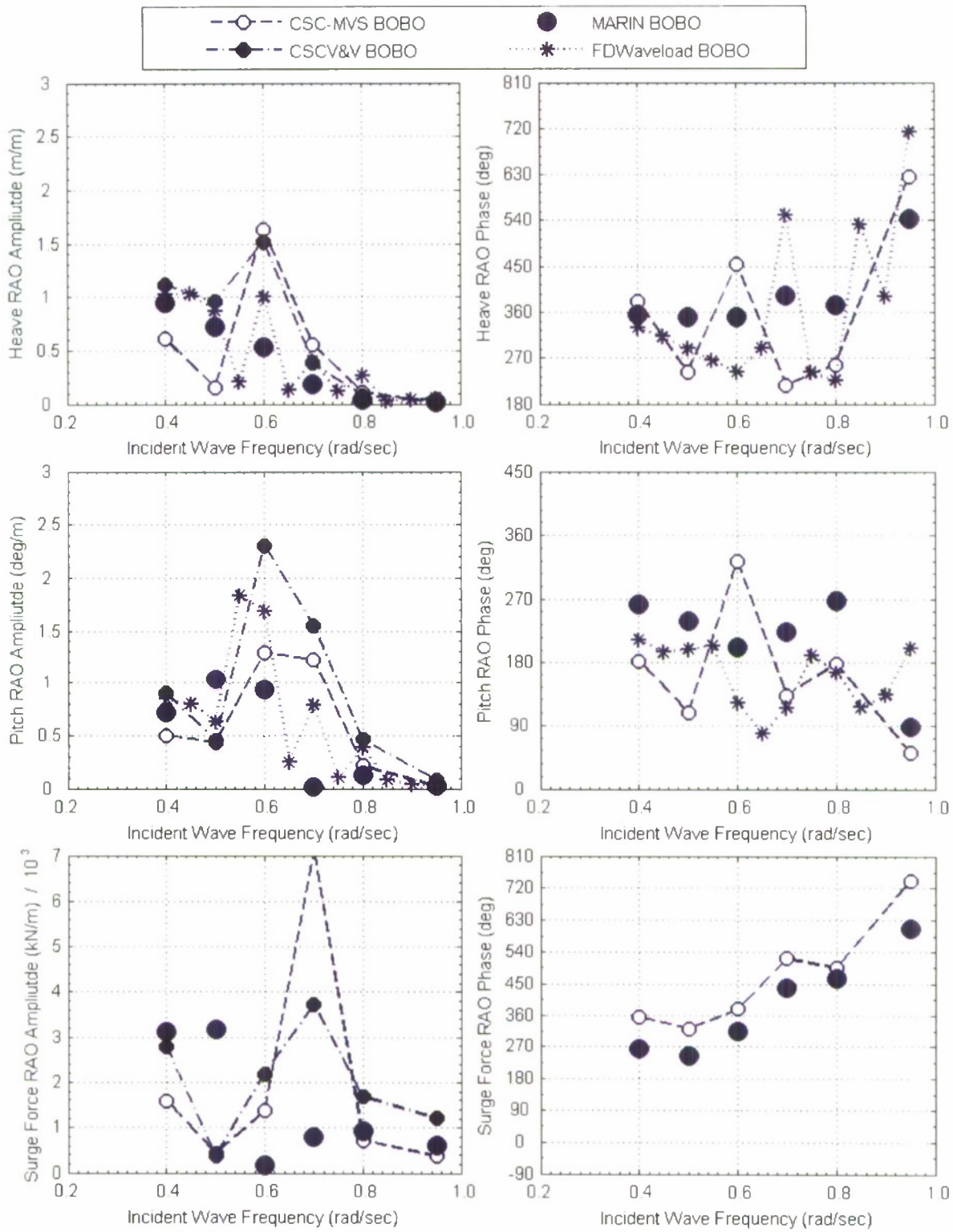

Figure A23. BOBO Heave and Pitch Motion and Surge Force RAO Amplitude and Phase for 33 meter separation, 150 degree wave heading, and 16 knots ship speed.

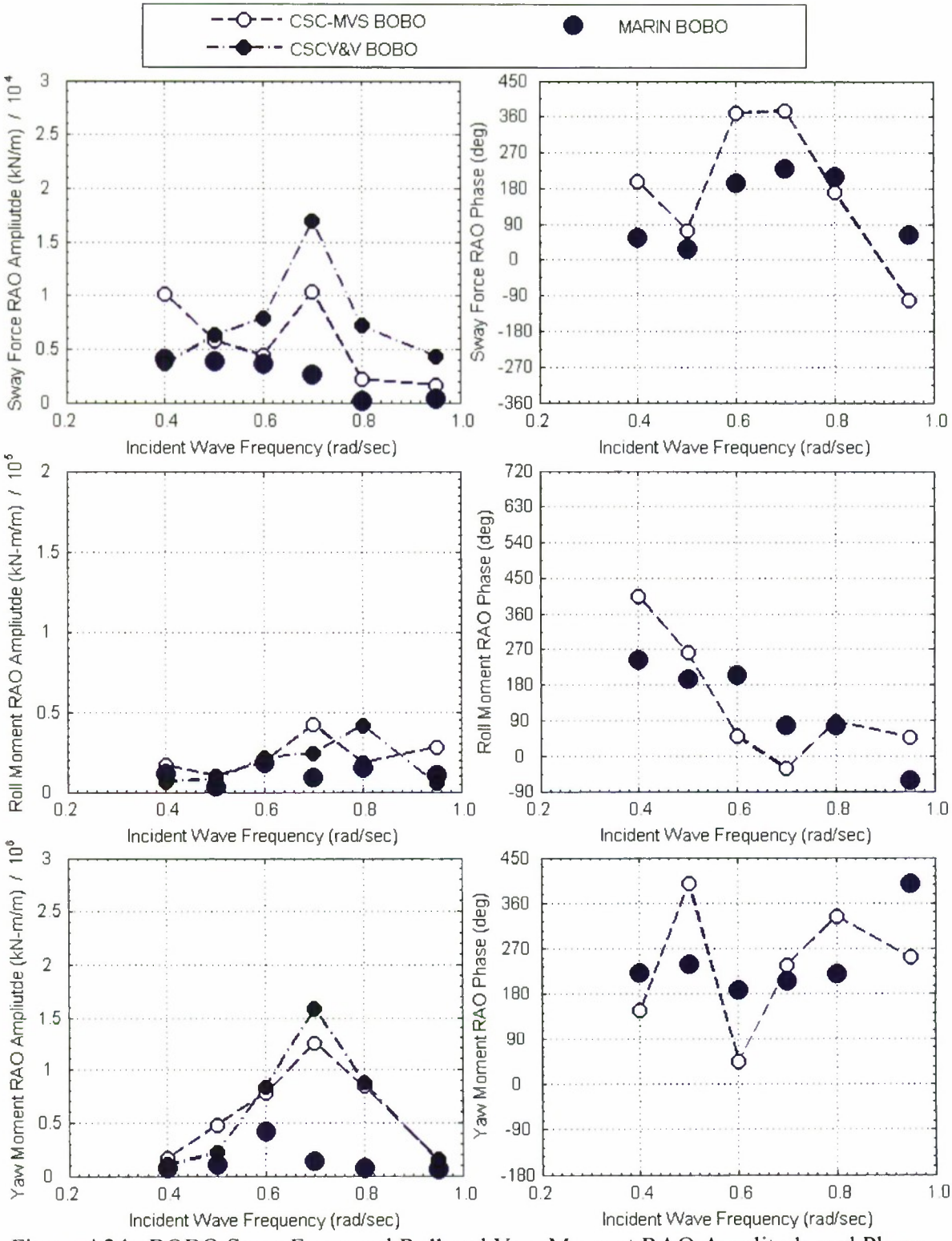

Figure A24. BOBO Sway Force and Roll and Yaw Moment RAO Amplitude and Phase for 33 meter separation, 150 degree wave heading, and 16 knots ship speed.

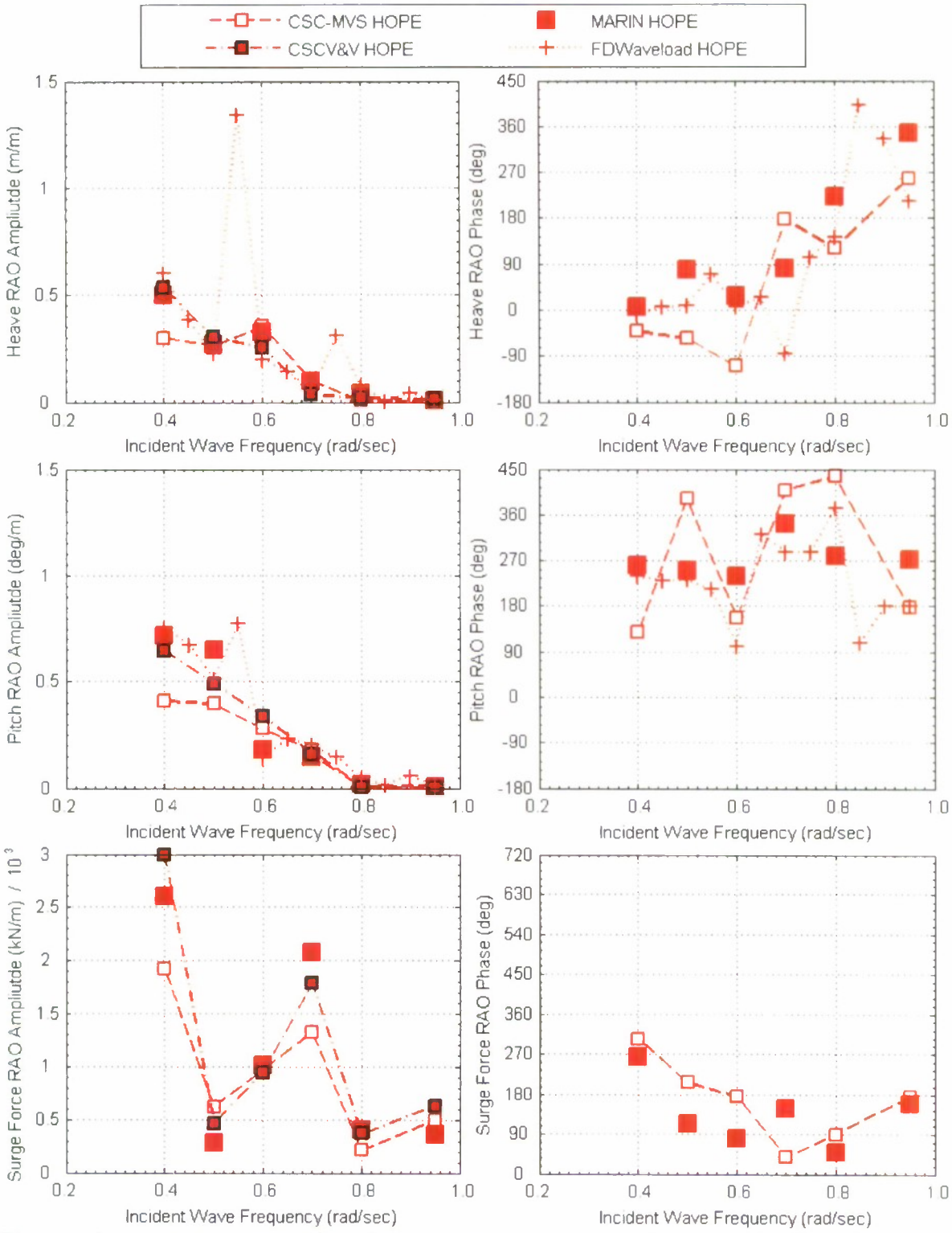

Figure A25. HOPE Heave and Pitch Motion and Surge Force RAO Amplitude and Phase for 33 meter separation, 180 degree wave heading, and 16 knots ship speed.

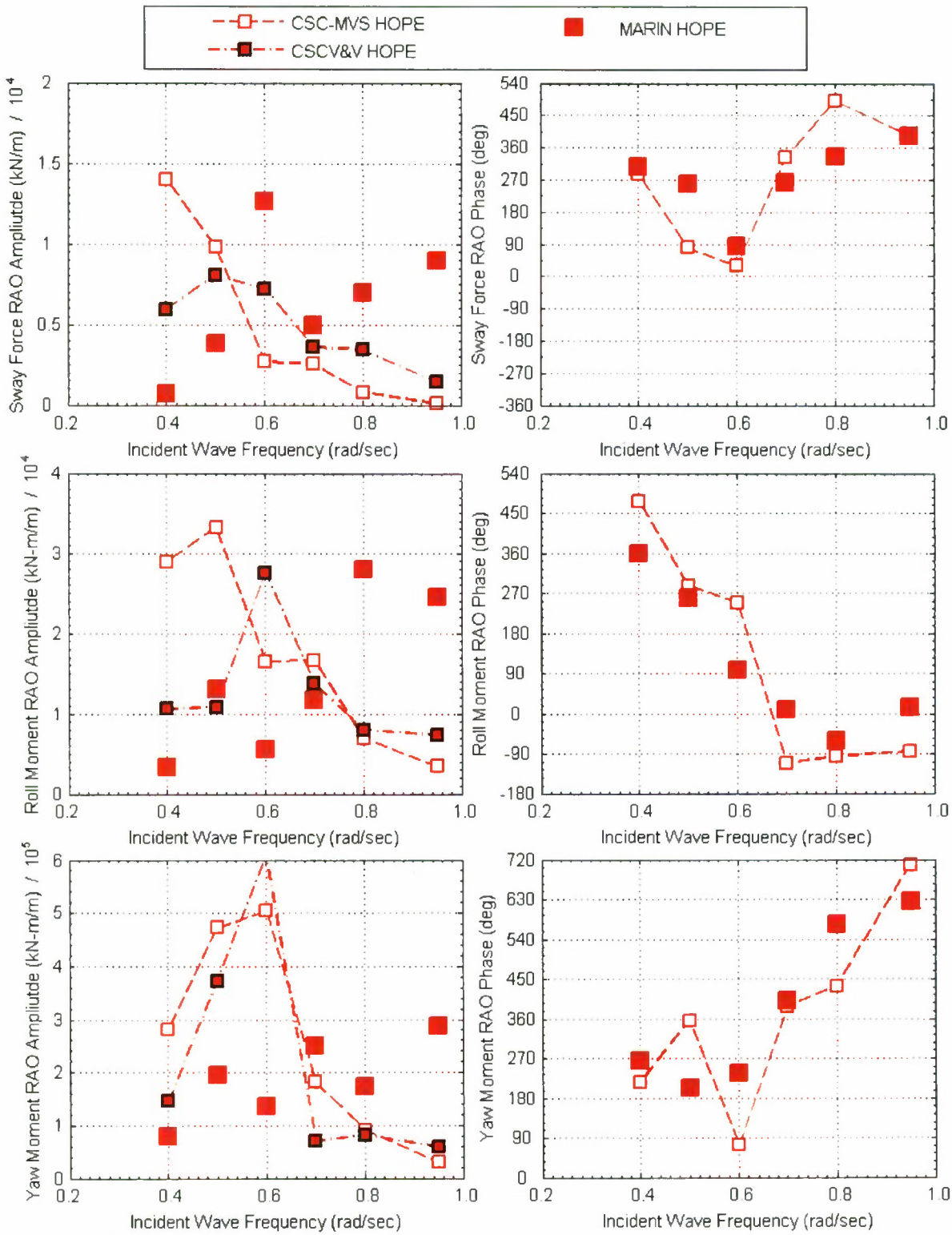

Figure A26. HOPE Sway Force and Roll and Yaw Moment RAO Amplitude and Phase for 33 meter separation, 180 degree wave heading, and 16 knots ship speed.

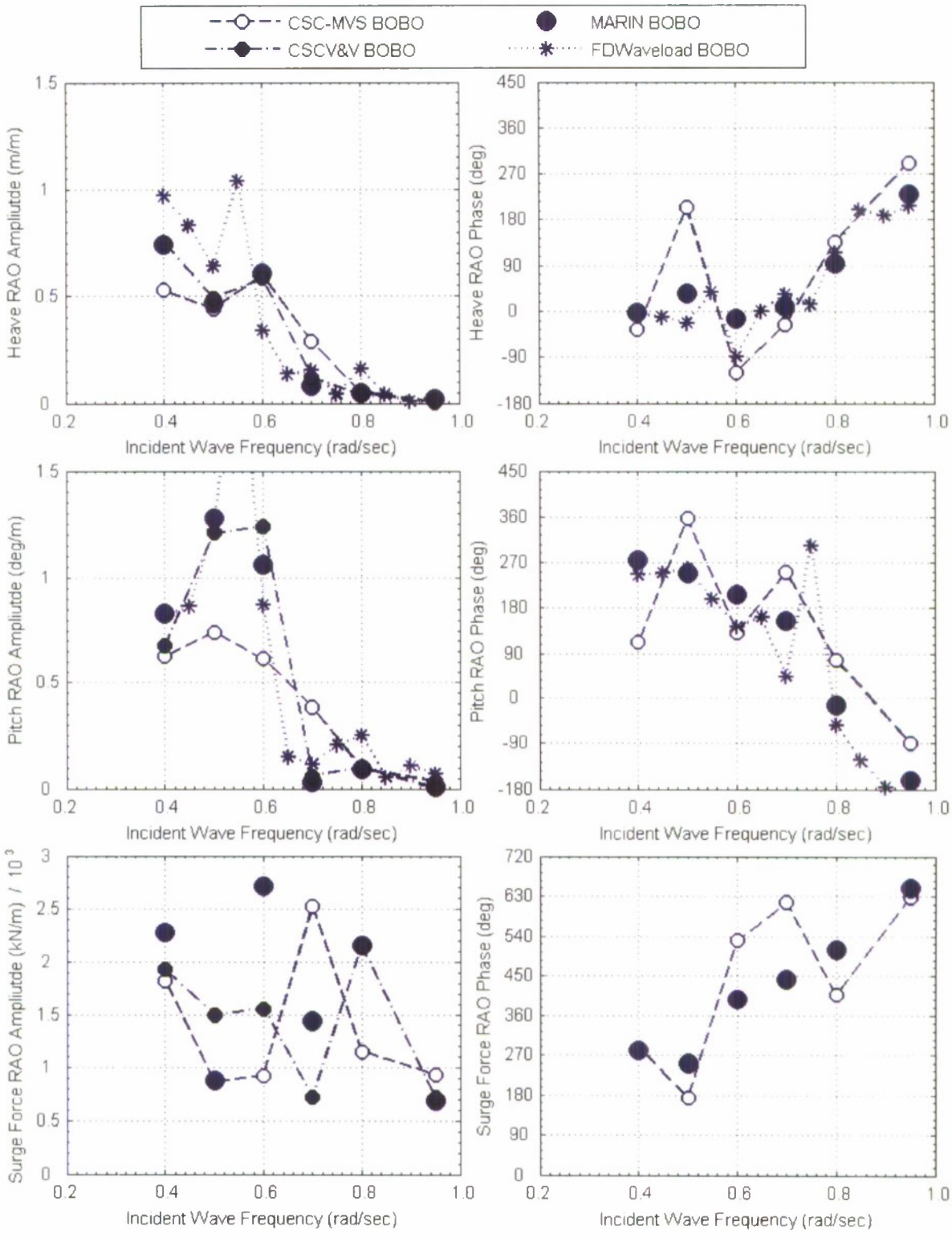

Figure A27. BOBO Heave and Pitch Motion and Surge Force RAO Amplitude and Phase for 33 meter separation, 180 degree wave heading, and 16 knots ship speed.

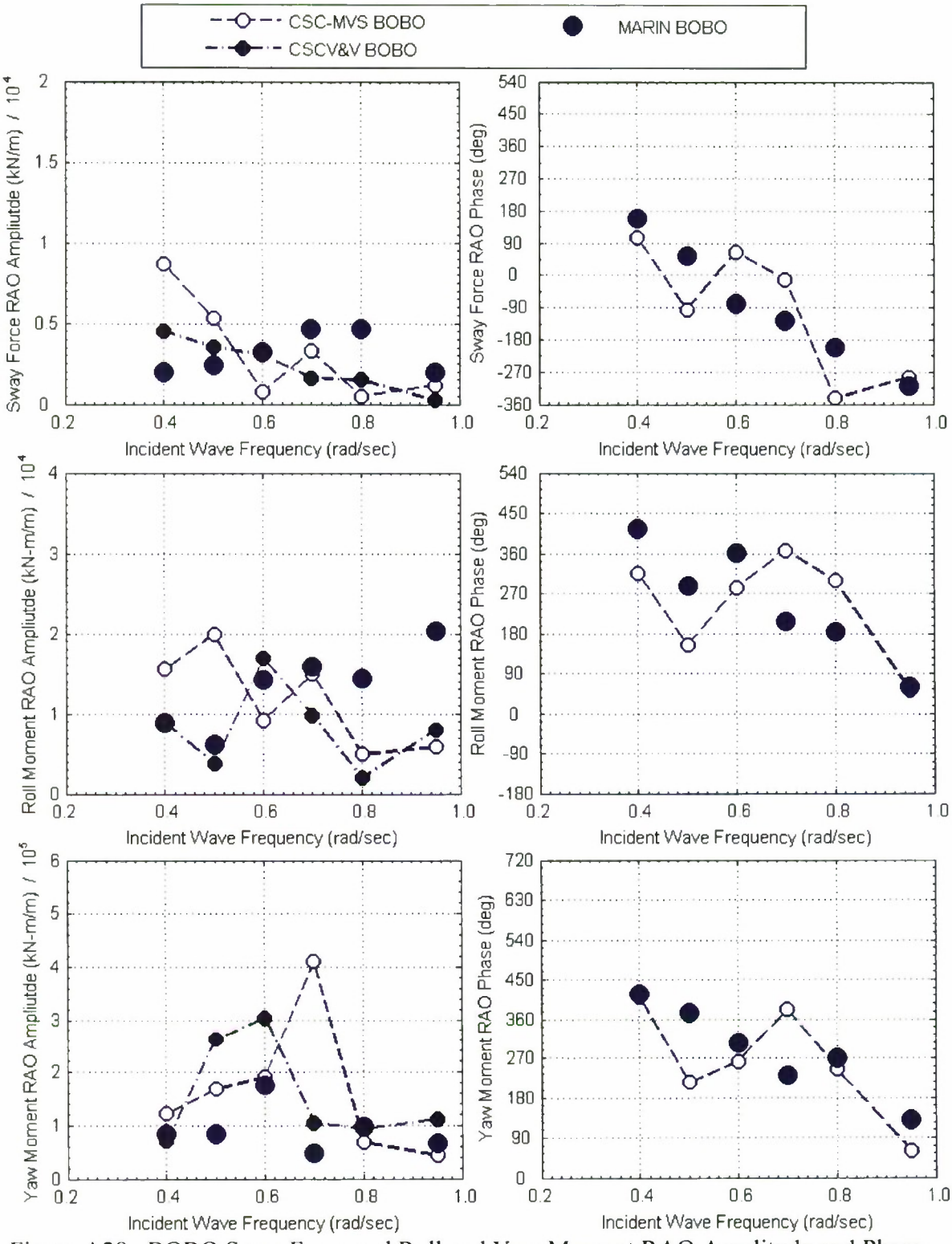

Figure A28. BOBO Sway Force and Roll and Yaw Moment RAO Amplitude and Phase for 33 meter separation, 180 degree wave heading, and 16 knots ship speed.

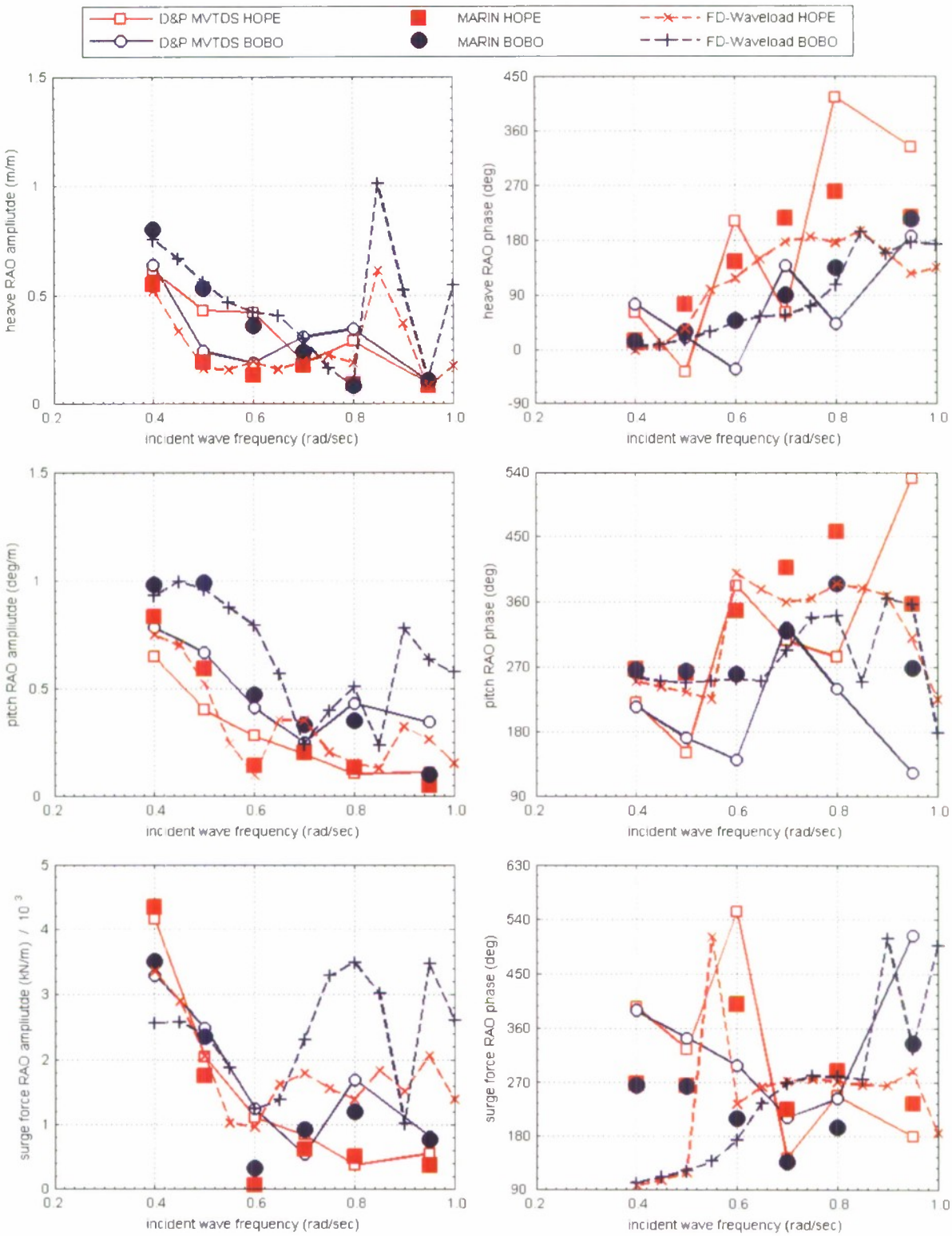

Figure B1. HOPE, BOBO Heave and Pitch and Surge Force RAO Amplitude and Phase for 3 meter separation, 180 degree wave heading, and 5 knots ship speed.

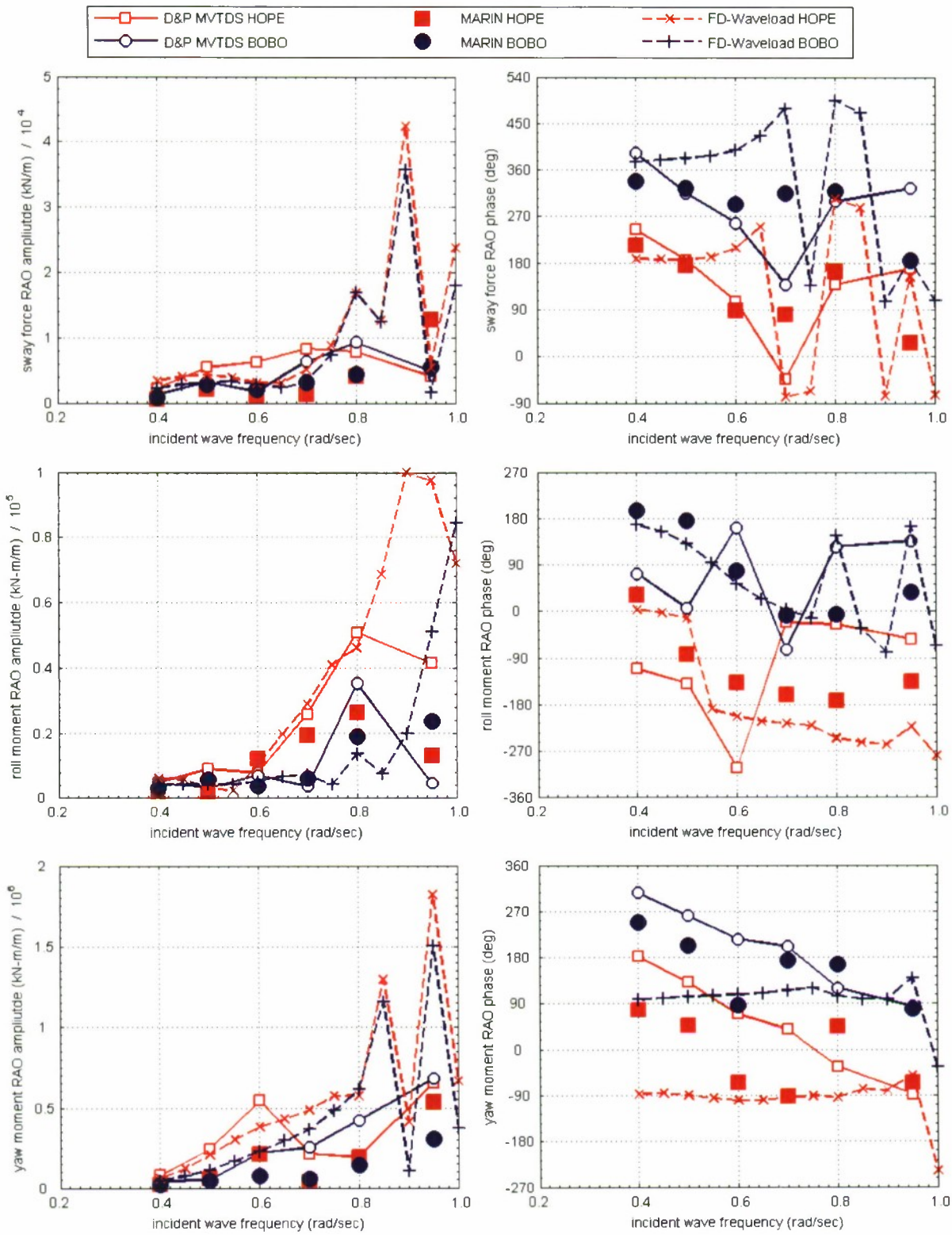

Figure B2. HOPE, BOBO Sway force and Roll and Yaw moment RAO Amplitude and Phase for 3 meter separation, 180 degree wave heading, and 5 knots ship speed.

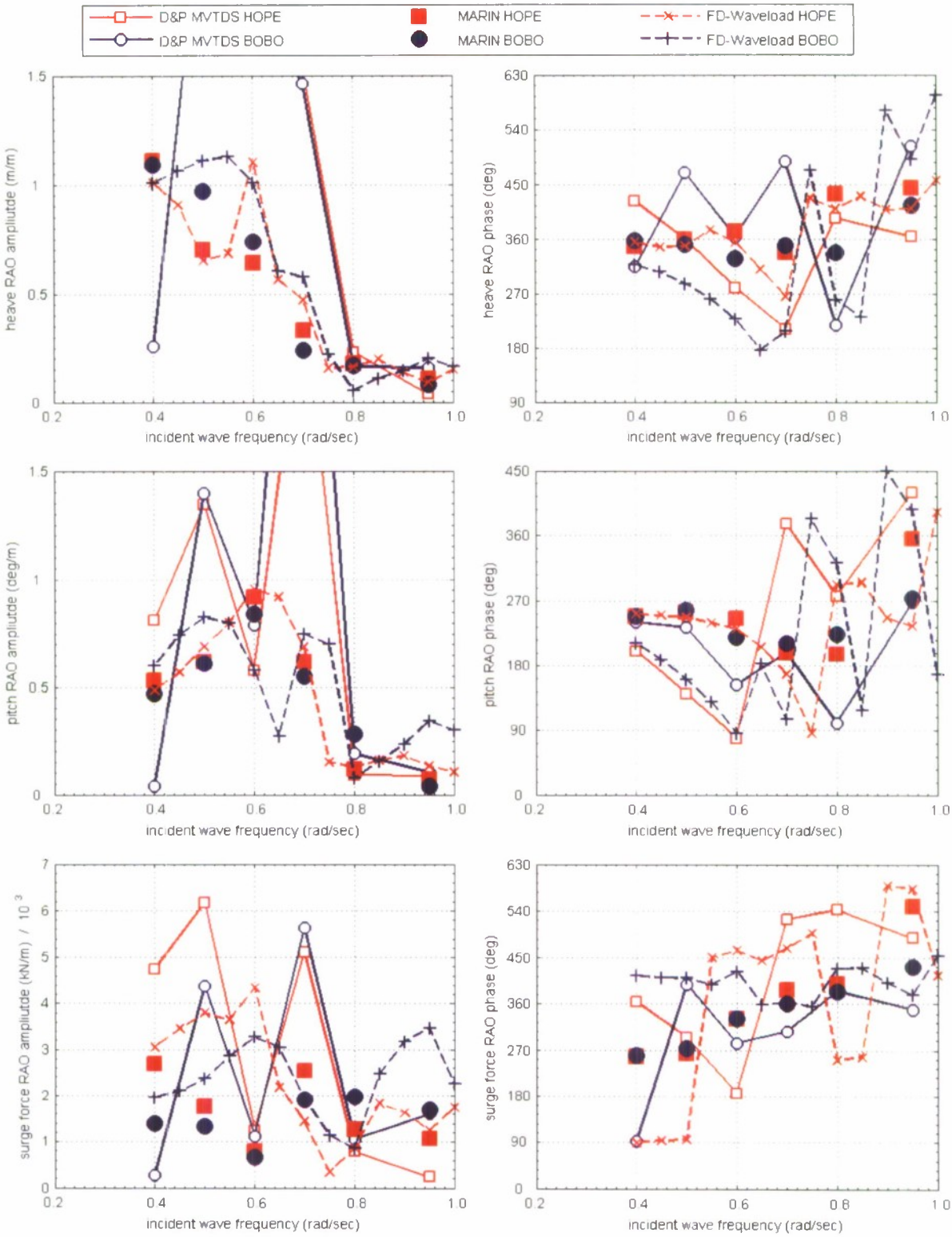

Figure B3. HOPE, BOBO Heave and Pitch and Surge Force RAO Amplitude and Phase for 16.5 meter separation, 120 degree wave heading, and 16 knots ship speed.

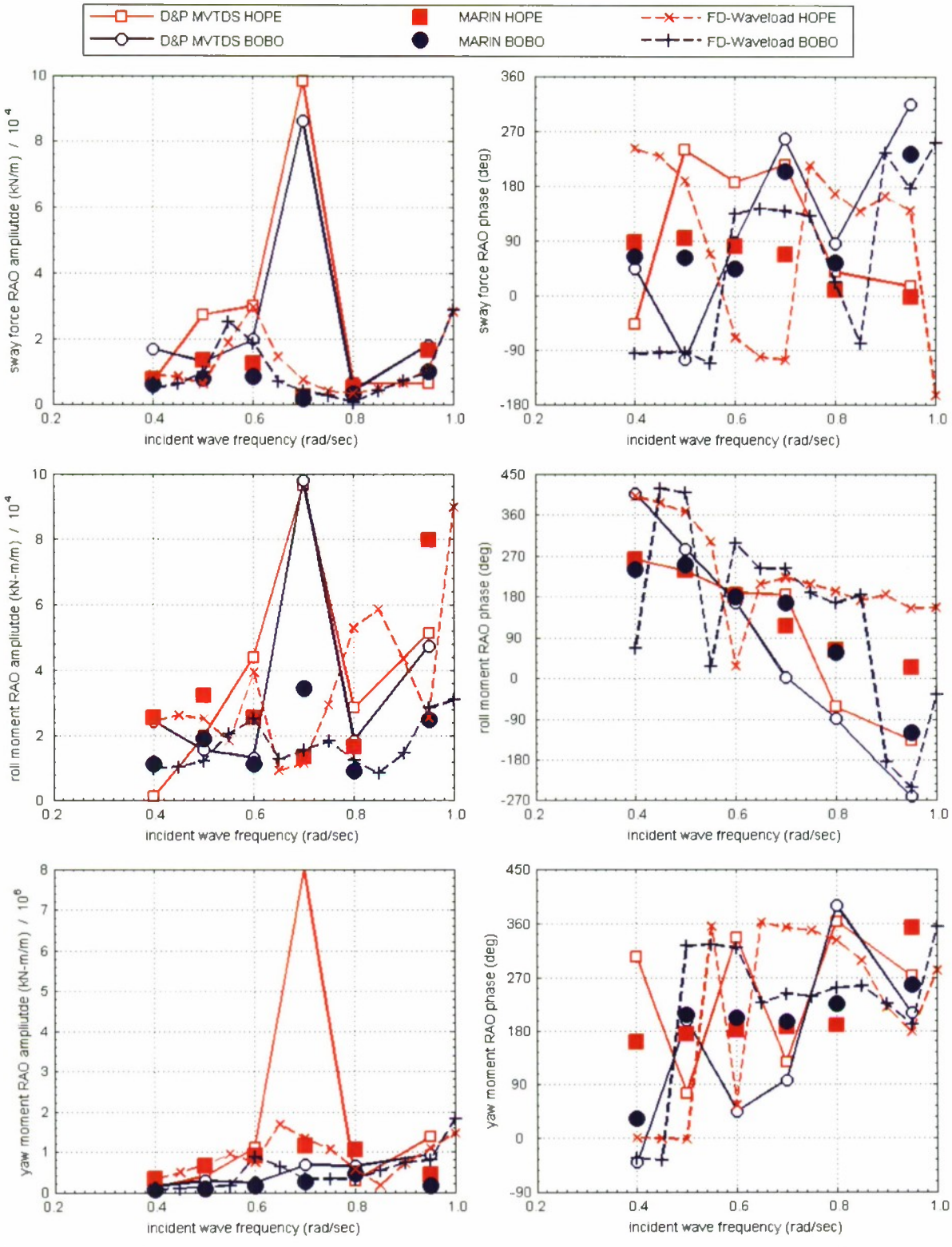

Figure B4. HOPE, BOBO Sway Foree and Roll and Yaw moment RAO Amplitude and Phase for 16.5 meter separation, 120 degree wave heading, and 16 knots ship speed.

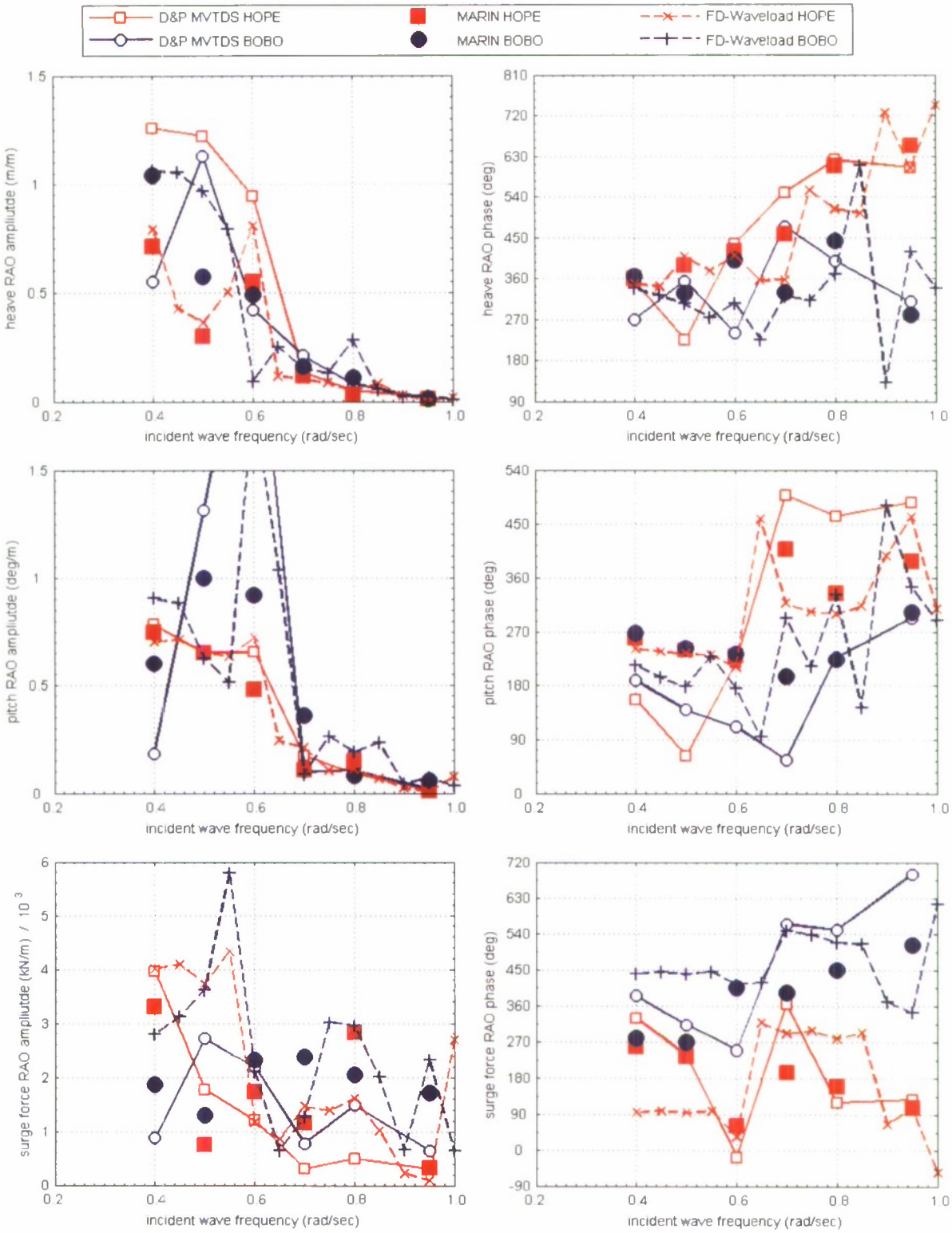

Figure B5. HOPE, BOBO Heave and Piteh and Surge Foree RAO Amplitude and Phase for 16.5 meter separation, 150 degree wave heading, and 16 knots ship speed.

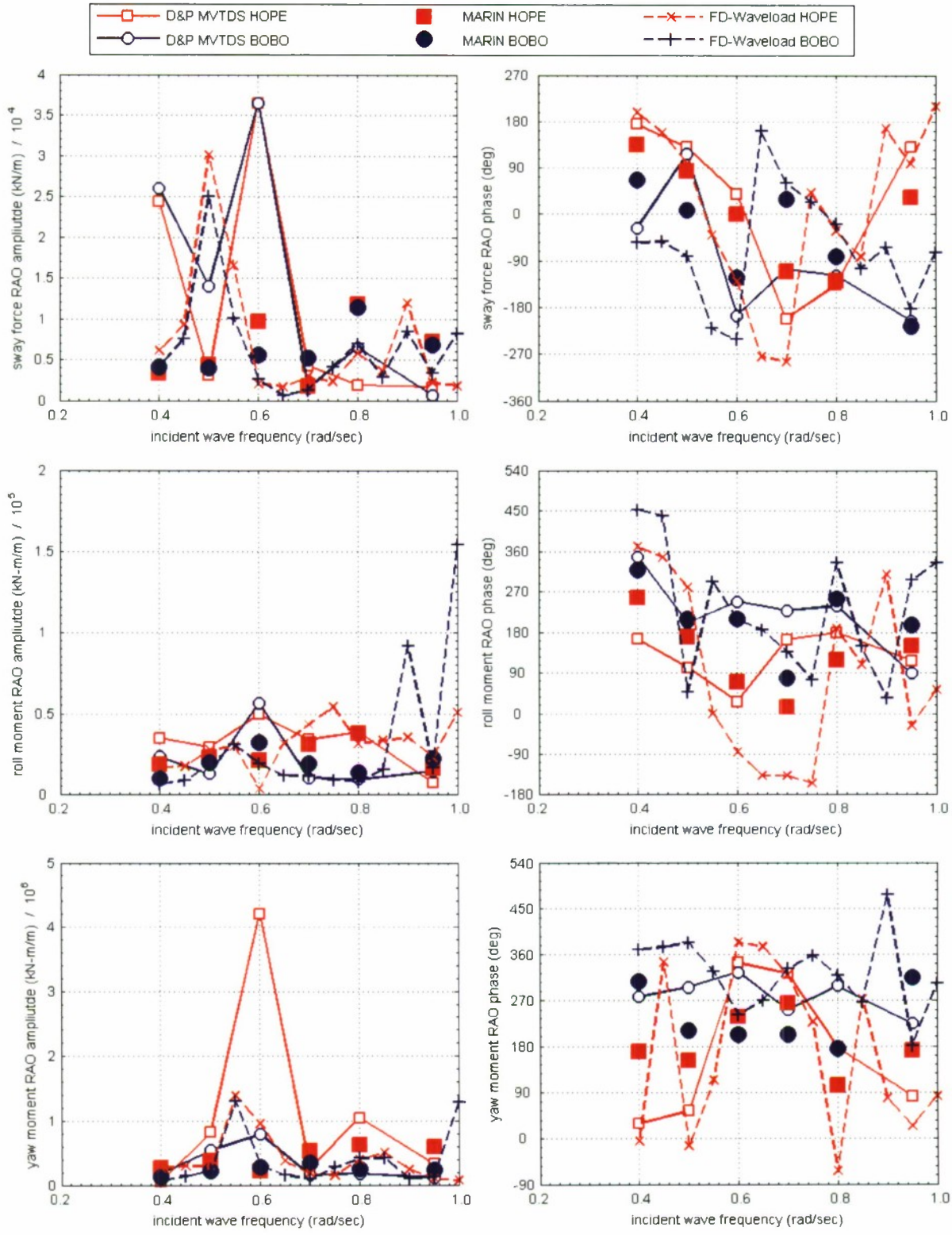

Figure B6. HOPE, BOBO Sway force and Roll and Yaw Moment RAO Amplitude and Phase for 16.5 meter separation, 150 degree wave heading, and 16 knots ship speed.

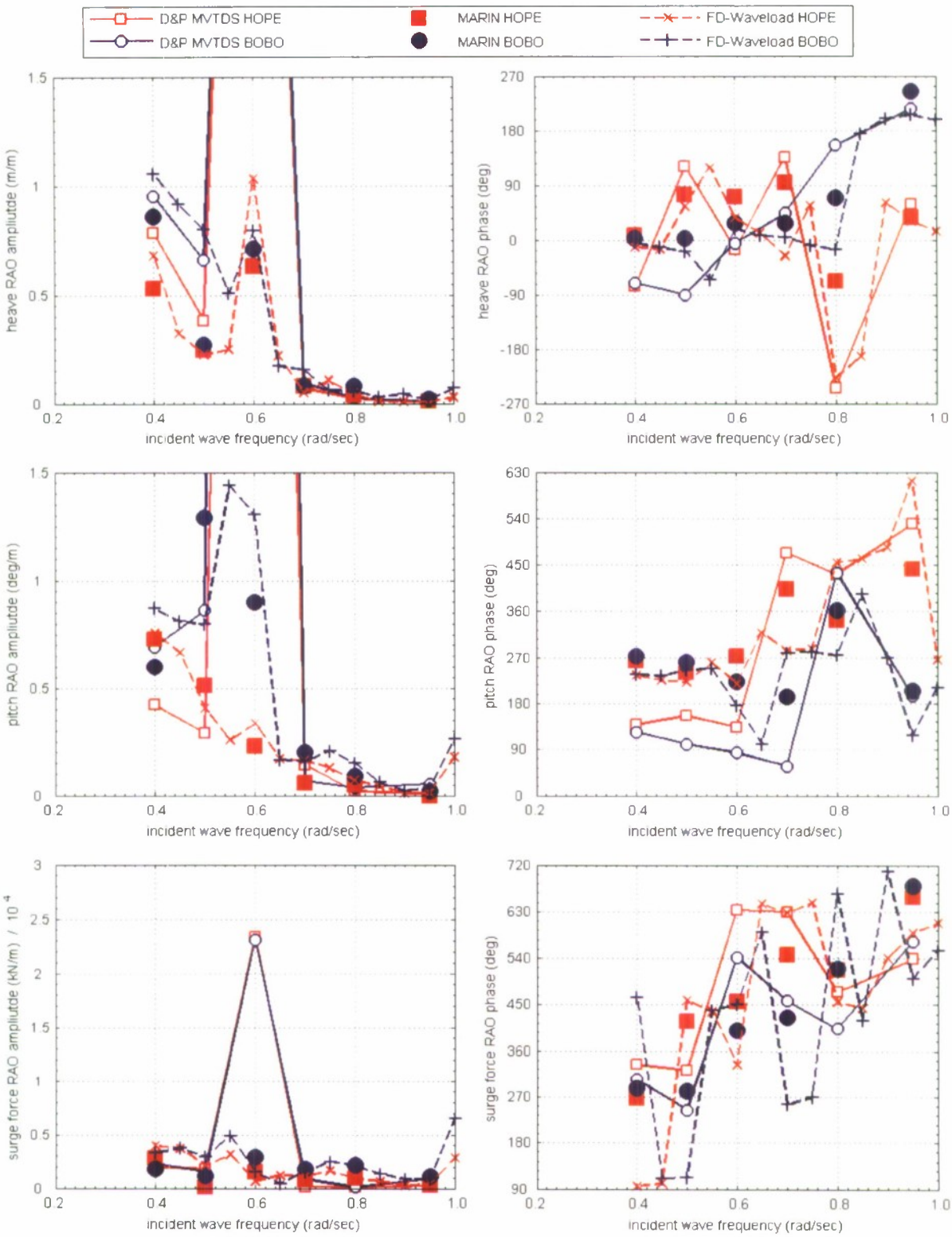

Figure B7. HOPE, BOBO Heave and Pitch and Surge Force RAO Amplitude and Phase for 16.5 meter separation, 180 degree wave heading, and 16 knots ship speed.

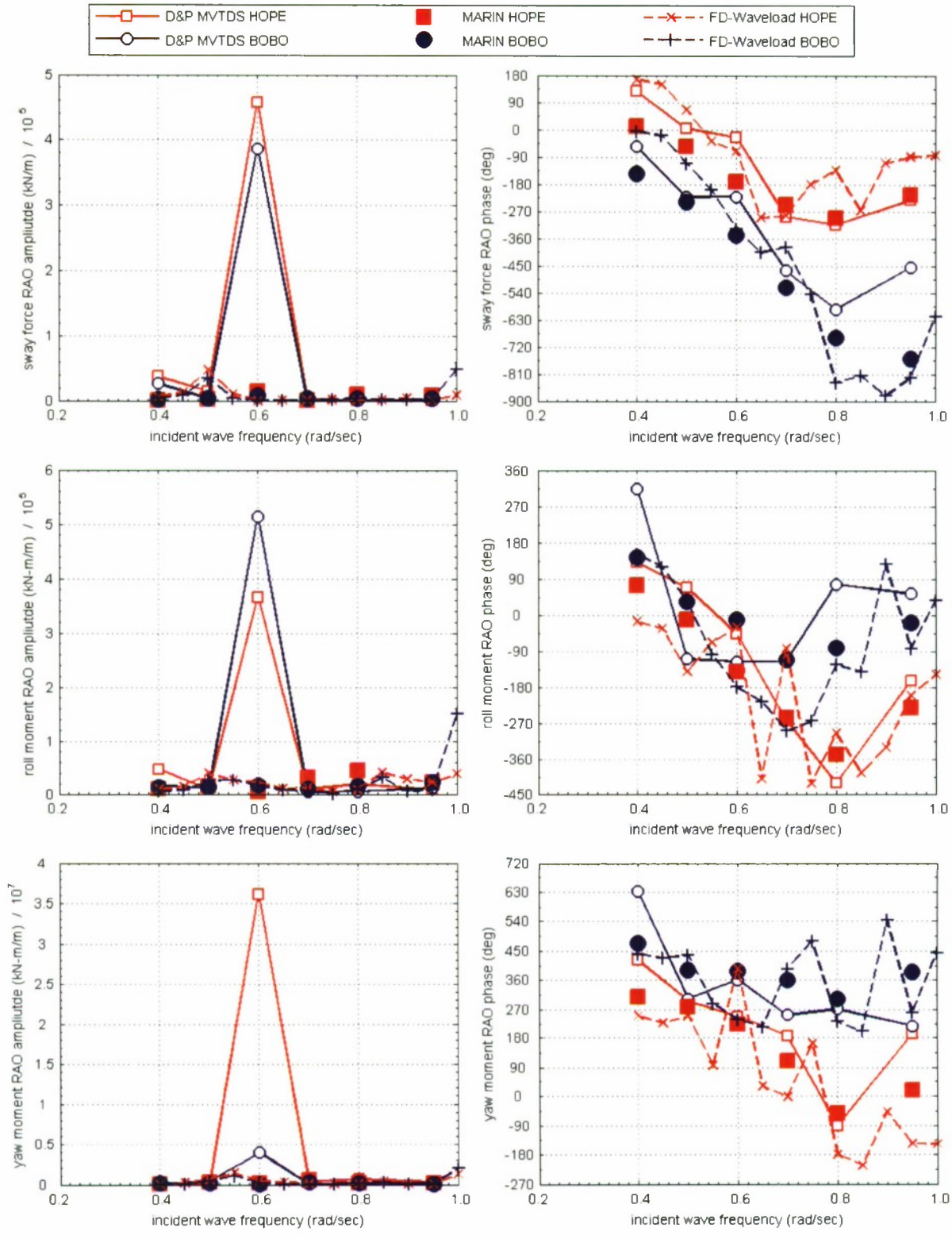

Figure B8. HOPE, BOBO Sway Force and Roll and Yaw Moment RAO Amplitude and Phase for 16.5 meter separation, 180 degree wave heading, and 16 knots ship speed.

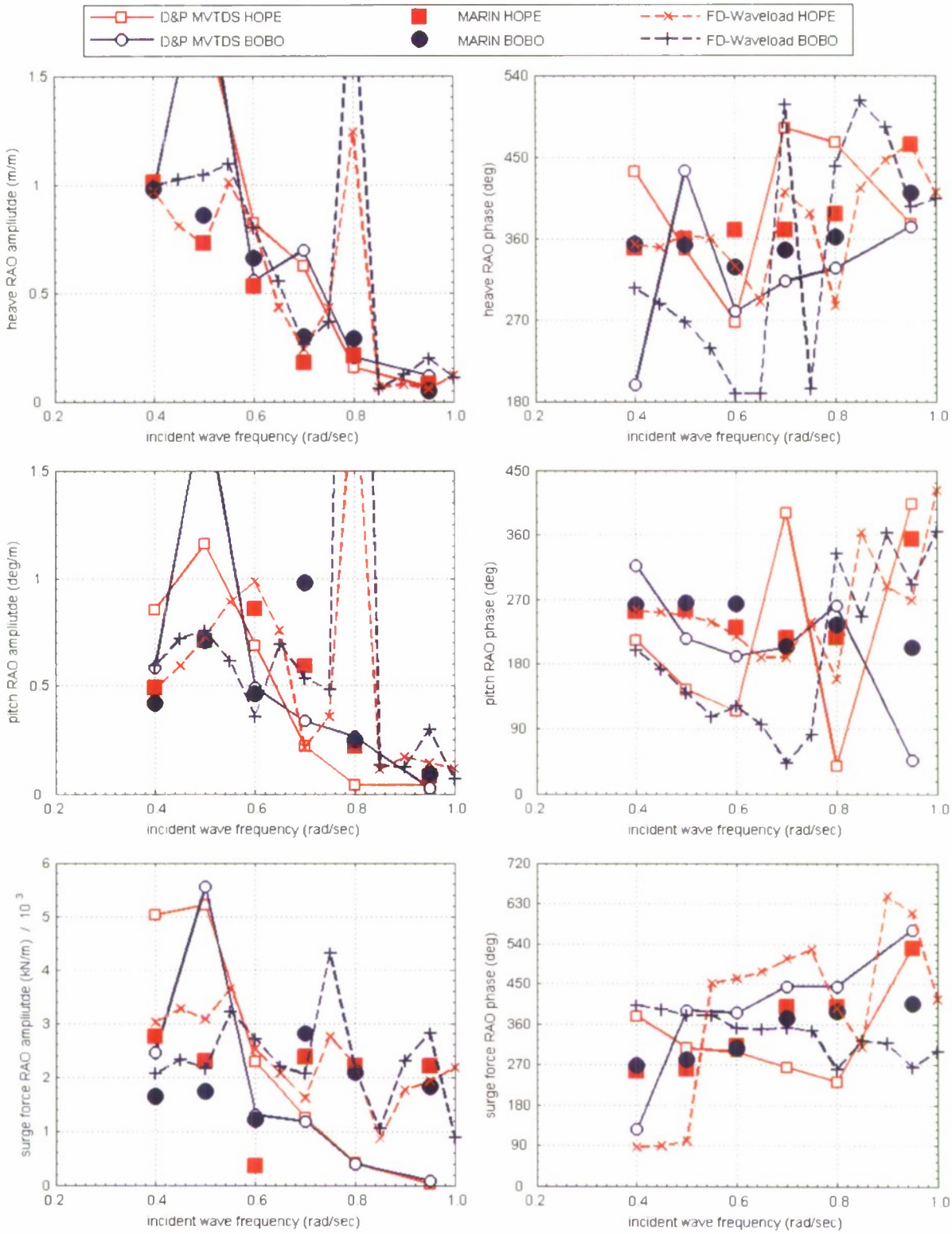

Figure B9. HOPE, BOBO Heave and Pitch and Surge Foree RAO Amplitude and Phase for 33 meter separation, 120 degree wave heading, and 16 knots ship speed.

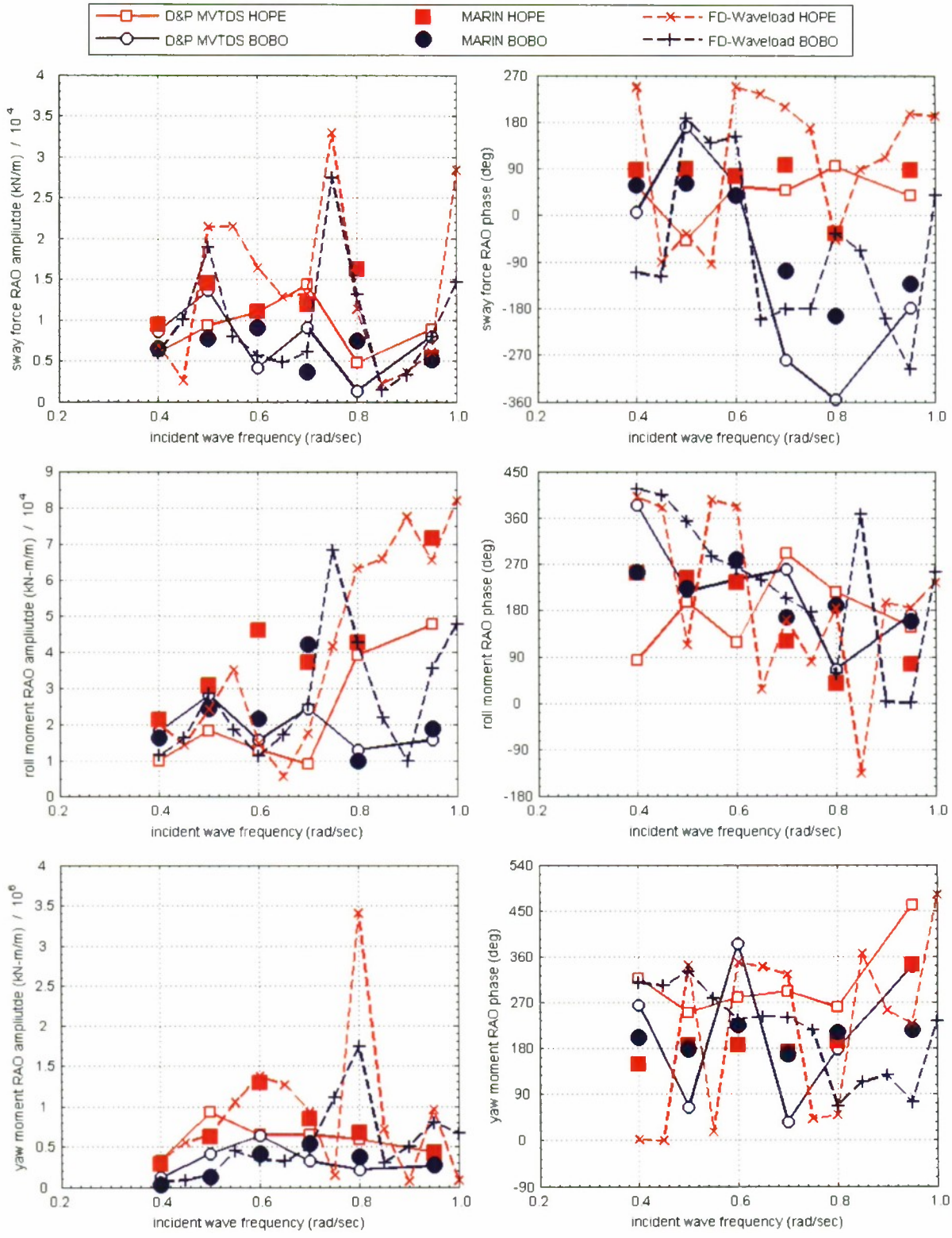

Figure B10. HOPE, BOBO Sway Force and Roll and Yaw Moment RAO Amplitude and Phase for 33 meter separation, 120 degree wave heading, and 16 knots ship speed.

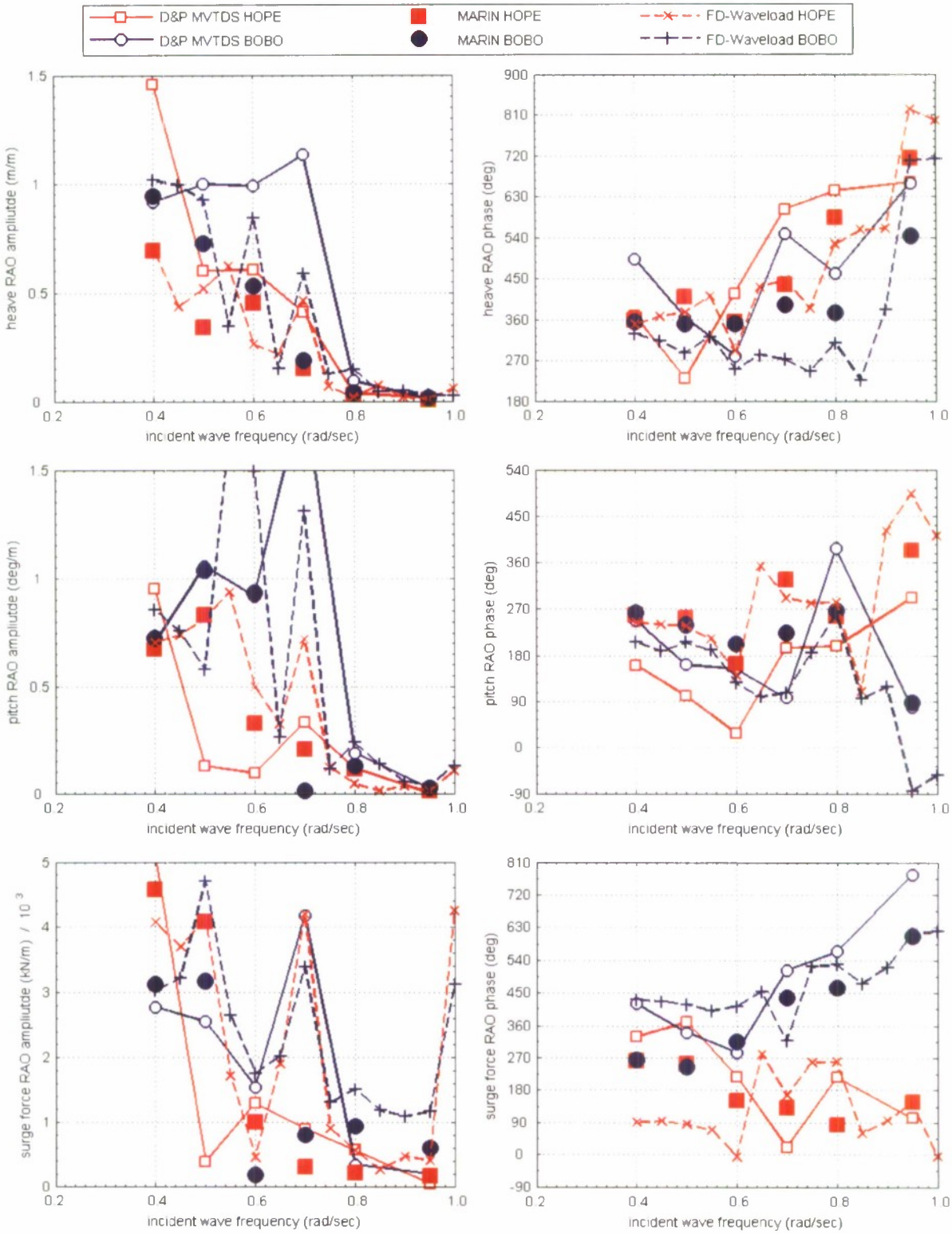

Figure B11. HOPE, BOBO Heave and Pitch and Surge Force RAO Amplitude and Phase for 33 meter separation, 150 degree wave heading, and 16 knots ship speed.

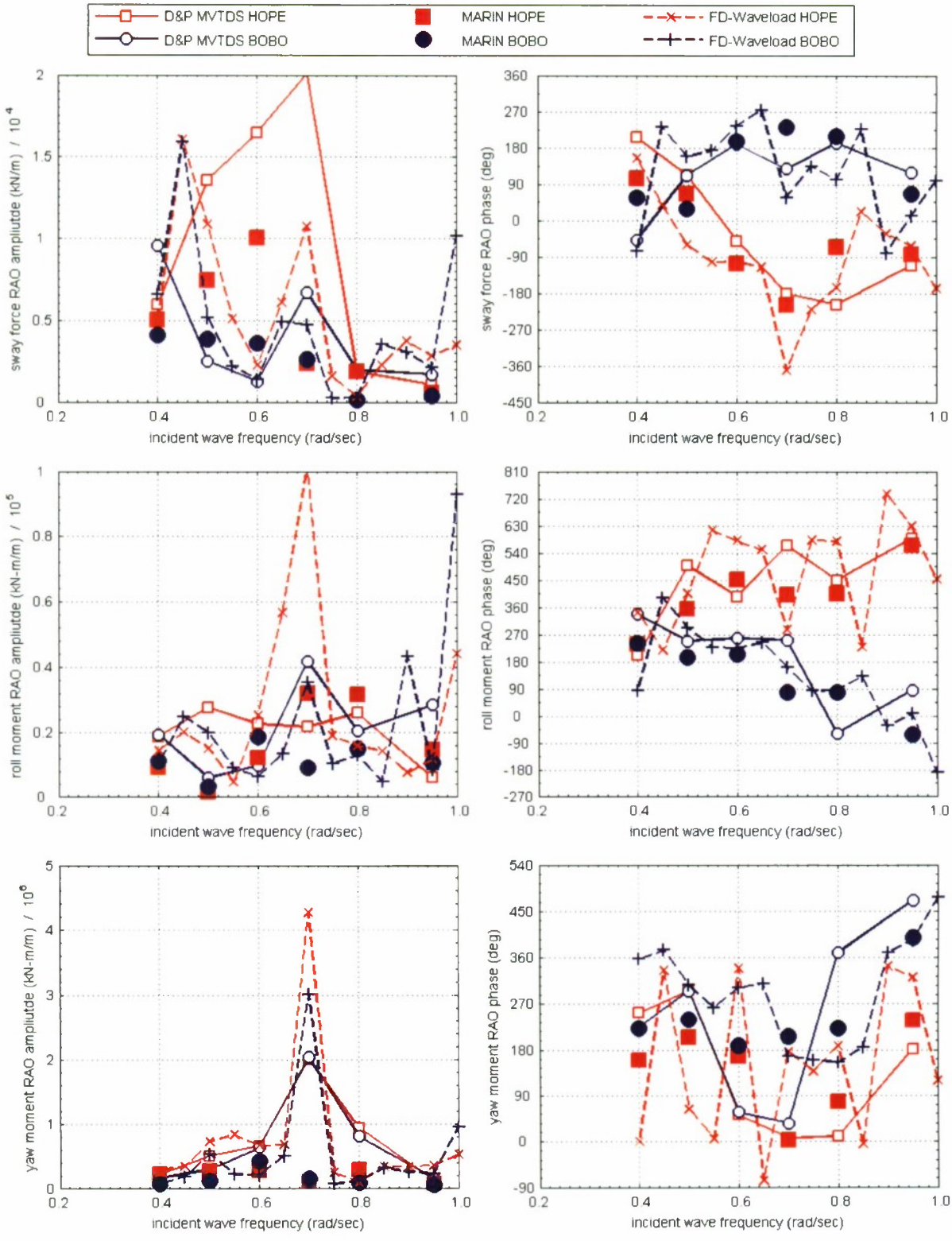

Figure B12. HOPE, BOBO Sway Force and Roll and Yaw Moment RAO Amplitude and Phase for 33 meter separation, 150 degree wave heading, and 16 knots ship speed.

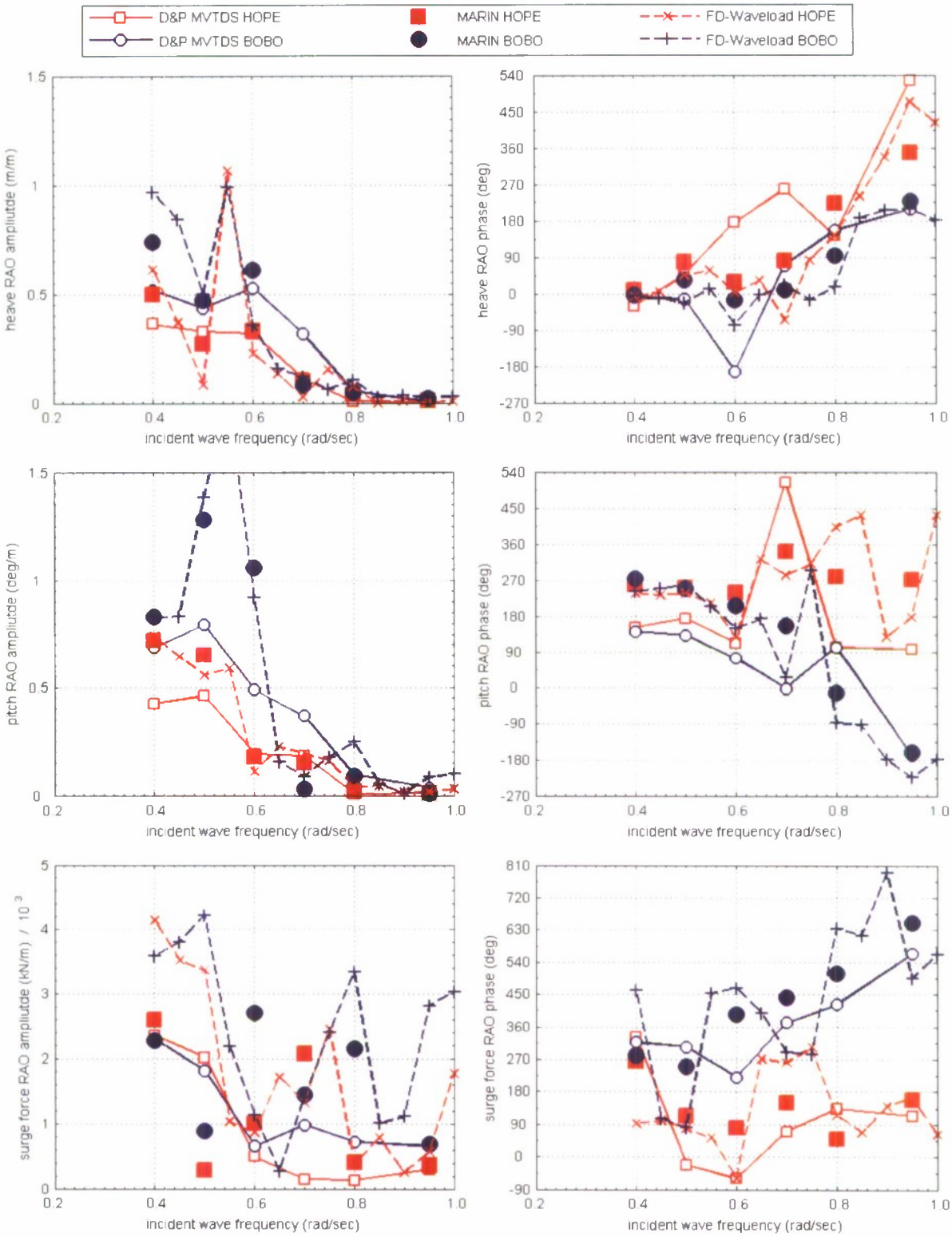

Figure B13. HOPE, BOBO Heave and Pitch and Surge Force RAO Amplitude and Phase for 33 meter separation, 180 degree wave heading, and 16 knots ship speed.

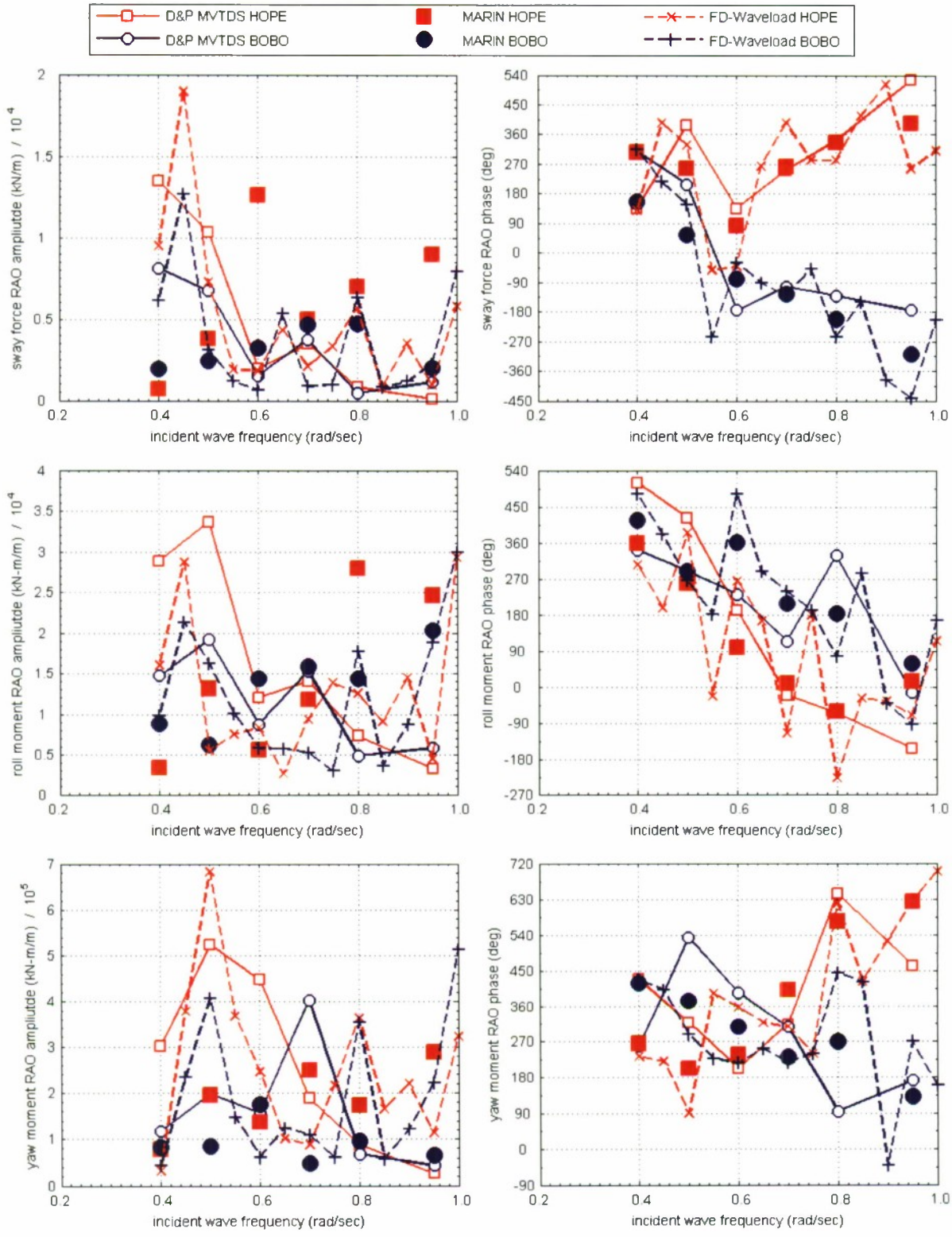

Figure B14. HOPE, BOBO Sway force and Roll and Yaw Moment RAO Amplitude and Phase for 33 meter separation, 180 degree wave heading, and 16 knots ship speed.

APPENDIX C. AQWA

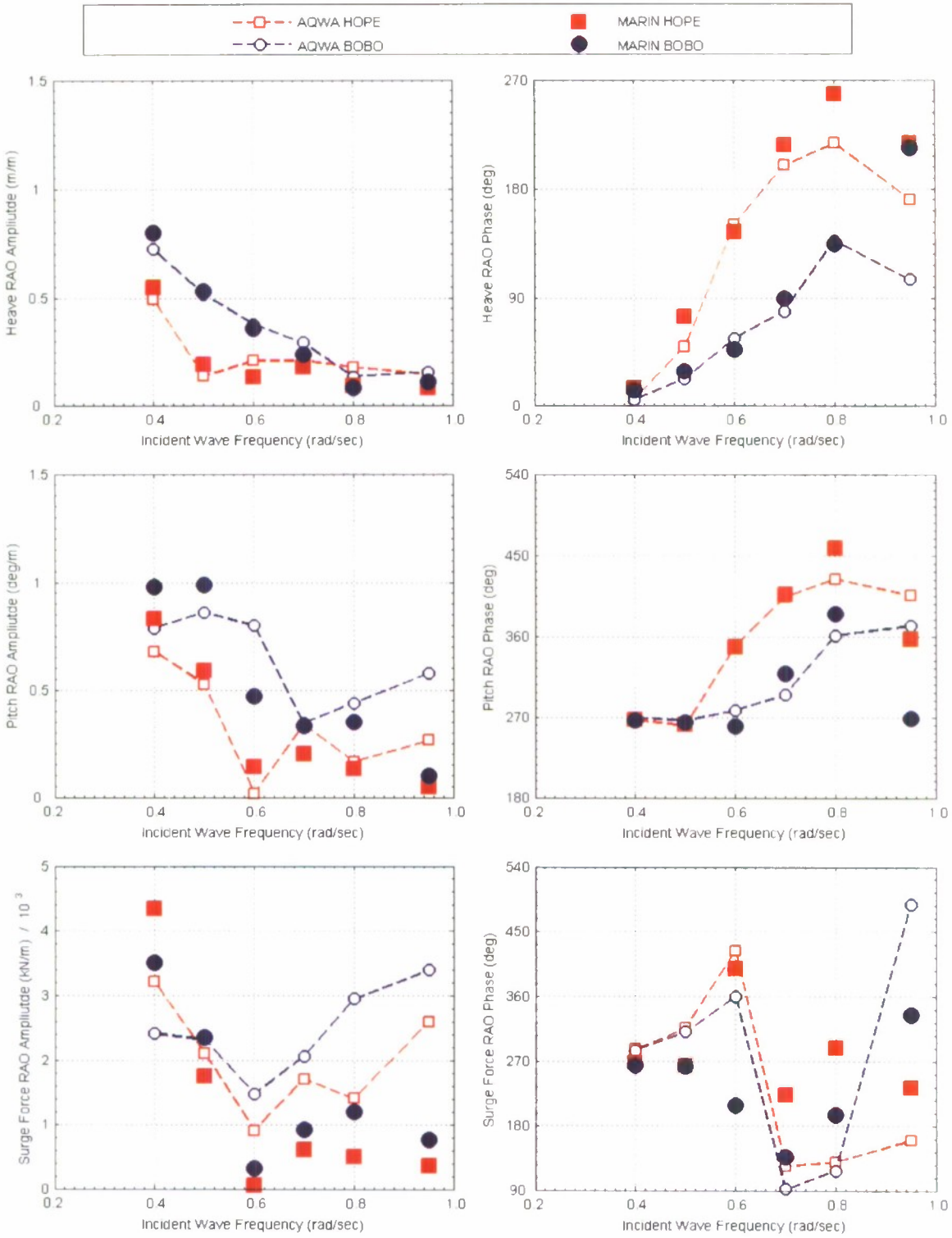

Figure C1. HOPE, BOBO Heave and Pitch and Surge Force RAO Amplitude and Phase for 3 meter separation, 180 degree wave heading, and 5 knots ship speed.

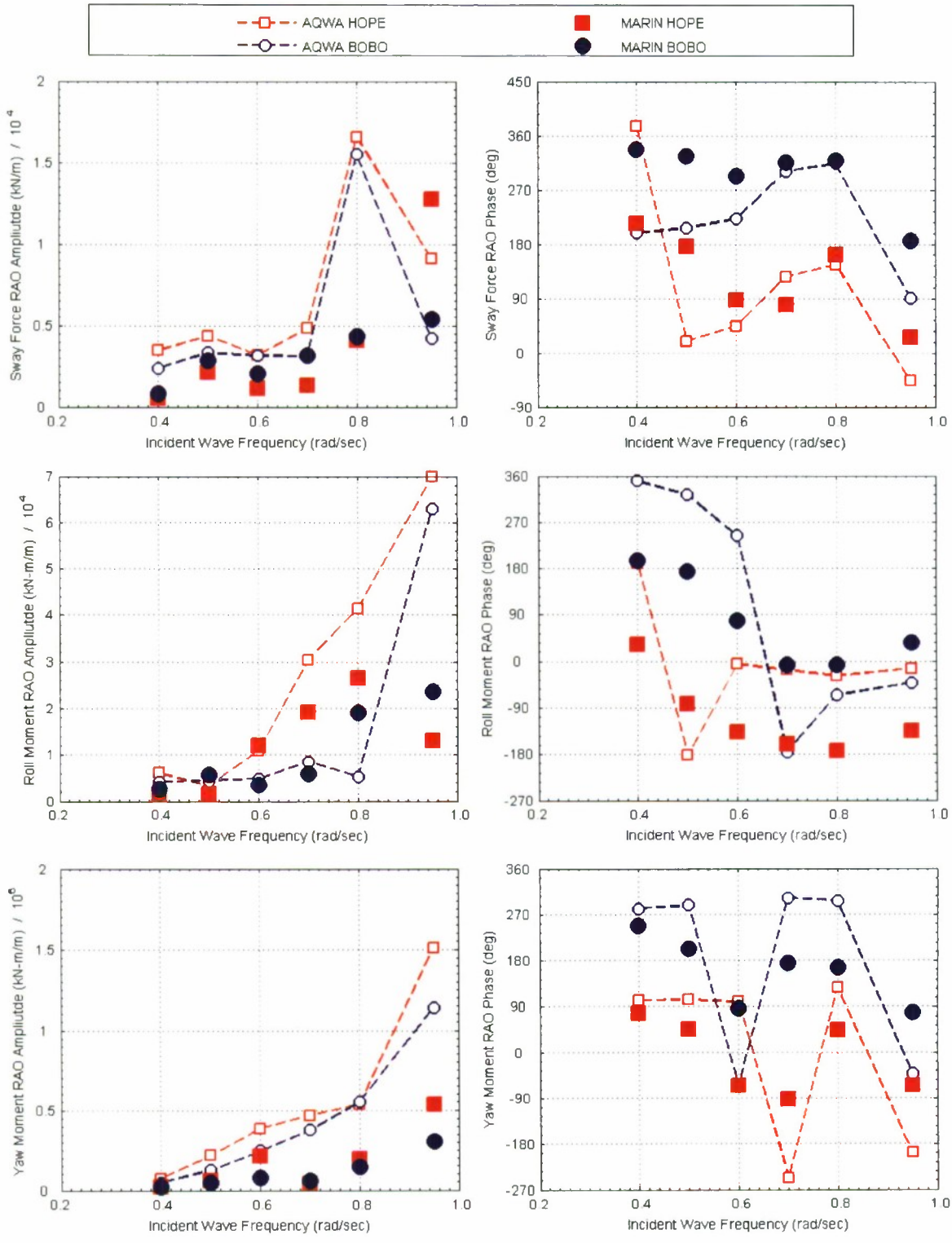

Figure C2. HOPE, BOBO Sway Force and Roll and Yaw Moment RAO Amplitude and Phase for 3 meter separation, 180 degree wave heading, and 5 knots ship speed.

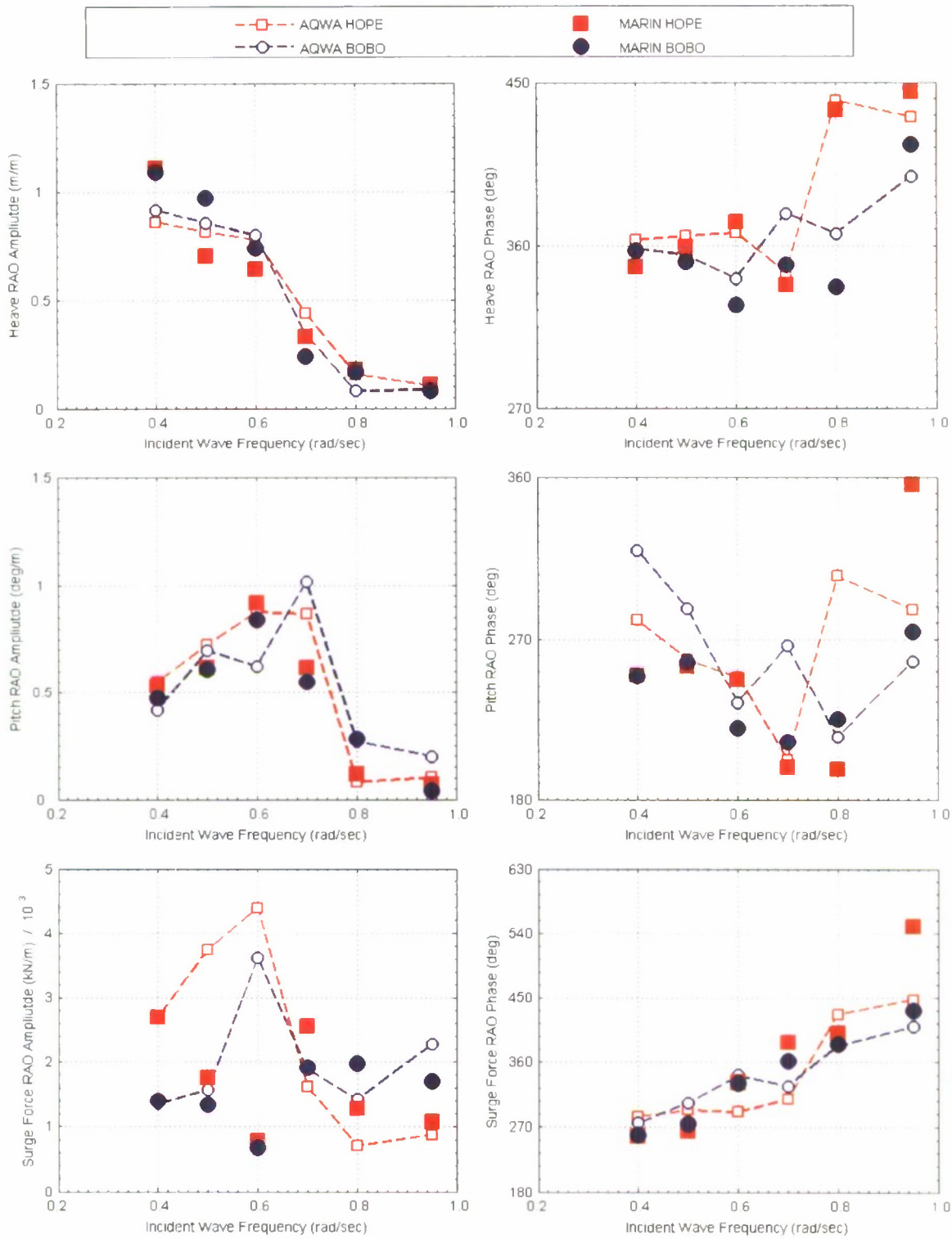

Figure C3. HOPE, BOBO Heave and Pitch and Surge Force RAO Amplitude and Phase for 16.5 meter separation, 120 degree wave heading, and 16 knots ship speed.

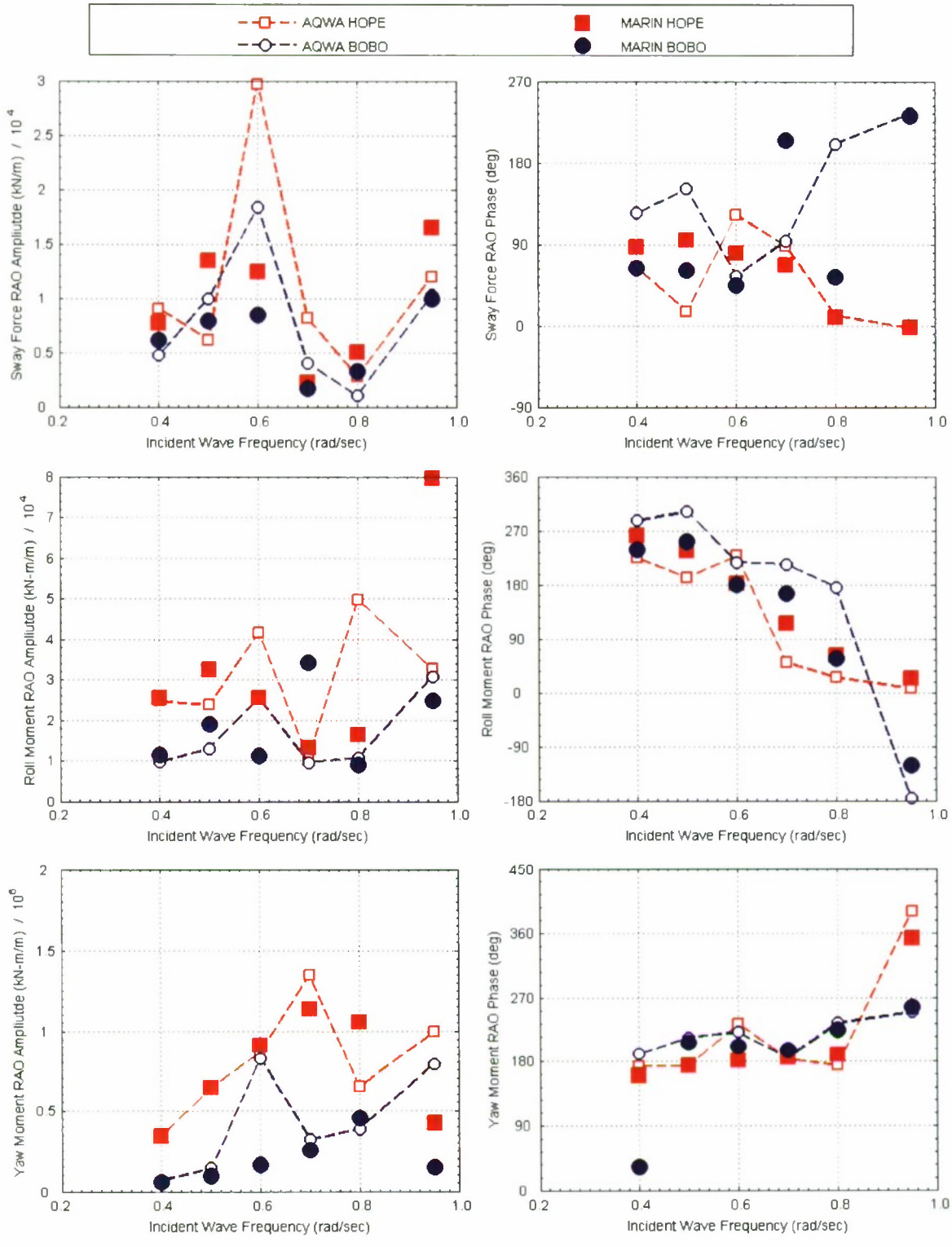

Figure C4. HOPE, BOBO Sway force and Roll and Yaw Moment RAO Amplitude and Phase for 16.5 meter separation, 120 degree wave heading, and 16 knots ship speed.

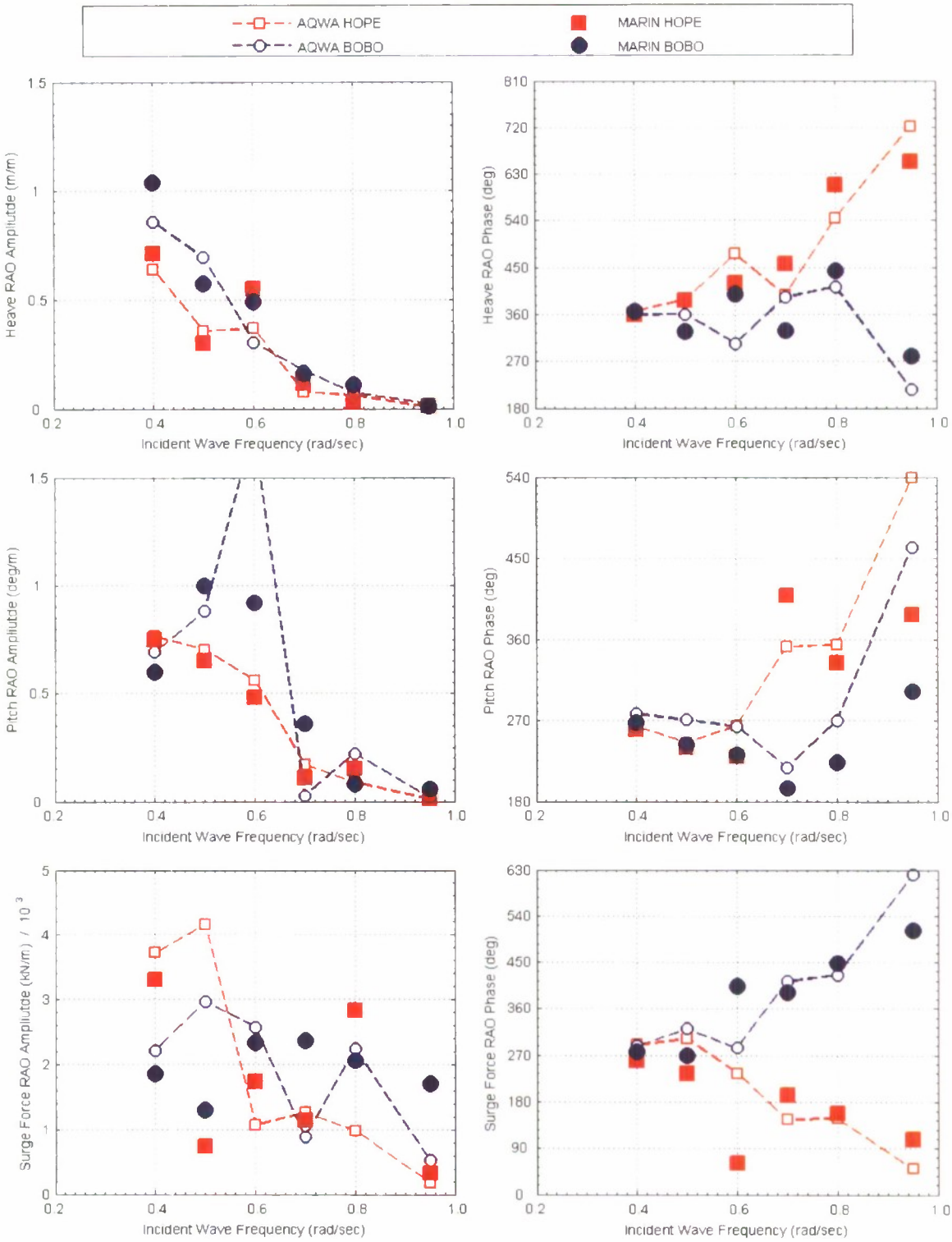

Figure C5. HOPE, BOBO Heave and Piteh and Surge Foree RAO Amplitude and Phase for 16.5 meter separation, 150 degree wave heading, and 16 knots ship speed.

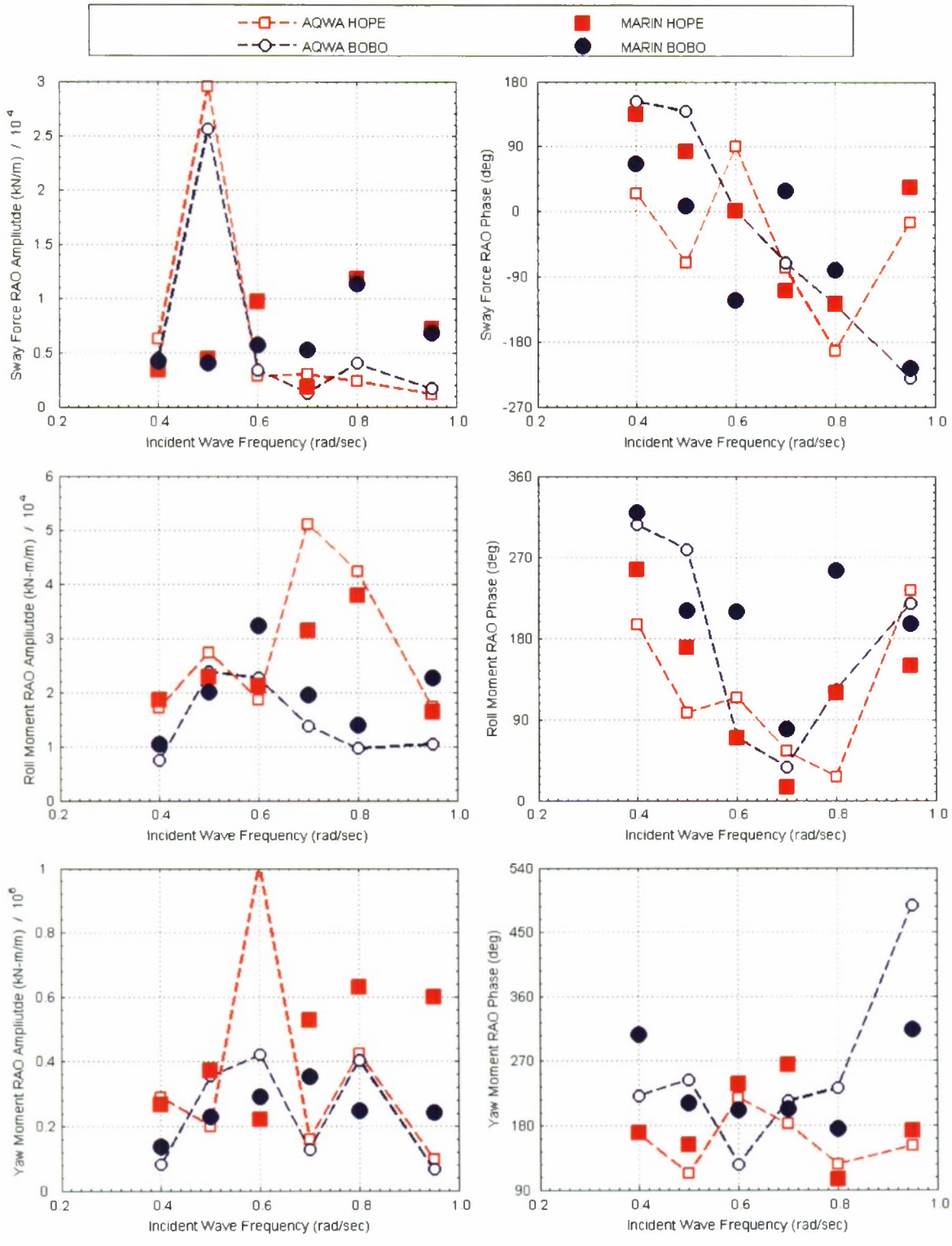

Figure C6. HOPE, BOBO Sway Force and Roll and Yaw Moment RAO Amplitude and Phase for 16.5 meter separation, 150 degree wave heading, and 16 knots ship speed.

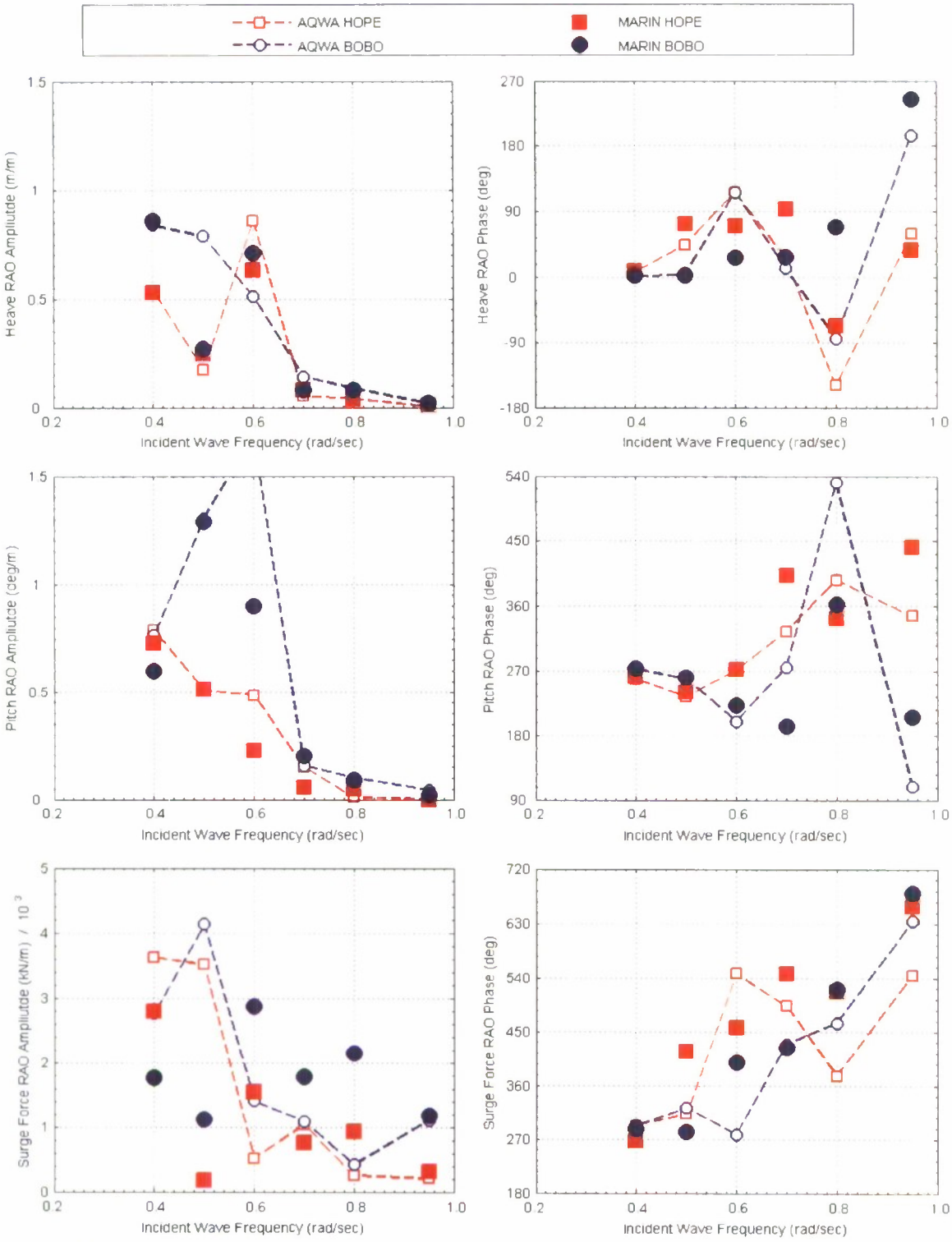

Figure C7. HOPE, BOBO Heave and Pitch and Surge Force RAO Amplitude and Phase for 16.5 meter separation, 180 degree wave heading, and 16 knots ship speed.

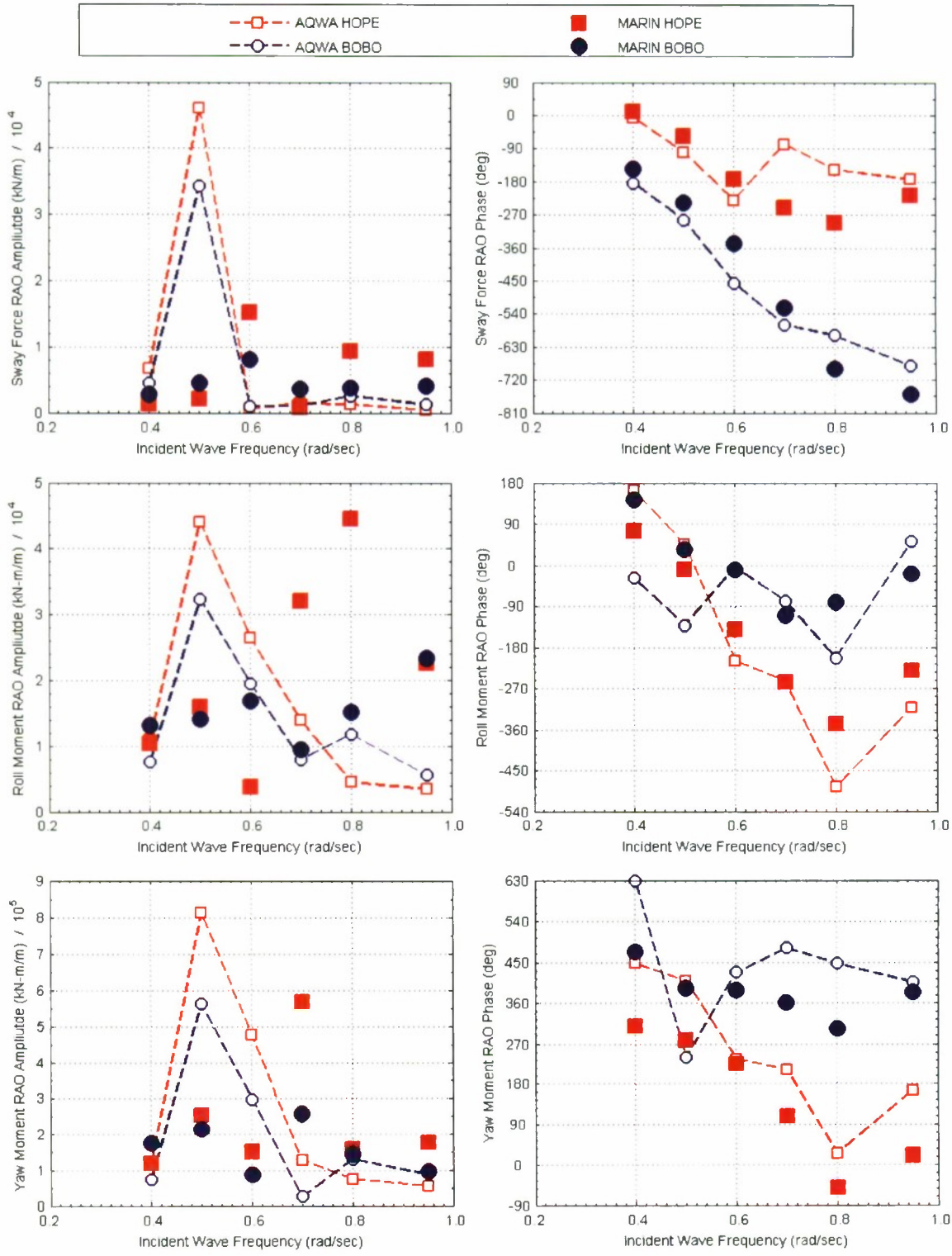

Figure C8. HOPE, BOBO Sway Force and Roll and Yaw Moment RAO Amplitude and Phase for 16.5 meter separation, 180 degree wave heading, and 16 knots ship speed.

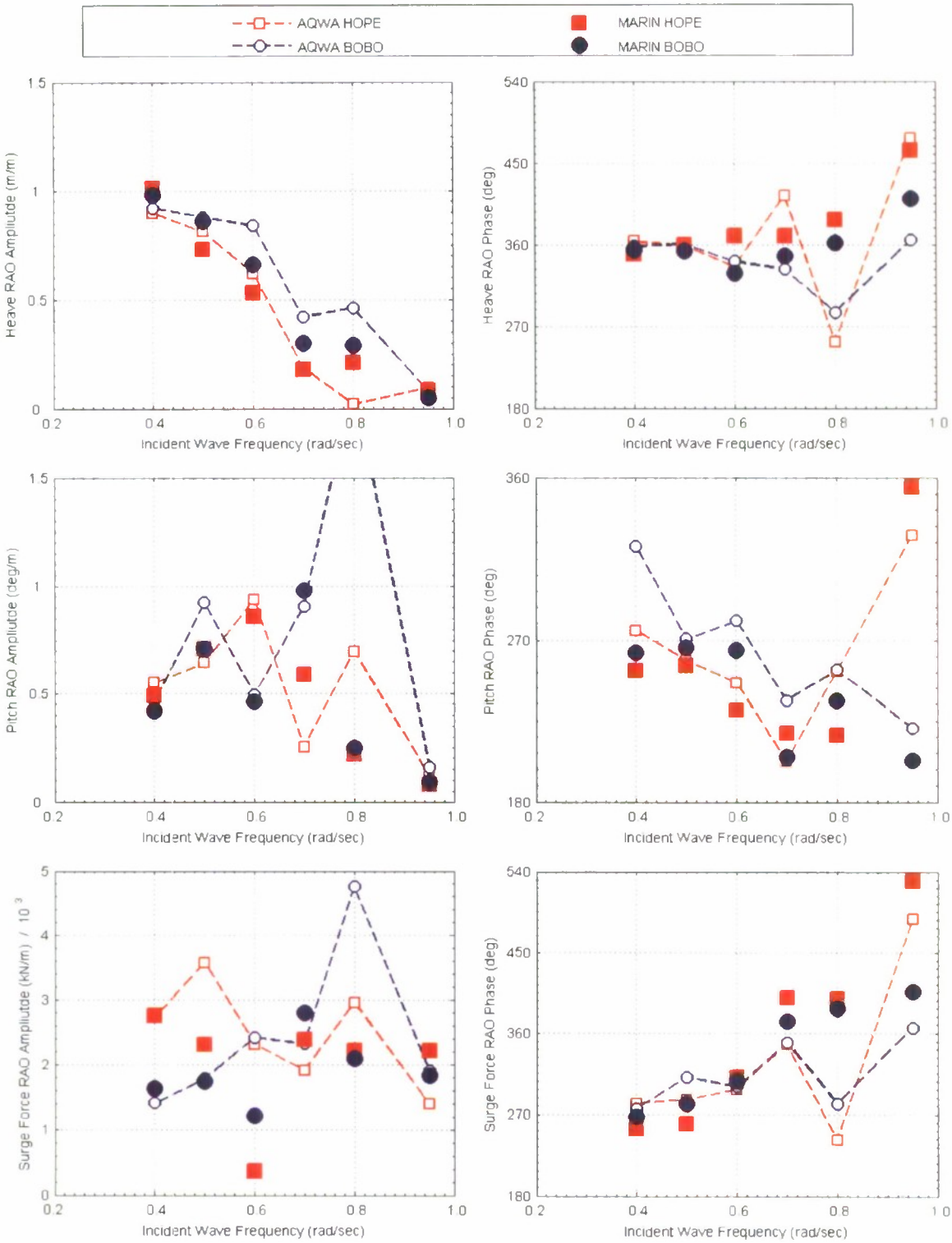

Figure C9. HOPE, BOBO Heave and Pitch and Surge Force RAO Amplitude and Phase for 33 meter separation, 120 degree wave heading, and 16 knots ship speed.

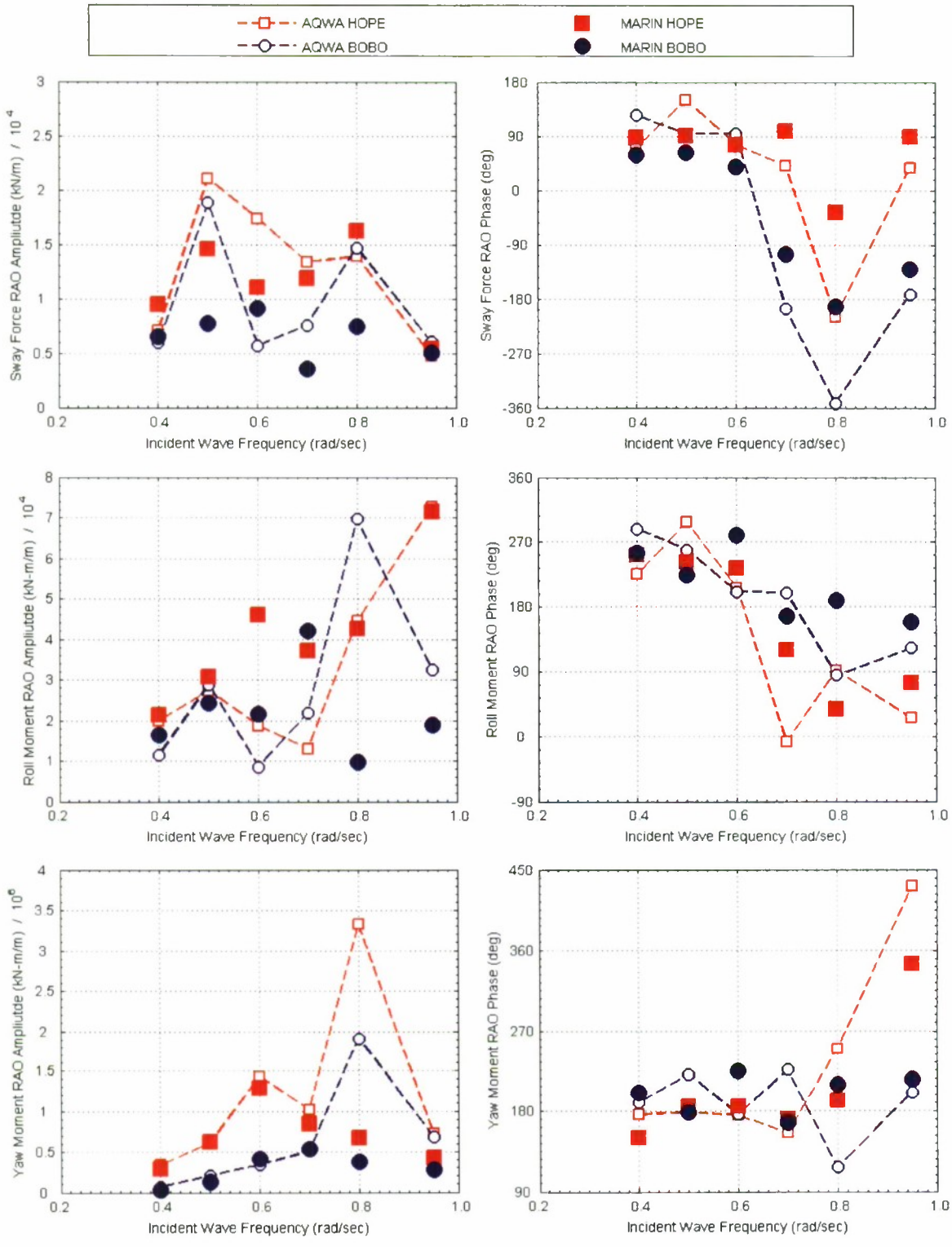

Figure C10. HOPE, BOBO Sway force and Roll and Yaw Moment RAO Amplitude and Phase for 33 meter separation, 120 degree wave heading, and 16 knots ship speed.

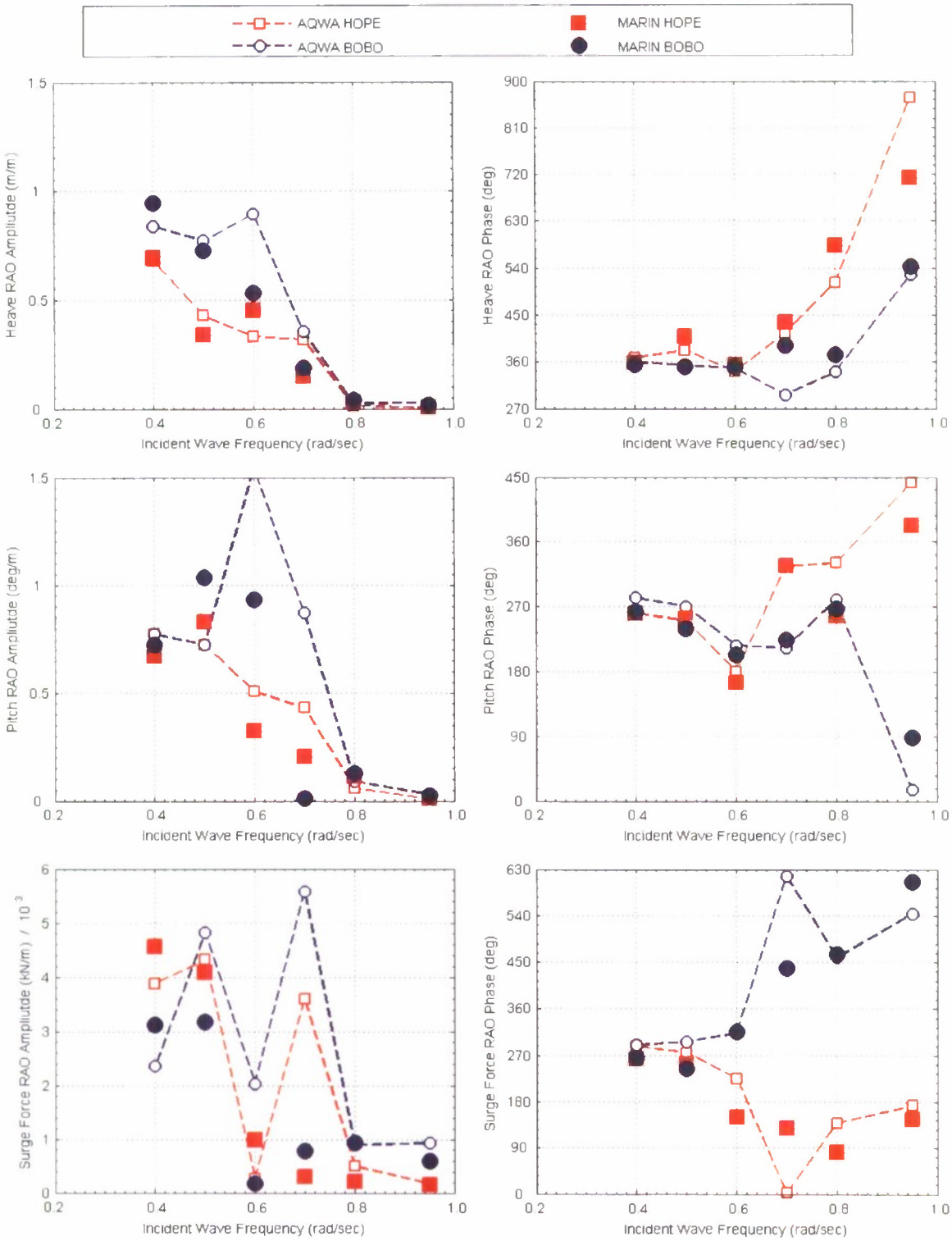

Figure C11. HOPE, BOBO Heave and Pitch and Surge Force RAO Amplitude and Phase for 33 meter separation, 150 degree wave heading, and 16 knots ship speed.

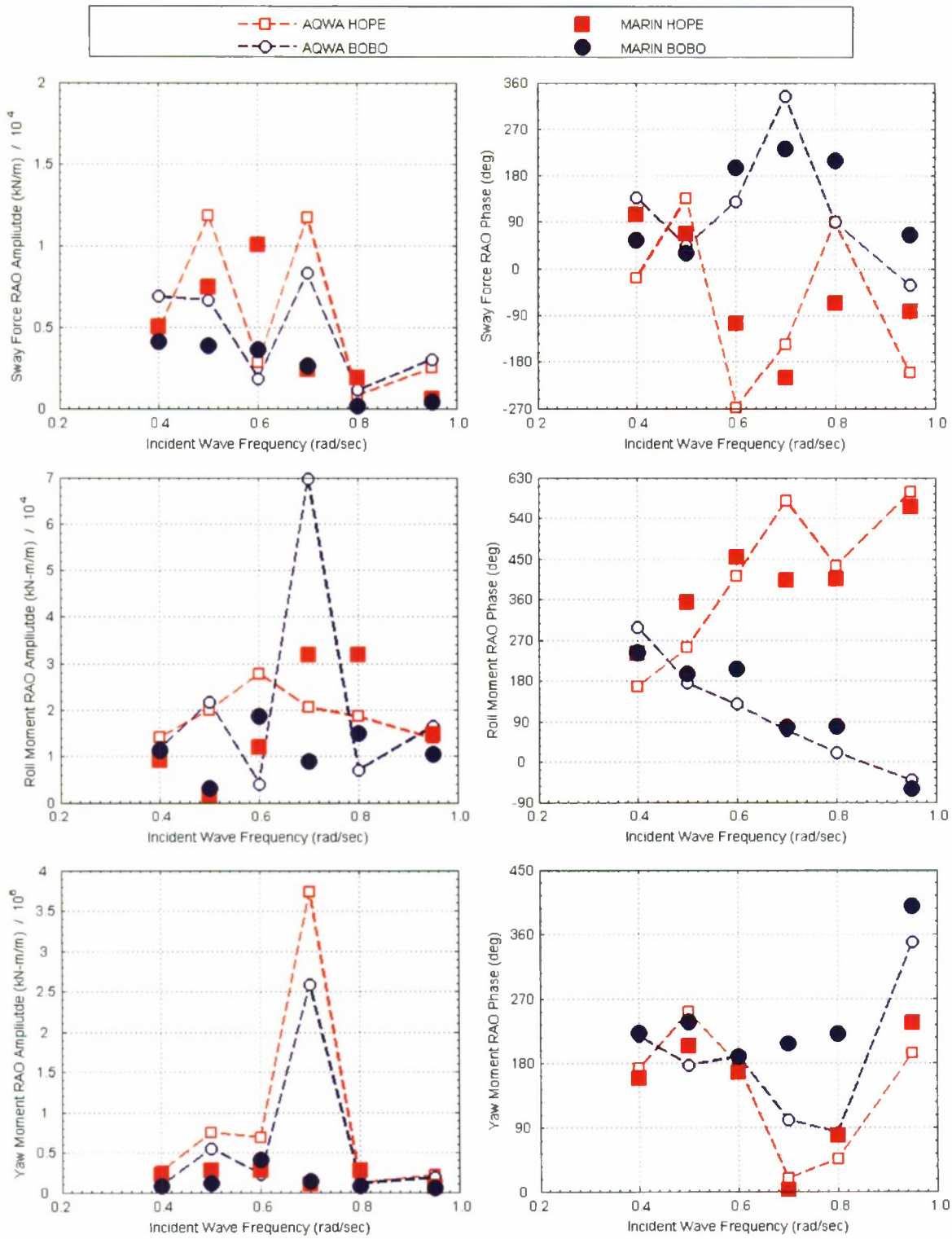

Figure C12. HOPE, BOBO Sway Force and Roll and Yaw Moment RAO Amplitude and Phase for 33 meter separation, 150 degree wave heading, and 16 knots ship speed.

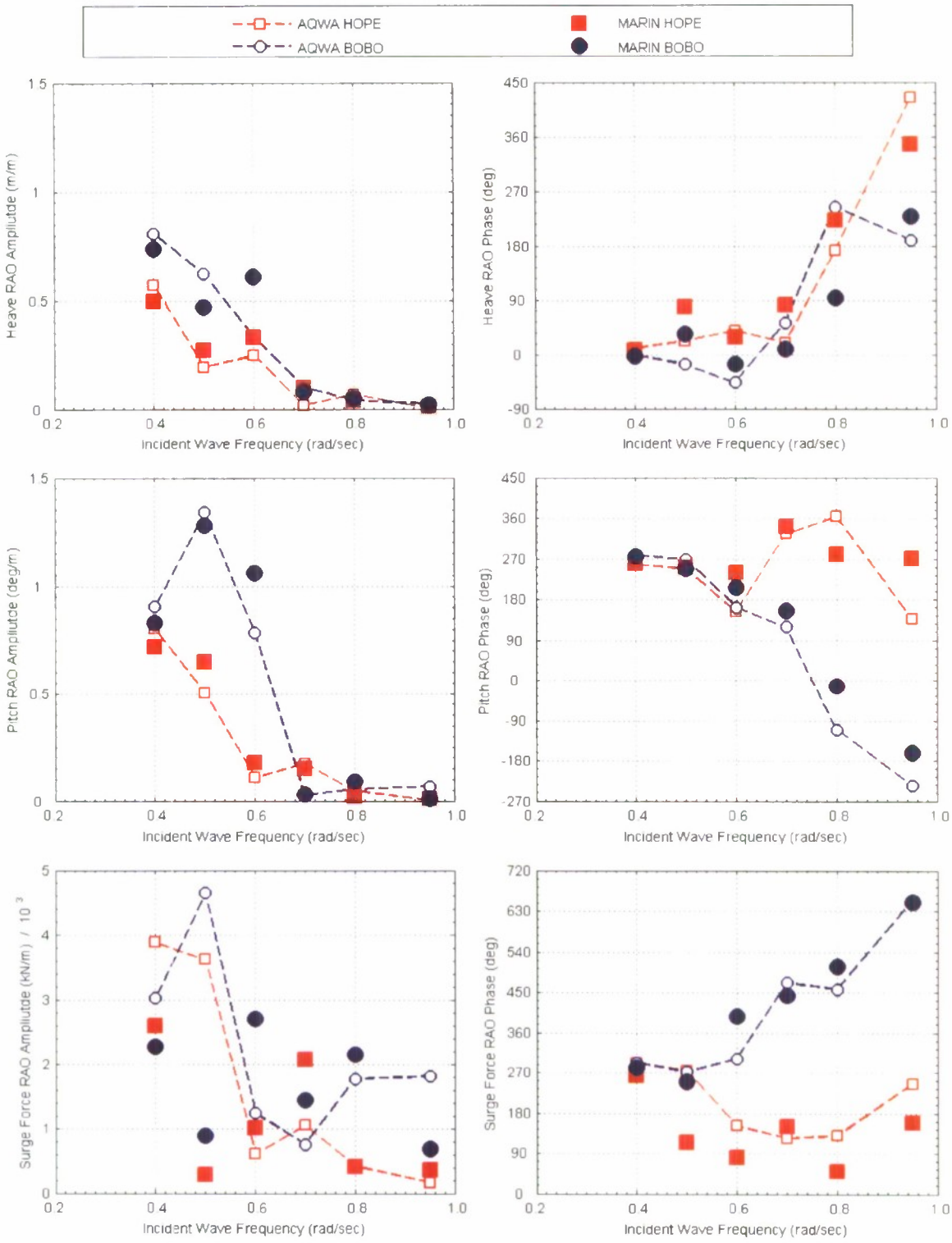

Figure C13. HOPE, BOBO Heave and Pitch and Surge Force RAO Amplitude and Phase for 33 meter separation, 180 degree wave heading, and 16 knots ship speed.

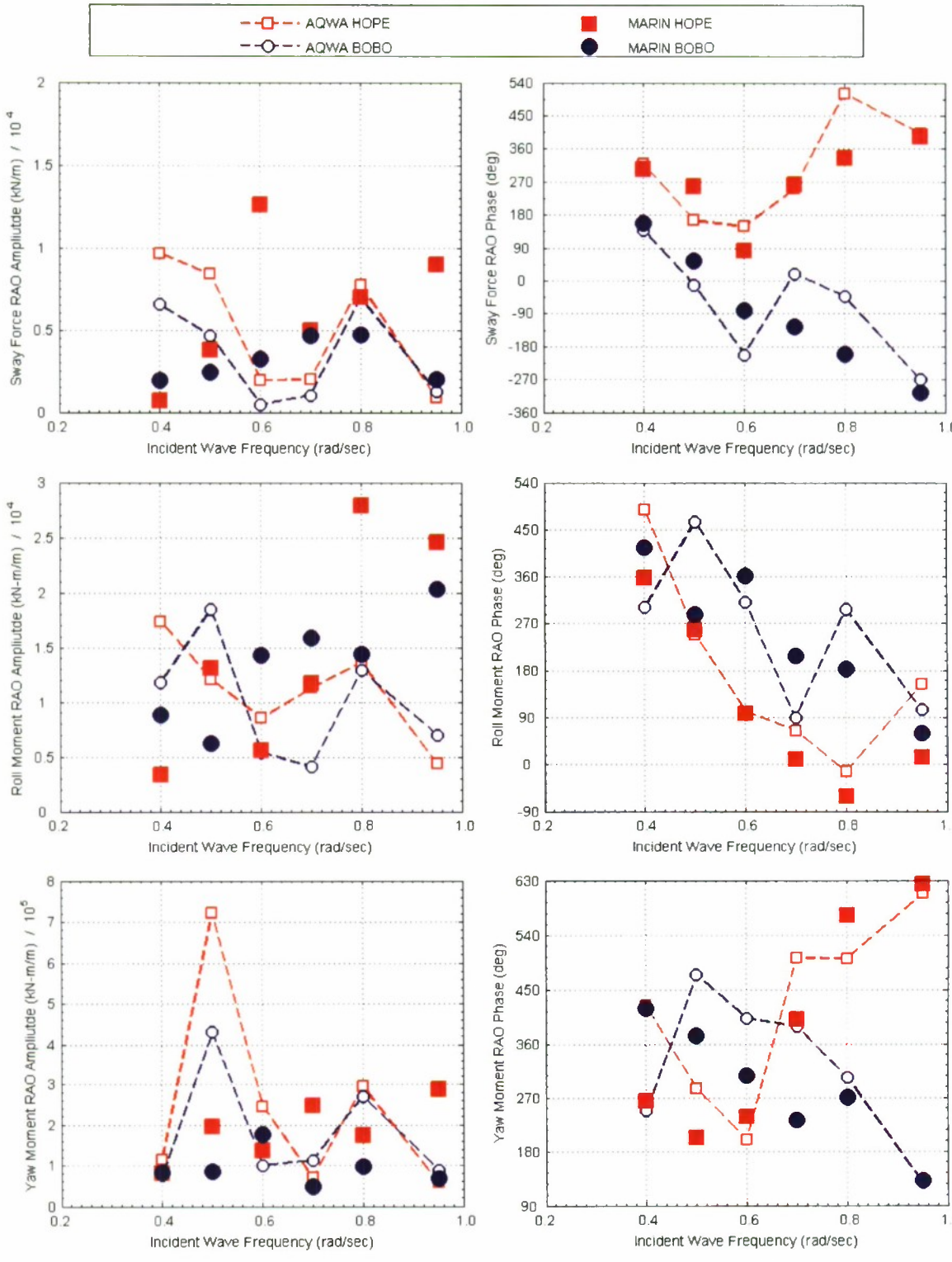

Figure C14. HOPE, BOBO Sway Force and Roll and Yaw Moment RAO Amplitude and Phase for 33 meter separation, 180 degree wave heading, and 16 knots ship speed.

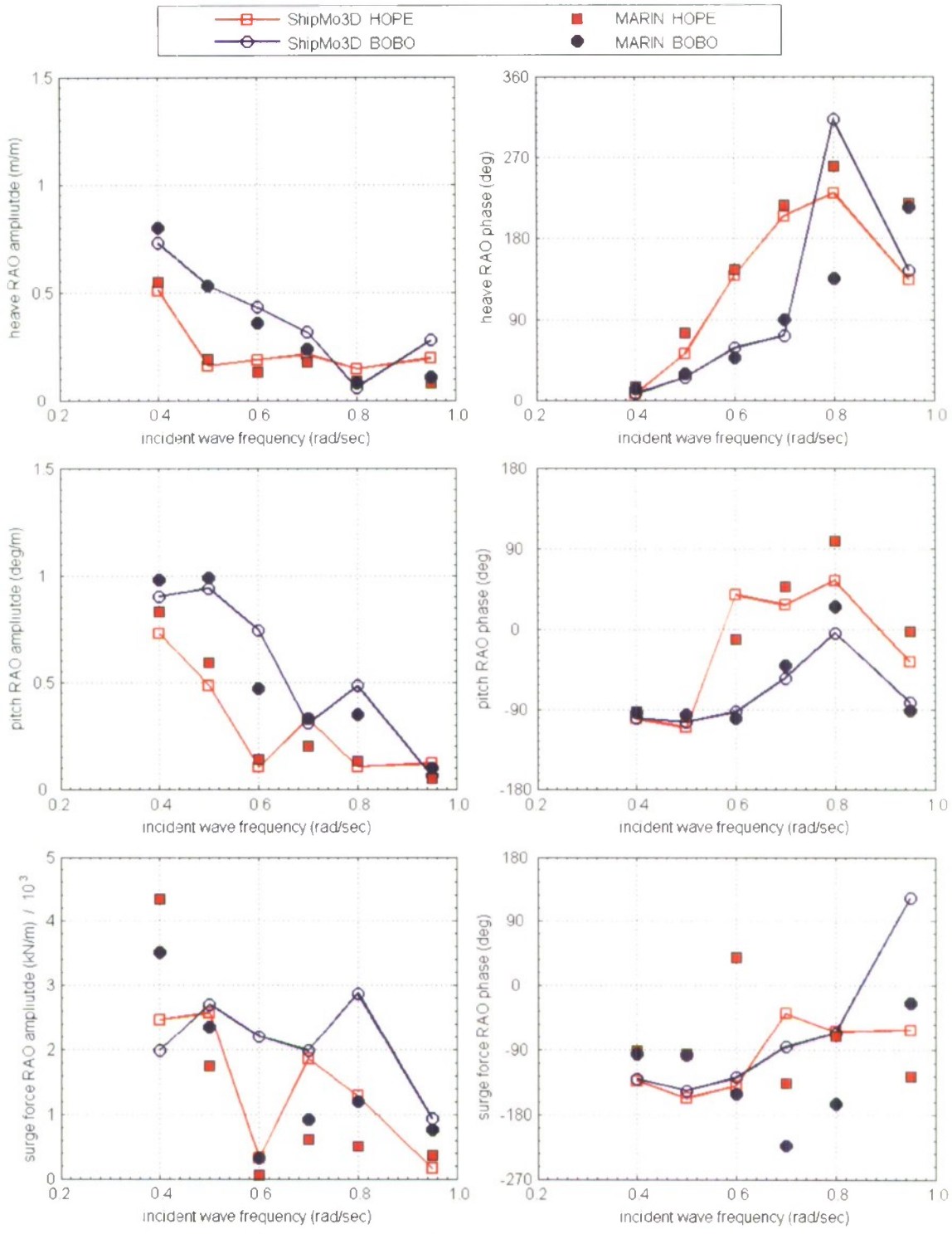

Figure D1. HOPE, BOBO Heave and Pitch and Surge Force RAO Amplitude and Phase for 3 meter separation, 180 degree wave heading, and 5 knots ship speed.

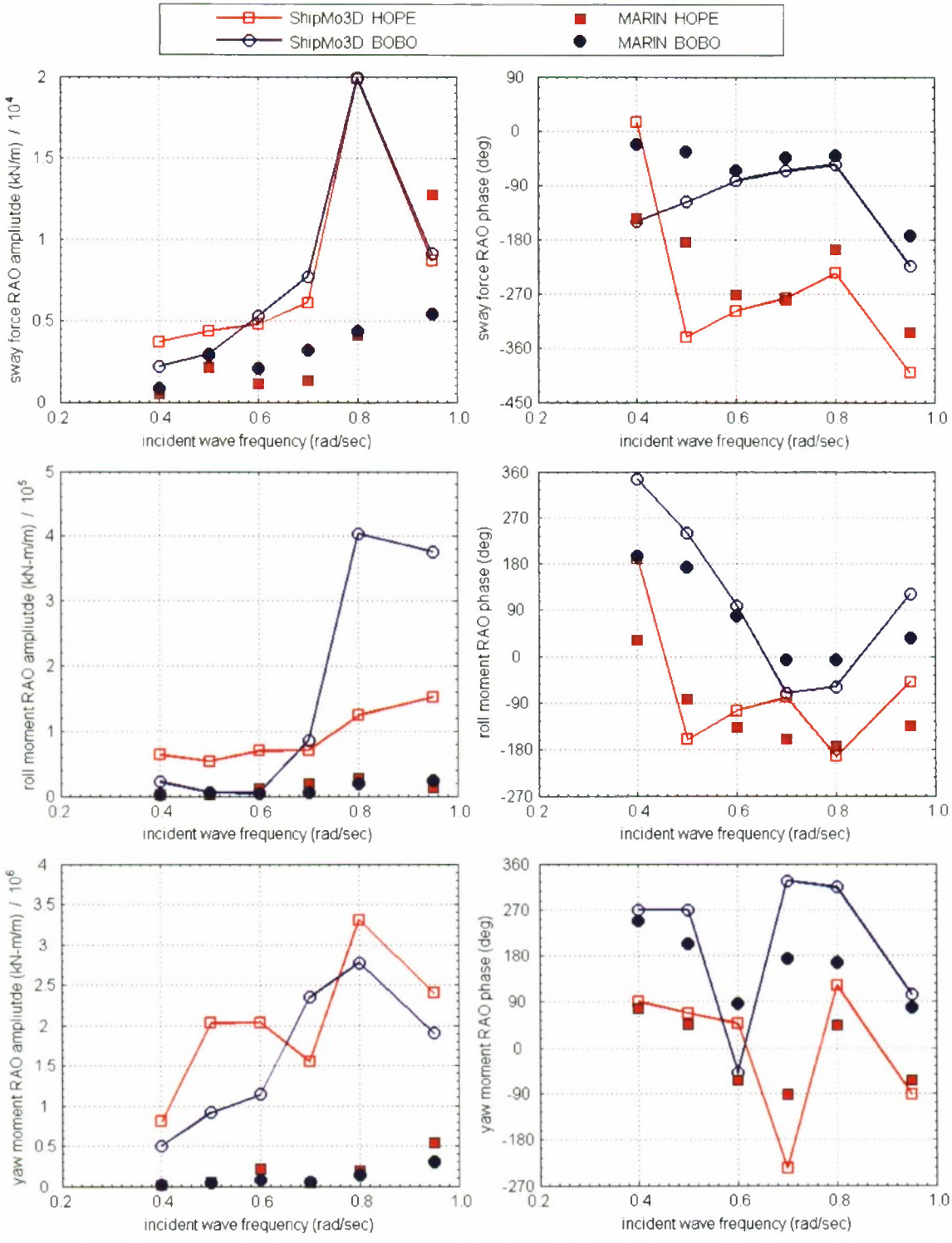

Figure D2. HOPE, BOBO Sway Force and Roll and Yaw Moment RAO Amplitude and Phase for 3 meter separation, 180 degree wave heading, and 5 knots ship speed.

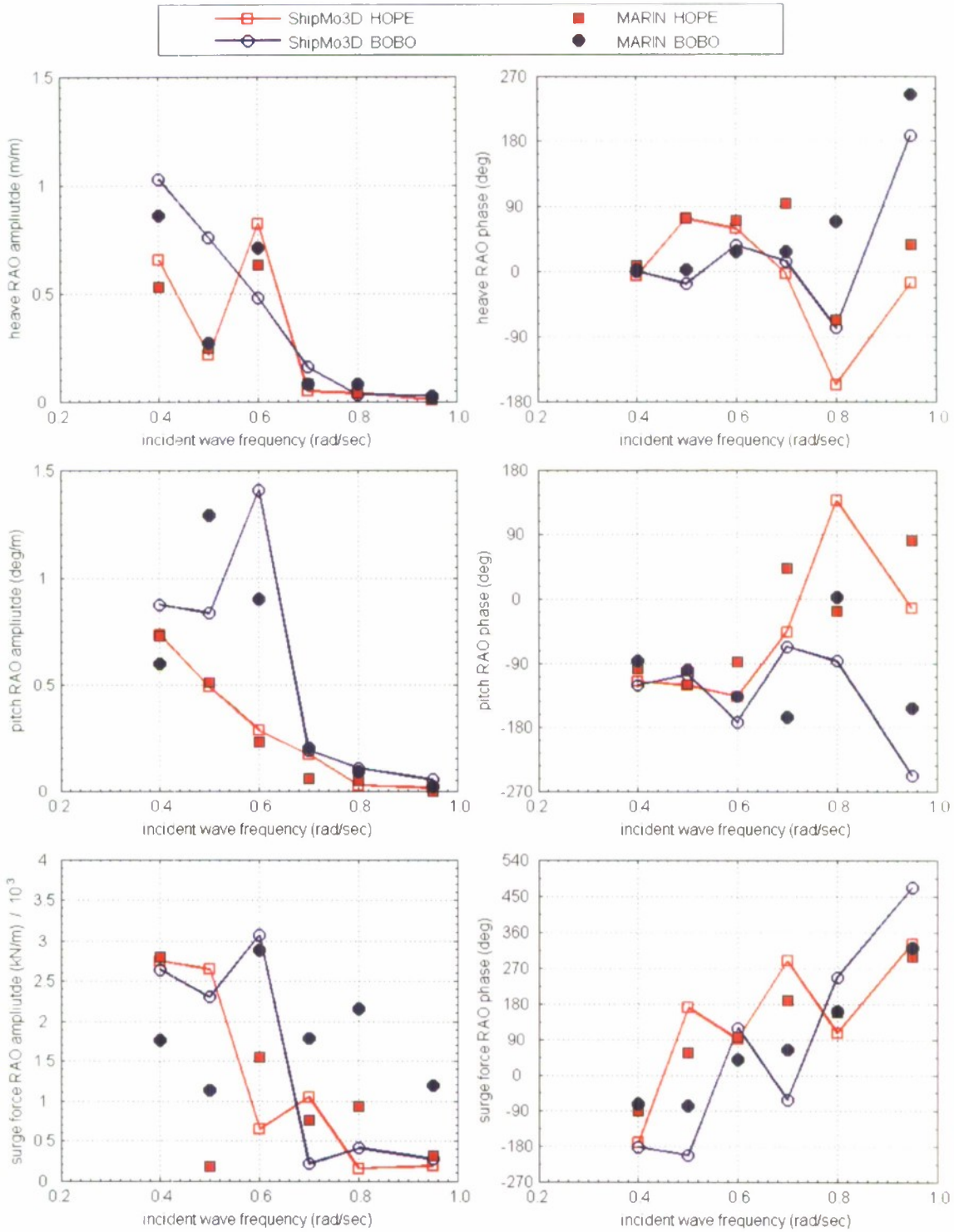

Figure D3. HOPE, BOBO Heave and Pitch Motions and Surge Force RAO Amplitude and Phase for 16.5 meter separation, 120 degree wave heading, and 16 knots ship speed.

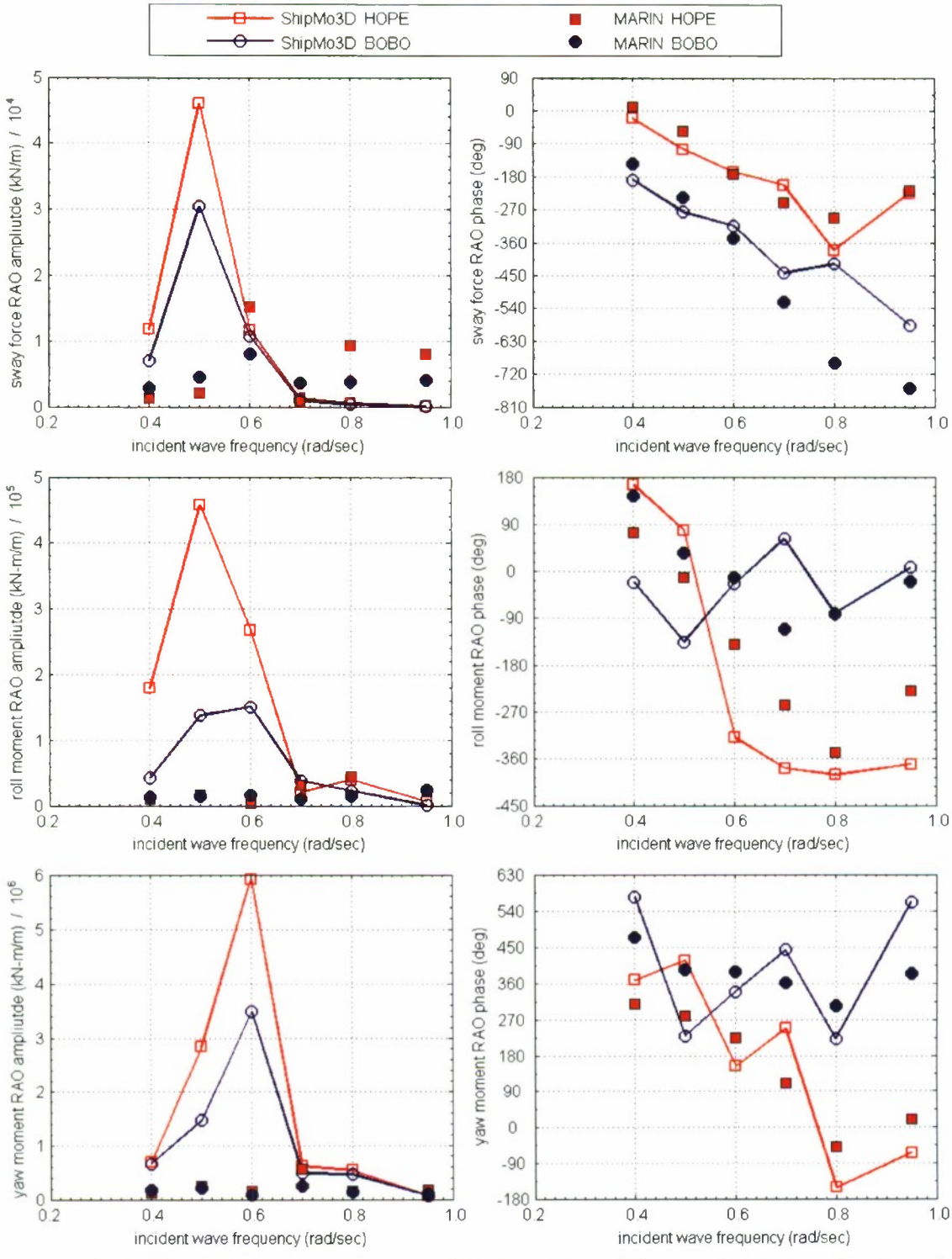

Figure D4. HOPE, BOBO Sway Force and Roll and Yaw Moment RAO Amplitude and Phase for 16.5 meter separation, 120 degree wave heading, and 16 knots ship speed.

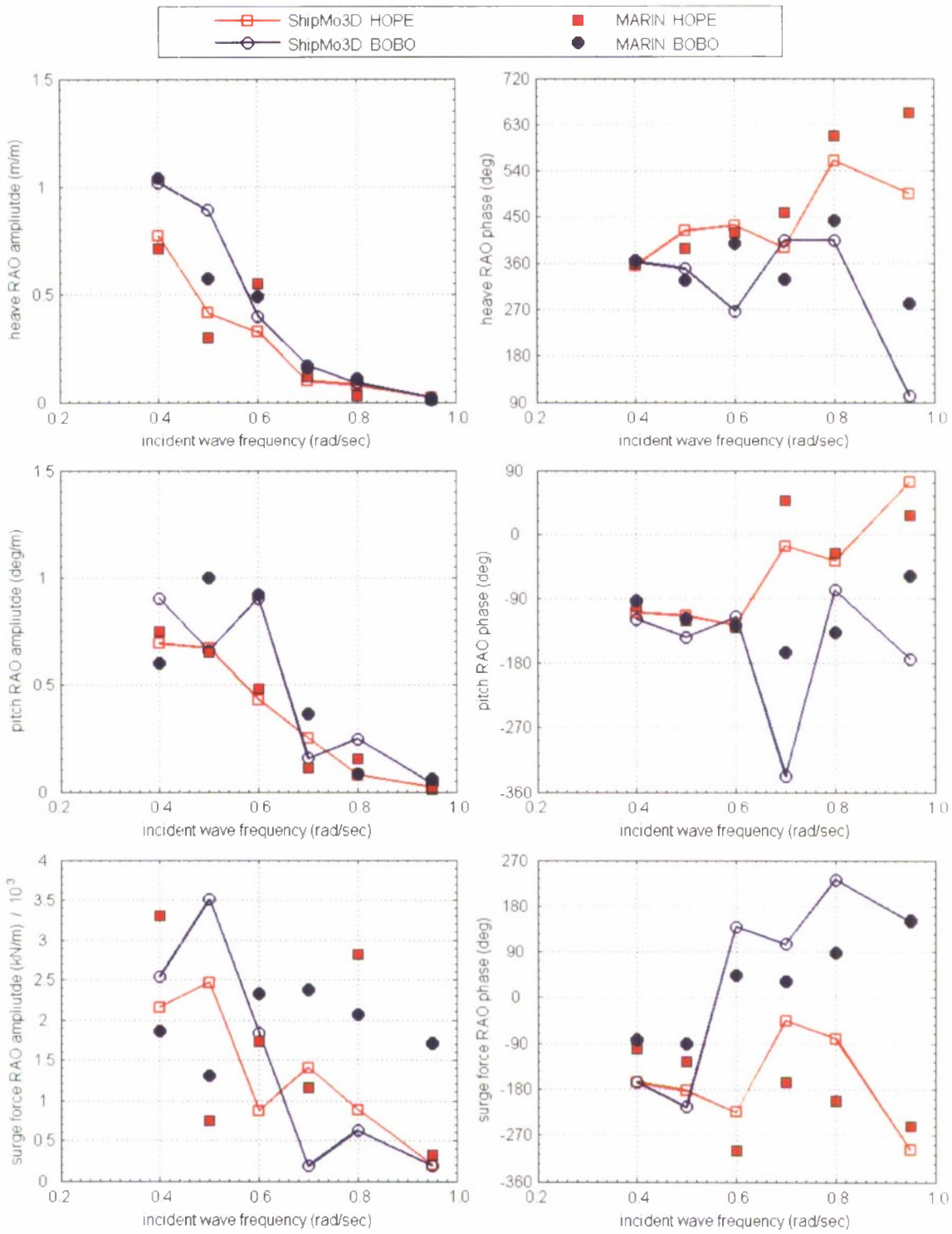

Figure D5. HOPE, BOBO Heave and Pitch Motions and Surge Force RAO Amplitude and Phase for 16.5 meter separation, 150 degree wave heading, and 16 knots ship speed.

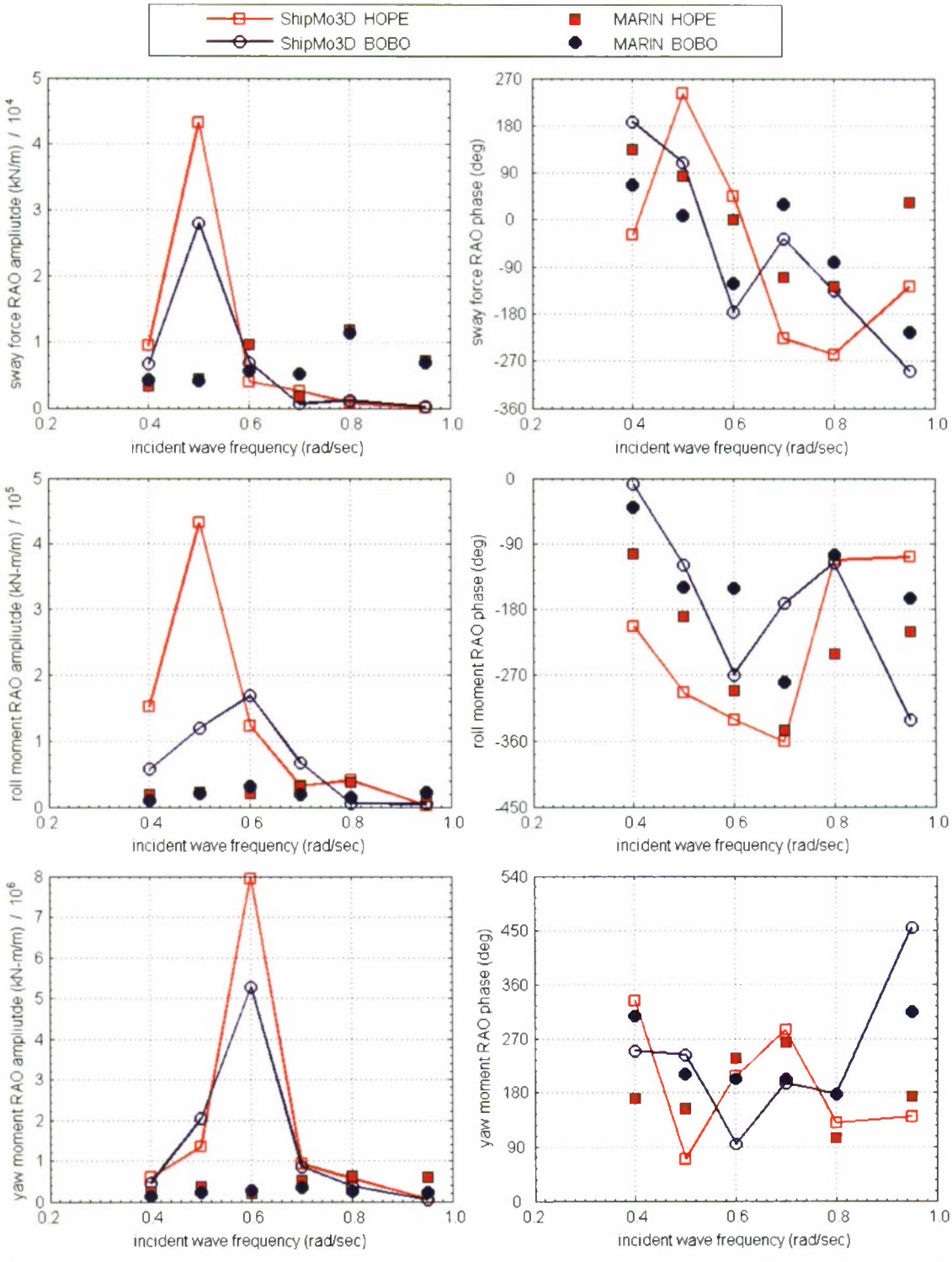

Figure D6. HOPE, BOBO Sway Force and Roll and Yaw Moment RAO Amplitude and Phase for16.5 meter separation, 150 degree wave heading, and 16 knots ship speed.

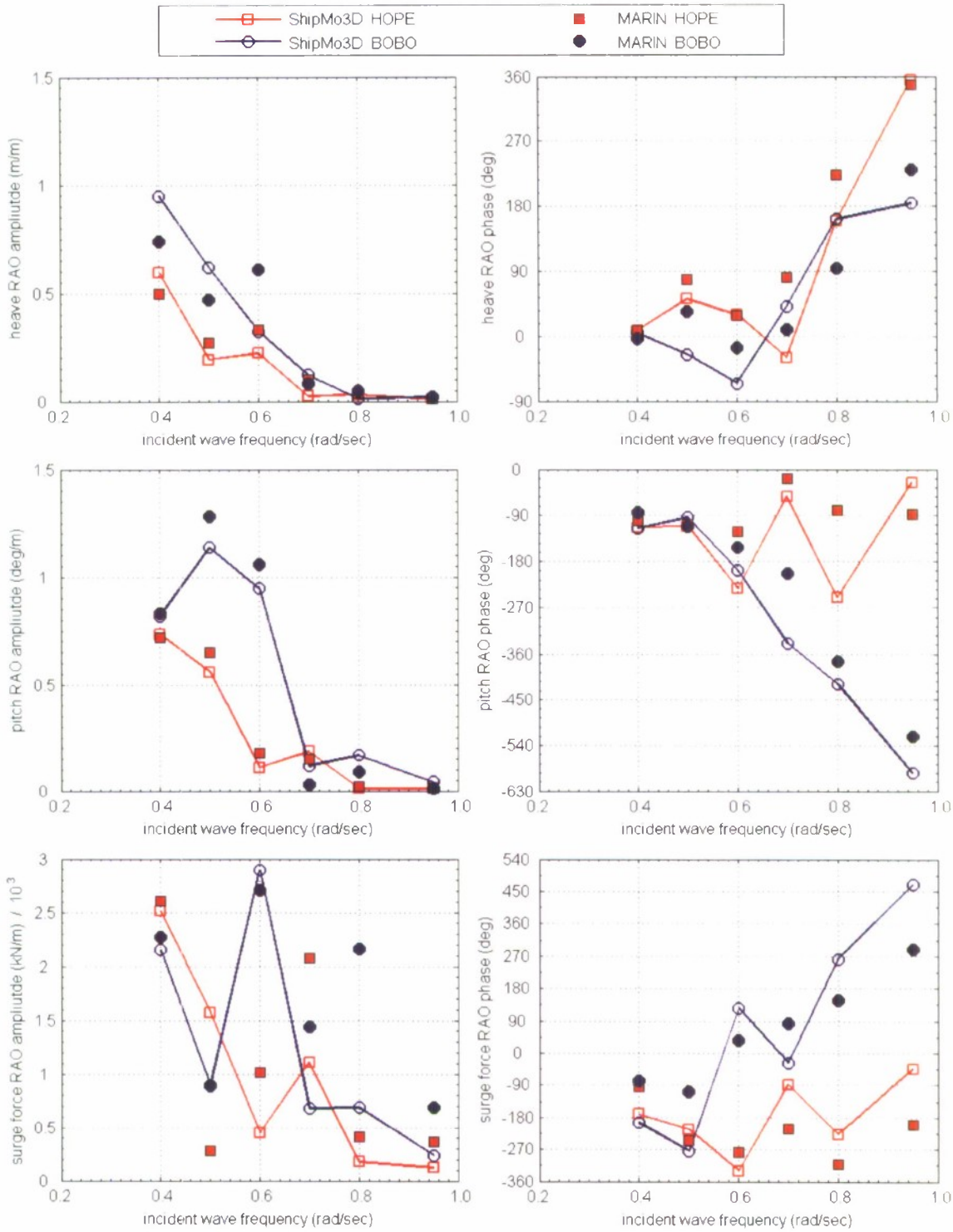

Figure D7. HOPE, BOBO Heave and Pitch Motions and Surge Force RAO Amplitude and Phase for 16.5 meter separation, 180 degree wave heading, and 16 knots ship speed.

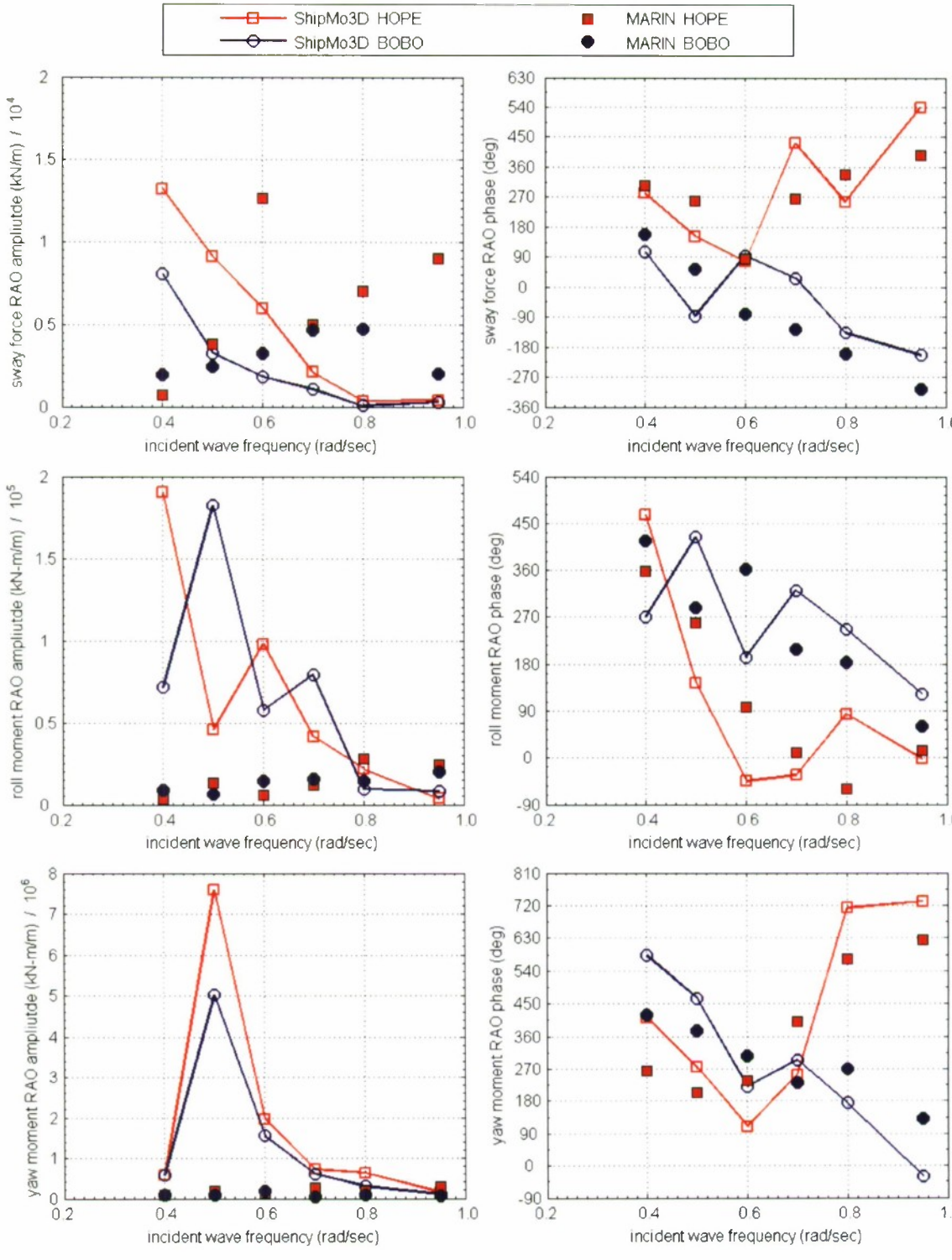

Figure D8. HOPE, BOBO Sway Force and Roll and Yaw Moment RAO Amplitude and Phase for16.5 meter separation, 180 degree wave heading, and 16 knots ship speed.

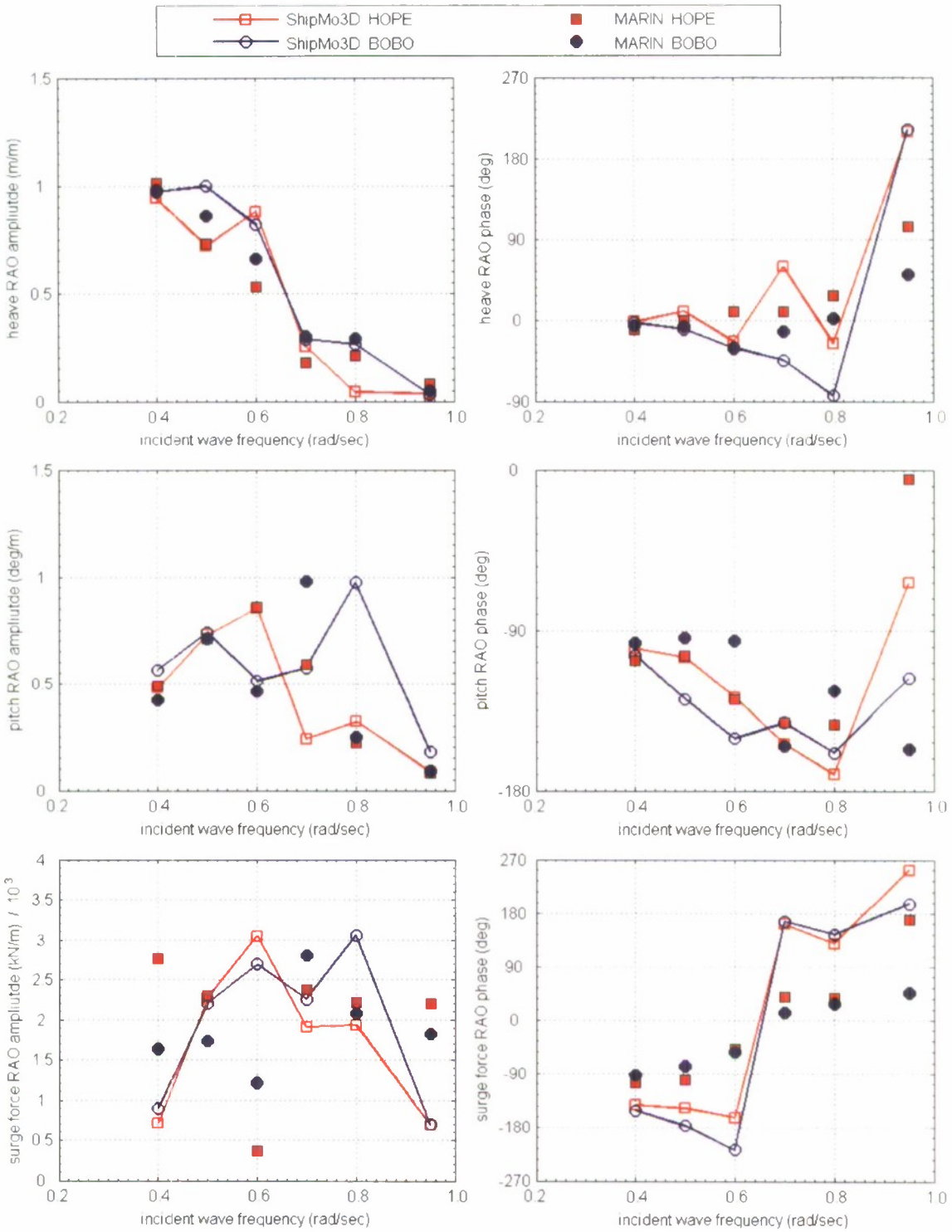

Figure D9. HOPE, BOBO Heave and Pitch Motions and Surge Force RAO Amplitude and Phase for 33 meter separation, 120 degree wave heading, and 16 knots ship speed.

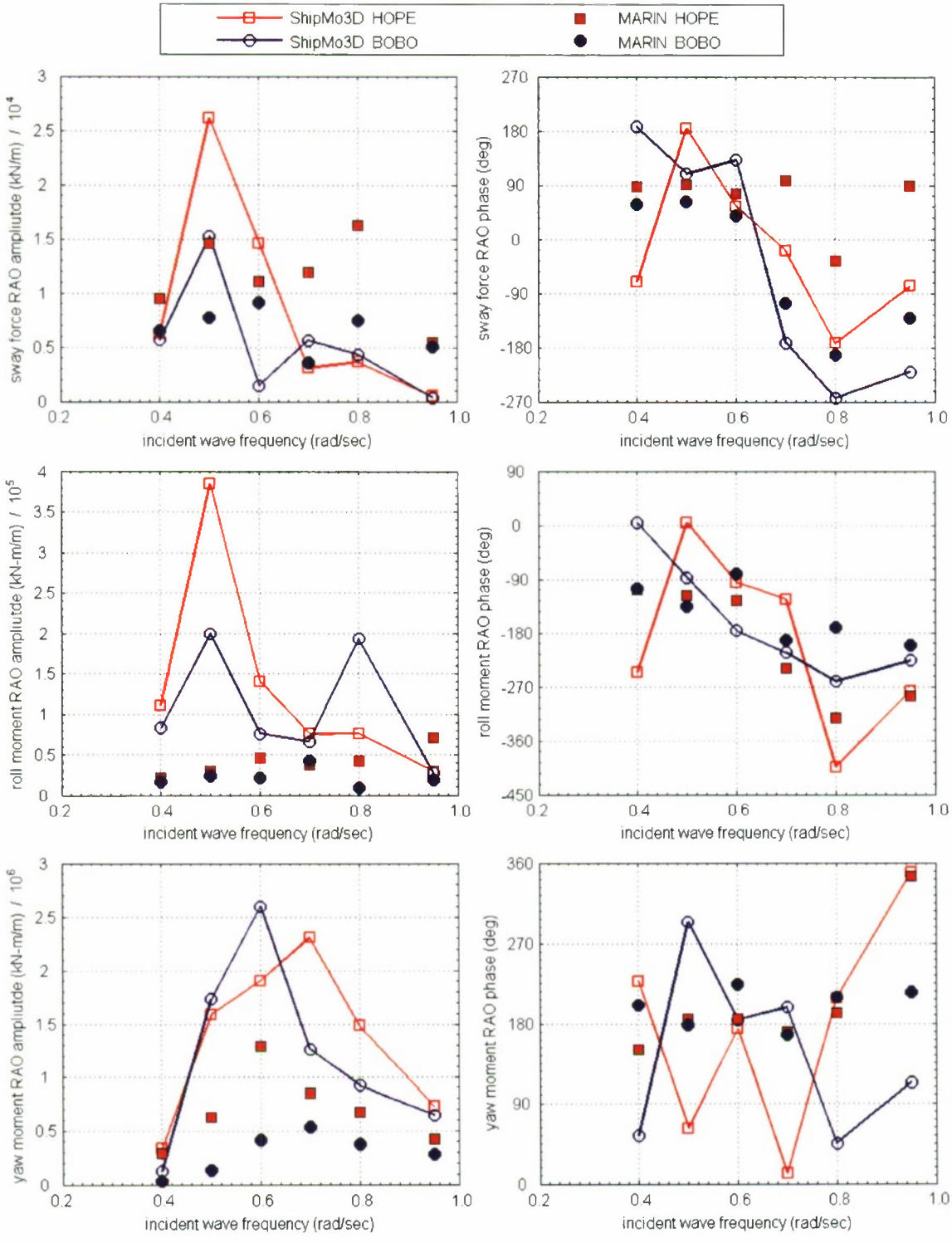

Figure D10. HOPE, BOBO Sway Force and Roll and Yaw Moment RAO Amplitude and Phase for 33 meter separation, 120 degree wave heading, and 16 knots ship speed.

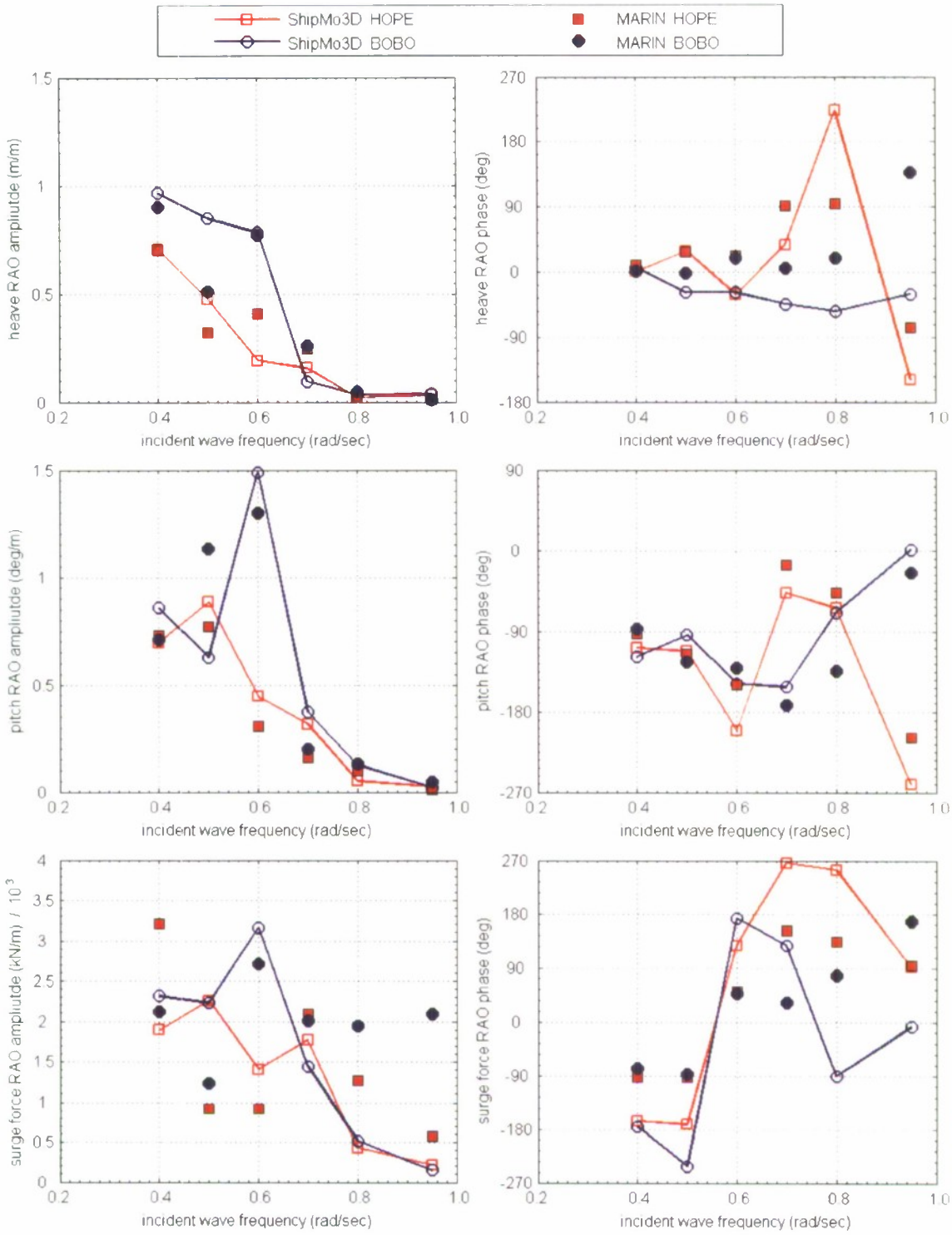

Figure D11. HOPE, BOBO Heave and Pitch Motions and Surge Force RAO Amplitude and Phase for 33 meter separation, 150 degree wave heading, and 16 knots ship speed.

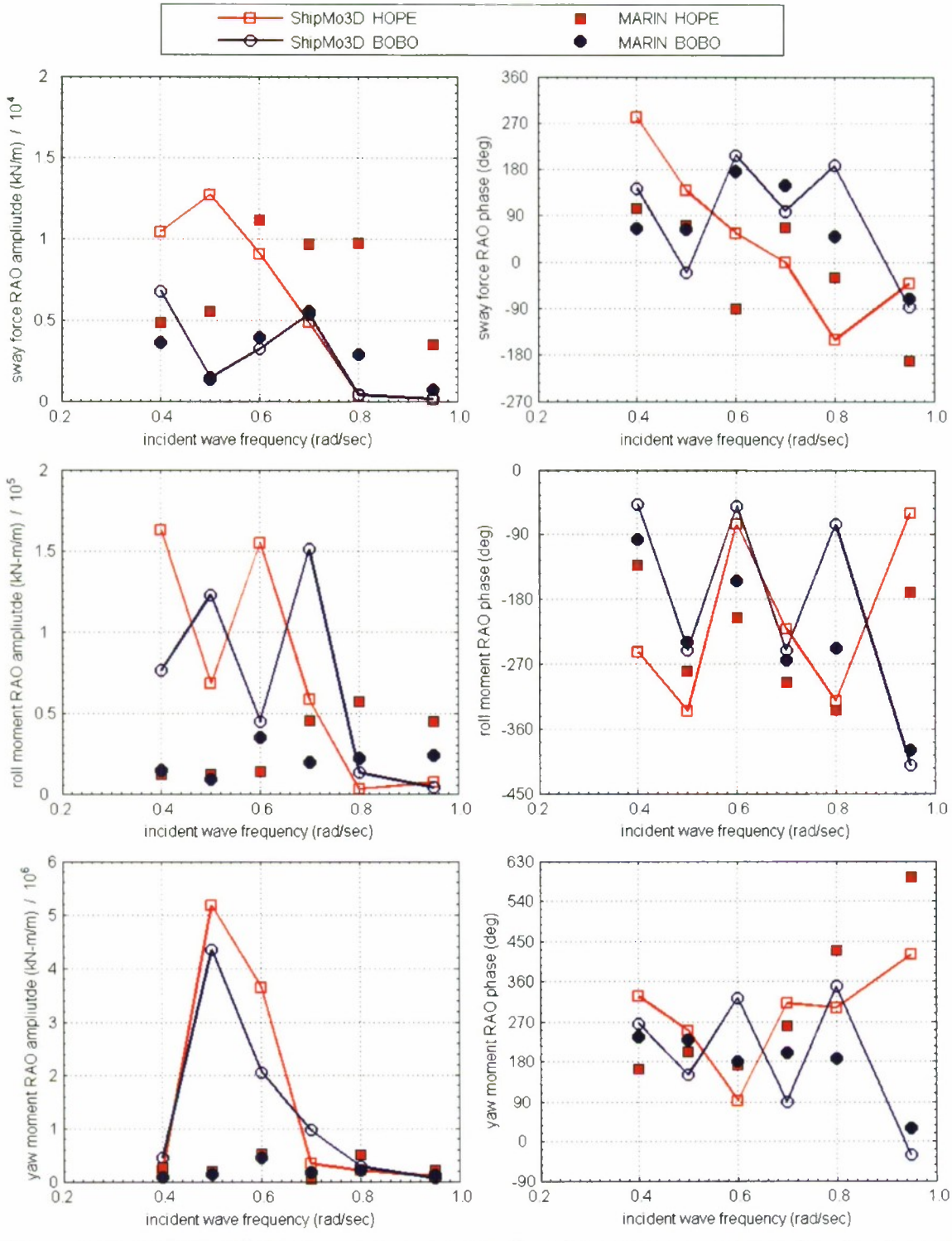

Figure D12. HOPE, BOBO Sway Force and Roll and Yaw Moment RAO Amplitude and Phase for 33 meter separation, 150 degree wave heading, and 16 knots ship speed.

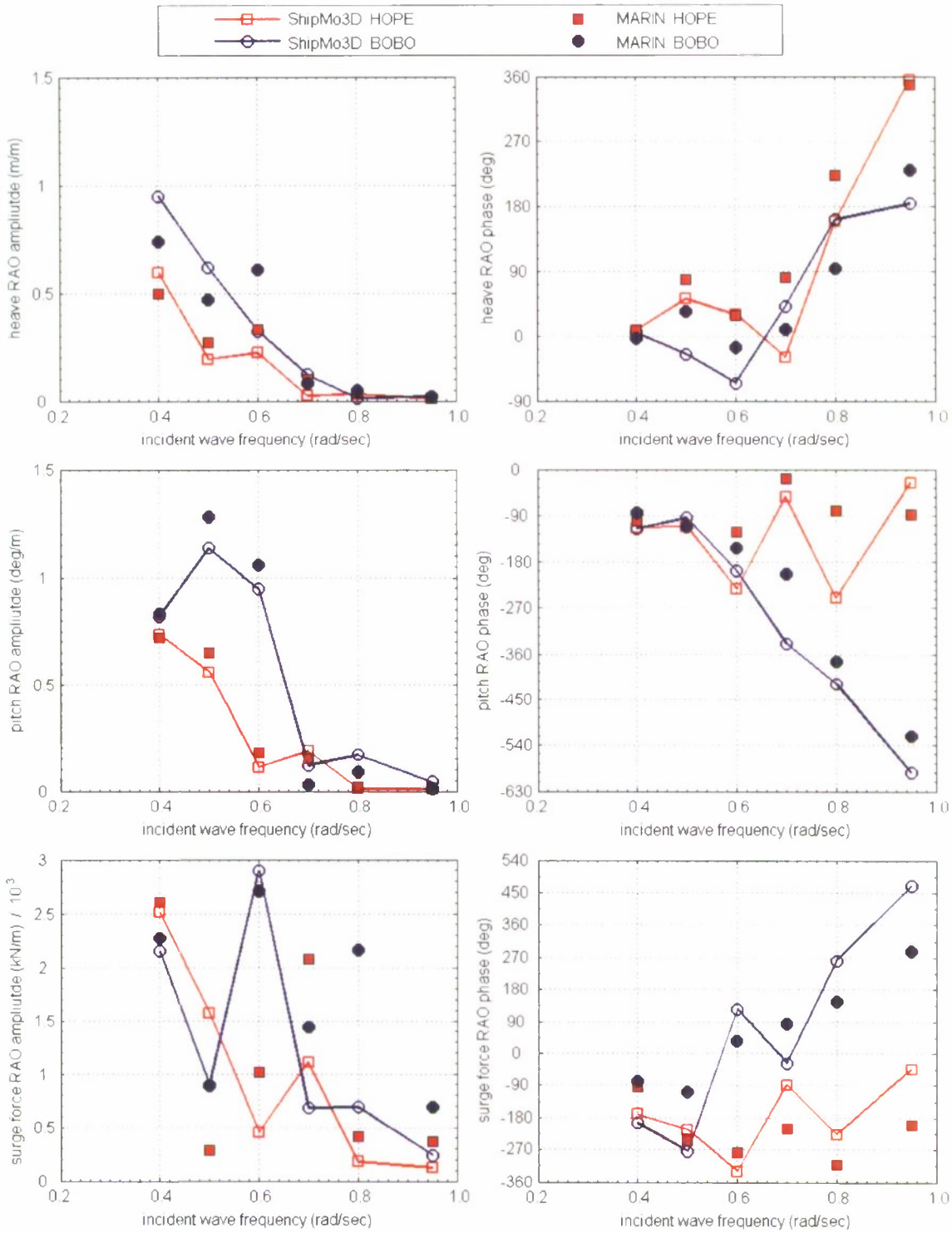

Figure D13. HOPE, BOBO Heave and Piteh Motions and Surge Foree RAO Amplitude and Phase for 33 meter separation, 180 degree wave heading, and 16 knots ship speed.

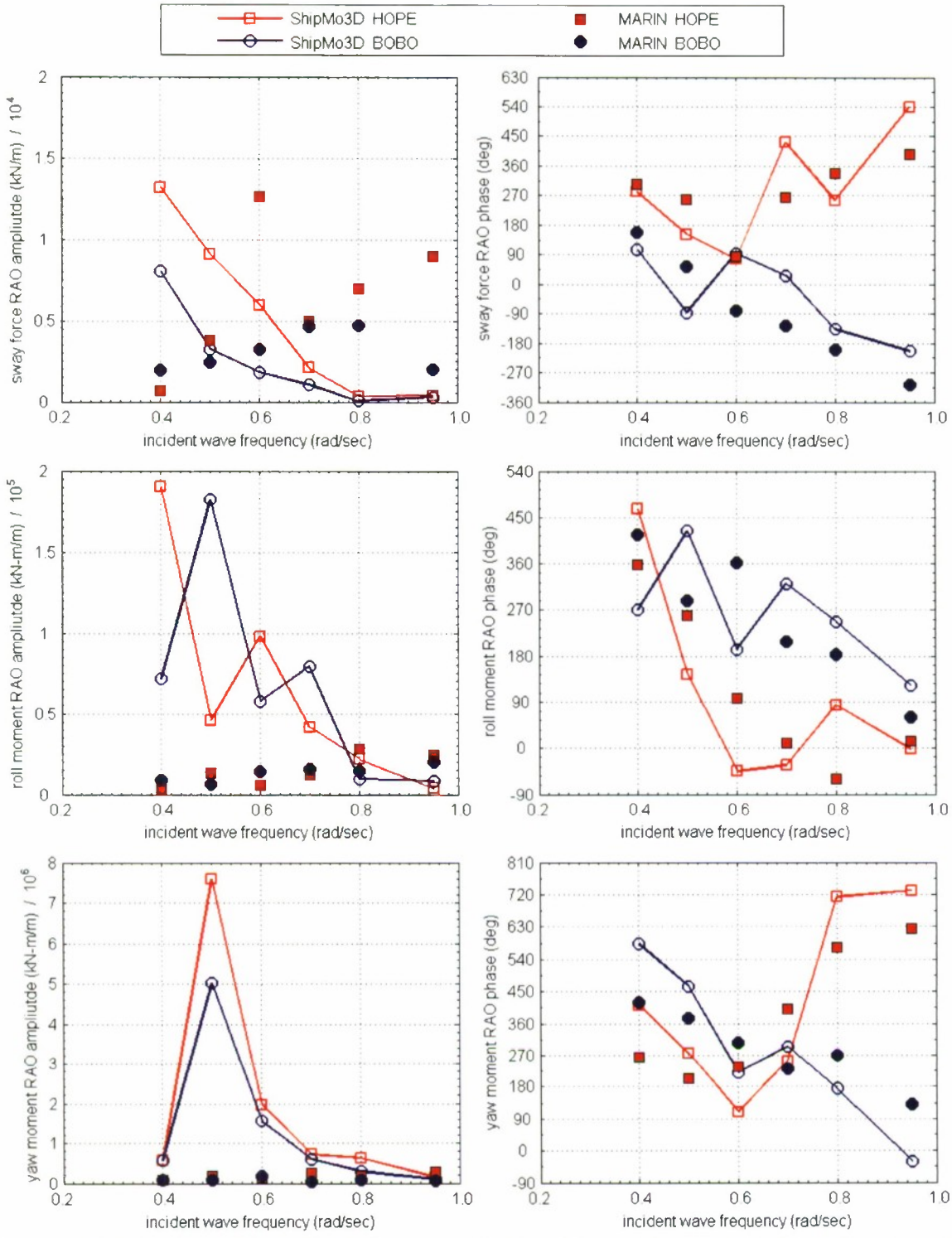

Figure D14. HOPE, BOBO Sway Force and Roll and Yaw Moment RAO Amplitude and Phase for 33 meter separation, 180 degree wave heading, and 16 knots ship speed.

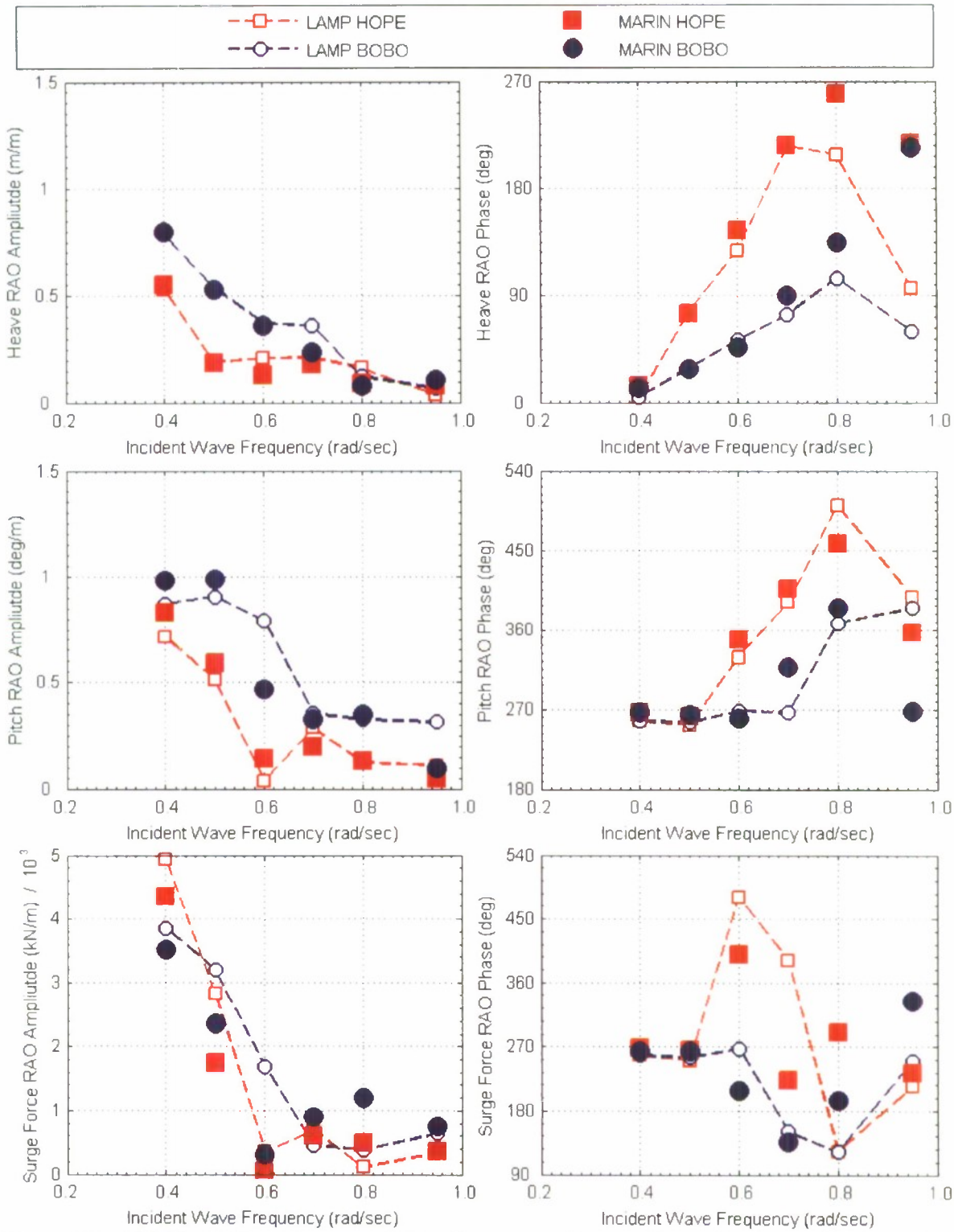

Figure E1. HOPE, BOBO Heave and Pitch Motion and Surge Force RAO Amplitude and Phase for 3 meter separation, 180 degree wave heading, and 5 knots ship speed.

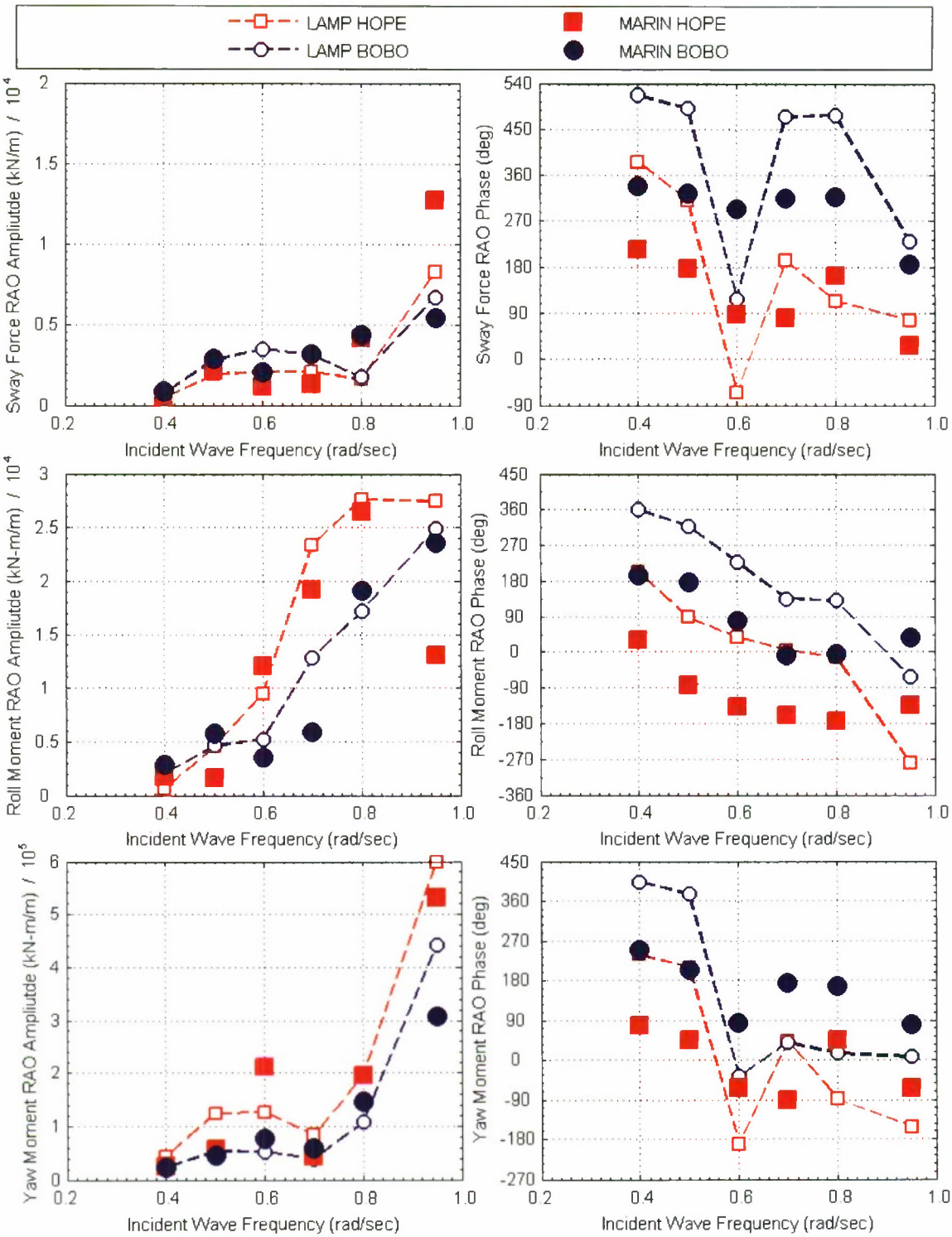

Figure E2. HOPE, BOBO Sway Force and Roll and Yaw Moment RAO Amplitude and Phase for 3 meter separation, 180 degree wave heading, and 5 knots ship speed.

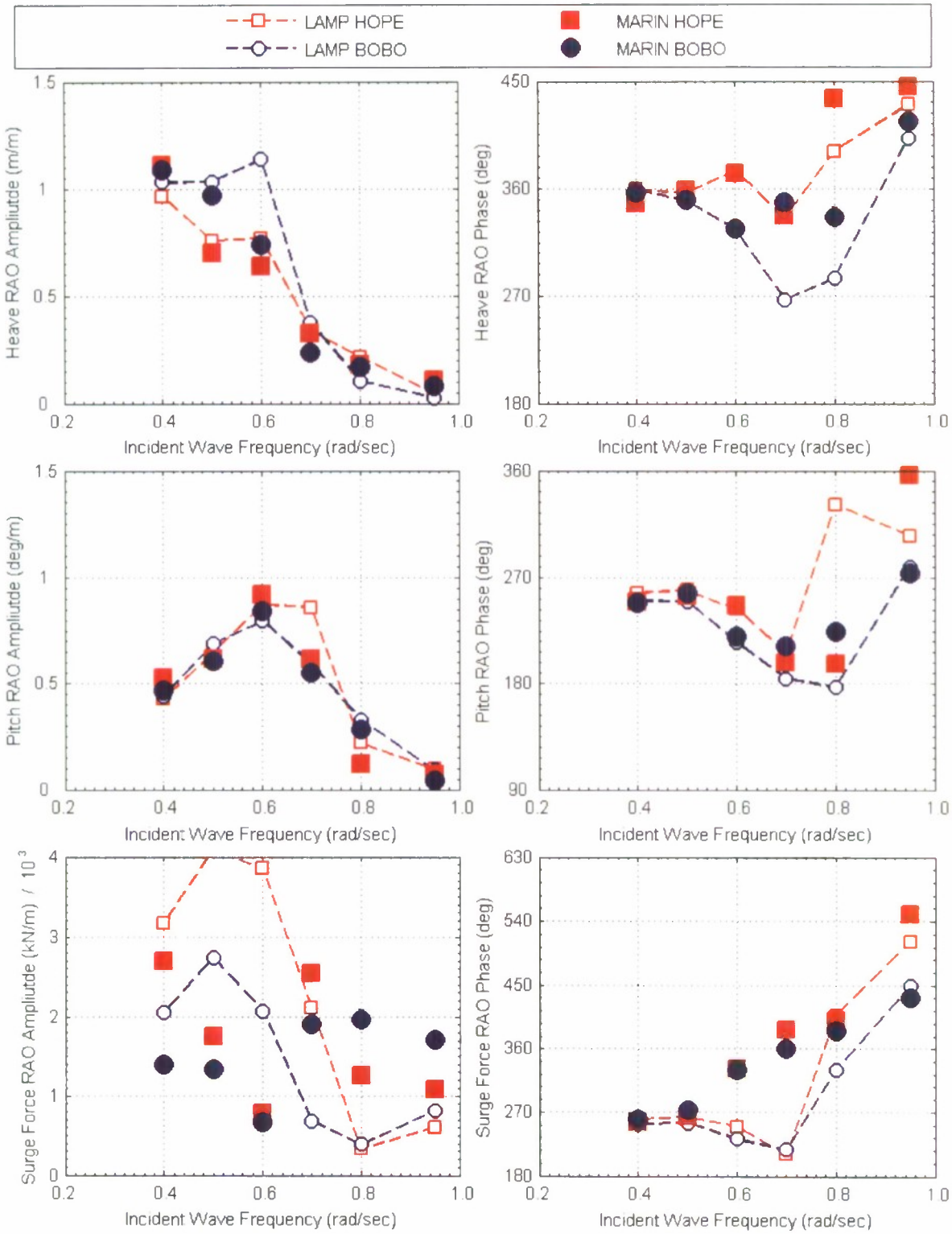

Figure E3. HOPE, BOBO Heave and Pitch Motion and Surge Force RAO Amplitude and Phase for 16.5 meter separation, 120 degree wave heading, and16 knots ship speed.

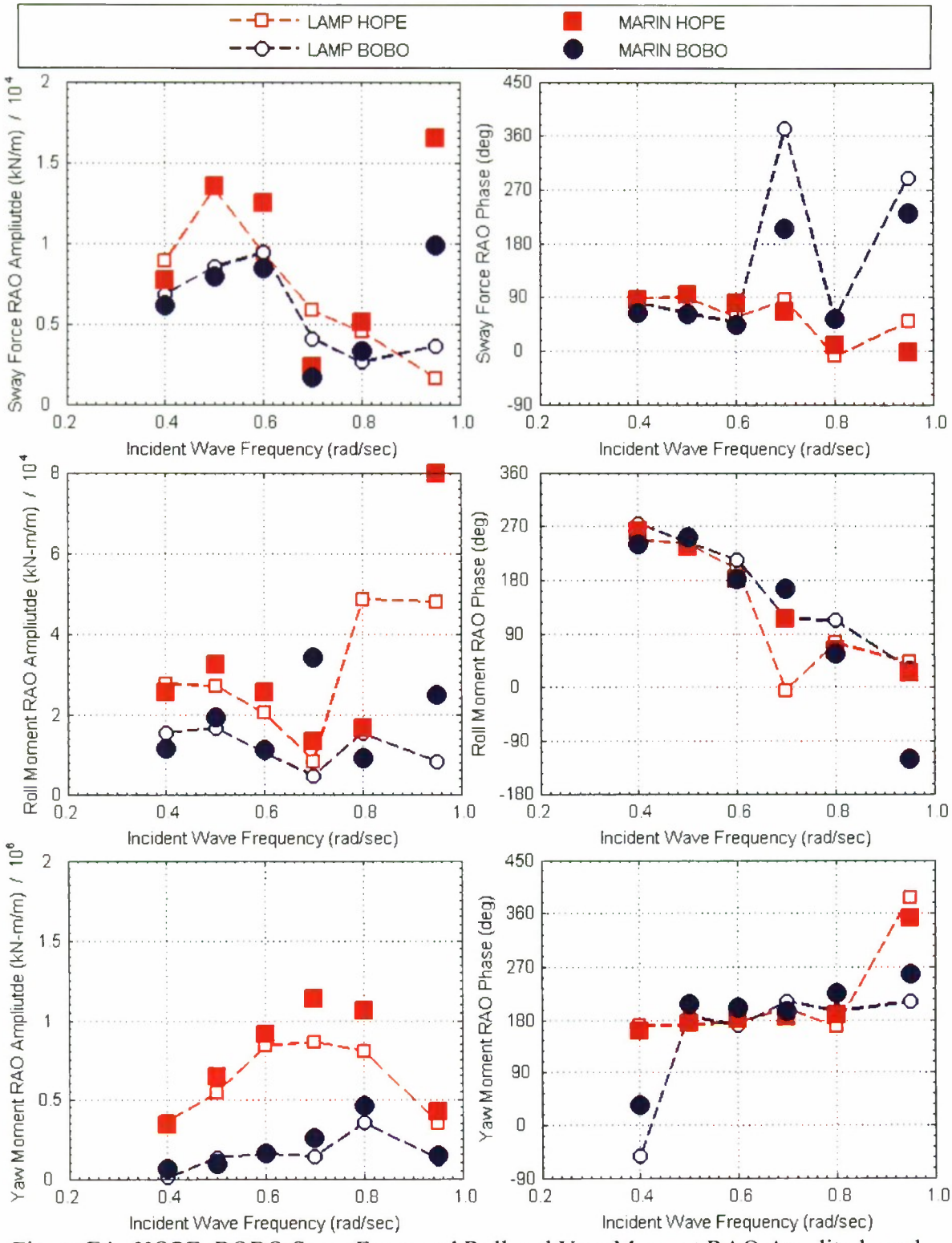

Figure E4. HOPE, BOBO Sway Force and Roll and Yaw Moment RAO Amplitude and Phase for 16.5 meter separation, 120 degree wave heading, and 16 knots ship speed.

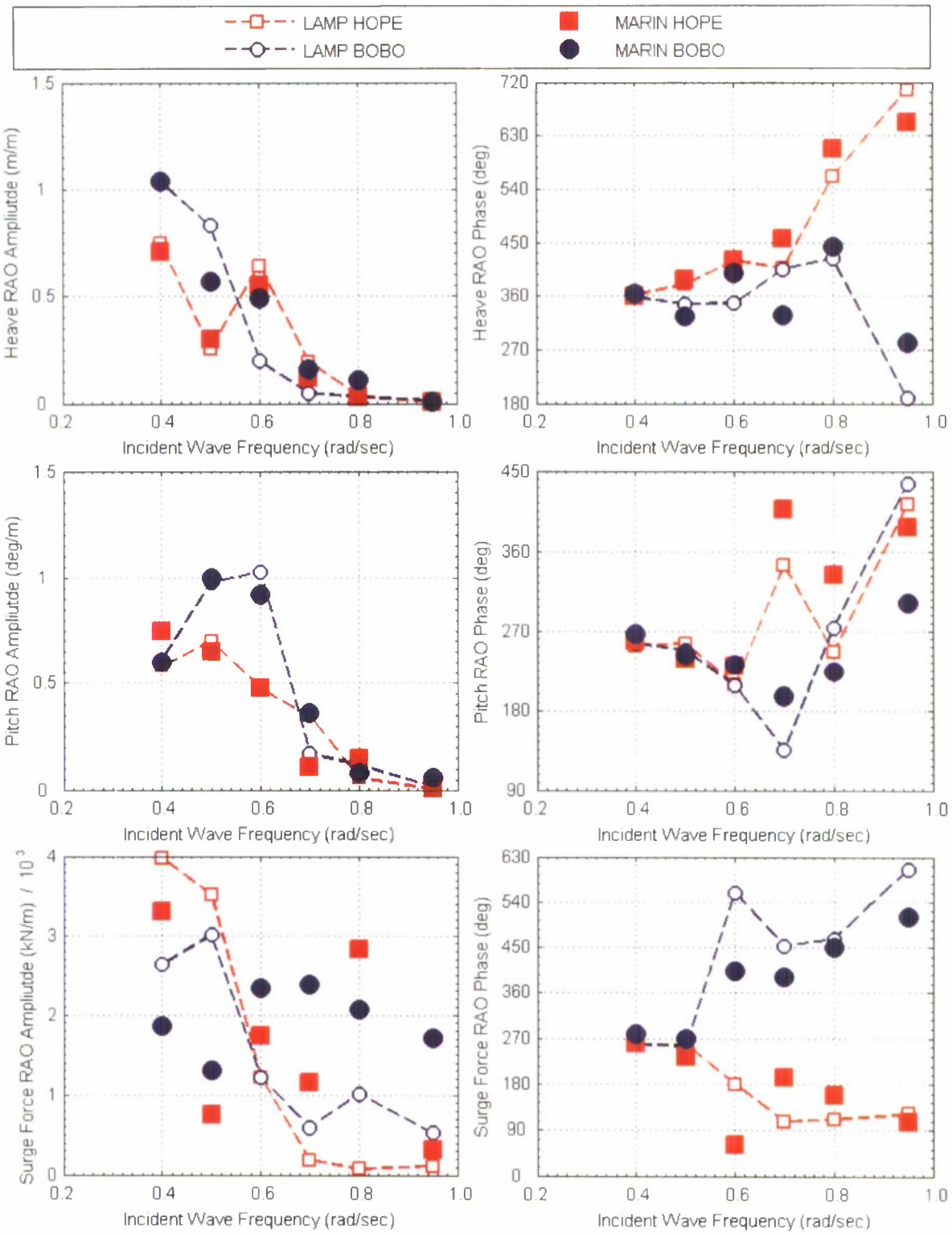

Figure E5. HOPE, BOBO Heave and Pitch Motion and Surge Force RAO Amplitude and Phase for 16.5 Meter Separation, 150 degree wave heading, and 16 knots ship speed.

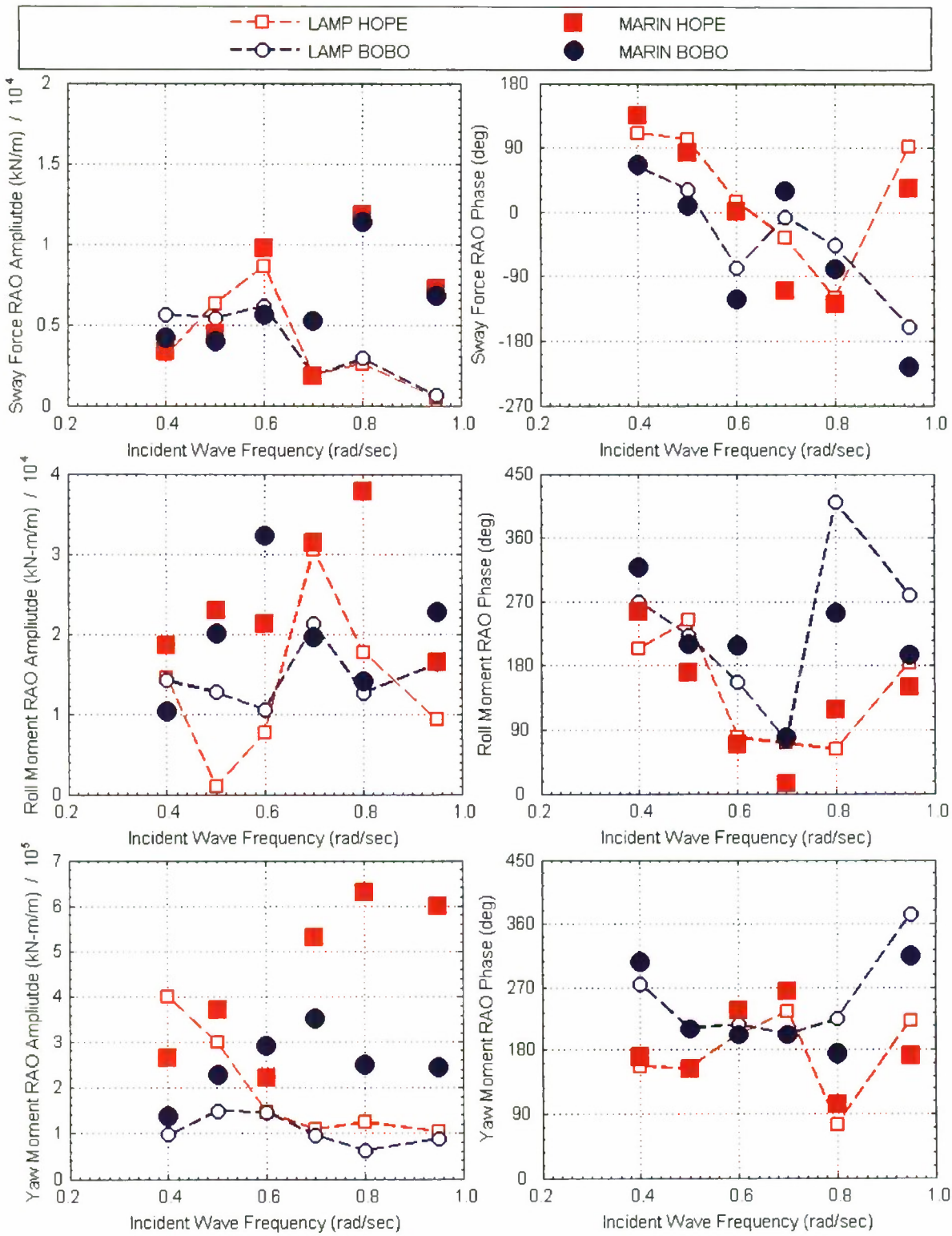

Figure E6. HOPE, BOBO Sway Force and Roll and Yaw Moment RAO Amplitude and Phase for 16.5 meter separation, 150 degree wave heading, and 16 knots ship speed.

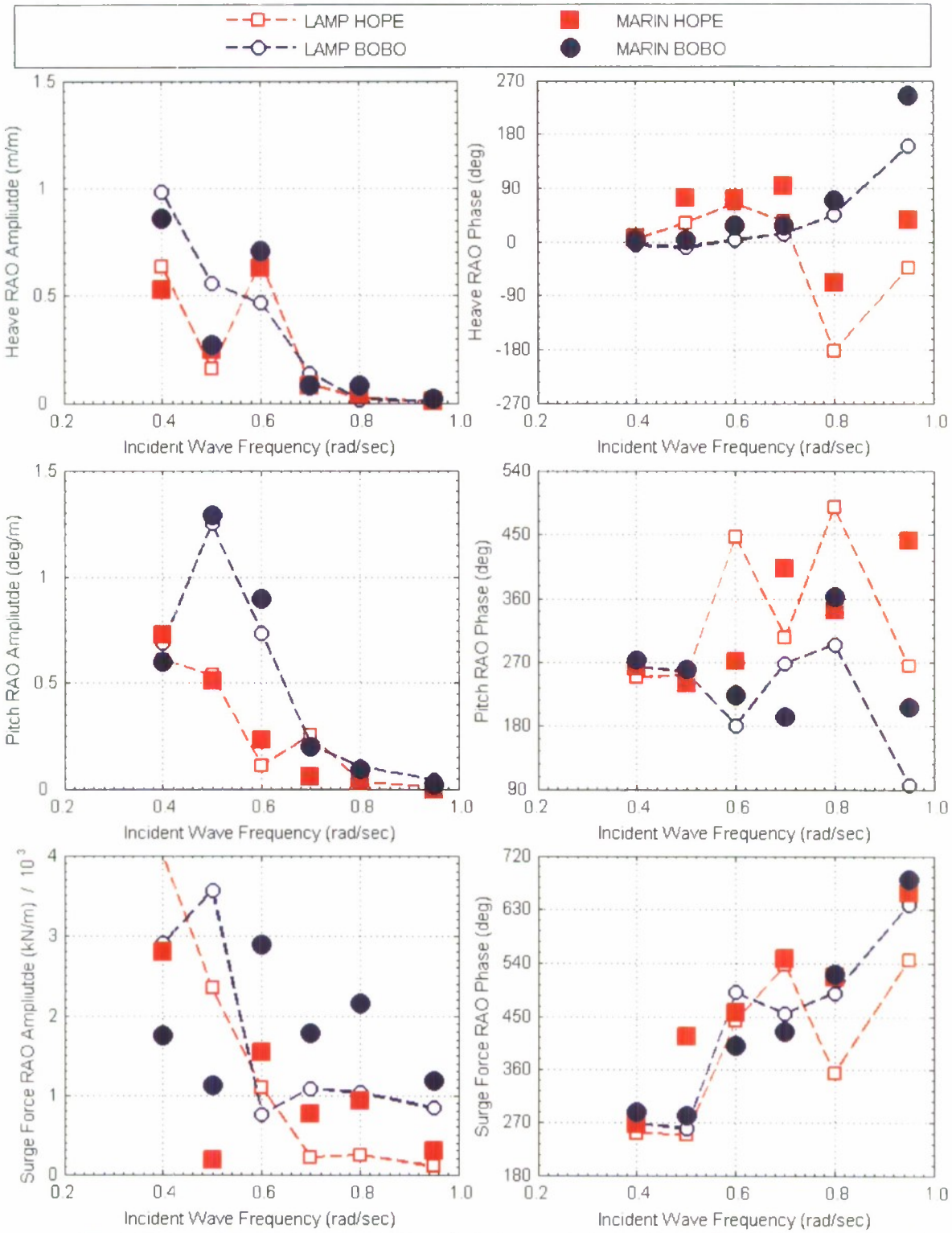

Figure E7. HOPE, BOBO Heave and Pitch Motion and Surge Force RAO Amplitude and Phase for 16.5 meter separation, 180 degree wave heading, and 16 knots ship speed.

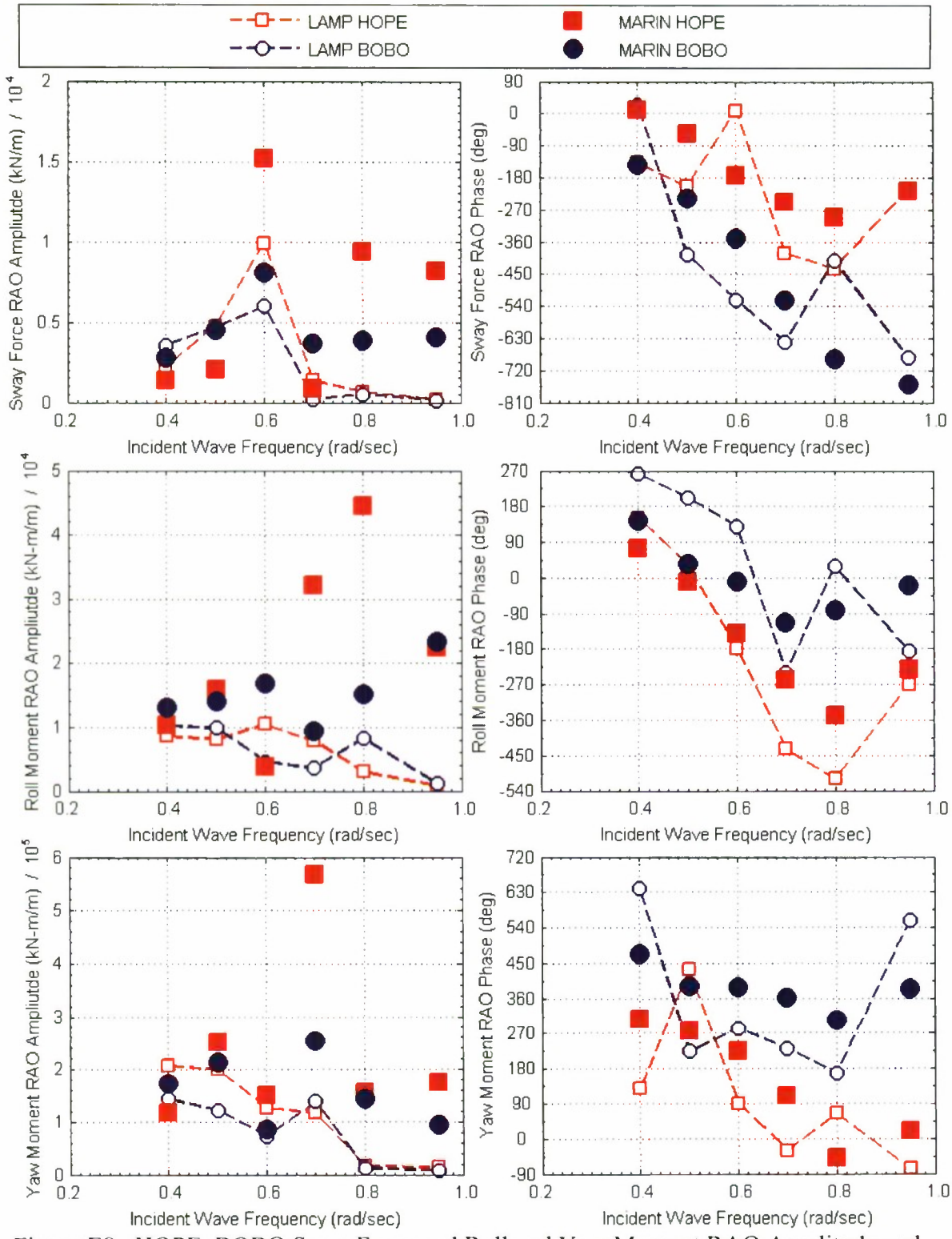

Figure E8. HOPE, BOBO Sway Force and Roll and Yaw Moment RAO Amplitude and Phase for 16.5 meter separation, 180 degree wave heading, and 16 knots ship speed.

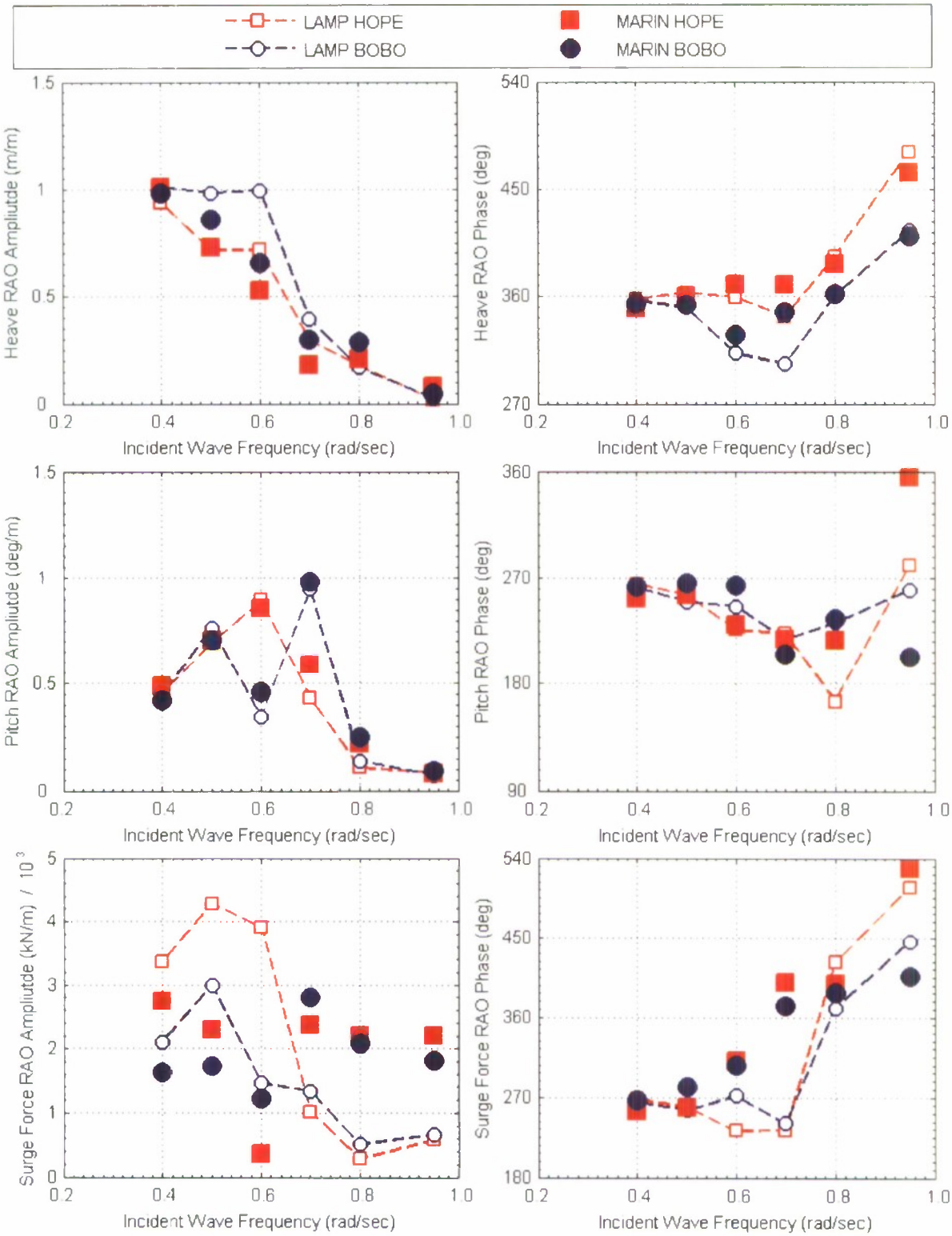

Figure E9. HOPE, BOBO Heave and Pitch Motion and Surge Force RAO Amplitude and Phase for 33 meter separation, 120 degree wave heading, and 16 knots ship speed.

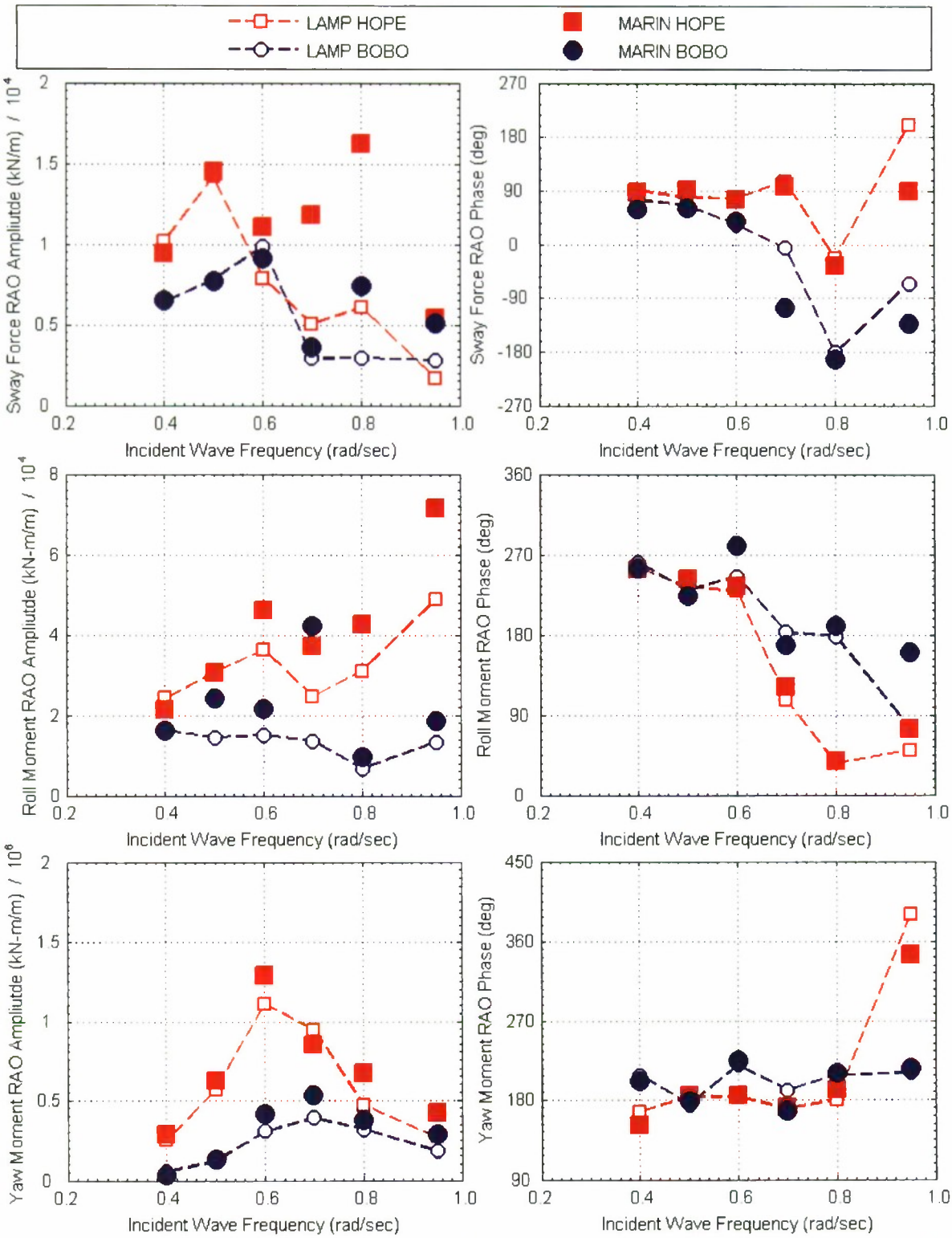

Figure E10. HOPE, BOBO Sway Force and Roll and Yaw Moment RAO Amplitude and Phase for 33 meter separation, 120 degree wave heading, and 16 knots ship speed.

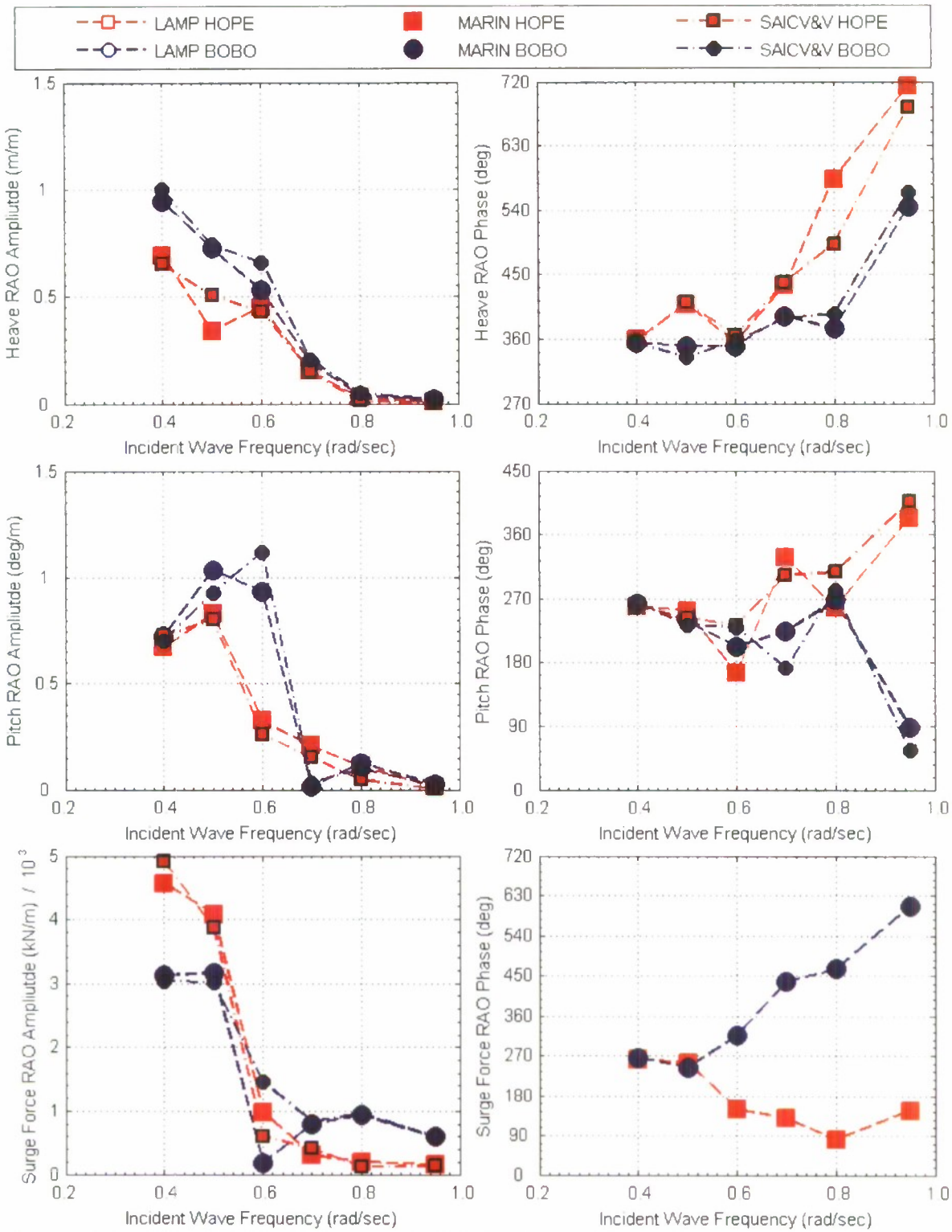

Figure E11. HOPE, BOBO Heave and Pitch Motion and Surge Force RAO Amplitude and Phase for 33 meter separation, 150 degree wave heading, and 16 knots ship speed.

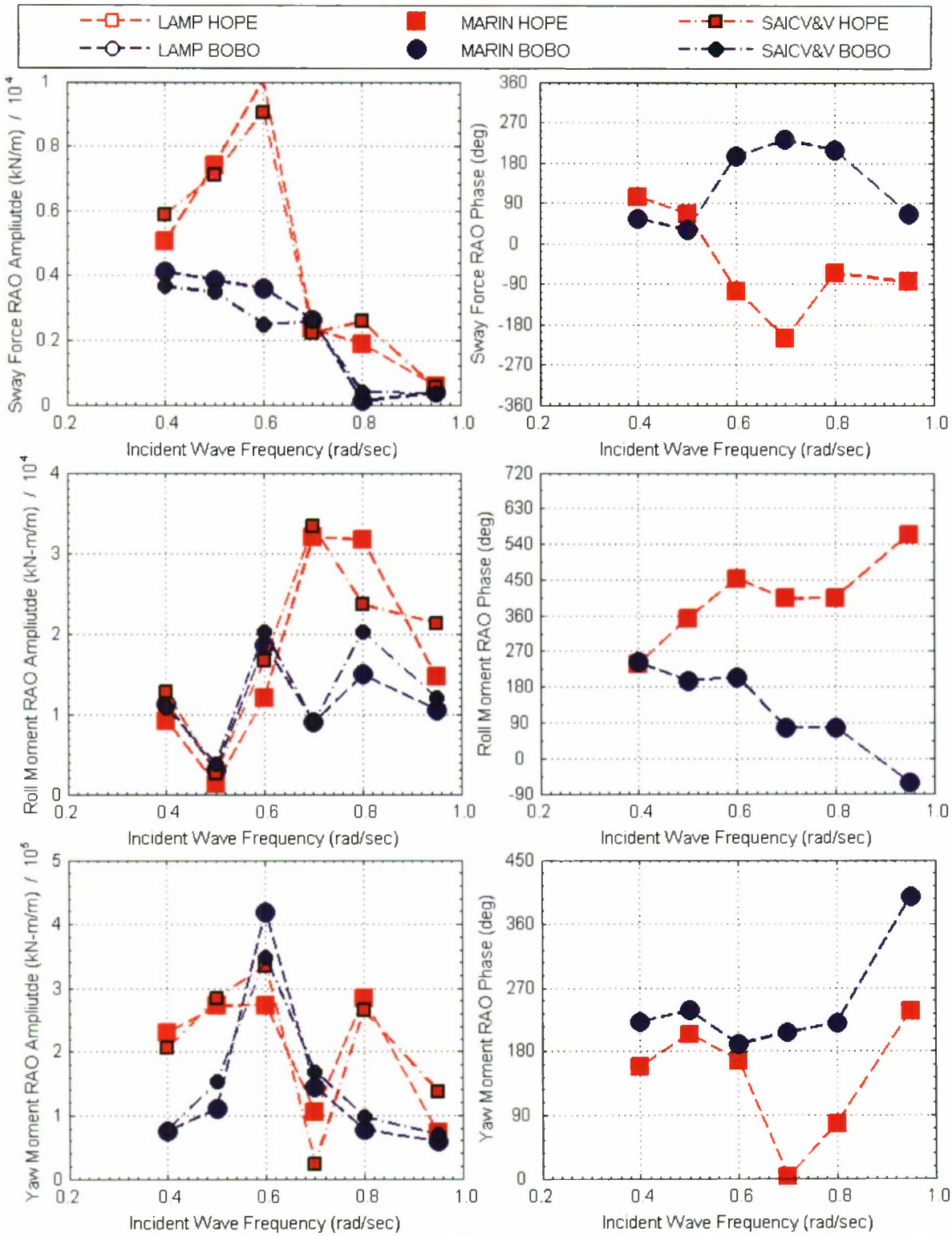

Figure E12. HOPE, BOBO Sway Force and Roll and Yaw Moment RAO Amplitude and Phase for 33 meter separation, 150 degree wave heading, and 16 knots ship speed.

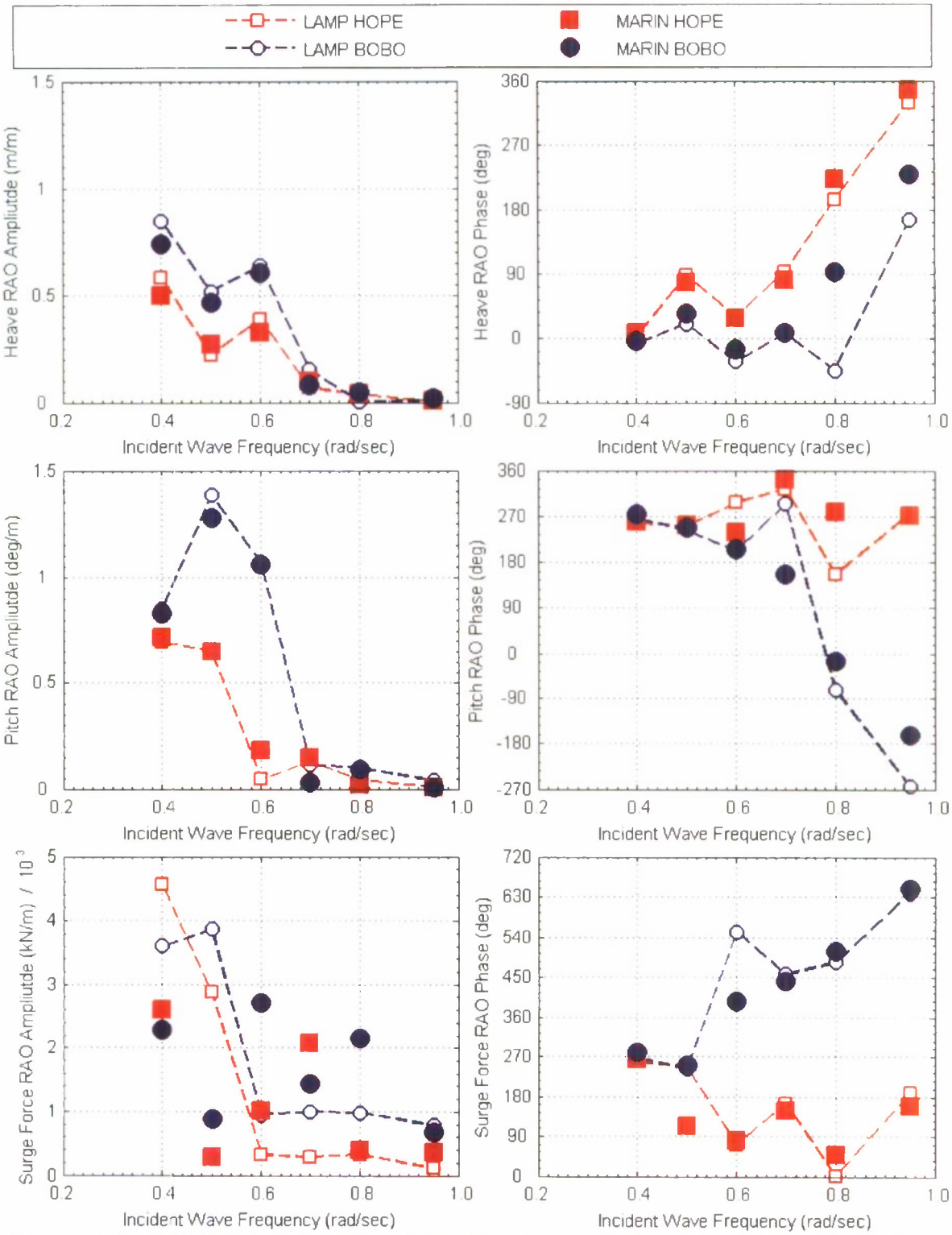

Figure E13. HOPE, BOBO Heave and Pitch Motion and Surge Force RAO Amplitude and Phase for 33 meter separation, 180 degree wave heading, and 16 knots ship speed.

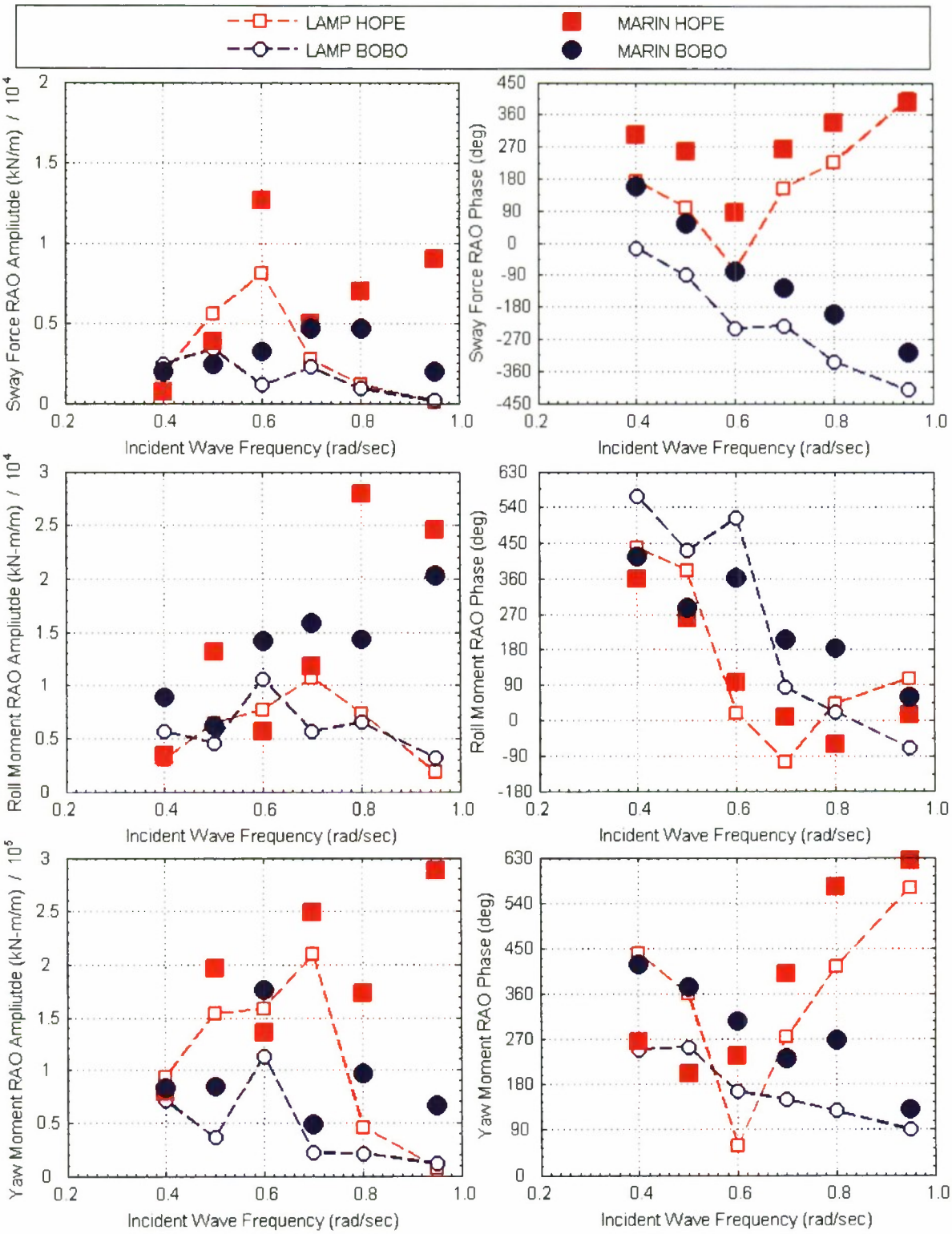

Figure E14. HOPE, BOBO Sway Force and Roll and Yaw Moment RAO Amplitude and Phase for 33 meter separation, 180 degree wave heading, and 16 knots ship speed.

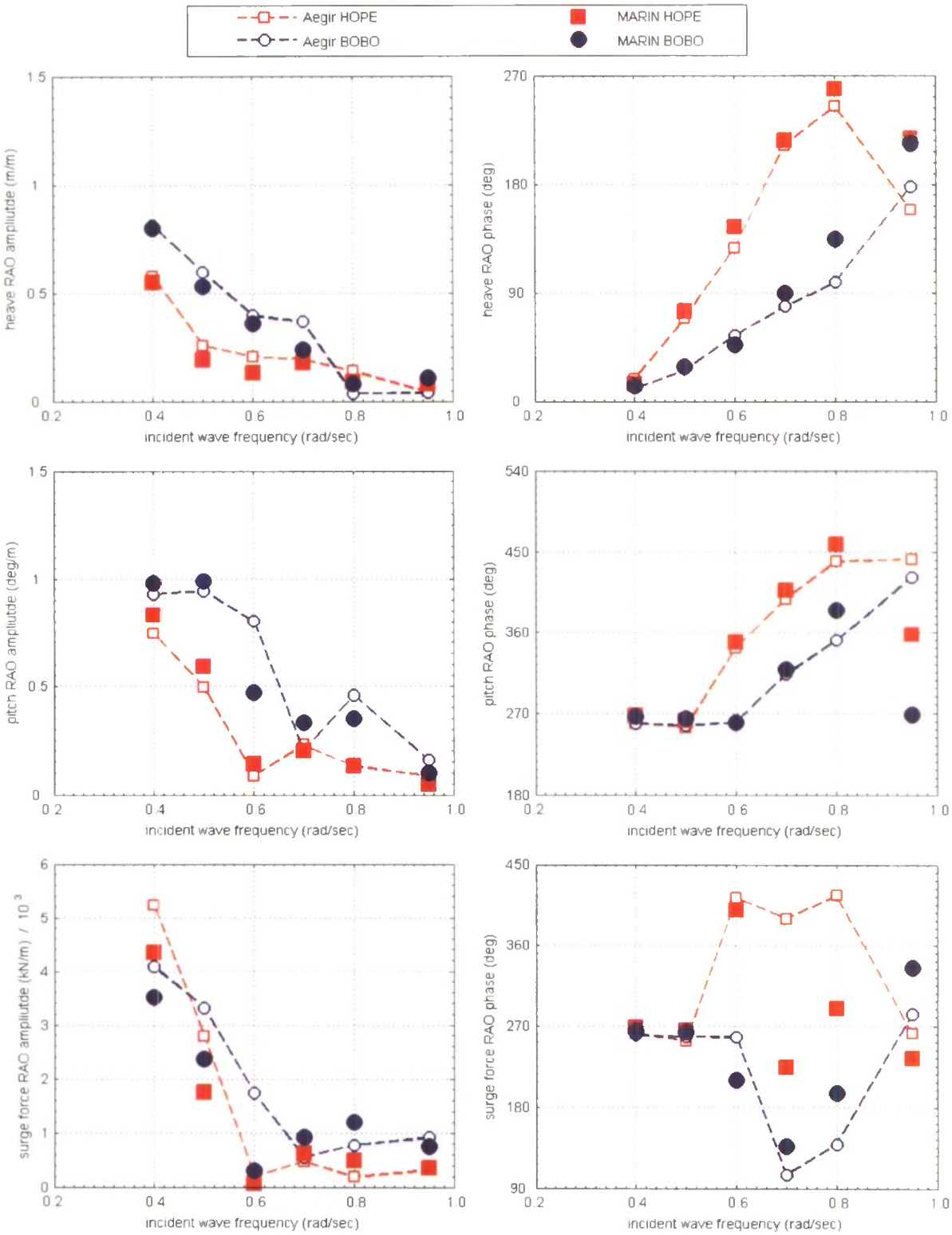

Figure F1. HOPE, BOBO Heave and Pitch Motion and Surge Force RAO Amplitude and Phase for 3 meter separation, 180 degree wave heading, and 5 knots ship speed.

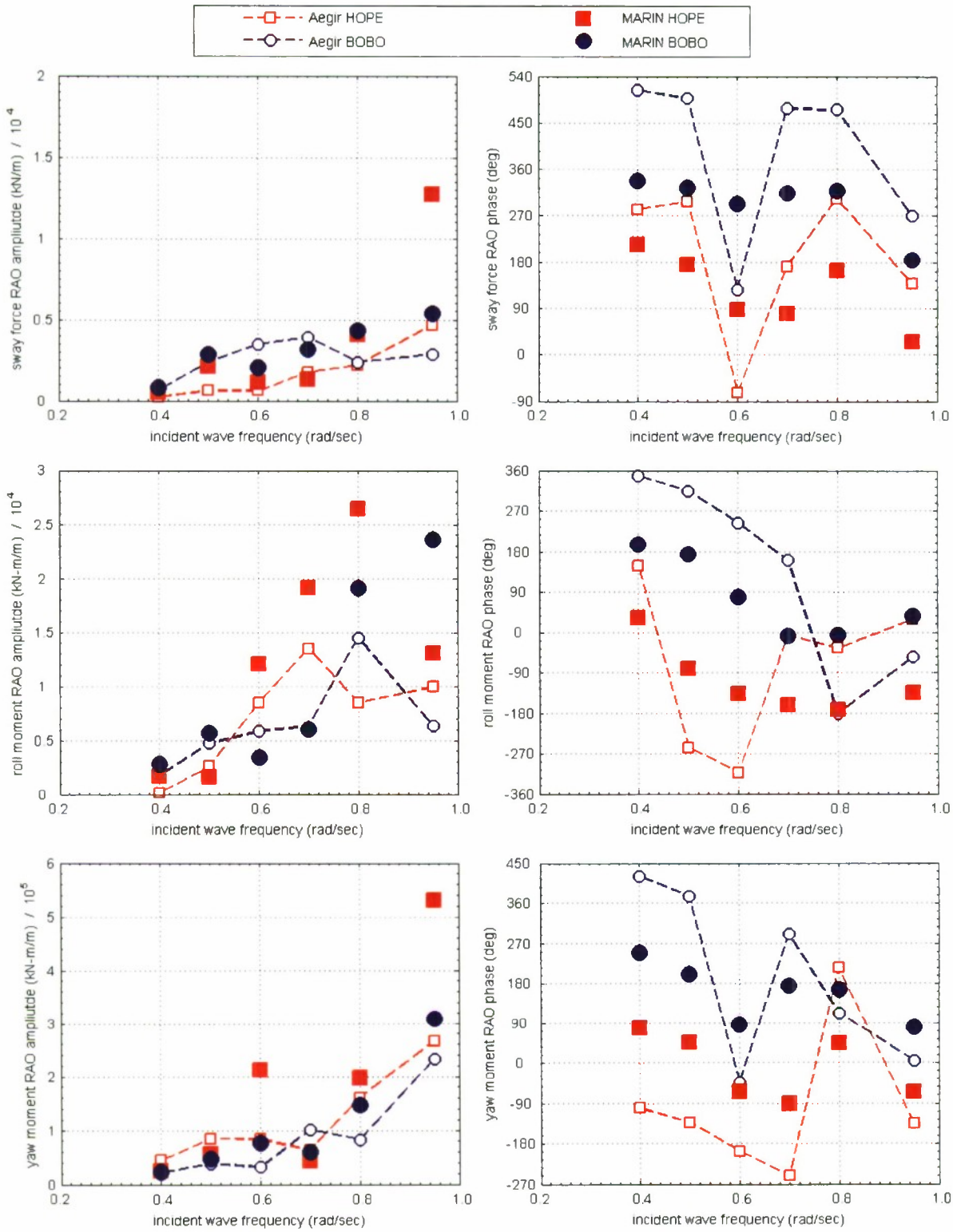

Figure F2. HOPE, BOBO Sway Force and Roll and Yaw Moment RAO Amplitude and Phase for 3 meter separation, 180 degree wave heading, and 5 knots ship speed.

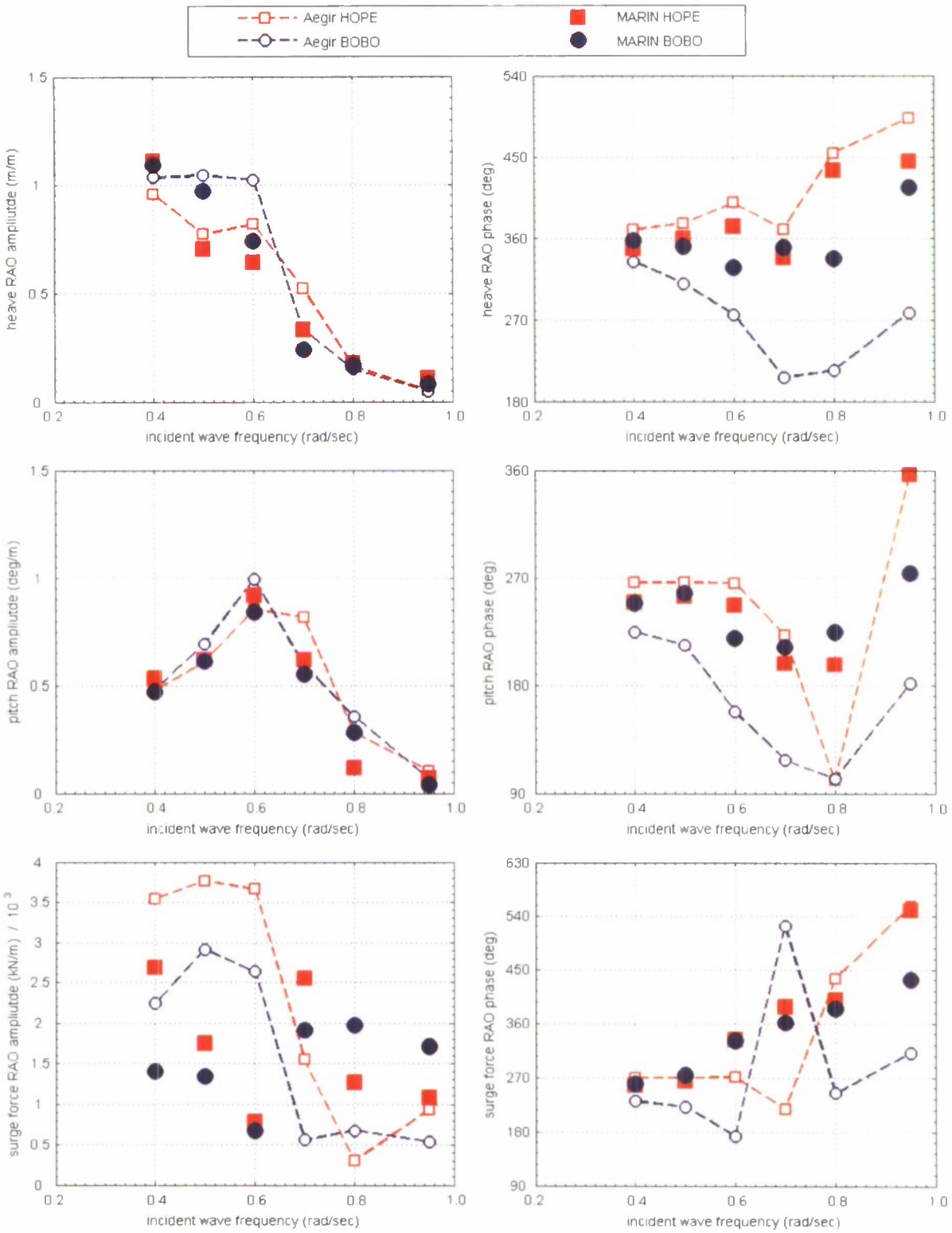

Figure F3. HOPE, BOBO Heave and Pitch Motion and Surge Force RAO Amplitude and Phase for 16.5 meter separation, 120 degree wave heading, and 16 knots ship speed.

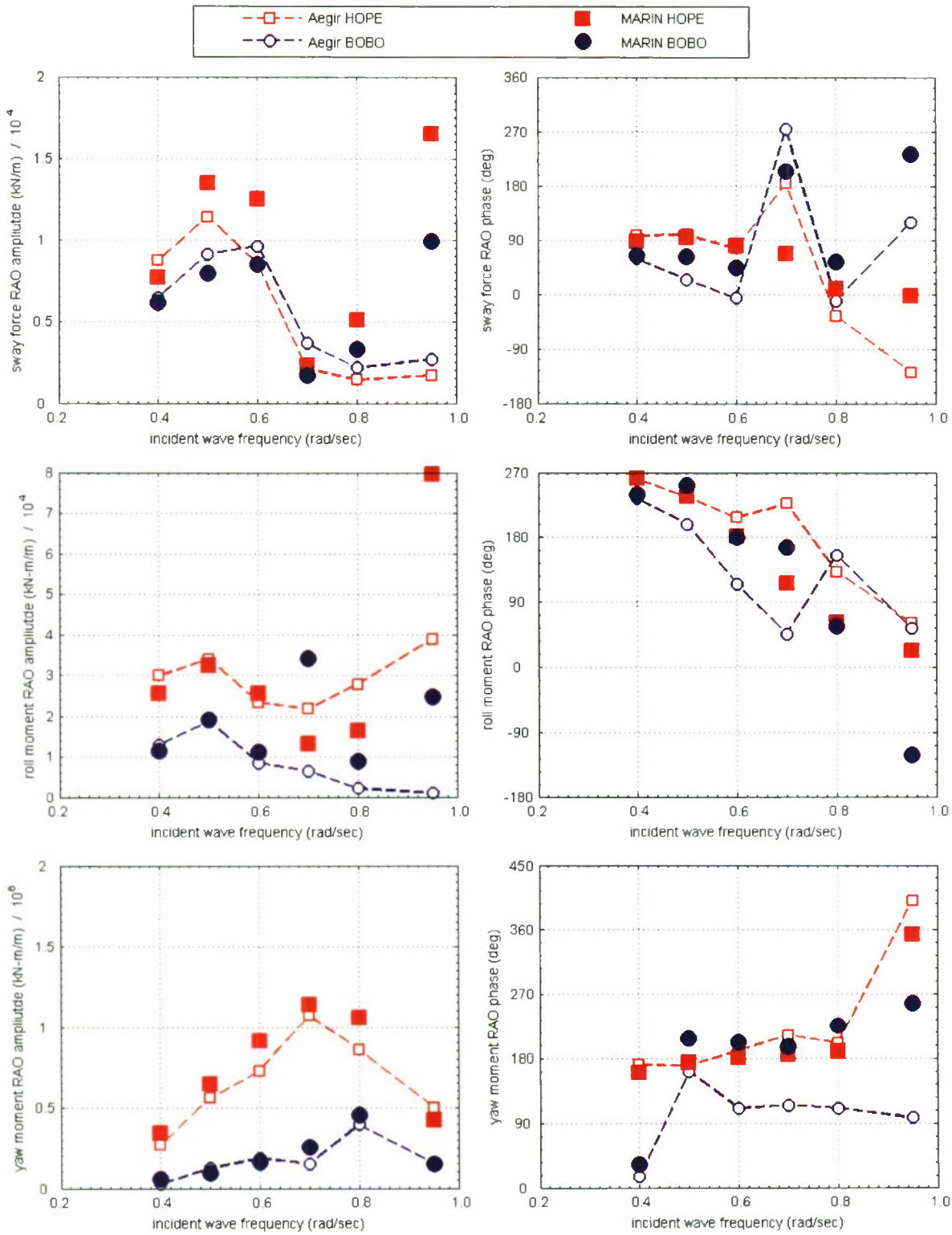

Figure F4. HOPE, BOBO Sway Force and Roll and Yaw Moment RAO Amplitude and Phase for 16.5 meter separation, 120 degree wave heading, and 16 knots ship speed.

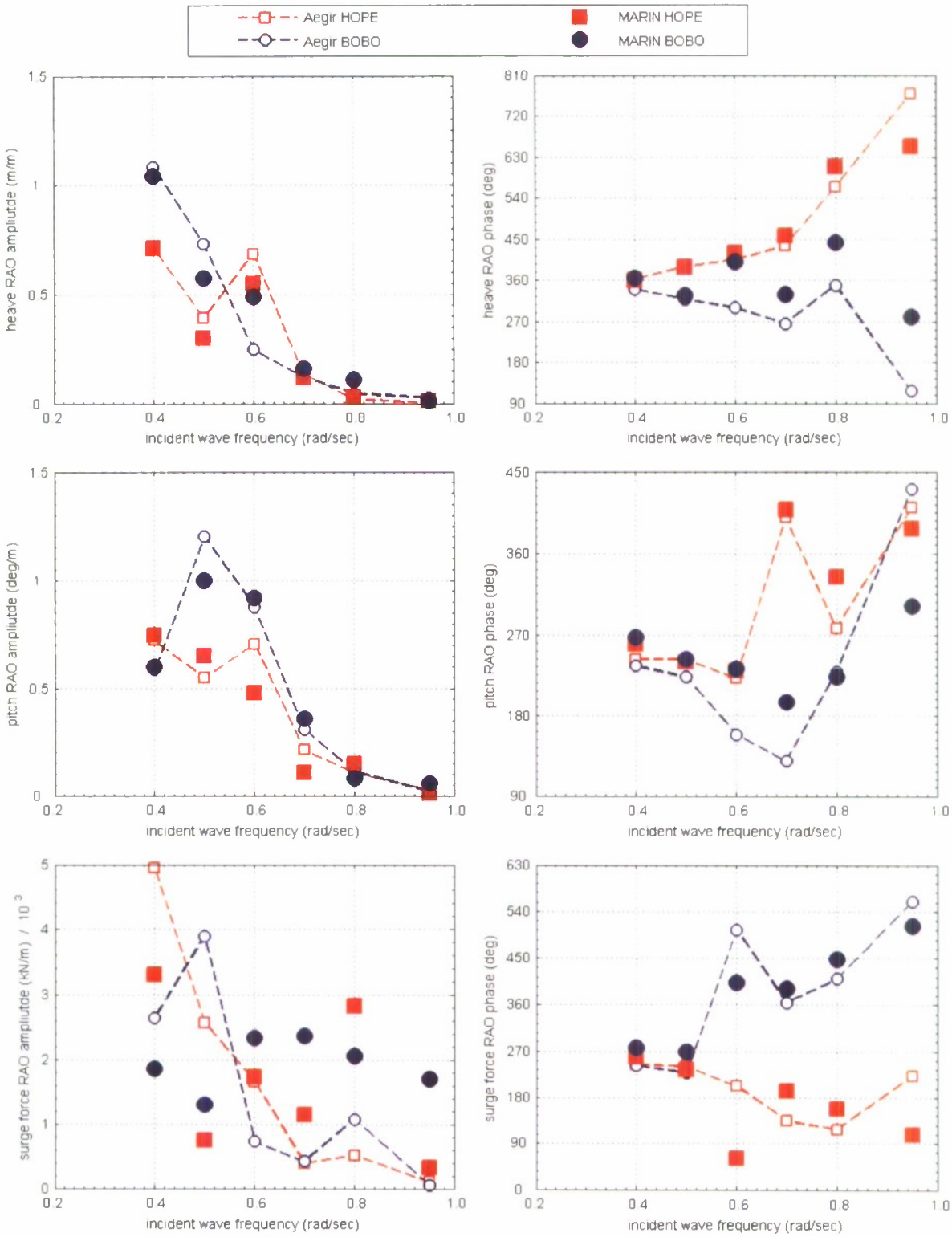

Figure F5. HOPE, BOBO Heave and Pitch Motion and Surge Force RAO Amplitude and Phase for 16.5 meter separation, 150 degree wave heading, and 16 knots ship speed.

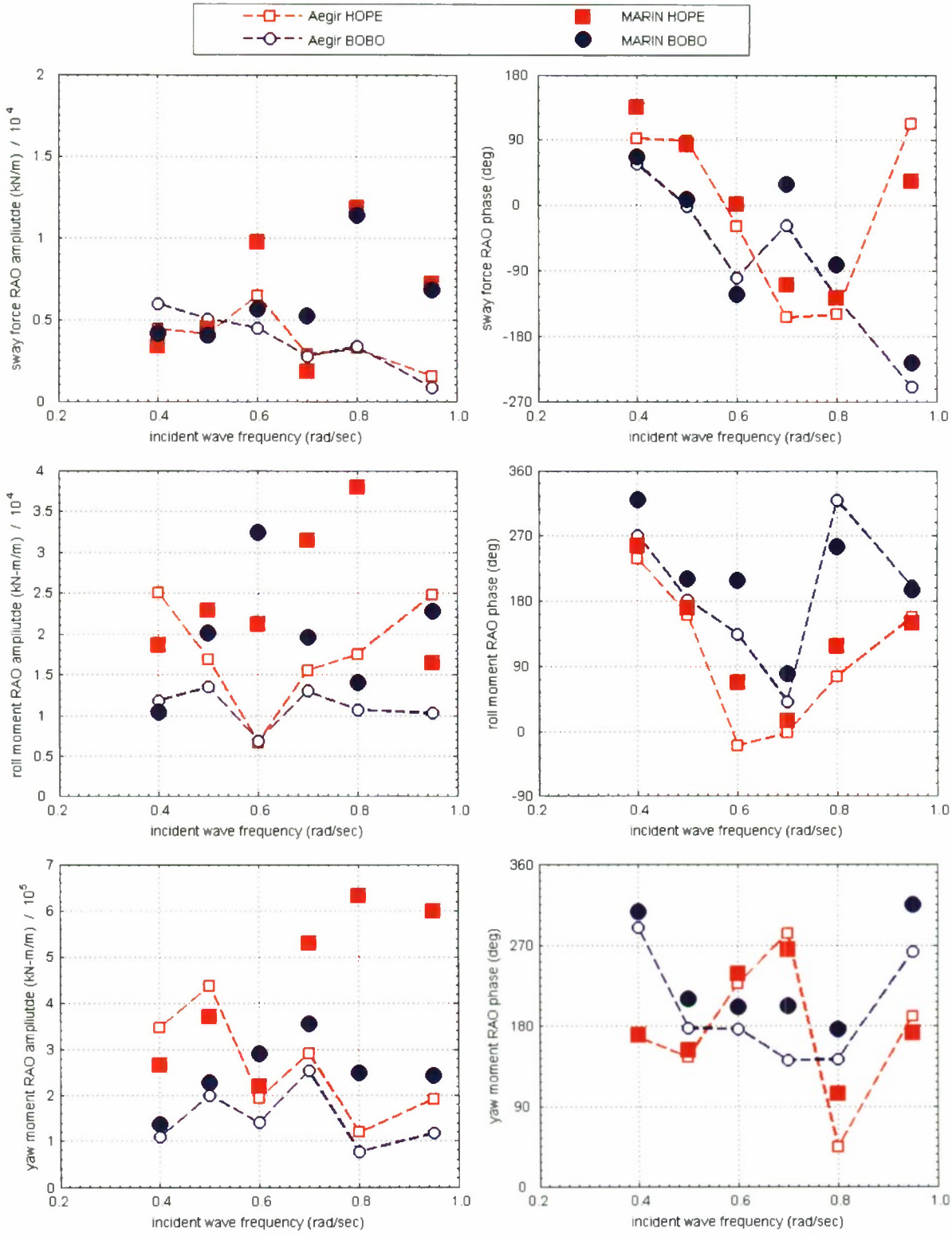

Figure F6. HOPE, BOBO Sway Force and Roll and Yaw Moment RAO Amplitude and Phase for 16.5 meter separation, 150 degree wave heading, and 16 knots ship speed.

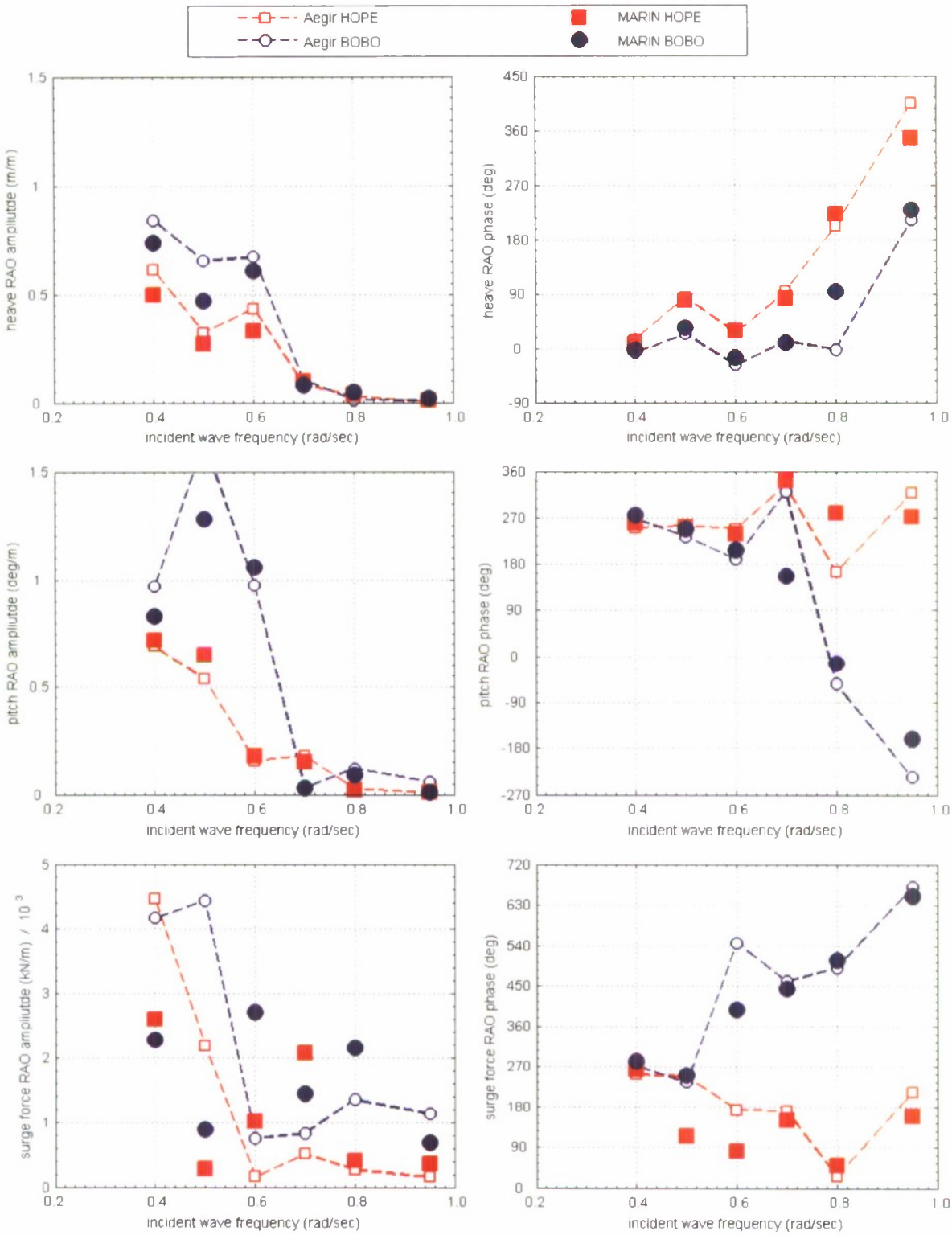

Figure F7. HOPE, BOBO Heave and Pitch Motion and Surge Force RAO Amplitude and Phase for 16.5 meter separation, 180 degree wave heading, and 16 knots ship speed.

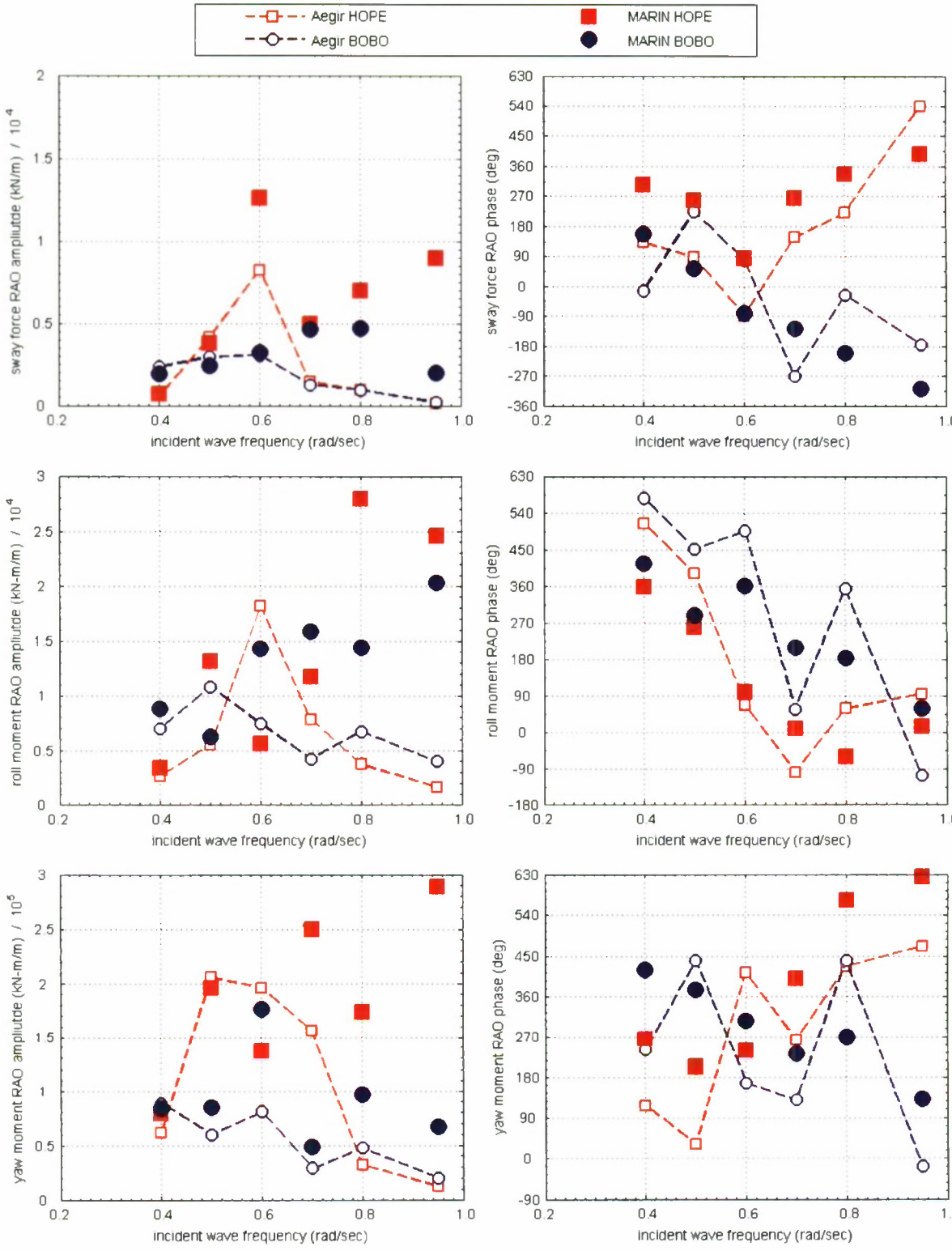

Figure F8. HOPE, BOBO Sway Force and Roll and Yaw Moment RAO Amplitude and Phase for 16.5 meter separation, 180 degree wave heading, and 16 knots ship speed.

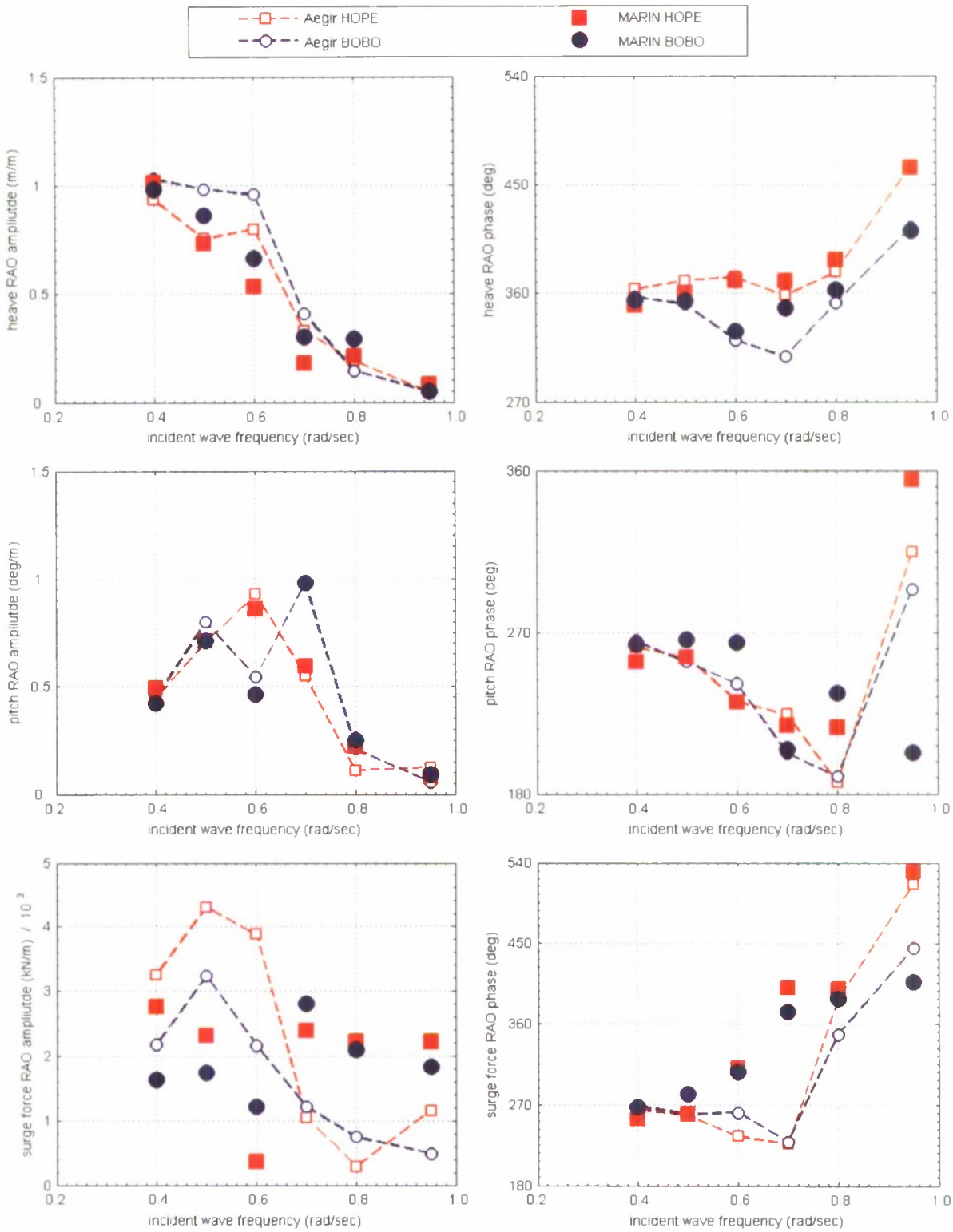

Figure F9. HOPE, BOBO Heave and Pitch Motion and Surge Force RAO Amplitude and Phase for 33 meter separation, 120 degree wave heading, and 16 knots ship speed.

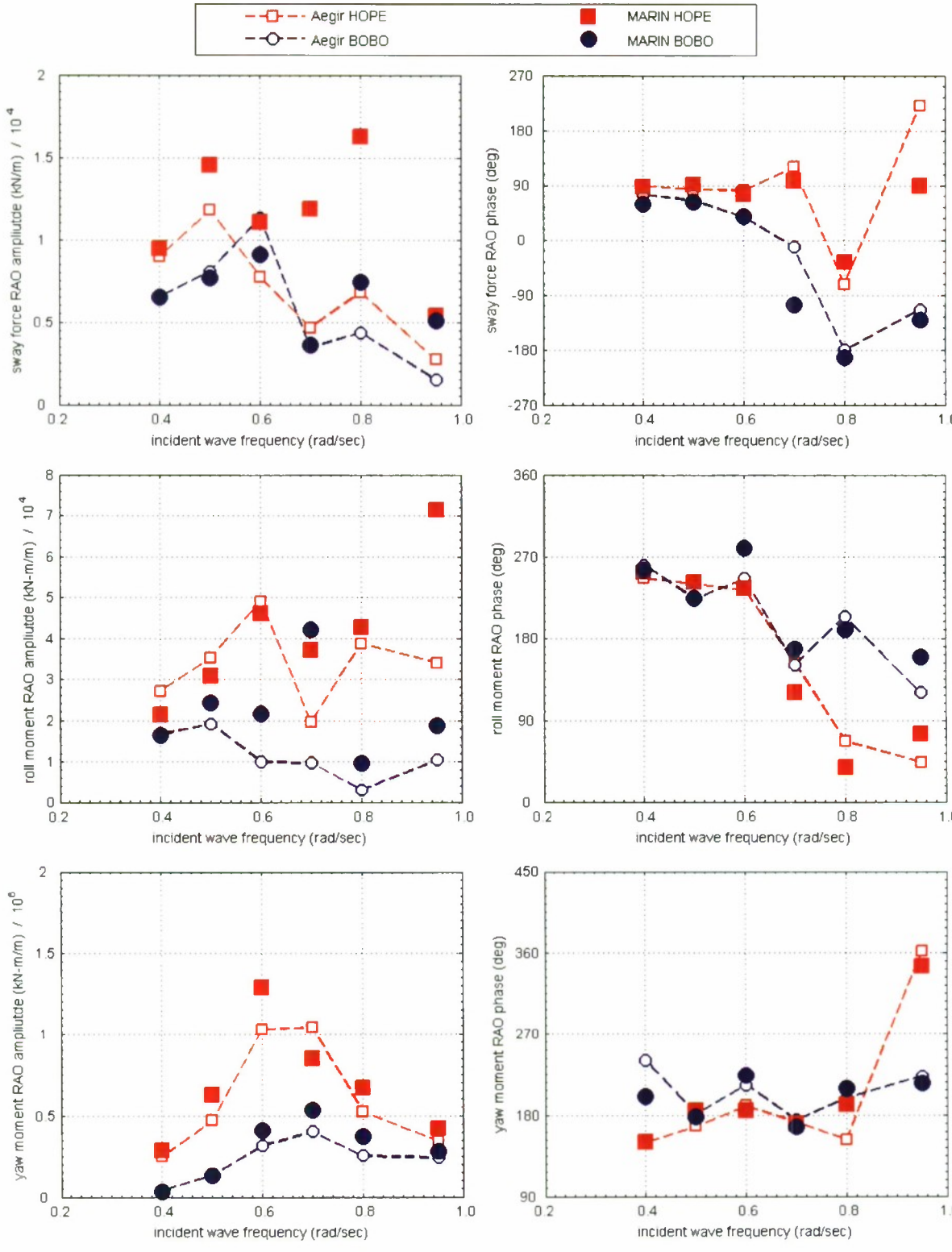

Figure F10. HOPE, BOBO Sway Force and Roll and Yaw Moment RAO Amplitude and Phase for 33 meter separation, 120 degree wave heading, and 16 knots ship speed.

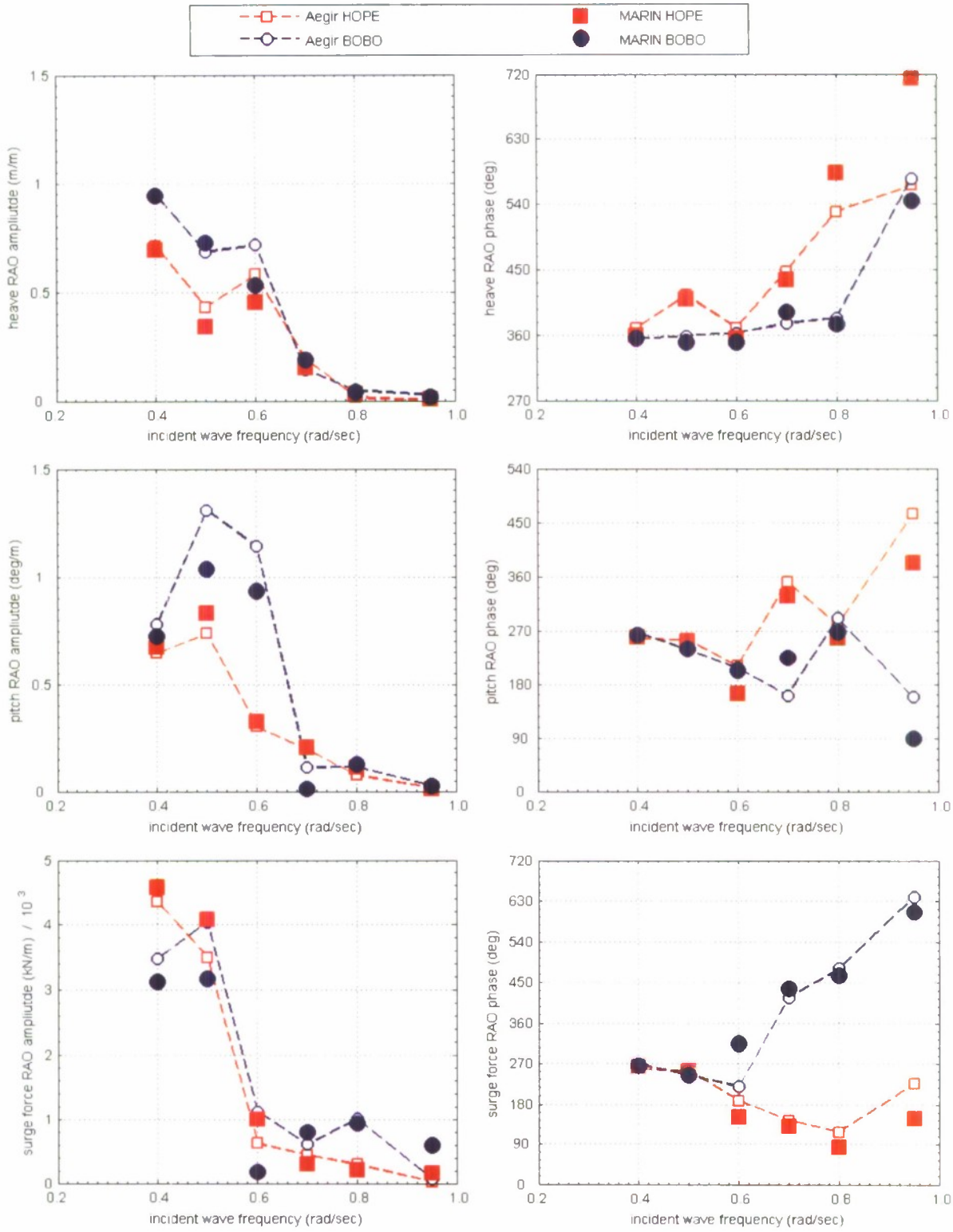

Figure F11. HOPE, BOBO Heave and Pitch Motion and Surge Force RAO Amplitude and Phase for 33 meter separation, 150 degree wave heading, and 16 knots ship speed.

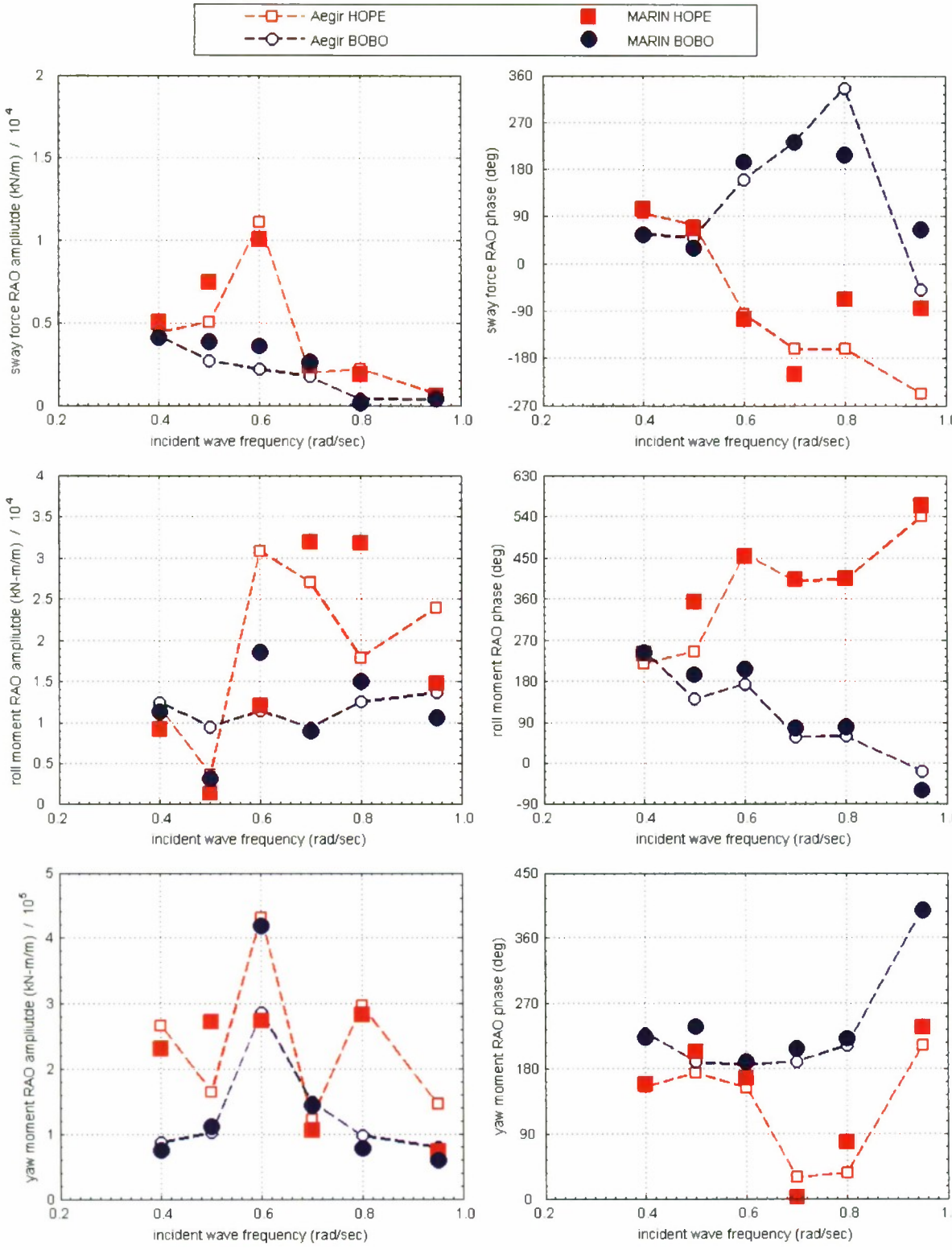

Figure F12. HOPE, BOBO Sway Force and Roll and Yaw Moment RAO Amplitude and Phase for 33 meter separation, 150 degree wave heading, and 16 knots ship speed.

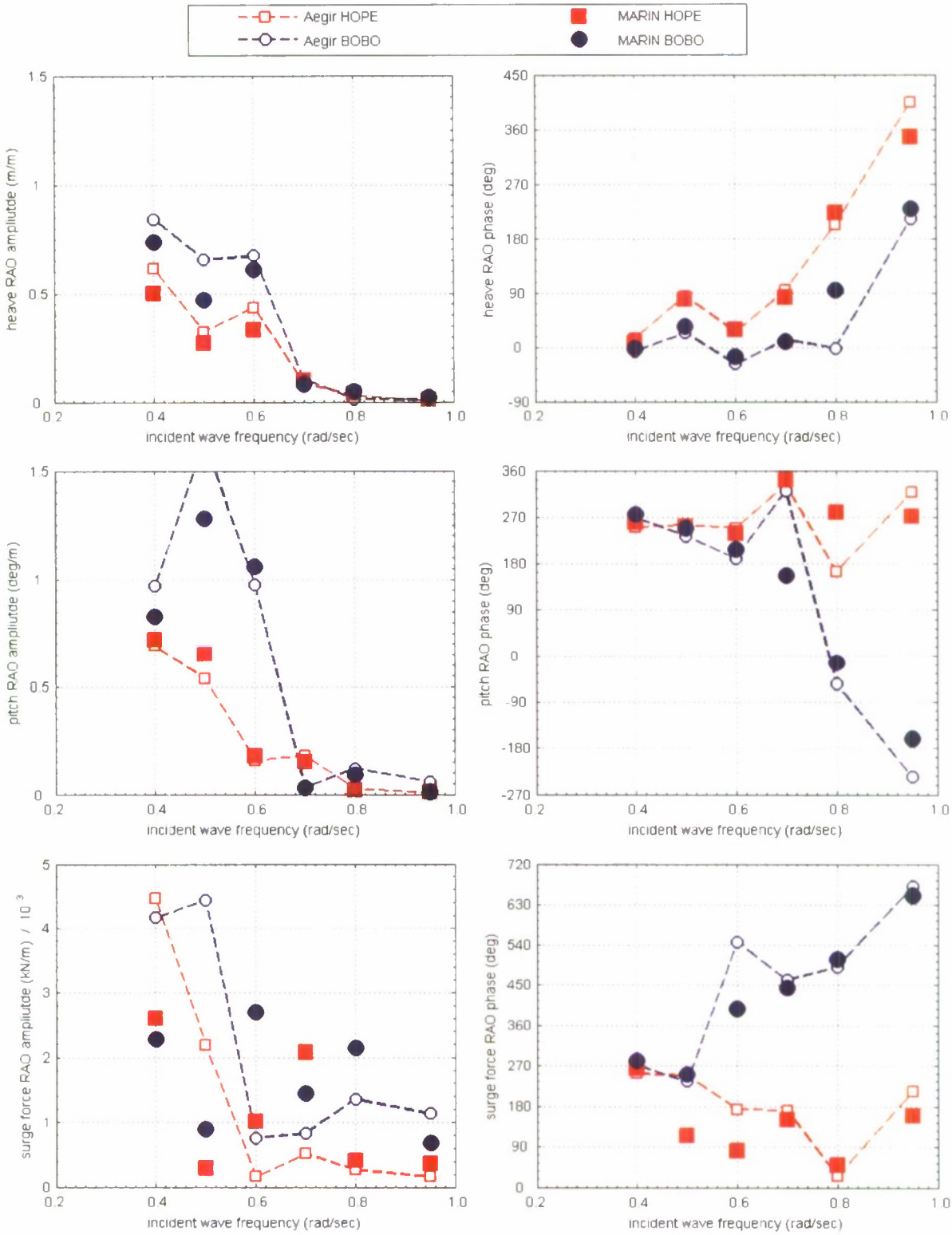

Figure F13. HOPE, BOBO Heave and Pitch Motion and Surge Force RAO Amplitude and Phase for 33 meter separation, 180 degree wave heading, and 16 knots ship speed.

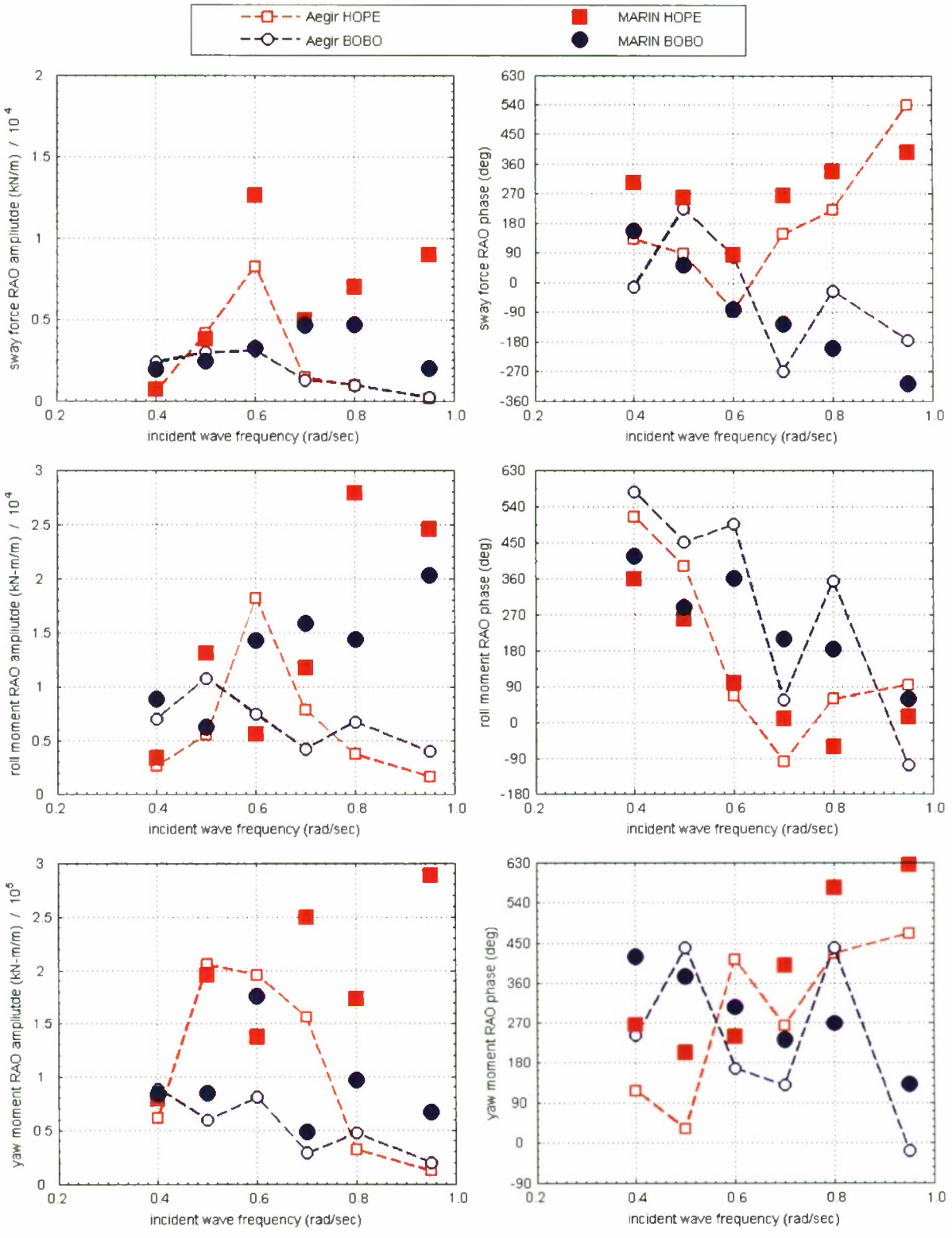

Figure F14. HOPE, BOBO Sway Force and Roll and Yaw Moment RAO Amplitude and Phase for 33 meter separation, 180 degree wave heading, and 16 knots ship speed.

APPENDIX G. PERCENT DIFFERENCE TABLES OF REMAINING CONDITIONS FOR HOPE AND BOBO

Table G1. Percent Difference for motion, force and moment amplitudes for HOPE, Test condition: 3 meter separation, 5 knots and 180 degree heading.

Amplitude Percent Differences for HOPE							
	MVS	MVTDS	FD-Waveload	AQWA	ShipMo3D	LAMP	AEGIR
Heave	13.63	16.65	4.86	7.64	6.83	5.11	5.53
Pitch	14.95	12.23	11.73	14.65	9.42	9.10	6.03
Surge	16.55	7.92	22.85	25.30	19.95	9.42	9.78
Sway	34.25	38.70	40.15	35.10	43.95	11.91	16.71
Roll	30.96	32.97	54.05	40.02	203.91	11.66	14.60
Yaw	23.47	22.64	64.12	55.35	287.24	7.37	12.94

Table G2. Percent Difference for motion, force and moment amplitudes for BOBO, Test condition: 3 meter separation, 5 knots and 180 degree heading.

Amplitude Percent Differences for BOBO							
	MVS	MVTDS	FD-Waveload	AQWA	ShipMo3D	LAMP	AEGIR
Heave	18.18	16.17	3.35	4.40	6.89	4.04	5.92
Pitch	19.76	16.73	19.85	20.77	10.00	13.09	12.15
Surge	23.96	10.48	39.38	37.20	31.62	18.82	18.50
Sway	23.56	22.66	44.82	36.70	67.19	13.24	17.24
Roll	35.32	32.50	27.23	42.23	592.02	9.65	18.75
Yaw	49.27	51.03	111.58	92.36	449.81	11.35	11.93

Table G3. Percent Difference for motion, force and moment phases for HOPE, Test condition: 3 meter separation, 5 knots and 180 degree heading.

Phase Percent Differences for HOPE							
	MVS	MVTDS	FD-Waveload	AQWA	ShipMo3D	LAMP	AEGIR
Heave	19.17	30.20	13.99	6.73	7.55	9.31	4.92
Pitch	25.25	29.85	12.30	4.07	7.82	6.34	6.30
Surge	22.18	23.90	28.06	19.96	20.79	21.25	16.32
Sway	17.89	16.18	27.14	23.06	21.02	31.19	32.33
Roll	15.14	33.93	17.53	36.99	21.11	45.63	42.54
Yaw	30.01	25.62	22.65	28.70	18.24	37.32	41.19

Table G4. Percent Difference for motion, force and moment phases for BOBO, Test condition: 3 meter separation, 5 knots and 180 degree heading.

Phase Percent Differences for BOBO							
	MVS	MVTDS	FD-Waveload	AQWA	ShipMo3D	LAMP	AEGIR
Heave	29.41	14.77	5.87	6.78	13.24	9.98	4.49
Pitch	27.35	25.93	8.84	8.03	3.47	9.74	9.71
Surge	21.40	27.42	26.18	22.94	22.73	11.41	9.18
Sway	17.57	20.22	24.90	20.65	14.68	40.99	42.62
Roll	27.28	31.06	17.99	35.80	20.05	38.73	41.31
Yaw	23.04	14.79	20.90	30.16	25.28	37.59	33.43

Table G5. Percent Difference for motion, force and moment amplitudes for HOPE, Test condition: 16.5 meter separation, 120 degree wave heading, and 16 knots ship speed.

Amplitude Percent Differences for HOPE							
	MVS	MVTDS	FD-Waveload	AQWA	ShipMo3D	LAMP	AEGIR
Heave	35.41	70.15	11.86	9.56	7.46	6.75	9.98
Pitch	64.41	55.91	5.17	8.80	5.14	9.88	9.57
Surge	37.81	54.48	38.45	36.87	28.83	38.94	39.54
Sway	182.26	140.83	38.80	38.92	45.39	23.67	25.99
Roll	22.63	37.40	24.03	22.75	175.30	17.00	14.39
Yaw	226.88	135.30	23.21	18.42	74.70	11.82	10.16

Table G6. Percent Difference for motion, force and moment amplitudes for BOBO, Test condition: 16.5 meter separation, 120 degree wave heading, and 16 knots ship speed.

Amplitude Percent Differences for BOBO							
	MVS	MVTDS	FD-Waveload	AQWA	ShipMo3D	LAMP	AEGIR
Heave	28.34	70.14	16.27	8.27	12.63	11.86	8.48
Pitch	82.45	56.15	16.98	12.83	18.54	3.86	4.99
Surge	78.65	54.01	40.92	25.29	33.57	41.36	47.33
Sway	262.61	177.29	27.72	27.05	38.51	17.01	18.96
Roll	93.15	55.54	23.35	26.40	221.49	29.03	30.53
Yaw	88.25	63.35	58.84	54.53	271.24	12.38	9.33

Table G7. Percent Difference for motion, force and moment phases for HOPE, Test condition: 16.5 meter separation, 120 degree wave heading, and 16 knots ship speed.

Phase Percent Differences for HOPE							
	MVS	MVTDS	FD-Waveload	AQWA	ShipMo3D	LAMP	AEGIR
Heave	34.82	19.25	7.84	2.45	4.77	3.60	7.57
Pitch	9.01	30.31	12.60	10.06	10.23	9.68	7.66
Surge	34.13	28.97	33.83	14.19	26.53	14.26	13.45
Sway	34.96	26.70	40.26	7.70	30.37	5.63	14.25
Roll	21.26	16.80	36.52	11.47	35.14	8.71	11.42
Yaw	24.18	33.00	43.90	5.74	21.76	4.01	5.11

Table G8. Percent Difference for motion, force and moment phases for BOBO, Test condition: 16.5 meter separation, 120 degree wave heading, and 16 knots ship speed.

Phase Percent Differences for BOBO							
	MVS	MVTDS	FD-Waveload	AQWA	ShipMo3D	LAMP	AEGIR
Heave	28.92	25.52	23.03	4.43	7.69	7.05	24.08
Pitch	22.62	11.23	27.59	9.04	7.64	4.34	20.34
Surge	34.54	22.01	22.47	5.24	34.72	15.72	30.69
Sway	26.72	18.28	25.85	19.49	29.21	11.50	15.83
Roll	24.93	30.86	34.77	16.49	23.75	15.63	23.99
Yaw	21.23	25.65	20.22	9.80	18.70	10.75	23.62

Table G9. Pereent Differenee for motion, foree and moment amplitudes for HOPE, Test condition: 16.5 meter separation, 150 degree wave heading, and 16 knots ship speed.

Amplitude Percent Differences for HOPE							
	MVS	MVTDS	FD-Waveload	AQWA	ShipMo3D	LAMP	AEGIR
Heave	6.86	28.58	6.54	5.85	7.22	3.91	3.89
Pitch	16.26	6.07	7.89	4.90	6.45	10.14	9.45
Surge	16.19	27.18	30.23	33.21	30.38	39.73	34.32
Sway	67.99	67.55	48.45	51.96	70.47	19.31	20.06
Roll	15.86	13.40	10.42	7.00	138.44	14.11	14.96
Yaw	37.35	82.05	27.80	30.30	146.42	25.06	19.54

Table G10. Pereent Differenee for motion, force and moment amplitudes for BOBO, Test condition: 16.5 meter separation, 150 degree wave heading, and 16 knots ship speed.

Amplitude Percent Differences for BOBO							
	MVS	MVTDS	FD-Waveload	AQWA	ShipMo3D	LAMP	AEGIR
Heave	9.67	18.42	15.34	8.50	7.32	11.55	8.59
Pitch	11.51	33.49	25.61	19.68	13.61	5.34	4.92
Surge	27.40	33.35	35.10	29.44	49.23	43.93	55.26
Sway	77.65	113.55	52.33	59.59	72.06	31.39	29.96
Roll	27.08	32.35	18.14	18.89	173.30	20.69	27.20
Yaw	41.54	45.66	23.07	31.73	290.63	31.63	22.11

Table G11. Pereent Difference for motion, foree and moment phases for HOPE, Test condition: 16.5 meter separation, 150 degree wave heading, and 16 knots ship speed.

Phase Percent Differences for HOPE							
	MVS	MVTDS	FD-Waveload	AQWA	ShipMo3D	LAMP	AEGIR
Heave	19.76	15.68	13.37	11.84	15.14	7.55	9.36
Pitch	24.57	28.23	11.34	12.59	6.48	10.29	5.41
Surge	19.56	17.46	25.50	17.84	22.50	13.63	17.50
Sway	15.85	14.91	25.17	23.15	35.79	9.12	10.35
Roll	28.16	20.58	35.92	18.21	22.69	13.10	8.52
Yaw	29.13	26.17	39.71	8.62	16.44	7.35	5.55

Table G12. Pereent Differenee for motion, foree and moment phases for BOBO, Test condition: 16.5 meter separation, 150 degree wave heading, and 16 knots ship speed.

Phase Percent Differences for BOBO							
	MVS	MVTDS	FD-Waveload	AQWA	ShipMo3D	LAMP	AEGIR
Heave	23.96	23.12	16.82	13.60	20.83	12.44	20.99
Pitch	30.08	21.17	19.76	13.78	19.17	13.21	15.10
Surge	26.85	34.71	33.75	15.50	24.21	16.82	13.52
Sway	33.09	21.16	21.08	23.17	21.81	8.93	8.33
Roll	33.99	16.12	24.63	19.37	21.62	16.60	12.07
Yaw	30.67	23.26	31.55	20.10	15.97	7.32	10.37

Table G13. Percent Difference for motion, force and moment amplitudes for HOPE, Test condition: 16.5 meter separation, 180 degree wave heading, and 16 knots ship speed.

Amplitude Percent Differences for HOPE							
	MVS	MVTDS	FD-Waveload	AQWA	ShipMo3D	LAMP	AEGIR
Heave	49.40	86.38	9.20	5.19	5.84	3.81	2.69
Pitch	104.43	177.82	6.68	8.17	4.17	8.86	6.36
Surge	72.42	129.23	22.59	31.59	23.14	26.47	28.71
Sway	271.75	514.22	81.13	80.79	75.96	26.22	23.42
Roll	41.15	97.52	20.81	26.88	189.73	21.66	18.29
Yaw	302.74	541.74	18.65	22.42	138.81	13.45	9.29

Table G14. Percent Difference for motion, force and moment amplitudes for BOBO, Test condition: 16.5 meter separation, 180 degree wave heading, and 16 knots ship speed.

Amplitude Percent Differences for BOBO							
	MVS	MVTDS	FD-Waveload	AQWA	ShipMo3D	LAMP	AEGIR
Heave	31.16	93.97	13.89	12.38	15.54	12.12	9.86
Pitch	121.40	192.16	16.59	13.55	16.72	4.41	11.06
Surge	130.10	141.64	30.56	46.27	37.37	45.62	53.30
Sway	321.25	602.06	65.68	66.46	63.11	20.23	19.06
Roll	154.83	258.64	21.75	23.82	168.33	26.44	22.30
Yaw	107.08	163.16	31.76	33.16	208.71	17.12	13.08

Table G15. Percent Difference for motion, force and moment phases for HOPE, Test condition: 16.5 meter separation, 180 degree wave heading, and 16 knots ship speed.

Phase Percent Differences for HOPE							
	MVS	MVTDS	FD-Waveload	AQWA	ShipMo3D	LAMP	AEGIR
Heave	23.43	21.37	16.68	11.44	12.31	14.32	18.03
Pitch	26.29	27.58	23.25	10.92	18.75	28.42	28.75
Surge	27.85	26.92	25.41	24.53	17.69	22.48	27.07
Sway	25.10	18.50	32.41	22.22	10.79	35.56	34.20
Roll	28.04	17.42	27.03	20.21	30.83	25.00	30.26
Yaw	27.84	20.62	30.70	27.94	27.64	38.00	41.81

Table G16. Percent Difference for motion, force and moment phases for BOBO, Test condition: 16.5 meter separation, 180 degree wave heading, and 16 knots ship speed.

Phase Percent Differences for BOBO							
	MVS	MVTDS	FD-Waveload	AQWA	ShipMo3D	LAMP	AEGIR
Heave	27.28	15.43	8.57	14.45	11.53	7.86	10.76
Pitch	25.10	30.90	16.81	17.31	16.67	14.35	14.55
Surge	27.09	21.04	41.12	12.86	31.48	11.04	9.94
Sway	27.78	20.31	29.32	18.76	21.25	35.89	41.93
Roll	30.36	30.27	21.46	26.50	25.32	38.43	35.70
Yaw	22.27	26.87	21.09	29.24	30.28	40.64	43.87

Table G17. Percent Differenee for motion, foree and moment amplitudes for HOPE, Test condition: 33 meter separation, 120 degree wave heading, and 16 knots ship speed.

Amplitude Percent Differences for HOPE							
	MVS	MVTDS	FD-Waveload	AQWA	ShipMo3D	LAMP	AEGIR
Heave	23.82	41.30	23.65	8.17	11.82	7.85	9.36
Pitch	17.04	30.43	46.05	20.55	9.50	7.01	6.25
Surge	35.42	63.54	22.06	27.48	36.55	57.56	53.75
Sway	43.46	26.84	22.34	20.29	45.82	25.56	26.54
Roll	18.37	26.17	20.06	13.81	151.93	13.93	16.79
Yaw	7.68	16.47	45.14	43.14	54.36	9.54	11.29

Table G18. Percent Differcnce for motion, force and moment amplitudes for BOBO, Test condition: 33 meter separation, 120 degree wave heading, and 16 knots ship speed.

Amplitude Percent Differences for BOBO							
	MVS	MVTDS	FD-Waveload	AQWA	ShipMo3D	LAMP	AEGIR
Heave	29.00	31.63	37.56	9.85	6.16	12.44	12.29
Pitch	15.94	26.11	81.18	27.44	18.51	4.63	3.40
Surge	41.29	57.99	24.47	28.06	31.72	36.72	43.03
Sway	48.10	50.08	48.09	49.78	47.34	15.25	17.09
Roll	18.59	14.04	33.83	45.94	203.21	21.13	25.54
Yaw	23.47	30.84	63.97	67.00	173.48	13.66	12.33

Table G19. Percent Difference for motion, force and moment phases for HOPE, Test condition: 33 meter separation, 120 degree wave heading, and 16 knots ship speed.

Phase Percent Differences for HOPE							
	MVS	MVTDS	FD-Waveload	AQWA	ShipMo3D	LAMP	AEGIR
Heave	39.38	22.09	8.86	11.20	11.99	3.35	2.22
Pitch	14.30	30.98	9.05	5.47	4.95	6.88	4.00
Surge	28.56	22.59	30.72	14.78	22.96	14.09	13.28
Sway	30.29	19.38	31.88	16.54	32.18	6.92	9.62
Roll	18.32	34.84	33.29	15.90	22.96	2.64	4.79
Yaw	28.12	29.41	41.04	9.26	18.01	3.62	3.73

Table G20. Pereent Difference for motion, force and moment phases for BOBO, Test condition: 33 meter separation, 120 degree wave heading, and 16 knots ship speed.

Phase Percent Differences for BOBO							
	MVS	MVTDS	FD-Waveload	AQWA	ShipMo3D	LAMP	AEGIR
Heave	27.03	18.25	24.51	7.52	13.24	3.22	3.07
Pitch	21.09	16.72	31.51	6.78	8.56	5.04	8.21
Surge	33.58	28.73	26.26	9.80	34.44	11.69	13.43
Sway	18.19	26.16	37.49	20.46	22.87	9.43	6.73
Roll	22.35	18.64	29.41	14.92	18.15	7.32	5.20
Yaw	24.63	29.15	29.22	12.39	27.82	2.13	3.74

Table G21. Percent Difference for motion, force and moment amplitudes for HOPE, Test condition: 33 meter separation, 150 degree wave heading, and 16 knots ship speed.

Amplitude Percent Differences for HOPE							
	MVS	MVTDS	FD-Waveload	AQWA	ShipMo3D	LAMP	AEGIR
Heave	17.22	23.25	9.22	4.76	8.15	2.93	5.96
Pitch	24.19	24.70	16.87	11.64	9.82	3.76	3.80
Surge	22.96	27.36	39.15	38.48	24.24	40.85	37.42
Sway	27.67	36.01	26.00	27.29	33.32	21.88	19.46
Roll	42.92	28.93	34.09	27.43	105.34	19.69	24.22
Yaw	58.69	38.14	70.51	62.08	114.55	10.31	6.48

Table G22. Percent Difference for motion, force and moment amplitudes for BOBO, Test condition: 33 meter separation, 150 degree wave heading, and 16 knots ship speed.

Amplitude Percent Differences for BOBO							
	MVS	MVTDS	FD-Waveload	AQWA	ShipMo3D	LAMP	AEGIR
Heave	31.62	27.80	17.66	9.90	10.60	10.03	6.98
Pitch	26.22	28.55	27.13	18.49	13.35	8.89	6.88
Surge	63.47	52.40	48.01	61.22	33.05	54.59	60.15
Sway	32.57	23.43	25.85	31.95	13.17	17.10	19.00
Roll	20.12	24.45	33.25	47.13	136.97	22.14	22.07
Yaw	78.02	91.17	116.62	102.06	222.92	9.02	11.79

Table G23. Percent Difference for motion, force and moment phases for HOPE, Test condition: 33 meter separation, 150 degree wave heading, and 16 knots ship speed.

Phase Percent Differences for HOPE							
	MVS	MVTDS	FD-Waveload	AQWA	ShipMo3D	LAMP	AEGIR
Heave	7.71	24.80	17.55	12.92	14.77	12.78	9.15
Pitch	20.95	38.45	9.36	6.84	7.92	12.14	5.13
Surge	30.95	25.42	27.77	20.28	21.44	11.41	14.79
Sway	27.90	25.61	24.78	29.63	33.75	11.48	15.42
Roll	21.63	20.58	27.93	27.03	23.19	9.98	13.00
Yaw	20.98	24.13	35.26	11.37	29.81	5.60	10.99

Table G24. Percent Difference for motion, force and moment phases for BOBO, Test condition: 33 meter separation, 150 degree wave heading, and 16 knots ship speed.

Phase Percent Differences for BOBO							
	MVS	MVTDS	FD-Waveload	AQWA	ShipMo3D	LAMP	AEGIR
Heave	28.30	30.46	25.42	8.22	17.08	5.62	5.36
Pitch	22.68	24.56	17.30	8.23	8.80	10.71	13.81
Surge	22.52	31.79	25.47	13.89	37.87	13.29	18.11
Sway	27.64	23.50	24.05	18.10	18.43	20.36	9.96
Roll	30.99	32.37	23.28	13.66	17.08	8.19	7.99
Yaw	32.99	28.86	18.07	14.85	27.08	4.05	4.52

Table G25. Percent Difference for motion, force and moment amplitudes for HOPE, Test condition: 33 meter separation, 180 degree wave heading, and 16 knots ship speed.

Amplitude Percent Differences for HOPE							
	MVS	MVTDS	FD-Waveload	AQWA	ShipMo3D	LAMP	AEGIR
Heave	4.51	4.34	8.49	5.81	5.96	3.86	4.96
Pitch	13.71	10.64	4.97	7.06	4.29	3.95	4.04
Surge	11.22	24.74	30.02	32.63	17.60	38.18	33.96
Sway	47.93	47.64	36.21	36.98	43.57	24.98	23.85
Roll	24.11	22.50	14.15	12.32	85.98	12.48	16.76
Yaw	16.25	16.43	15.10	15.59	139.88	6.81	7.74

Table G26. Percent Difference for motion, force and moment amplitudes for BOBO, Test condition: 33 meter separation, 180 degree wave heading, and 16 knots ship speed.

Amplitude Percent Differences for BOBO							
	MVS	MVTDS	FD-Waveload	AQWA	ShipMo3D	LAMP	AEGIR
Heave	8.08	10.19	10.26	9.11	12.26	5.41	7.16
Pitch	20.07	20.15	6.88	6.47	6.03	3.41	8.55
Surge	27.23	29.34	56.89	48.62	17.83	46.19	55.07
Sway	33.67	33.28	24.04	29.63	33.32	21.15	18.27
Roll	19.95	19.38	13.80	20.08	143.35	17.28	19.35
Yaw	17.26	18.00	29.80	21.62	238.65	8.92	7.55

Table G27. Percent Difference for motion, force and moment phases for HOPE, Test condition: 33 meter separation, 180 degree wave heading, and 16 knots ship speed.

Phase Percent Differences for HOPE							
	MVS	MVTDS	FD-Waveload	AQWA	ShipMo3D	LAMP	AEGIR
Heave	28.08	30.21	19.95	11.93	9.72	3.57	4.83
Pitch	31.20	38.81	19.84	15.13	18.24	9.54	8.89
Surge	18.44	25.49	24.62	20.95	24.03	11.18	15.46
Sway	22.01	23.11	32.24	17.03	24.44	31.54	41.24
Roll	25.51	28.08	33.52	17.81	26.44	27.28	28.90
Yaw	27.82	29.50	18.94	21.65	34.35	39.56	43.21

Table G28. Percent Difference for motion, force and moment phases for BOBO, Test condition: 33 meter separation, 180 degree wave heading, and 16 knots ship speed.

Phase Percent Differences for BOBO							
	MVS	MVTDS	FD-Waveload	AQWA	ShipMo3D	LAMP	AEGIR
Heave	20.53	17.40	10.95	14.81	12.22	11.26	6.73
Pitch	28.08	30.91	17.04	12.72	15.88	14.85	14.81
Surge	23.77	23.48	39.72	9.75	35.88	10.44	10.81
Sway	29.13	29.10	23.00	25.45	31.94	37.99	44.14
Roll	27.51	24.10	23.17	28.78	31.99	40.00	43.77
Yaw	21.11	32.26	23.89	25.91	30.51	32.32	37.33

[This page is intentionally blank]

REFERENCES

1. Computer Seienees Corporation, "Multi-Vessel Simulator User's Manual Version 1.0," Computer Seienees Corporation/Advanced Marine Center, August 2006.
2. BMT Designers & Planners, "Multiple Vessel Time Domain Simulator," prepared for the NSWC Carderoek Division Code 5500, September, 2007.
3. Weems, K., "LAMP-MULTI: A LAMP Version for Multiple, Interaeting Bodies in Waves User's Guide," Version 3.1.2, Seienee Applieations International Corporation, Advaneed Systems and Teehnology Division, February 2007.
4. Kring, D.C., Milewski, W.M. and Fine, N.E., "Validation of a NURBS-Based BEM for Multihull Ship Seakeeping," Proeeedings of the 25th Symposium on Naval Hydrodynamics, St. John's Newfoundland and Labrador, Canada, 2004.
5. Century Dynamies, "AQWA-LINE Manual," AQWA Support Manager, Century Dynamies Limited, 2006.
6. WAMIT Ine., "WAMIT User Manual Versions 6.3, 6.3PC, 6.3S, 6.3S-PC," WAMIT Ine., 2006.
7. Martee Limited, "FD-Waveload 2007 A-CSC User's Guide," SM-07-02 A Rev 1, September 2007.
8. van't Veer, A.P. and van Engelenburg R., "Multi Body Interaetion Model Tests Bob Hope and Bobo," MARIN order number 19037 in "Multivessel Tests TAKR 300 (Bob Hope) & T-AK 3008 (2nd Lt. John P. Bobo) Volume III: Test Report," Computer Seienees Corporation/Advaneed Marine Center, September 2006.
9. van't Veer, A.P. and van Engelenburg R., "Multi Body Interaetion Model Tests Bob Hope and Bobo," MARIN order number 19037 in "Multivessel Tests TAKR 300 (Bob Hope) & T-AK 3008 (2nd Lt. John P. Bobo) Volume I: Test Plan," Computer Seienees Corporation/Advaneed Marine Center, September 2006.
10. van't Veer, A.P. and van Engelenburg R., "Multi Body Interaetion Model Tests Bob Hope and Bobo," MARIN order number 19037 in "Multivessel Tests TAKR 300 (Bob Hope) & T-AK 3008 (2nd Lt. John P. Bobo) Volume II: Model Measurement Report," Computer Seienees Corporation/Advaneed Marine Center, September 2006.
11. ISO, "Guide to the Expression of Uneertainty in Measurement," International Organization for Standardization, Geneva, Switzerland, 1995.
12. Stern, F., et. al., *Computational Hydrodynamic Tools for High-Speed Sealift: Phase II Final Report, IIHR Technical Report No. 465*, University of Iowa, June 2008.
13. Ogilvie, T. F. and E. O. Tuek 1969. *A rational strip theory of ship motions: Part 1*, Teehnieal Report 013, Dept. of Naval Arehiteeture and Marine Engineering, University of Miehigan.
14. Newman, J.N., "Progress in wave load eomputations on offshore structures", Invited Lecture, 23th OMAE Conferenee, Vaneouver, Canada, 2004. (available at http://www.wamit.eom/publieations.html)

15. C.-H. Lee, J.N. Newman and X. Zhu "An extended boundary-integral-equation method for the removal of irregular-frequency effects," *International Journal for Numerical Methods in Fluids*, **23**, 637-660, 1996

16. Katsuro Kijima, "On the Practical Prediction Method for Ship Maneuvering Characteristics", Proceedings, MARSIM '03, August 2003.

INITIAL REPORT DISTRIBUTION

Number of copies			
Hard	PDF	Organization	Name
10	6	ONR	Hess (5), Cooper (1), Mangum (1), Main (1), Purtell (1), Rispin (1)
2	2	NAVSEA 05Z	Waters (1), Croekett (1)
3	3	NAVSEA PMS 385	Fink (1), Rauseh (1), Huffman (1)
1	1	ABS	Ingram (1)
1		DTIC	
		NSWCCD Code	Name
	1	2420	Hardy
	1	3442	TIC
	1	5060	Walden
15	6	5500	Silver (10), Hughes (1), Conrad (1), S. Lee (1), Klamo (1), Applebee (1)